PhD Program in Translational and Molecular Medicine

DIMET

University of Milano-Bicocca

School of Medicine and Faculty of Science

Targeting *JAK2* and *PAX5* Rearrangements in a Preclinical Model of Childhood Acute Lymphoblastic Leukemia

Tutor: Prof. Giovanni Cazzaniga

Co-tutor: Dr.ssa Grazia Fazio

Coordinator: Prof. Francesco Mantegazza

Dr. Manuel Quadri

Matr. 785990

XXXV cycle

Academic Year 2021-2022

Table of Contents

Chapter 1

Introduction

1. Acute Lymphoblastic Leukemia

Acute lymphoblastic leukemia (ALL) is the most common pediatric cancer and represents 85% of all the pediatric leukemias (Inaba, et al. 2013; Harrison, et al. 2001; Inaba, et al. 2021). It is characterized by an abnormal expansion of immature lymphoid progenitors, also called lymphoblasts, which arise in the bone marrow and could infiltrate both hematopoietic organs (as spleen and peripheral blood) and non-hematopoietic organs as central nervous system (Tasian, et al. 2015). Based on the clinical course of the disease, leukemias are divided into chronic leukemias, defined by the proliferation of more differentiated/mature cells, or acute leukemias, characterized by the presence of undifferentiated cells, called blasts, in peripheral blood and bone marrow, which infiltrate hematopoietic and non-hematopoietic organs. Acute leukemias have a rapid course and a bad prognosis (Inaba, et al. 2013). Morphological and histological analysis, flowcytometry immunophenotyping, based on cluster differentiation (CD) molecules surface expression, and identification of cytogenetic-molecular abnormalities in bone marrow and peripheral blood of patients are used for the diagnosis of ALL. CD identification by flowcytometry define the different lineage commitment and the differentiative states of the expanded clonal leukemic blasts, leading to the classification of ALL into two forms: B cell precursor-ALL (BCP-ALL), derived from alterations of B lymphocytes precursors (85% of cases in Caucasian population), and T-ALL, with aberrant T cell precursors (15% of cases) (Harrison, et al. 2017). The ALL remains the main cause of death in children and young adults (Inaba, et al 2013). Indeed, even though the improvement of multidrug chemotherapy

protocols and novel therapies based on prognostic factors led to a better prognosis with complete remission in 85% of cases, 20% of patients still relapse with only 20-45% of cure rate (Nguyen, et al. 2008; Bourquin and Izraeli, 2010; Conter, et al. 2010).

Remarkably, many factors have to be considered in the leukemogenesis process, as ALL arises from several interactions between exogenous (e.g. infections) and endogenous (e.g. inflammation and oxidative stress), genetic inherited alterations and chance (Inaba, et al. 2013), from ALL initiation, usually in utero, through the evolution to overt disease (Greaves, et al. 2003).

Molecular analysis defined the main genetic alterations found in leukemic cells, which determine pathogenesis and prognosis of the disease, divided in aberrant expression of proto-oncogenes, chromosomal translocations, hyper and hypodiploidies, and contributing to leukemic transformation of hematopoietic cells (Pui, et al. 2004; Tasian, et al. 2015). Rearrangements and translocations (primary events) lead to the deregulation of transcriptional and epigenetic events which are usually not sufficient to evolve in leukemic transformation, while the accumulation of additional alterations as mutations and microdeletions (secondary events) are responsible for the evolvement to a leukemic state through involvement of survival and proliferation pathways (Bhojwani, et al 2015).

The first class of translocations is defined by oncogenes inserted in the regulatory region of transcriptionally active genes leading to deregulated protein expression, as in the case of EPOR and CRLF2 rearrangements (Mullighan, et al. 2009).Conversely, the second class of translocations is represented by fusion proteins derived by the

juxtaposition of sequences of two different genes, leading to a chimeric protein with altered functions from the two original unaltered genes, including 'Philadelphia Chromosome', alterations of the subsets of Philadelphia-like patients, ETV6 and PAX5 rearrangements (Tasian, et al. 2015; Den Boer, et al. 2009; Mullighan, et al. 2009) among the others.ETV6 is one of the most frequently rearranged genes (Bohlander, et al. 2005), with the t(12;21) ETV6::RUNX1 translocations present in 25% pediatric ALL, in which the N-term of ETV6, fundamental gene for hematopoietic stem cells migration in bone marrow, is fused at the C-term with the complete RUNX1, a component of the core binding factor essential for the hematopoiesis. RUNX1 transcriptional function is inhibited by ETV6 in the chimer protein (Pui, et al. 2004), therefore downstream there is an altered signaling, even though the prognosis of affected patients is still excellent, with 90% event free survival (Tasian, et al. 2015). However, PAX5::ETV6 remains the most frequent fusion in B-ALL (Jia and Gu, 2022), involving PAX5, a master regulator of B cell development. PAX5, whose gene is altered in 30% of B-ALL cases (Mullighan, et al. 2007), is a very promiscuous gene, with several known partner genes generating multiple chimeric fusion proteins, such as PAX5::AUTS2 and PAX5::JAK2. TCF3, also known as E2A, is frequently involved in fusion proteins, with the TCF3::PBX t(1;19) translocation affecting 26% of B-ALL cases, although it does not have a prognostic role in the ongoing treatment protocol. TCF3::PBX1 fusion protein blocks the expression of both HOX genes and TCF3 targets, resulting in leukemia evolution (Pui, et al. 2004). KMT2A/MLL rearrangements are present in only 3% of B-ALL pediatric patients, while they represent a key alteration in infant leukemia, in which they

represent 80% of cases, having the MLL::AF4 t(4;11) translocation as the most frequent and associated with a bad prognosis (Roberts and Mullighan, 2015).

Hyperdiploidy represents the largest genetic entity in pediatric B-ALL (30-35%) (Moorman, et al. 2010), with increased number of chromosomes from 52 to 67(Haas and Borkhardt, 2022), and it is associated with low risk (Enshaei, et al. 2021), while hypodiploidy has a lower incidence and a number of chromosome lower than 44 (Ghavazi, et al. 2015) and it is associated with a dismal outcome (Pui, et al. 2019). There are finally mutations and deletions as frequent alterations in B-ALL, such as the ones involving PAX5 (30%), IKZF1 (15%) and EBF1(5%) (Mullighan, et al. 2013).

2.JAK2 in Philadelphia-like BCP-ALL

2.1 Philadelphia-like BCP-ALL subgroup

The most frequent genetic aberrations in ALL in young adults (25% of cases), and less frequent in children (3-4%), is the t(9;22) translocation, also known as 'Philadelphia Chromosome', involving non receptor tyrosine kinase ABL1 at 3' in 9q34 fused with the B cell receptor BCR at 5' in 22q11 'Philadelphia positive' or Ph+ patients carry the fusion oncoprotein BCR::ABL1, which alters proliferations, survival and renewal of cells, representing a constitutively active kinase (Bernt, et al. 2014). Fundamental has been the introduction of tyrosine kinase inhibitors (TKIs) for BCR::ABL1, as the prognosis of Ph+ ALL was highly unfavorable, even though the low incidence of the disease before TKIs introduction (Biondi, et al. 2012; Biondi, et al. 2018; Aricò, et al. 2010, Schrappe, et al. 2016). This approach of targeted therapy using TKIs has led to the development of the concept of personalized medicine, considering an increasing number of targetable alterations.

Philadelphia-like (Ph-like) has been defined as a new high-risk subgroup (Den Boer, et al. 2009; Mullighan, et al. 2009),characterized by a genetic expression pattern similar to the one of the Philadelphia positive ALL, despite not having the typical chromosomal fusion BCR-ABL1. About 90% of the Ph-like or BCR-ABL1-like subgroup carry an additional lesion (Herold and Gokbuget, 2017), mainly affecting *ABL1/ABL2*, *PDGFRB/A*, *MCSF1R*, *CRLF2*, *PAX5*, *EPOR* and *JAK2* genes (Roberts, et al. 2017; Boer, at al. 2017; Shiraz, et al. 2020; Fazio, et al. 2022). Ph-like genomic profile is heterogeneous, peculiarly defined by lesions activating tyrosine kinases and/or signaling

pathways downstream kinase receptors, making this ALL class a good candidate for alternative treatment therapies with specific kinase inhibitors. Based on the kinase-activating lesion, Ph-like can be subdivided in 4 subtypes: 1. alterations in JAK/STAT pathway genes (CRLF2, JAK2, EPOR, IL7R, SH2B3 mainly), 2. ABL class alterations (ABL1, ABL2, CSF1R, LYN, PDGFRA, and PDGFRB), 3. uncommon Ras pathway mutations (NRAS, KRAS, NF1, PTPN11, CBL), and 4. rare kinase fusions (NTRK3, PTK2B, BLNK) (Tran and Tasian, 2021). Interestingly, more than 60 genetic rearrangements involving 15 genes of kinases and/or cytokine receptors have been described among the Ph-like with, among the others, more than 25 frequent partner genes (Roberts, et al. 2017). Therefore, depending on the type of kinase involved in the rearrangement, a more general distinction in ABL-class or JAK2-class can be done, which is particularly relevant to better understand to whom class of tyrosine kinase inhibitor there could be the appropriate sensibility of treatment (Boer, et al. 2017). The rearrangements involving kinases are mainly in-frame, keeping their kinase domain at the 3'. CRLF2 is among the genes involved in rearrangements in Ph-like, in which they show higher incidence in children affected by Down Syndrome. (Roberts, et al. 2017; Tasian, et al. 2017). Moreover, half of the children carrying *CRLF2* rearrangements in Ph-like (Roberts, et al. 2014; Tasian, et al. 2017) present concurrent mutations mainly in *JAK2*, but also in *JAK1*, which lead to the JAK/STAT pathway activation in association to CRLF2 overexpression (Roberts, et al. 2014; Mullighan, et al. 2009). *JAK2* and *EPOR* rearrangements represent 5-7% of Ph-like cases. *JAK2* is a 3' promiscuous gene with about 30 described 5' partner genes, as *PAX5*,

ATF7IP, *BCR*, *ETV6*, *PCM1* among the others. (Tran and Tasian, 2021; Tasian, et al. 2017; Shiraz, et al. 2020), while 3' *EPOR* showed fewer partner genes involving the enhancer region of immunoglobulin loci (Iacobucci, et al. 2016). In both cases, the JAK/STAT pathway activation has been observed (Tasian, et al. 2017; Roberts, et al. 2017; Iacobucci, et al. 2017).Multiple alterations influence JAK/STAT pathway signaling, as mutations in *IL7R*, *TYK2* rearrangements, mutations in *JAK1-3* and deletions in *SH2B3*, frequently associated to rearrangements which originate oncoprotein involving several genes as *PAX5*, *ETV6*, *CREBBP* among the others (Roberts, et al. 2017).

The JAK/STAT pathway is an appealing potential therapeutic target for Ph-like ALL in children, as the majority of kinase activating aberrations characterizing Ph-like alters JAK/STAT signaling (Tran and Tasian, 2021). Indeed, preclinical studies on patient-derived xenografts (PDX) and engineered Ba/F3 carrying different JAK/STAT pathway alterations (CRLF2 rearrangements, JAK mutations, JAK2 fusions among the others) showed *in-vitro* and *in-vivo* activity to different JAK inhibitors (Maude, et al. 2012; Wu, et al. 2015). Moreover, preclinical data showed that the therapeutic combination approach, acting on multiple oncogenic networks, could be more effective, such as the combination of JAK and mTOR inhibitors in CRLF2 rearranged primary leukemic cells and PDX (Tasian and Loh, 2011; Tasian, et al. 2017).

Several clinical trials are currently ongoing, testing the efficacy of some drugs on Ph-like patients as dasatinib, targeting ABL class alterations, or as ruxolitinib, targeting JAK/STAT pathway alterations, among the others (Tran and Tasian, 2021).

2.2 JAK2, a fundamental hematopoietic regulator

JAK2 is a non-receptor tyrosine kinase belonging to the Janus kinases (JAK1, JAK3, Tyk2). Fundamental for the hematopoiesis, JAK2 is involved in multiple cellular activities and signaling pathways, as proliferation and survival of cells among the others. When altered, JAK2 leads to multiple pathologies. Indeed, due to its pathogenic tendency, JAK2 is the most studied member of the Janus kinases, mainly in myeloproliferative neoplasms and some forms of leukemias and lymphomas (Tran and Tasian, 2021). Located on the short arm of chromosome 9 (9p24), JAK2 is defined by 7 JAK homology (JH) domains, divided into one FERM domain (JH5-7), one Src2-like (SH2-like) homology domain (JH3-4), one pseudokinase domain (JH2) and one tyrosine kinase domain (JH1), from the N-term to the C-term respectively. To note, FERM domain is fundamental for the binding of N-term of JAK2 to the cytoplasmatic end of an activated cytokine receptor, while the pseudokinase domain regulates the JH1 domain, which is activated through the phosphorylation of Tyr1007-1008 inside its catalytic loop of activation (Bousoik and MontazeriAliabadi, 2018; Mullally, et al. 2016). The binding of a cytokine or hormone to the extracellular part of surface receptors, as for growth factor, IFNγ, IL-3 and GM-CSF (Granulocyte-macrophage colony-stimulating factor), leads to a receptor dimerization process. As a consequence, JAK2 dimerizes and a transphosphorylation of JH1 Tyr1007-1008 is responsible for JAK2 activation that initiates its main downstream signaling pathway, the JAK/STAT (signal transducer and activator of transcription) one in addition to multiple downstream signaling pathways, as the Ras/MAPK and PI3K/AKT pathways among the

others, with a progressive transduction of the signal inside the cells (Silvennoinen, et al. 2013).

JAK2 is positively and negatively highly regulated through multiple mechanisms, as by JH2 domain itself, or through SOCS (suppressors of cytokine signaling) and SHP (protein tyrosine phosphatase) proteins, or by phosphorylation mechanisms (Silvennoinen, et al. 2013). To note, JH2 domain negatively regulates JAK2 in absence of ligands on one side, while contributes to JAK2 activation when a ligand binds a receptor correlated to JAK2 itself (Steeghs, et al. 2017). To have JAK2 transphosphorylation, the two JH1 domains have to be accessible to each other. Without stimuli, JH2 blocks the formation of the catalytic connection fundamental for JH1 domains activation, also phosphorylating JH2 Ser523 and Tyr520 keeping JAK2 in a closed and inactive conformation. This specific regulation is crucial, as observed when, due to the presence of the biggest number of mutations occurring in the interface JH1/JH2, the autoinhibition of JAK2 is lost in JAK2 mutated, which is therefore hyperactivated (Zhang, et al. 2018).

Beside Tyr1007-1008, at least 20 additional residues have been identified as residues subjected to phosphorylation after cytokine stimulation (Silvennoinen, et al. 2013). JAK/STAT pathway is the main signaling pathway activated after JAK2 autophosphorylation in Y1007-1008, leading to the phosphorylation of several targets, including STAT3 and STAT5 which create stable homo and heterodimers in their SH2 domains. They translocate inside the nucleus of the cell, acting as transcription factors binding their target promoters on the DNA, regulating proliferation, differentiation and apoptosis of the cell. (Heimm, et al. 1999; Quintas-Cardama, et al. 2013; Bousoik and

MontazeriAliabadi, 2018). STAT3 and STAT5 have been widely studied in cancer biology as they regulate many targets such as inflammatory genes, oncogenes and genes involved in apoptosis (Bousoik and Montazeri, 2018). Considering the fundamental roles of JAK2, STAT3 and STAT5, the JAK/STAT pathway is frequently subjected to alteration peculiar to ALL Ph-like (Tasian, et al. 2017).

2.3 JAK2 alterations from mutations to rearrangements

In literature, copy number variations, mutations and chromosomal translocations have been described as alterations of JAK2 in leukemia and lymphomas. While in recent years JAK2 mutations have been widely studied, its rearrangements are still poorly characterized, being structurally and clinically rarer and defined by more variability (Ehrentraut, et al. 2013). Somatic activating mutations of JAK2 have been described in polycythemia vera, and rarely they have a germinal origin representing rare hereditary forms of polycythemia vera; moreover, acquired or somatic mutations of JAK2 have been frequently found in MPN and acute leukemia (Baxter, et al. 2005). $JAK2_{V617F}$ mutation is the most frequent mutation of JAK2, first described in 2005 and nowadays observed in 90% of polycythemia vera cases and in 50% of myelofibrosis patients (Baxter, et al. 2005). It is a gain of function mutation as resides inside exon 14 of the pseudokinase domain of JAK2, causing a constitutive activation of kinase domain of JAK2, as JH2 domain loses its autoinhibitory activity, that leads to a cellular growth independent of the cytokines of the hematopoietic cells carrying the mutation (Quintas-Cardama, et al. 2013; Vainchenker and Constantinescu, 2013). Focusing on B-ALL patients carrying the $JAK2_{V617F}$ mutation, there is frequently a co-presence of CRLF2

overexpression, in which CRLF2 protein binds alfa subunit of interleukin receptor forming TSLP receptor which becomes the cytokine scaffold for the signaling of JAK2m proteins. Moreover, the co-presence of CRLF2 overexpression and $JAK2_{V617F}$ mutation leads to an hyperactivation of STAT5 and to the cytokine-independent growth of hematopoietic progenitors cell lines (Malin, et al. 2010). In B-ALL, CRLF2 is frequently involved in rearrangements of two types: P2RY8::CRLF2, derived from a PAR1 deletion of chromosome X, and IGH::CRLF2, derived from translocation t(X;14)(Palmi, et al. 2012). Moreover, activating mutations of JAK2 are identified in half of the cases of ALL carrying CRLF2 rearrangements, with the JAK2R683G in JH2 domain to be the most frequent. CRLF2r and JAK2m are present in 60% of children with down syndrome affected by B-ALL (Hertzberg, et al. 2010; Mullighan, et al. 2009).

On the other side, JAK2 rearrangements are found in 5% of pediatric Ph-like ALL and are associated with the poorest outcomes compared with other Ph-like ALL subtypes (Iacobucci and Roberts, 2021). JAK2 retains its catalytic domain (usually exons 19-25) at 3' in frame with a partner gene at 5' of the fusion gene (Tran and Tasian, 2021; Downes, et al. 2022). As the partner gene at 5' is usually highly expressed in B cells, its promoter should induce a high expression of the derived fusion, but the molecular mechanism by which JAK2 fusion genes lead to constitutive JAK2 activation remains largely unknown (Downes, et al. 2022). The main supposed mechanism of activation of JAK2 fusion genes is through their homodimerization via domains in the partner genes (Medves and Demoulin, 2012). Moreover, the loss of JAK2 autoregulatory JH2 domain in presence of fusions, may be an additional

way of activation independent of cytokine stimuli (Schinnerl, et al. 2015). Downstream JAK2 rearrangements, the signaling activation is evaluated, generally of STAT3 and STAT5 (Den Boer, et al. 2009; Tasian, et al 2017; Tran and Tasian, 2021; Downes, et al. 2022). Nowadays, fusion genes involving JAK2 are identified by multiple techniques, as karyotype, FISH, RT-PCR and Sanger and next generation sequencing (NGS). About 30 genes have been found to be partner genes of JAK2 in the ALL, with PAX5 recognized as the most recurrent (28.7%) (Den Boer, et al. 2009; Gu, et al, 2019; Tran and Tasian, 2021; Downes, et al. 2022). Among the other more frequent fusion genes there are BCR::JAK2 (12.8%), ETV6::JAK2 (9.6%), SSBP2::JAK2 (6.4%) and ATF7IP::JAK2 (3.2%) (Roberts, et al. 2014; Downes, et al. 2022; Quintas-Cardama and Verstovsek, 2013). PAX5::JAK2 fusion has been described as the only one able to get inside the nucleus of the cells, where it acts on STATs and additional PAX5 target genes (Schinnerl, et al. 2015; Jurado, et al. 2022), using therefore a different mechanism of activation from the cytokine-independent oligomerization supposed to be followed by the other recurrent fusion genes.

As observed in other Ph-like ALL subtypes, JAK2r are often co-occurring with deletions in genes related to B-cell development including IKZF1(Mullighan, et al. 2008), whose most common alteration is the exons 3-6 deletion, which encodes for the dominant negative IK6 isoform of IKAROS, lacking the N-terminal DNA binding domain (Shiraz, et al. 2020). IKAROS IK6 is unable to bind DNA to regulate the expression of genes required for B-cell differentiation (Downes, et al. 2022). Moreover, additional genomic alterations co-

occurring with JAK2 rearrangements and involved in B-cell pathways are deletions of PAX5, CDKN2A/B, RAG1/2, ETV6 among the others, and mutations within IKZF1 and KRAS (Roberts, et al. 2012; Roberts, et al. 2017). Despite the evidence of a prognostic significance of some of these additional alterations in Ph-like ALL, their influence on JAK2r patient survival rates is still to be better elucidated (Pui, et al. 2017; Zhang, et al. 2018; Downes, et al. 2022).

2.4 JAK2 targeting

JAK2 altered ALL still lacks effective drugs maintaining their specificity for JAK2, with low toxicity. The still poor outcome of ALL patients carrying JAK2 alterations in Ph-like highlights the urgent need of novel specific drugs with reduced toxicity to target these high-risk subgroups of patients (Roberts and Mullighan, 2015; Tran and Tasian, 2021). JAK/STAT signaling pathway is one of the deregulated pathways in Ph-like ALL and it could be considered their major therapeutic target, even though JAK inhibitors have been less well studied in patients with ALL to date, in particular JAK2 rearrangements still lack a specific inhibitor (Tran and Tasian, 2021). When altered, JAK2 can be targeted by tyrosine kinase inhibitors (TKIs), which are mainly divided into type I and type II TKIs, even though the allosteric JAK inhibitors, also defined type III inhibitors, have been recently developed. HDAC inhibitors, as givinostat, HSP90 inhibitors and PROTACS, are instead the most recent approaches currently in use in *ex-vivo* and *in-vivo* settings to induce a degradation of JAK2 as a novel therapeutic approach, alone or in combination with TKIs of type I and II. Interestingly, in the setting of B-ALL, antibody based and

immunotherapies, involving CAR-T cells among the others, are appealing alternatives in case of relapsed/refractory B-ALL. Combination regimens of TKIs and standard chemotherapy drugs seem to be a promising target therapy for JAK2 alterations, as for the JAK2 fusions. Currently, there are clinical trials for ALL patients carrying JAK2 rearrangements exclusively with ruxolitinib, a type-I TKI (Downes, et al. 2022; Tran and Tasian, 2021).

2.5 JAK2 type-I TKIs

In 6 years after the identification of the $JAK2_{V617F}$ mutation, ruxolitinib, a TKI of type I, was FDA-approved as targeted JAK2 inhibitor for MF and PV (Levine, et al. 2007). In 2019 fedratinib was added as FDA-approved JAK2 inhibitor, for the treatment of MF (Mullally, et al. 2020). Ruxolitinib and fedratinib are type-I JAK inhibitors, which bind the ATPbinding site of JAK2 in its active conformation (Leroy and Constantinescu, 2017). Unfortunately, their application in MF revealed some issues related to type-I JAK2 inhibition. Despite ruxolitinib therapy significantly reduced splenomegaly and symptoms (Bose and Verstovsek, 2020), adverse effects were evaluated in COMFORT-1 and COMFORT-2 trials for MF (Harrison, et al. 2017) and in the RESPONSE-III trial for PV (Alimam and Harrison, 2017). The toxicity associated with ruxolitinib may be due to suppression of other JAK family kinases, such as TYK2 and JAK3 and due to the immunosuppression of some types of cells (Quintas-Cardama, et al. 2010; Harrison, et al. 2017). Moreover, it was observed that ruxolitinib binding induces pJAK2 accumulation by preventing JAK2 dephosphorylation and degradation (Tvorogov, et al. 2018; Ross, et al.

2021). Ruxolitinib is still the best available therapy (BAT) for MF, even though it showed low efficacy, dose-dependent toxicity and withdrawal syndrome in MPNs (Downes, et al. 2022). In Ph-like ALL,*ex-vivo* and *in-vivo m*odels carrying JAK2 fusions, ruxolitinib treatment of JAK2r significantly reduced cell viability and STAT5 phosphorylation (Steeghs, et al. 2017; Roberts, et al. 2017; Downes, et al. 2022). However, ruxolitinib showed differential preclinical activity due to the level of JAK pathway oncogene addiction and/or to paradoxical JAK2 hyperphosphorylation with prolonged treatment (Maude, et al. 2012; Boer and den Boer, et al. 2017). To note, ruxolitinib treatment of PAX5::JAK2 primary leukemic cells induced pJAK2 accumulation and hyperphosphorylation (Boer, et al. 2017). Ruxolitinib JAK2 inhibition in combination with chemotherapy may improve outcomes for JAK2 rearrangements in patients of ALL (Schrappe, et al. 2012; Roberts, et al. 2017; Downes, et al. 2021).

Currently fedratinib is the most selective JAK2 inhibitor with a lower immunosuppressive state than ruxolitinib. Unfortunately, also fedratinib has been associated with dose dependent side effects (Mullally, et al. 2020).

Considering the low sensibility data of the TKIs treatment, including ruxolitinib (IC50 of 2 μM), and their side effects in the treatment of B-ALL (Springuel, et al. 2014; Roberts, et al. 2012), novel type-II TKIs could be used to overcome TKIs limitations to treat Ph-like ALL patients with JAK2 rearrangements.

2.6 JAK2 type-II TKIs

Type-II JAK inhibitors bind the inactive conformation of JAK2 in its ATP-binding site (Leroy and Constantinescu, 2017). Type-II JAK inhibitors are still ATP-competitive as type-I TKIs, but they also bind an allosteric pocket of JAK2 resulting in a higher specificity for their target (Li, et al. 2019). BBT594 was the first type-II JAK inhibitor developed, specifically to target resistant cells carrying BCR::ABL1 (Andraos, et al. 2012), followed by the development of a potent type-II JAK inhibitor, CHZ868, with high selectivity towards JAK2 (Meyer, et al. 2015). CHZ868 has shown potent efficacy in *in-vitro* (cell lines) and *in-vivo* (murine models) preclinical settings of MPN and B-ALL. On JAK2 mutated cell lines and primary samples, CHZ868 treatment inhibited the proliferation and blocked the phosphorylation of JAK2, STAT3 and STAT5, contrary to the persistent phosphorylation induced on JAK2 by ruxolitinib treatment (Andraos, et al. 2012; Meyer, et al. 2015; Tvorogov, et al. 2018), suggesting that CHZ868 treatment could avoid pJAK2 accumulation, preventing heterodimeric JAK2 activation and CHZ868 inhibitor persistence (Meyer, et al. 2015; Tvorogov, et al. 2018). CHZ868 treatment reduced pJAK2 and induced apoptosis of B-ALL cell lines carrying CRLF2r co-occurring with a JAK2 mutation, while CHZ868 treatment on PDXs (patient-derived xenografts) derived from B-ALL samples carrying CRLF2r and JAK2 mutations, increased mice survival and reduced splenomegaly (Wu, et al. 2015). Interestingly, CHZ868 proved to synergize with dexamethasone in a leukemia murine model carrying CRLF2/JAK2 alterations (Wu, et al. 2015). Moreover, CHZ868 withdrawal was not associated with a STAT5 signaling rebound (Tvorogov, et al. 2018), highlighting that

type-II JAK2 inhibition may benefit of absent withdrawal syndrome (Meyer, et al. 2015; Wu, et al. 2015; Tvorogov, et al. 2018). The presence of $JAK2_{L884P}$ mutation gives resistance to both BBT594 and CHZ868, pointing out that a possible resistance mechanism of type-II JAK inhibitors could derive from acquired mutations in JAK2 ATP-binding site (Wu, et al. 2015; Leroy and Constantinescu, 2017; ,Downes et al. 2022). Resistance mechanisms of type-II JAK inhibitors treatment still need to be further studied to consider their introduction in clinics, but their promising results *ex-vivo* and *in-vivo* may consider type-II JAK inhibitors for the treatment of JAK2 alterations in B-ALL, with no withdrawal syndrome and persistence which are frequent in type-I JAK inhibitors (Downes, et al. 2021).

3. PAX5, key regulator of B cells

3.1 B cell development

Pluripotent hematopoietic stem cells (PHSCs), characterized by self-renewal, are the originating cells of multiple progenitors of the hematopoietic system, with reduced differentiation potential, which follow a binary commitment in each step of development and deeper specialization (Busslinger, et al. 2004). Multipotential progenitors (MPP) may originate, at the step of distinction into myeloid and lymphoid lineages, common myeloid progenitors (CMPs) or early lymphoid progenitors (ELPs). RAG1 and RAG2 expression (recombinant activating gene 1 and 2), followed by initiation of the immunoglobulin heavy chain (IgH) locus rearrangements, lead ELPS to their dual eventual differentiation in thymic precursors of the T-cell lineage (early T-cell-lineage progenitors, ETPs) or bone-marrow common lymphoid progenitors (CLPs). CLPS may generate B cells, Tcells, dendritic cells (DCs) and natural killer (NK) cells. (Cobaleda, et al. 2008).

Focusing on CLPs, pro-B cells expressing the B cell marker B220 enter the B-cell-differentiation pathway, followed by CD19 expression and completion of IgH diversity (DH)-to-joining (JH) gene-segment rearrangement by pre-BI cells. Then in large pre-BII cells the IgH locus continues to rearrange its variable (V)-region gene segments generating complete VH–DJH alleles. When Rag1 and Rag2 expression is ceased with subsequent expression of the completely rearranged IgH gene at the cell surface, followed by the assembling with the surrogate immunoglobulin light chains (IgLs), VpreB and λ5, together with the

signaling molecules Igαand Igβ, the pre-B-cell receptor (pre-BCR) is completely assembled. Expression of the pre-BCR is a crucial checkpoint in early B-cell development. Signaling through the pre-BCR stimulates a proliferative clonal expansion of large pre-BII cells, followed by re-expression of RAGs and rearrangement at the IgL locus in small pre-BII cells. (Fazio, et al. 2011)

The immature B-cell stage, defined by the surface expression of an assembled BCR, are tested by a secondary immunoglobulin gene rearrangement, known as receptor editing, resulting in their elimination by apoptosis or inactivation by anergy if they don't successfully pass the examination. Otherwise, immature B cells leave the bone marrow and get to the spleen differentiating into their mature counterparts through three transitional stages (T1, T2 and T3), based on the expression of various cell-surface markers. Transitional B cells can be negatively selected in the periphery which becomes a crucial checkpoint for the generation of mature B cells. The transition of immature B cells to mature B cells is crucially regulated by BAFF and its receptor. In the spleen, about 10% of mature splenic B cells are marginal zone B cells, positioned at the blood–lymphoid tissue interface, identified as the main responsible for humoral immune responses to protein antigens. With the help of T cells, they form germinal centers, where germinal center B cells proliferate rapidly and modify immunoglobulins. After about 10 days from the immunization, the germinal center reaction reaches its peak, subsequently slowly vanishing, generating memory B cells and effector plasma cells, following still unclear mechanism of development (Bemark, et al. 2015; Fazio, et al. 2011)

3.2 Transcription factors in B cell development

Transcription factors play a central role in the B cells, coordinating their development, maturation and function (Matthias, et al. 2005). A pool of key transcription factors that include SPI1/PU.1 (an ets-family member), Ikaros, Bcl11a (a zinc finger transcription factor), TCF3/E2A (a helix-loop-helix protein), EBF (early B cell factor) and PAX5 (paired box protein 5), cooperate in a regulatory network over B cell development (Fuxa, et al. 2007).

PU.1controls B cell development in a dose-dependent manner. At low expression, PU.1 favors B cell development priming modifications of the chromatin to facilitate transcriptional activation. Conversely, when expressed at high concentrations in early progenitors, PU.1 might block B cell specific gene expression by inhibiting histone acetylation and bearing the methylation of gene targets, favoring macrophages formation (Hagman and Lukin, 2005). Ikaros controls the development of lymphoid progenitors, while early B lymphopoiesis is blocked before the pre-pro-B stage when Bcl11a is not expressed (Fuxa, et al. 2007).

TCF3, EBF and PAX5 were found to be essential for the differentiation of CLPs in pro-B cells. To note, B cells are blocked at the pro-B or pre-B stage when any of these 3 factors is lacking (Matthias, et al. 2005). TCF3 and EBF determine primary B cell fate coordinating the expression of B cell specific genes. (Matthias, et al. 2005, Fuxa, et al. 2007). Without TCF3 or EBF, B cell development is blocked at early progenitor stages of development, but EBF can activate the B cell lineage program in absence of TCF3 or PU.1. On the other side, B cell development is not rescued by expression of PAX5 without EBF expression (Hagman, et al. 2006). EBF is suggested to be capable of

initiating the activation of transcriptionally quiescent genes (Hagman, et al. 2005). However, PAX5 expression is fundamental to commit B cell progenitors to the B lymphoid lineage after the activation of the B lymphocyte transcription program (Fuxa, et al. 2007). PAX5 is also the responsible of the first checkpoint of B cell development, as it represses B lineage nonspecific genes simultaneously activating B lineage specific genes inside multi-lineage progenitors (Cobaleda, et al. 2007).

3.3 Signaling pathways in precursor B cells

Two are the main wide signaling pathways which regulate survival, proliferation, and differentiation of B cells: IL7R (receptor) downstream pathway, and pre-BCR downstream pathway.

IL7Rα and γc (chain) constitute IL7R, and when α chain expression increases there is the passage from CLPs to LMMPs. IL7 is required for the proliferation and survival of B cells progenitors. With activated IL7 signaling, pro-B and pre-B cells proliferate in the bone marrow and migrate to spleen, lymph nodes and blood (Clark, et al. 2014). The activation of IL7 pathway starts when IL7 binds its receptor, inducing the receptor dimerization that activates JAK3, pre-bound to the cytoplasmic region of the receptor, causing several phosphorylations which serve as binding sites for STAT5, which is also phosphorylated by SRC. STAT5 homodimerize, translocate to the nucleus, where it acts as a transcription factor (Vainchenker, et al. 2013). This transient signaling is terminated by multiple ways, as internalization and degradation of the receptor, dephosphorylation of the receptor and of JAK3 by phosphatases, recruitment of negative regulators, as SOCS proteins, interactions of STAT5 proteins with protein inhibitors (Vainchenker, et al. 2013). When the signal is constitutively active,

there could be the evolution to oncogenesis. Il7R and pre-BCR are strictly correlated and balanced (Clark, et al. 2014). Expression of the pre-BCR by pro-B cells upregulates IL7R expression on the cell surface, increasing the responsiveness of these cells to IL7, resulting in the selection of pre-BCR positive cells in conditions in which IL7 concentration is low. pre-B cells expansion during B-cell development in vivo is limited when pre-BCR itself renders pre-B cells less responsive to IL7 (Ochiai, et al. 2012).

The pre-BCR, on the surface of pre-BI cells, is constituted by the coupling of μ heavy chain with surrogate light chain components VpreB (Vpreb1) and λ5 (Igll1). The pre-BCR is present on the surface of the pre-BI cells. Its extracellular part is linked to Igα and Igβ, 2 signaling chains which represent the sites where the components of the pre-BCR signaling cascade are activated, with consequent regulation of proliferation and survival on one side, and growth arrest and differentiation on the other side. The pre-BCR is therefore a checkpoint in early B cell development.Without a functional heavy chain rearrangement, the negative selection leads to cell apoptosis, while with functional rearrangement, the cell survives and the pre-BCR ensures proliferation and differentiation signaling (Rickert, et al. 2013). One of the main mediators of the dual function of the pre-BCR is SYK, inducing proliferation and survival through the activation of downstream survival pathways, as the PI3K pathway, or favoring the differentiation through BLNK activation (Deane, et al. 2004; Chiu, et al. 2002). Phosphorylated PI3K signaling pathway is inactivated by BLNK, after its phosphorylation. FoxO factors, triggered by BLNK, activate the RAG enzymes, and allow for immunoglobulin light chain

rearrangement (Herzog, et al. 2009). Indeed, Blnk-/- pre-B cells are blocked at the pre-BI stage of development, constantly proliferating (Jumaa, et al. 1999). All these signaling molecules at the pre-BCR checkpoint maintain the balance between negative selection of non-functional B cells (apoptosis) and leukemic transformation is granted by the cooperation of all these signaling effectors in the pre-BCR network.

To note, the JAK/STAT pathway is among the other additional pathways regulating B-cell having a fundamental role in the regulation of proliferation, differentiation, survival and apoptosis of the cells. JAK2 and STATs are key regulators of multiple targets inside B-cells, such as inflammatory genes, oncogenes and genes involved in apoptosis (Bousoik and Montazeri, 2018).

3.4 PAX5 gene and protein

The PAX5 gene is a member of the paired box (PAX) gene family of fundamental transcription factors for B lymphoid lineage commitment, whose family is composed by 9 members from PAX1 to PAX9 (Morrison, et al. 1998). Each of these members, through a paired box domain constituted by a conserved 128aa sequence at the N-term, binds target sequences in the DNA. From pro-B to mature B cells, PAX5 regulates B lymphocytes throughout B cell development (Matthias, et al. 2005). PAX5 encodes for the B cell specific activator protein (BSAP) and is expressed in B lymphocytes, the developing CNS, fetal liver, and adult testis (Cobaleda, et al. 2007).

Located on chromosome 9p13, *PAX5* gene is organized in 10 exons and encodes for a transcript of 8536bp, giving rise to a coding sequence of 1176 bp which encodes for a protein of 391 residues (Ghia, et al. 1998).

The ultimate sequence of PAX5 protein may differ due to alternative transcripts generated by mRNA splicing of *PAX5* (Arseneau, et al. 2009). Alternative splicing of PAX5 may be essential for the regulation of PAX5 targets during the lineage B development. Indeed, PAX5 isoforms may downregulate or upregulate target genes with a finely regulated process fundamental for B cell differentiation in plasma cells (Zwollo, et al. 1997).

PAX5 is a homeodomain protein, member of a class of transcription factors containing a DNA-binding domain with homology to the Drosophila melanogaster homeodomain regulatory proteins. The characteristic feature of PAX protein family is this conserved 'paired' domain, defined by a bipartite nature consisting of an N-term (PAI or NTD) and a C-terminal subdomain (RED or NTD), connected by a central linker. Each of the two subregions consists of a helix– turn–helix motif that binds different half-site in target sequences for PAX5 in the major groove of the DNA of the cell (Golub, et al. 1994). Moreover, PAX5 transcriptional activity is finely regulated by its other domains: an octamer (OP) that inhibits PAX5 transcriptional activity, a partial homeodomain (HD) which associates with the TATA-binding protein of the basal transcription machinery, and the TAD (transactivation domain) and ID (inhibitory domains) domains that, forming the potent C-terminal regulatory region of PAX5, cooperate with activating and repressing activity on PAX5 (Cobaleda, et al. 2007).

3.5 PAX5 role and target genes

PAX5 fulfills a dual role in B lineage commitment by activating B cell specific genes while simultaneously repressing lineage inappropriate

genes. Localized in the nucleus, this transcription factor regulates B cell development (Matthias, et al. 2005; Cobaleda, et al. 2007). The activation of transcription mediated by TCF3 and EBF alone is not sufficient for B cell maturations. In B cells TCF3 and EBF expression is normal in PAX5 mutations in homozygous but rearrangement at the IgH locus is impaired blocking the development at the pro-B state (Matthias, et al. 2005; Delogu, et al. 2006) Pax5-/- pre-BI cells show hematopoietic stem cell features as multipotency and self-renewal, and ability to differentiate in macrophages, osteoclasts, DCs, granulocytes or NK cells after *in-vitro* stimulation, but even into T cells and erythrocytes *in-vivo*. Conversely, without the introduction of PAX5, they can't differentiate in B cells. (Rolink, et al. 2002). Moreover, peripheral mature B cells in mice with conditional PAX5 deletion can dedifferentiate back to early uncommitted progenitors in the bone marrow, leading to the rescue of T lymphopoiesis in T cell deficient mice, generating functional T cells (Cobaleda, et al. 2007). When Pax5 absence co-occur with a strong BCR signaling mature B cells differentiate into plasma cells, while the inactivation of Pax5 in presence of absent BCR signaling leads to dedifferentiation to uncommitted progenitors (Cobaleda, et al. 2007).

The transcription factor PAX5 acts at the level of chromatin, being essential for the formation of chromatinic domains at the promoters level of its target genes, which are involved in signaling, adhesion, migration, B cell differentiation among the others(Schebesta, et al. 2007). PAX5 represses B lineage inappropriate genes and activates B cell lineage genes in B lymphocytes, acting as a transcriptional activator and as a repressor on different target genes (Nutt, et al. 1998). As a

repressor, PAX5 acts on several genes involved in multiple biological activities such as cell adhesion and migration, receptor signaling, cellular metabolism and B cell commitment. Remarkably, PAX5 represses specific genes that lead to other lineages commitment and are reactivated in committed pro-B cells and mature B cells following conditional Pax5 deletion (Cobaleda, et al. 2007), such as Lck (T cells) (Souabni 2002), Flt3 and Sca1 (progenitor cells) (Holmes, et al. 2006), CD33 (myeloid cells) (Morrison, et al. 1998), Sdc1 (plasma cells) (Delogu, et al. 2006). As an activator PAX5 controls B cell development and functions through a complex regulatory network of key proteins involved in B cell signaling, adhesion, migration, antigen presentation, and germinal center B cell formation. Indeed, it regulates signaling cascade from the pre-BCR and the surface of cells, to transcription in the nucleus regulating multiple genes such as Cd19, Cd79a/Iga, Blnk, Vpreb3, Igk and Bach2 (Schebesta, et al. 2007). Interestingly, PAX5 is considered a metabolic gatekeeper, as IKZF1, reducing glucose uptake and consumption in PAX5wt cells, while in presence of heterozygous deletion of PAX5, glycolysis increases as marked glucose uptake and ATP production are observed (Chan, et al. 2017). In conclusion, PAX5 activated target genes encode for essential components of the pre-BCR and BCR signaling pathways, while the transcriptional repression induced by PAX5 is fundamental to limit lineage commitment that differ from B-cells (Fuxa, et al. 2007). To note, the repression induced by PAX5 is continuously required, as reactivation of PAX5 repressed targets is observed following conditional deletion of PAX5 in proB and mature B cells (Fuxa, et al. 2007).

3.6 Oncogenic role of PAX5 in B-ALL

PAX5 is one of the most common targets of genetic alterations in B-ALL, represented by copy number variations, point mutations, intragenic amplifications (iAMP), and translocations, (Jia and Gu, 2022). PAX5 alterations cluster and partially overlaps Ph-like subgroup of B-ALL, as evaluated in gene expression analysis (Gu, et al. 2019, Fazio, et al. 2022).

Among the copy number alterations involving PAX5, **deletions** are the most frequent, being divided in wide range or focal deletions depending on the amount of PAX5 gene affected (Jia and Gu, 2022). They usually affect one allele of PAX5 with absent or altered expression of the truncated protein, leading to a loss of function (Mullighan, et al. 2007). In B-ALL deletions of PAX5 usually co-occur with other alterations, indicating that the presence of other oncogenic lesions is needed to overt leukemia (Mullighan, et al. 2007), as observed in case of a complex karyotype (Mullighan, et al. 2007), or with additional fusions as in Ph-like ALL (Auer, et al. 2014). In mouse models monoallelic deletion leading to PAX5 haploinsufficiency is responsible for susceptibility of B cell oncogenic transformation. Indeed, mice have normal B cell development, when they are characterized by heterozygous PAX5 loss, but they spontaneously develop B cell leukemia when they acquire other oncogenic events (Heltemes-Harris, et al. 2011). Therefore, PAX5 deletions tends to disrupt only one allele, representing cooperating events in B-ALL (Jia and Gu, et al. 2022).

The second most common PAX5 variants observed in B-ALL are **point mutations** (7-10%) (Mullighan, et al. 2008), whose majority are missense which impair DNA binding as they are located in the DNA-

binding domain (Gu, et al. 2019). Both NTD and CTD subdomains of the paired domain of PAX5 contribute to DNA binding, with NTD having greater affinity between the two, therefore being more enriched in mutations (Gu, et al. 2019). The most frequent mutation of the DNA binding domain of PAX5 is the PAX5 P80R (Mullighan, et al. 2009), whose affected B-ALL patients are classified as a novel subtype, with a peculiar GEP with co-occurring biallelic alterations of PAX5, homozygous deletion of CDKN2A/B, and activating mutations of RAS signaling (Gu, et al. 2019). PAX5 P80R decreases the regulatory activity of PAX5 deregulating B cell lineage genes, blocking blasts in the pre-pro-B stage (Gu, et al. 2019). The prognosis of PAX5 P80R patients is significantly better than PAX5alterated patients, which includes rearrangements and amplifications among the others (Gu, et al. 2019).

With an incidence of 0.5-1.4%, PAX5 intragenic amplifications (**PAX5-iAmp**) have been found in B-ALL (Schwab, et al. 2017). B-ALL cases with PAX5-iAmp cluster into the PAX5alt subtype from transcriptome analysis (Gu, et al., 2019), and matched diagnosis and relapse samples maintain PAX5-iAmp, indicating a role of driver lesion for leukemia development in B-ALL (Schwab 2017). PAX5 amplifications are usually in exons 2-5, site of the DNA-binding and octapeptide domains of PAX5 (Schwab, et al. 2017; Gu, et al. 2019). As PAX5 amplifications involve the DNA-binding domain of the gene, there may be an altered binding to the target genes due to increased number of binding domains in PAX5, with consequent alterations in B cell differentiation and transformation (Jia and Gu, 2022).

PAX5 rearrangements due to **translocations** occur in about 4% of pediatric B-ALL patients (Pui, et al. 2019). PAX5 maintains its DNA binding domain still localizing in the nucleus at the N-term of the fusion. PAX5 is a very promiscuous gene, having several C-term partner genes, that can encode for transcription factors (e.g. ETV6), structural proteins (e.g. POM121), kinases (e.g. JAK2), among the others. PAX5 fusions are subjected to multiple DNA binding and gene regulations (Fortschegger, et al. 2014). PAX5 fusions represent 30% of PAX5alt B-ALL, not including PAX5::JAK2(Gu, et al. 2019). It is supposed that the fusion protein binds the DNA with a dominant-negative effect, altering wild type PAX5 activity (Kawamata, et al. 2012). Two most recurrent fusion genes in B-ALL are PAX5::ETV6 and PAX5::JAK2. PAX5::ETV6 maintains the paired box and helix-loop-helix domain of PAX5 fused with the DNA binding domain of ETV6 (Gu, et al. 2019). PAX5::ETV6 has an opposite dominant effect on PAX5 target genes (Fazio, et al. 2013). Dominant negative fusions of PAX5 are thought to antagonize PAX5wt function, as reported in mouse models in which PAX5 fusions compete with PAX5wt protein levels (Cazzaniga, et al. 2015; Kuwamata, et al. 2012) and its target gene levels, such as by the downregulation of CD19 (Fazio, et al. 2008), among the other genes (Fazio, et al. 2013). PAX5::JAK2 has its peculiar gene expression profile that shifts this fusion from PAX5alt patients into the Ph-like subgroup of B-ALL (Gu, et al. 2019), as it maintains the kinase domain of JAK2 (Nebral, et al. 2009). PAX5::JAK2 is the only JAK2 fusion protein that localizes in the nucleus of the cell, deregulating PAX5 targets and activating JAK/STAT signaling. (Schinnerl, et al. 2015). Considering the setting of a knock-in mouse

model, B-ALL rapidly developed by only PAX5::JAK2 without other cooperating mutations, implicating PAX5::JAK2 key role as dual hits to drive leukemogenesis, represented by PAX5 haploinsufficiency and constitutively active kinase activity (Jurado, et al. 2022).

3.7 PAX5 targeting in B-ALL

No FDA-approved drugs are available for PAX5 alterations. Several approaches, depending on the specific alterations of PAX5 and on the mechanisms of action underlying the PAX5alt deregulation in B cells, could be used to develop the ideal targeting strategy. GEPs could drive the search for specific biomarkers that could be used to develop targeted therapies, depending on the type of PAX5 alteration considered (Gu, et al. 2022). Considering PAX5 metabolic gatekeeper function, drugs acting on deregulated metabolic effectors due to PAX5 deficiency, with increased glycolysis and ATP production, could deprive the leukemic cells of their essential fuel (Chan, et al. 2017). Indeed, agonists against CNR2 and TXNIP, two central effectors of energy supply restrictions in B cells, showed synergistic effect in combination with glucocorticoids bringing ATP levels to normal levels in B cells (Chan, et al. 2017). Moreover, in B-ALL patients carrying PAX5 deletions energy nonpermissive state can be reintroduced with restorations of PAX5 (Chan, et al. 2017). Targeting PAX5 downstream deregulated pathways could overcome the deregulated networks of signaling in B leukemic cells. Treatment with kinase inhibitors resulted in increased apoptosis of leukemic cells, acting on LCK in *in-vitro*, *ex-vivo* and *in-vivo* models of B-ALL (Cazzaniga, et al. 2015; Fazio, et al. 2022). Moreover, the reactivation through drugs of divergent silenced pathways by PAX5 alterations could inhibit leukemia transformation (Chan, et al. 2020).

Long but also brief restoration of PAX5 in B-ALL cells and mouse models disables leukemia initiating power, enabling differentiation and maturation of B cells through disease remissive state (Hart, et al. 2018). Pharmacological inhibition of IL-6 inhibits leukemic cells as it blocks PAX5 heterozygosis-enhanced IL-6 expression that was observed to sustain proliferation of leukemic cells (Isidro-Hernandez, et al. 2020).

4. Pediatric ALL treatment to get a personalized medicine

The treatment of acute lymphoid leukemias uses therapeutic combinations and treatment schemes among the most specialized in oncology. Since the 60s, the largest part of drugs applied in nowadays treatment were available, such as methotrexate, vincristine and asparaginase as first line treatment which increased the percentage and number of complete remission (RC). Later cyclophosphamide and anthracycline, used for consolidation of 6-mercaptopurine and methotrexate, have been applied for the central nervous system intrathecal prophylaxis making ALL treatment more effective and specific (CALLCG, 2009). Fundamental is the continuous effort of clinical research to get better doses and ways of administration, going to a personalized medicine depending on the subtype of leukemia considered with high specificity associated with the lowest toxicity achievable. Indeed, the identification of specified categories of patients based on immunophenotypic and/or cytogenic characteristics have required specific, differentiated and more intensive therapeutic approaches, in some cases being able to get to a target therapy, as for imatinib for BCR::ABL1(Biondi, et al. 2018) and ABL-class targeted

therapies (den Boer, et al. 2020). To note, target therapies of PAX5 and JAK2 alterations in B-ALL patients are among the future goals to reach, as highlighted by the multiple *ex-vivo* and *in-vivo* studies developed in recent years. (Jia and Gu, 2022; Tran and Tasian, 2021).

Nowadays, for B-ALL in adults and children, the conventional common treatment is divided into three therapeutic phases:

1. Induction, used to eradicate the biggest number of leukemic cells to reestablish normal hematopoiesis.

2. Consolidation/Intensification to eradicate eventual resistant leukemic clones, meaning to eradicate the quote of minimal residual disease (MRD) after the induction.

3. Maintenance with an antineoplastic therapy at low doses for 2-3 years, to prevent eventual refractory disease.

To note, CNS prophylaxis is included to avoid leukemia involvement in the meninges and cerebral parenchyma, known to be a potential secondary site for leukemia as not all the chemotherapy drugs cross at blood-barrier (Pui, et al. 2008).

The application of international intensive multicentric protocols based on early response to the treatment as main prognostic stratification factor has increased the survival of children affected by ALL (Pui, et al. 2015). Indeed, the introduction of the evaluation of the early response to the therapy, beyond the biological characteristics from the diagnosis, has led on one side to the intensification of treatment in high-risk patients, both towards treatment failure risk and relapse, and on the other side to reduce doses and use of drugs potentially toxic for low-risk patients. The BFM group first created in the 80s a therapeutic protocol based on intensive induction with multiple drugs, late

consolidation and intensification, reaching an increase in the event free survival from 50% in 1981 to 70% in 1995 till 85% nowadays (Conter, et al. 2010). Reinduction, a long-time maintenance, intensification in high-risk patients and a better risk stratification based on molecular MRD, have led to this EFS improvement (Conter, et al. 2010). To note, combinatory strategies with drugs not particularly myelotoxic such as corticosteroids, vincristine, asparaginase, methotrexate and antimetabolites, in addition to the limitation of the intracranial radiotherapy to only some types of ALL, has helped to increase the EFS of B-ALL children (90% low risk, 77% intermediate risk, 50% high risk) (Conter, et al. 2010; Conter, et al. 2014). The aim is to increase the current outcome reducing the treatment related toxicity better refining the stratification of risk categories considering the early response to treatment and the novel biological characteristics of the disease (e.g., IKAROS plus). Fundamental is the urgent identification of alternative treatments to combine with standard chemotherapy to improve the prognosis of children identified as high risk. Remarkably, the AIEOP-BFM ALL 2017 protocol considers the prospective evaluation of the efficacy of some specific drugs, such as bortezomib, blinatumomab and kinase inhibitors, in high-risk children affected by B-ALL. Next generation sequencing is fundamental for the identification of molecular alterations, as mutations and rearrangements, in pediatric patients of B-ALL, in order to define the genetic background of the children and to increase the possibility to define novel therapeutic targets. To note, there is the need to find novel targets for the pediatric patients with bad prognosis carrying genetic alterations that are still not included in already defined categories with targeted treatment. As

already previously described, novel applications with preclinical and clinical studies are undergoing for the treatment of B-ALL patients carrying JAK2 and PAX5 alterations. Remarkably, JAK2 and PAX5 rearrangements still lack their specific drugs, urging to develop a personalized medicine for those high-risk categories, considering in particular the delicate group of pediatric B-ALL patients.

Promising results derive from the application of targeted inhibitors of apoptotic proteins to treat children and adults with relapsed/refractory ALL, currently evaluated in early phase clinic pediatric trials (Tran and Tasian, 2021). Indeed, Venetoclax, a selective inhibitor of BCL2, an anti-apoptotic protein, showed efficacy in combination with standard chemotherapy (Place, et al. 2020). Moreover, it had synergistic effect in combination with dasatinib or ponatinib in Ph+ ALL cell lines and PDX models (Leonard, et al. 2016) and showed potent anti-leukemic activity in combination with MCL-1 inhibitors Ph+ and Ph-like ALL PDXs (Moujalled, et al. 2020).

5. SCOPE OF THE THESIS

The aim of the project of the thesis is the development of a preclinical target strategy towards pediatric patients of B-ALL carrying JAK2 and/or PAX5 rearrangements, with the final aim to get to a personalized medicine in this subset of pediatric B-ALL, which still lacks their specific and effective drugs. Therefore, to define our cohorts, we profited of the screening continuously performed in our laboratory for all the Italian AIEOP centers of large cohort of Italian pediatric leukemic patients by next generation sequencing approach on RNA. Primary patients' cells have been expanded *in-vivo* in NSG mice, in order to obtain the blast cells to set up our *ex-vivo* and *in-vivo* experiments.

First, focusing on JAK2 rearrangements, we test the efficacy of a novel kinase inhibitor of type II, CHZ868, to evaluate whether it could have higher specificity than ruxolitinib on JAK2r, both in *ex-vivo* co-culture of blasts cell on a layer of human bone marrow stroma (HBMS), to reproduce the bone marrow niche, and *in-vivo* in mice xenotransplant with primary cells carrying JAK2 fusions. We aim also to verify if it could have synergistic or additive effects in combination with standard chemotherapy drugs and tyrosine kinase inhibitors.

Secondly, in the PAX5r setting, we aim to define and characterize the peculiar molecular profile of pediatric patients with PAX5 fusions integrating NGS findings with gene expression. We investigate both the prognostic evidence and the altered signaling pathways sustaining leukemia evolvement downstream PAX5 fusion genes. Further, we develop the most specific preclinical strategy of

targeting with novel drugs both *ex-vivo* and *in-vivo*, as applied for the JAK2r patients, aiming to define a potential therapy for those patients. We moreover analyze infant germline for KMT2A/MLL rearrangements to find by NSG approach an eventual enrichment of fusion genes, as the one involving PAX5, in those fragile patients.

Further, we aim to better understand the basis of leukemia development and maintenance in PAX5 and JAK2 rearranged pediatric cases. To achieve this purpose, we want to take advantage of high through put technologies in protein studies, such as the CyTOF, a single cells mass spectrometry approach that allows to simultaneously detect a wide pool of proteins using antibodies labeled with heavy metal ions. We develop and apply a panel to classify our patients derived xenograft (PDXs) samples into the different subpopulations of B cell development, from HSC to mature B cells, observing eventual changes of expression of specific markers (surface and intracellular) after stimulation and drug treatment. Moreover, we aim to define by CyTOF the basal metabolic state in presence of PAX5 and JAK2 fusions in leukemia.

Finally, we aim to improve the spectra of FDA-approved drugs that may be considered for future developments for the treatment of JAK2 and PAX5 rearrangements through a wide high throughput drug screening.

Our results aim to provide a better understanding of JAK2 and PAX5 rearrangements targeting in the setting of pediatric B-ALL following an integrative approach from primary material of patients to blasts-HBMS co-culture, to mice xenografts, hoping the define a personalized medicine to target JAK2 and PAX5 rearrangements.

REFERENCES

Alimam S, Harrison C. Experience with ruxolitinib in the treatment of polycythaemia vera. Ther Adv Hematol. 2017 Apr;8(4):139-151. doi: 10.1177/2040620717693972. Epub 2017 Apr 1. Erratum in: Ther Adv Hematol. 2017 Sep;8(9):273.

Andraos R, Qian Z, Bonenfant D, et al. Modulation of activation-loop phosphorylation by JAK inhibitors is binding mode dependent. Cancer Discov. 2012 Jun;2(6):512-523. doi: 10.1158/2159-8290.CD-11-0324. Epub 2012 May 3.

Aricò M, Schrappe M, Hunger SP, et al. Clinical outcome of children with newly diagnosed Philadelphia chromosome-positive acute lymphoblastic leukemia treated between 1995 and 2005. *J Clin Oncol*. 2010;28(31):4755-4761. doi:10.1200/JCO.2010.30.1325

Arseneau JR, Laflamme M, Lewis SM, et al. Multiple isoforms of PAX5 are expressed in both lymphomas and normal B-cells. Br J Haematol. 2009 Nov;147(3):328-38. doi: 10.1111/j.1365-2141.2009.07859.x.

Auer F, Rüschendorf F, Gombert M, et al. Inherited susceptibility to pre B-ALL caused by germline transmission of PAX5 c.547G>A. Leukemia. 2014 May;28(5):1136-8. doi: 10.1038/leu.2013.363.

Baxter EJ, Scott LM, Campbell PJ, et al. Acquired mutation of the tyrosine kinase JAK2 in human myeloproliferative disorders. Lancet. 2005 Mar 19-25;365(9464):1054-61. doi: 10.1016/S0140-6736(05)71142-9.

Bemark M. Translating transitions - how to decipher peripheral human B cell development. J Biomed Res. 2015 Jul;29(4):264-84. doi: 10.7555/JBR.29.20150035.

Bernt KM, Hunger SP. Current concepts in pediatric Philadelphia chromosome-positive acute lymphoblastic leukemia. Front Oncol. 2014 Mar 25;4:54. doi: 10.3389/fonc.2014.00054.

Bhojwani D, Yang JJ, Pui CH. Biology of childhood acute lymphoblastic leukemia. Pediatr Clin North Am. 2015 Feb;62(1):47-60. doi: 10.1016/j.pcl.2014.09.004.

Biondi A, Gandemer V, De Lorenzo P, et al. Imatinib treatment of paediatric Philadelphia chromosome-positive acute lymphoblastic leukaemia (EsPhALL2010): a prospective, intergroup, open-label, single-arm clinical trial. Lancet Haematol. 2018 Dec;5(12):e641-e652. doi: 10.1016/S2352-3026(18)30173-X.

Biondi A, Schrappe M, De Lorenzo P, et al. Imatinib after induction for treatment of children and adolescents with Philadelphia-chromosome-positive acute lymphoblastic leukaemia (EsPhALL): a randomised, open-label, intergroup study. *Lancet Oncol*. 2012;13(9):936-945. doi:10.1016/S1470-2045(12)70377-7

Boer, J.M., Steeghs, E.M., Marchante, et al. (2017) Tyrosine kinase fusion genes in pediatric BCR-ABL1-like acute lymphoblastic leukemia. *Oncotarget,* **8,** 4618-4628.

Bohlander SK. ETV6: a versatile player in leukemogenesis. Semin Cancer Biol. 2005 Jun;15(3):162-74. doi: 10.1016/j.semcancer.2005.01.008.

Bose P, Verstovsek S. JAK Inhibition for the Treatment of Myelofibrosis: Limitations and Future Perspectives. Hemasphere. 2020 Jul 21;4(4):e424. doi: 10.1097/HS9.0000000000000424.

Bourquin JP, Izraeli S. Where can biology of childhood ALL be attacked by new compounds? Cancer Treat Rev. 2010 Jun;36(4):298-306. doi: 10.1016/j.ctrv.2010.02.005.

Bousoik E, Montazeri Aliabadi H. "Do We Know Jack" About JAK? A Closer Look at JAK/STAT Signaling Pathway. Front Oncol. 2018 Jul 31;8:287. doi: 10.3389/fonc.2018.00287.

Busslinger M. Transcriptional control of early B cell development. Annu Rev Immunol. 2004;22:55-79. doi: 10.1146/annurev.immunol.22.012703.104807.

Cazzaniga V, Bugarin C, Bardini M, Giordan M, te Kronnie G, Basso G, Biondi A, Fazio G, Cazzaniga G. LCK over-expression drives STAT5 oncogenic signaling in

PAX5 translocated BCP-ALL patients. Oncotarget. 2015 Jan 30;6(3):1569-81. doi: 10.18632/oncotarget.2807.

Chan LN, Chen Z, Braas D, et al. Metabolic gatekeeper function of B-lymphoid transcription factors. Nature. 2017 Feb 23;542(7642):479-483. doi: 10.1038/nature21076. Epub 2017 Feb 13. Erratum in: Nature. 2018 Jun;558(7711):E5.

Chan LN, Murakami MA, Robinson ME, et al. Signalling input from divergent pathways subverts B cell transformation. Nature. 2020 Jul;583(7818):845-851. doi: 10.1038/s41586-020-2513-4.

Childhood Acute Lymphoblastic Leukaemia Collaborative Group (CALLCG). Beneficial and harmful effects of anthracyclines in the treatment of childhood acute lymphoblastic leukaemia: a systematic review and meta-analysis. British Journal of Haematology 2009;145: 376-388.

Chiu CW, Dalton M, Ishiai M, et al. BLNK: molecular scaffolding through 'cis'-mediated organization of signaling proteins. EMBO J. 2002 Dec 2;21(23):6461-72. doi: 10.1093/emboj/cdf658.

Clark MR, Mandal M, Ochiai K, Singh H. Orchestrating B cell lymphopoiesis through interplay of IL-7 receptor and pre-B cell receptor signalling. Nat Rev Immunol. 2014 Feb;14(2):69-80. doi: 10.1038/nri3570. Epub 2013 Dec 31.

Cobaleda C, Busslinger M. Developmental plasticity of lymphocytes. Curr Opin Immunol. 2008 Apr;20(2):139-48. doi: 10.1016/j.coi.2008.03.017. Epub 2008 May 9.

Cobaleda C, Schebesta A, Delogu A, Busslinger M. Pax5: the guardian of B cell identity and function. Nat Immunol. 2007 May;8(5):463-70. doi: 10.1038/ni1454.

Conter V, Aricò M, Basso G, et al. Long-term results of the Italian Association of Pediatric Hematology and Oncology (AIEOP) Studies 82, 87, 88, 91 and 95 for

childhood acute lymphoblastic leukemia. Leukemia. 2010 Feb;24(2):255-64. doi: 10.1038/leu.2009.250.

Conter V, Bartram CR, Valsecchi MG, et al. Molecular response to treatment redefines all prognostic factors in children and adolescents with B-cell precursor acute lymphoblastic leukemia: results in 3184 patients of the AIEOP-BFM ALL 2000 study. Blood. 2010 Apr 22;115(16):3206-14. doi: 10.1182/blood-2009-10-248146.

Conter V, Valsecchi MG, Parasole R, et al. Childhood high-risk acute lymphoblastic leukemia in first remission: results after chemotherapy or transplant from the AIEOP ALL 2000 study. Blood. 2014 Mar 6;123(10):1470-8. doi: 10.1182/blood-2013-10-532598.

Deane JA, Fruman DA. Phosphoinositide 3-kinase: diverse roles in immune cell activation. Annu Rev Immunol. 2004;22:563-98. doi: 10.1146/annurev.immunol.22.012703.104721.

Delogu A, Schebesta A, Sun Q, et al. Gene repression by Pax5 in B cells is essential for blood cell homeostasis and is reversed in plasma cells. Immunity. 2006 Mar;24(3):269-81. doi: 10.1016/j.immuni.2006.01.012.

den Boer ML, Cario G, Moorman AV, et al. Outcomes of paediatric patients with B-cell acute lymphocytic leukaemia with ABL-class fusion in the pre-tyrosine-kinase inhibitor era: a multicentre, retrospective, cohort study. Lancet Haematol. 2021 Jan;8(1):e55-e66. doi: 10.1016/S2352-3026(20)30353-7. Epub 2020 Dec 22.

Den Boer ML, van Slegtenhorst M, De Menezes RX, et al. A subtype of childhood acute lymphoblastic leukaemia with poor treatment outcome: a genome-wide classification study. Lancet Oncol. 2009 Feb;10(2):125-34. doi: 10.1016/S1470-2045(08)70339-5. Epub 2009 Jan 8.

Downes CE, McClure BJ, McDougal DP, et al. *JAK2* Alterations in Acute Lymphoblastic Leukemia: Molecular Insights for Superior Precision Medicine

Strategies. Front Cell Dev Biol. 2022 Jul 12;10:942053. doi: 10.3389/fcell.2022.942053.

Downes CEJ, McClure BJ, Bruning JB, et al. Acquired JAK2 mutations confer resistance to JAK inhibitors in cell models of acute lymphoblastic leukemia. NPJ Precis Oncol. 2021 Aug 10;5(1):75. doi: 10.1038/s41698-021-00215-x.

Ehrentraut S, Nagel S, Scherr ME, et al. t(8;9)(p22;p24)/PCM1-JAK2 activates SOCS2 and SOCS3 via STAT5. PLoS One. 2013;8(1):e53767. doi: 10.1371/journal.pone.0053767. Epub 2013 Jan 23.

Enshaei A, Vora A, Harrison CJ, Moppett J, Moorman AV. Defining low-risk high hyperdiploidy in patients with paediatric acute lymphoblastic leukaemia: a retrospective analysis of data from the UKALL97/99 and UKALL2003 clinical trials [published correction appears in Lancet Haematol. 2021 Dec;8(12):e874]. *Lancet Haematol*. 2021;8(11):e828-e839. doi:10.1016/S2352-3026(21)00304-5

Fazio G, Bresolin S, Silvestri D, et al. PAX5 fusion genes are frequent in poor risk childhood acute lymphoblastic leukaemia and can be targeted with BIBF1120. EBioMedicine. 2022 Sep;83:104224. doi: 10.1016/j.ebiom.2022.104224. Epub 2022 Aug 16.

Fazio G, Cazzaniga V, Palmi C, et al. PAX5/ETV6 alters the gene expression profile of precursor B cells with opposite dominant effect on endogenous PAX5. Leukemia. 2013 Apr;27(4):992-5. doi: 10.1038/leu.2012.281. Epub 2012 Oct 1. PMID: 23090680.

Fazio G, Palmi C, Rolink A, et al. PAX5/TEL acts as a transcriptional repressor causing down-modulation of CD19, enhances migration to CXCL12, and confers survival advantage in pre-BI cells. Cancer Res. 2008 Jan 1;68(1):181-9. doi: 10.1158/0008-5472.CAN-07-2778.

Fazio, G., Biondi, A. & Cazzaniga, G. The role of PAX5 in ALL. 1st edn, (InTech Open Access Publisher, 2011).

Fortschegger K, Anderl S, Denk D, Strehl S. Functional heterogeneity of PAX5 chimeras reveals insight for leukemia development. Mol Cancer Res. 2014 Apr;12(4):595-606. doi: 10.1158/1541-7786.MCR-13-0337.

Fuxa M, Skok JA. Transcriptional regulation in early B cell development. Curr Opin Immunol. 2007 Apr;19(2):129-36. doi: 10.1016/j.coi.2007.02.002.

Ghazavi F, Lammens T, Van Roy N, et al. Molecular basis and clinical significance of genetic aberrations in B-cell precursor acute lymphoblastic leukemia. Exp Hematol. 2015 Aug;43(8):640-53. doi: 10.1016/j.exphem.2015.05.015.

Ghia P, ten Boekel E, Rolink AG, Melchers F. B-cell development: a comparison between mouse and man. Immunol Today. 1998 Oct;19(10):480-5. doi: 10.1016/s0167-5699(98)01330-9.

Golub TR, Barker GF, Lovett M, Gilliland DG. Fusion of PDGF receptor beta to a novel ets-like gene, tel, in chronic myelomonocytic leukemia with t(5;12) chromosomal translocation. Cell. 1994 Apr 22;77(2):307-16. doi: 10.1016/0092-8674(94)90322-0.

Greaves MF, Wiemels J. Origins of chromosome translocations in childhood leukaemia. Nat Rev Cancer. 2003 Sep;3(9):639-49. doi: 10.1038/nrc1164.

Gu Z, Churchman ML, Roberts KG, et al. PAX5-driven subtypes of B-progenitor acute lymphoblastic leukemia. Nat Genet. 2019 Feb;51(2):296-307. doi: 10.1038/s41588-018-0315-5.

Haas OA, Borkhardt A. Hyperdiploidy: the longest known, most prevalent, and most enigmatic form of acute lymphoblastic leukemia in children. Leukemia. 2022 Dec;36(12):2769-2783. doi: 10.1038/s41375-022-01720-z.

Hagman J, Lukin K. Early B-cell factor 'pioneers' the way for B-cell development. Trends Immunol. 2005 Sep;26(9):455-61. doi: 10.1016/j.it.2005.07.001. Erratum in: Trends Immunol. 2005 Dec;26(12):625.

Hagman J, Lukin K. Transcription factors drive B cell development. Curr Opin Immunol. 2006 Apr;18(2):127-34. doi: 10.1016/j.coi.2006.01.007. Epub 2006 Feb 7.

Harrison CJ. Acute lymphoblastic leukaemia. Best Pract Res Clin Haematol. 2001 Sep;14(3):593-607. doi: 10.1053/beha.2001.0156.

Harrison CN, Mead AJ, Panchal A, et al. Ruxolitinib vs best available therapy for ET intolerant or resistant to hydroxycarbamide. Blood. 2017 Oct 26;130(17):1889-1897. doi: 10.1182/blood-2017-05-785790.

Hart MR, Anderson DJ, Porter CC, et al. Activating PAX gene family paralogs to complement PAX5 leukemia driver mutations. PLoS Genet. 2018 Sep 14;14(9):e1007642. doi: 10.1371/journal.pgen.1007642.

Heim MH. The Jak-STAT pathway: cytokine signalling from the receptor to the nucleus. J Recept Signal Transduct Res. 1999 Jan-Jul;19(1-4):75-120. doi: 10.3109/10799899909036638.

Heltemes-Harris LM, Willette MJ, Ramsey LB, et al. Ebf1 or Pax5 haploinsufficiency synergizes with STAT5 activation to initiate acute lymphoblastic leukemia. J Exp Med. 2011 Jun 6;208(6):1135-49. doi: 10.1084/jem.20101947. Epub 2011 May 23.

Herold T, Gökbuget N. Philadelphia-Like Acute Lymphoblastic Leukemia in Adults. Curr Oncol Rep. 2017 May;19(5):31. doi: 10.1007/s11912-017-0589-2.

Hertzberg L, Vendramini E, Ganmore I, et al. Down syndrome acute lymphoblastic leukemia, a highly heterogeneous disease in which aberrant expression of CRLF2 is associated with mutated JAK2: a report from the International BFM Study Group. Blood. 2010 Feb 4;115(5):1006-17. doi: 10.1182/blood-2009-08-235408. Epub 2009 Nov 24.

Herzog S, Reth M, Jumaa H. Regulation of B-cell proliferation and differentiation by pre-B-cell receptor signalling. Nat Rev Immunol. 2009 Mar;9(3):195-205. doi: 10.1038/nri2491.

Holmes ML, Carotta S, Corcoran LM, Nutt SL. Repression of Flt3 by Pax5 is crucial for B-cell lineage commitment. Genes Dev. 2006 Apr 15;20(8):933-8. doi: 10.1101/gad.1396206.

Iacobucci I, Li Y, Roberts KG, Dobson SM, et al. Truncating Erythropoietin Receptor Rearrangements in Acute Lymphoblastic Leukemia. Cancer Cell 2016;29(2):186–200.

Iacobucci I, Mullighan CG. Genetic Basis of Acute Lymphoblastic Leukemia. J Clin Oncol. 2017 Mar 20;35(9):975-983. doi: 10.1200/JCO.2016.70.7836. Epub 2017 Feb 13.

Iacobucci I, Roberts KG. Genetic Alterations and Therapeutic Targeting of Philadelphia-Like Acute Lymphoblastic Leukemia. Genes (Basel). 2021 May 1;12(5):687. doi: 10.3390/genes12050687.

Inaba H, Greaves M, Mullighan CG. Acute lymphoblastic leukaemia. Lancet. 2013 Jun 1;381(9881):1943-55. doi: 10.1016/S0140-6736(12)62187-4. Epub 2013 Mar 22.
Inaba H, Pui CH. Advances in the Diagnosis and Treatment of Pediatric Acute Lymphoblastic Leukemia. J Clin Med. 2021 Apr 29;10(9):1926. doi: 10.3390/jcm10091926.
Isidro-Hernández M, Mayado A, Casado-García A, et al. Inhibition of inflammatory signaling in Pax5 mutant cells mitigates B-cell leukemogenesis. Sci Rep. 2020 Nov 5;10(1):19189. doi: 10.1038/s41598-020-76206-y.

Jia Z, Gu Z. *PAX5* alterations in B-cell acute lymphoblastic leukemia. Front Oncol. 2022 Oct 25;12:1023606. doi: 10.3389/fonc.2022.1023606.

Jumaa H, Wollscheid B, Mitterer M, et al. Abnormal development and function of B lymphocytes in mice deficient for the signaling adaptor protein SLP-65. Immunity. 1999 Nov;11(5):547-54. doi: 10.1016/s1074-7613(00)80130-2.

Jurado S, Fedl AS, Jaritz M, et al. The PAX5-JAK2 translocation acts as dual-hit mutation that promotes aggressive B-cell leukemia via nuclear STAT5 activation. EMBO J. 2022 Apr 4;41(7):e108397. doi: 10.15252/embj.2021108397. Epub 2022 Feb 14.

Kawamata N, Pennella MA, Woo JL, Berk AJ, Koeffler HP. Dominant-negative mechanism of leukemogenic PAX5 fusions. Oncogene. 2012 Feb 23;31(8):966-77. doi: 10.1038/onc.2011.291. Epub 2011 Jul 18

Leonard JT, Rowley JS, Eide CA, et al. Targeting BCL-2 and ABL/LYN in Philadelphia chromosome-positive acute lymphoblastic leukemia. Sci Transl Med. 2016 Aug 31;8(354):354ra114. doi: 10.1126/scitranslmed.aaf5309

Leroy E, Constantinescu SN. Rethinking JAK2 inhibition: towards novel strategies of more specific and versatile Janus kinase inhibition. Leukemia. 2017 May;31(5):1023-1038. doi: 10.1038/leu.2017.43. Epub 2017 Jan 25. Erratum in: Leukemia. 2017 Dec;31(12):2853.

Levine RL, Pardanani A, Tefferi A, Gilliland DG. Role of JAK2 in the pathogenesis and therapy of myeloproliferative disorders. Nat Rev Cancer. 2007 Sep;7(9):673-83. doi: 10.1038/nrc2210.

Li B, Rampal RK, Xiao Z. Targeted therapies for myeloproliferative neoplasms. Biomark Res. 2019 Jul 16;7:15. doi: 10.1186/s40364-019-0166-y.
Malin S, McManus S, Cobaleda C, et al. Role of STAT5 in controlling cell survival and immunoglobulin gene recombination during pro-B cell development. Nat Immunol. 2010 Feb;11(2):171-9. doi: 10.1038/ni.1827. Epub 2009 Nov 29.

Matthias P, Rolink AG. Transcriptional networks in developing and mature B cells. Nat Rev Immunol. 2005 Jun;5(6):497-508. doi: 10.1038/nri1633. PMID: 15928681.

Maude SL, Tasian SK, Vincent T, et al. Targeting JAK1/2 and mTOR in murine xenograft models of Ph-like acute lymphoblastic leukemia. Blood. 2012 Oct 25;120(17):3510-8. doi: 10.1182/blood-2012-03-415448. Epub 2012 Sep 6

Medves S, Demoulin JB. Tyrosine kinase gene fusions in cancer: translating mechanisms into targeted therapies. J Cell Mol Med. 2012 Feb;16(2):237-48. doi: 10.1111/j.1582-4934.2011.01415.x.

Meyer SC, Keller MD, Chiu S, et al. CHZ868, a Type II JAK2 Inhibitor, Reverses Type I JAK Inhibitor Persistence and Demonstrates Efficacy in Myeloproliferative Neoplasms. Cancer Cell. 2015 Jul 13;28(1):15-28. doi: 10.1016/j.ccell.2015.06.006.

Moorman AV, Ensor HM, Richards SM, et al. Prognostic effect of chromosomal abnormalities in childhood B-cell precursor acute lymphoblastic leukaemia: results from the UK Medical Research Council ALL97/99 randomised trial. Lancet Oncol. 2010 May;11(5):429-38. doi: 10.1016/S1470-2045(10)70066-8.

Morrison AM, Nutt SL, Thévenin C, et al. Loss- and gain-of-function mutations reveal an important role of BSAP (Pax-5) at the start and end of B cell differentiation. Semin Immunol. 1998 Apr;10(2):133-42. doi: 10.1006/smim.1998.0115.

Moujalled DM, Hanna DT, Hediyeh-Zadeh S, et al. Cotargeting BCL-2 and MCL-1 in high-risk B-ALL. Blood Adv. 2020 Jun 23;4(12):2762-2767. doi: 10.1182/bloodadvances.2019001416.

Mullally A, Hood J, Harrison C, Mesa R. Fedratinib in myelofibrosis. Blood Adv. 2020;4(8):1792-1800. Blood Adv. 2020 Jul 28;4(14):3315. doi: 10.1182/bloodadvances.2020002897.

Mullally A. Underlying mechanisms of the JAK2V617F mutation in the pathogenesis of myeloproliferative neoplasms. Pathologe. 2016 Nov;37(Suppl 2):175-179. English. doi: 10.1007/s00292-016-0240-2.

Mullighan CG, Goorha S, Radtke I, et al. Genome-wide analysis of genetic alterations in acute lymphoblastic leukaemia. Nature. 2007 Apr 12;446(7137):758-64. doi: 10.1038/nature05690.

Mullighan CG, Phillips LA, Su X, et al. Genomic analysis of the clonal origins of relapsed acute lymphoblastic leukemia. Science. 2008 Nov 28;322(5906):1377-80. doi: 10.1126/science.1164266.

Mullighan CG. Genomic analysis of acute leukemia. Int J Lab Hematol. 2009 Aug;31(4):384-97. doi: 10.1111/j.1751-553X.2009.01167.x. Epub 2009 May 18.

Mullighan CG. Genomic characterization of childhood acute lymphoblastic leukemia. *Semin Hematol*. 2013;50(4):314-324. doi:10.1053/j.seminhematol.2013.10.001

Nebral K, Denk D, Attarbaschi A, et al. Incidence and diversity of PAX5 fusion genes in childhood acute lymphoblastic leukemia. Leukemia. 2009 Jan;23(1):134-43. doi: 10.1038/leu.2008.306. Epub 2008 Nov 20. PMID: 19020546.

Nguyen K, Devidas M, Cheng SC, La M, Raetz EA, et al. Children's Oncology Group. Factors influencing survival after relapse from acute lymphoblastic leukemia: a Children's Oncology Group study. Leukemia. 2008 Dec;22(12):2142-50. doi: 10.1038/leu.2008.251. Epub 2008 Sep 25

Nutt SL, Morrison AM, Dörfler P, et al. Identification of BSAP (Pax-5) target genes in early B-cell development by loss- and gain-of-function experiments. EMBO J. 1998 Apr 15;17(8):2319-33. doi: 10.1093/emboj/17.8.2319. PMID: 9545244; PMCID: PMC1170575.

Ochiai K, Maienschein-Cline M, Mandal M, et al. A self-reinforcing regulatory network triggered by limiting IL-7 activates pre-BCR signaling and differentiation. Nat Immunol. 2012 Jan 22;13(3):300-7. doi: 10.1038/ni.2210.

Palmi C, Vendramini E, Silvestri D, et al. Poor prognosis for P2RY8-CRLF2 fusion but not for CRLF2 over-expression in children with intermediate risk B-cell precursor acute lymphoblastic leukemia. Leukemia. 2012 Oct;26(10):2245-53. doi: 10.1038/leu.2012.101. Epub 2012 Apr 9.

Place AE, Karol SE, Forlenza CJ, et al. Pediatric Patients with Relapsed/Refractory Acute Lymphoblastic Leukemia Harboring Heterogeneous Genomic Profiles Respond to Venetoclax in Combination with Chemotherapy. Blood 2020:2793.

Pui CH, Nichols KE, Yang JJ. Somatic and germline genomics in paediatric acute lymphoblastic leukaemia. *Nat Rev Clin Oncol*. 2019;16(4):227-240. doi:10.1038/s41571-018-0136-6

Pui CH, Rebora P, Schrappe M, et al. Outcome of Children With Hypodiploid Acute Lymphoblastic Leukemia: A Retrospective Multinational Study. J Clin Oncol. 2019 Apr 1;37(10):770-779. doi: 10.1200/JCO.18.00822. Epub 2019 Jan 18.

Pui CH, Relling MV, Downing JR. Acute lymphoblastic leukemia. N Engl J Med. 2004 Apr 8;350(15):1535-48. doi:10.1056/NEJMra023001.
Pui CH, Roberts KG, Yang JJ, Mullighan CG. Philadelphia Chromosome-like Acute Lymphoblastic Leukemia. Clin Lymphoma Myeloma Leuk. 2017 Aug;17(8):464-470. doi: 10.1016/j.clml.2017.03.299.

Pui CH, Robison LL, Look AT. Acute lymphoblastic leukaemia. Lancet. 2008 Mar 22;371(9617):1030-43. doi: 10.1016/S0140-6736(08)60457-2. PMID: 18358930.

Pui CH, Yang JJ, Hunger SP, et al. Childhood Acute Lymphoblastic Leukemia: Progress Through Collaboration. J Clin Oncol. 2015 Sep 20;33(27):2938-48. doi: 10.1200/JCO.2014.59.1636. Epub 2015 Aug 24.

Quintás-Cardama A, Vaddi K, Liu P, et al. Preclinical characterization of the selective JAK1/2 inhibitor INCB018424: therapeutic implications for the treatment of myeloproliferative neoplasms. Blood. 2010 Apr 15;115(15):3109-17. doi: 10.1182/blood-2009-04-214957. Epub 2010 Feb 3.

Quintás-Cardama A, Verstovsek S. Molecular pathways: Jak/STAT pathway: mutations, inhibitors, and resistance. Clin Cancer Res. 2013 Apr 15;19(8):1933-40. doi: 10.1158/1078-0432.CCR-12-0284. Epub 2013 Feb 13.

Rickert RC. New insights into pre-BCR and BCR signalling with relevance to B cell malignancies. Nat Rev Immunol. 2013 Aug;13(8):578-91. doi: 10.1038/nri3487. Erratum in: Nat Rev Immunol. 2013 Sep;13(9):701.

Roberts KG, Li Y, Payne-Turner D, et al. Targetable kinase-activating lesions in Ph-like acute lymphoblastic leukemia. N Engl J Med. 2014 Sep 11;371(11):1005-15. doi: 10.1056/NEJMoa1403088.

Roberts KG, Morin RD, Zhang J, et al. Genetic alterations activating kinase and cytokine receptor signaling in high-risk acute lymphoblastic leukemia. Cancer Cell. 2012 Aug 14;22(2):153-66. doi: 10.1016/j.ccr.2012.06.005.

Roberts KG, Mullighan CG. Genomics in acute lymphoblastic leukaemia: insights and treatment implications. Nat Rev Clin Oncol. 2015 Jun;12(6):344-57. doi: 10.1038/nrclinonc.2015.38. Epub 2015 Mar 17.

Roberts KG. The biology of Philadelphia chromosome-like ALL. Best Pract Res Clin Haematol. 2017 Sep;30(3):212-221. doi: 10.1016/j.beha.2017.07.003. Epub 2017 Jul 6.

Rolink AG, Schaniel C, Bruno L, Melchers F. In vitro and in vivo plasticity of Pax5-deficient pre-B I cells. Immunol Lett. 2002 Jun 3;82(1-2):35-40. doi: 10.1016/s0165-2478(02)00016-0. PMID: 12008032.

Ross DM, Babon JJ, Tvorogov D, Thomas D. Persistence of myelofibrosis treated with ruxolitinib: biology and clinical implications. Haematologica. 2021 May 1;106(5):1244-1253. doi: 10.3324/haematol.2020.262691

Schebesta A, McManus S, Salvagiotto G, et al. Transcription factor Pax5 activates the chromatin of key genes involved in B cell signaling, adhesion, migration, and immune function. Immunity. 2007 Jul;27(1):49-63. doi: 10.1016/j.immuni.2007.05.019. Epub 2007 Jul 19. PMID: 17658281.

Schinnerl D, Fortschegger K, Kauer M, et al. The role of the Janus-faced transcription factor PAX5-JAK2 in acute lymphoblastic leukemia. Blood. 2015 Feb 19;125(8):1282-91. doi: 10.1182/blood-2014-04-570960. Epub 2014 Dec 16.

Schrappe M, Bleckmann K, Zimmermann M, et al. Reduced-Intensity Delayed Intensification in Standard-Risk Pediatric Acute Lymphoblastic Leukemia Defined by Undetectable Minimal Residual Disease: Results of an International Randomized Trial (AIEOP-BFM ALL 2000). J Clin Oncol. 2018 Jan 20;36(3):244-253. doi: 10.1200/JCO.2017.74.4946. Epub 2017 Nov 17.

Schrappe M, Hunger SP, Pui CH, et al. Outcomes after induction failure in childhood acute lymphoblastic leukemia. N Engl J Med. 2012 Apr 12;366(15):1371-81. doi: 10.1056/NEJMoa1110169. PMID: 22494120; PMCID: PMC3374496.

Schwab C, Nebral K, Chilton L, et al. Intragenic amplification of *PAX5*: a novel subgroup in B-cell precursor acute lymphoblastic leukemia? Blood Adv. 2017 Aug 14;1(19):1473-1477. doi: 10.1182/bloodadvances.2017006734. PMID: 29296789; PMCID: PMC5728462.

Shiraz P, Payne KJ, Muffly L. The Current Genomic and Molecular Landscape of Philadelphia-like Acute Lymphoblastic Leukemia. Int J Mol Sci. 2020 Mar 22;21(6):2193. doi: 10.3390/ijms21062193.

Silvennoinen O, Ungureanu D, Niranjan Y, et al. New insights into the structure and function of the pseudokinase domain in JAK2. Biochem Soc Trans. 2013 Aug;41(4):1002-7. doi: 10.1042/BST20130005.

Souabni A, Cobaleda C, Schebesta M, Busslinger M. Pax5 promotes B lymphopoiesis and blocks T cell development by repressing Notch1. Immunity. 2002 Dec;17(6):781-93. doi: 10.1016/s1074-7613(02)00472-7.

Springuel L, Hornakova T, Losdyck E, et al. Cooperating JAK1 and JAK3 mutants increase resistance to JAK inhibitors. Blood. 2014 Dec 18;124(26):3924-31. doi: 10.1182/blood-2014-05-576652. Epub 2014 Oct 28.

Steeghs EMP, Jerchel IS, de Goffau-Nobel W, et al. *JAK2* aberrations in childhood B-cell precursor acute lymphoblastic leukemia. Oncotarget. 2017 Sep 16;8(52):89923-89938. doi: 10.18632/oncotarget.21027.

Tasian SK, Hurtz C, Wertheim GB, et al. High incidence of Philadelphia chromosome-like acute lymphoblastic leukemia in older adults with B-ALL. Leukemia. 2017 Apr;31(4):981-984. doi: 10.1038/leu.2016.375. Epub 2016 Dec 9.

Tasian SK, Loh ML, Hunger SP. Childhood acute lymphoblastic leukemia: Integrating genomics into therapy. Cancer. 2015 Oct 15;121(20):3577-90. doi: 10.1002/cncr.29573. Epub 2015 Jul 20.

Tasian SK, Loh ML. Understanding the biology of CRLF2-overexpressing acute lymphoblastic leukemia. Crit Rev Oncog. 2011;16(1-2):13-24. doi: 10.1615/critrevoncog.v16.i1-2.30.

Tran TH, Tasian SK. Has Ph-like ALL Superseded Ph+ ALL as the Least Favorable Subtype? Best Pract Res Clin Haematol. 2021 Dec;34(4):101331. doi: 10.1016/j.beha.2021.101331. Epub 2021 Oct 23.

Tvorogov D, Thomas D, Liau NPD, et al. Accumulation of JAK activation loop phosphorylation is linked to type I JAK inhibitor withdrawal syndrome in myelofibrosis. Sci Adv. 2018 Nov 28;4(11):eaat3834. doi: 10.1126/sciadv.aat3834.

Vainchenker W, Constantinescu SN. JAK/STAT signaling in hematological malignancies. Oncogene. 2013 May 23;32(21):2601-13. doi: 10.1038/onc.2012.347. Epub 2012 Aug 6. PMID: 22869151.

Wu SC, Li LS, Kopp N, et al. Activity of the Type II JAK2 Inhibitor CHZ868 in B Cell Acute Lymphoblastic Leukemia. Cancer Cell. 2015 Jul 13;28(1):29-41. doi: 10.1016/j.ccell.2015.06.005.

Zhang Q, Shi C, Han L, et al. Inhibition of mTORC1/C2 signaling improves anti-leukemia efficacy of JAK/STAT blockade in *CRLF2* rearranged and/or *JAK* driven Philadelphia chromosome-like acute B-cell lymphoblastic leukemia. Oncotarget. 2018 Jan 17;9(8):8027-8041. doi: 10.18632/oncotarget.24261.

Zwollo P, Arrieta H, Ede K, et al. The Pax-5 gene is alternatively spliced during B-cell development. J Biol Chem. 1997 Apr 11;272(15):10160-8. doi: 10.1074/jbc.272.15.10160.

Chapter 2

Preclinical study of the efficacy of the novel kinase inhibitor CHZ868 for the treatment of the pediatric acute lymphoblastic leukemia with JAK2 rearrangements

Preclinical study of the efficacy of the novel kinase inhibitor CHZ868 for the treatment of the pediatric acute lymphoblastic leukemia with JAK2 rearrangements

Manuscript in preparation

Running Title

CHZ868 targets *JAK2* rearrangements in pediatric Philadelphia-like BCP-ALL

Authors

Manuel Quadri[1], Claudia Saitta[1], Sonia Palamini[1], Chiara Palmi[1], Jia-Wey Tu[2], Titus Watrin[2], Sanil Bhatia[2], Arndt Borkhardt[2], Andrea Biondi[1], Giovanni Cazzaniga[1-3], Grazia Fazio[1].

[1]Tettamanti Research Center, Dept. Pediatrics, University of Milano-Bicocca, Fondazione MBBM/San Gerardo Hospital, Monza, Italy.
[2]Department of Pediatric Oncology, Hematology and Clinical Immunology, Medical Faculty, Heinrich Heine University Düsseldorf, Düsseldorf, Germany
[3]Medical Genetics, School of Medicine and Surgery, University of Milano-Bicocca, Monza, Italy;

ABSTRACT

Background: Risk-based treatment is curative for 85% of children with B-cell precursor acute lymphoblastic leukemia (BCP-ALL), however relapse remains a leading cause of mortality, urging the need of novel

molecular targeted therapies. JAK2, a non-receptor tyrosine kinase, is rearranged in 5% of the 'Philadelphia-like' cases. While *JAK2* mutations have been widely studied, *JAK2* fusion genes are still poorly characterized.

Aim: This study aims to develop a target strategy in preclinical models of JAK2 fusion genes in BCP-ALL pediatric patients, using the novel inhibitor CHZ868.

Methods: RNA Next Generation Sequencing was applied to find JAK2 fusions in a cohort of high risk BCP-ALL pediatric patients. *In-vivo* expansion of patients' cells has been carried out in NSG mice. CHZ868 ex-vivo pharmacological treatment, versus ruxolitinib and standard chemotherapy, have been evaluated. Moreover, a wide throughput ex-vivo screening of 174 FDA-approved drugs was performed. After *ex-vivo* and *in-vivo* treatments with single selected drugs, phosphoflow and apoptosis assays were done.

Results. We identified 13 pediatric cases carrying a JAK2 fusion with different partners, where PAX5 gene was the only recurrent. We expanded cells from 4 cases in mice, carrying PAX5::JAK2, ATF7IP::JAK2 and ZEB2::JAK2, respectively. We demonstrated that the basal activation of pY1007-1008-JAK2 and its downstream effectors, pS727-STAT3 and pY694-STAT5, can targeted by CHZ868, a new class-II tyrosine kinase inhibitor (TKI). We appreciated a mean inhibition of 33-71% of pY1007-1008 after 30 minutes, till -40-50% after 48h, with consequent decrease of pS727-STAT3, pY694-STAT5 and PI3K-AKT pathway effectors. After 48h monotherapy treatment by

CHZ868, we also detected decreased cell viability (20-75% at IC50), which increased in the combination with dexamethasone.

In PAX5::JAK2, we also performed treatments with BIBF1120/Nintedanib, LCK inhibitor (activated downstream to PAX5 fusions) which synergizes with CHZ868 (-45%, at IC50). Moreover, ruxolitinib caused autophagy, as confirmed by higher levels of LC3-II versus untreated cells (+45%, $p<0.01$) and increased active caspase 3 in ruxolitinib and chloroquine (autophagy inhibitor) combination (+20% $p<0.01$). Instead, CHZ868 alone or with chloroquine did not induce autophagy.

Finally, we demonstrated the *in-vivo* efficacy of CHZ868 in PAX5::JAK2, ATF7IP::JAK2 and ZEB2::JAK2 patient-derived-xenografts, with a significant reduction of leukemic CD10+/CD19+ cells in hematopoietic organs after two weeks of 30mg/Kg daily treatment of CHZ868.

We moreover decided to apply a high-throughput *ex-vivo* screening of a library of 174 FDA-approved drugs in clinical trials, on 4 PDXs samples carrying JAK2 fusions (PAX5::JAK2, ATF7IP::JAK2, ZEB2::JAK2 and GIT2::JAK2), to check if other inhibitors may be available for JAK2 targeting. While we confirmed that ruxolitinib was not effective on JAK2 cohort at the tested dosages (8nM-25uM), this screening led us to identify specific and non-toxic drugs for rearranged JAK2 cohort, such as AT9283 ($p<0.05$) (pan-Aurora inhibitor) and Birinapant (Smac mimetic) ($p<0.05$), among the others.

Summary/Conclusion: CHZ868 is a promising drug for the treatment of JAK2 fusions. Further studies will focus on the preclinical

combination of CHZ868 with the recently screened drugs found to be specifically effective on JAK2 fusions.

INTRODUCTION

Acute lymphoblastic leukemia (ALL) is the most common pediatric cancer and represents 85% of all the pediatric leukemias (Inaba, et al. 2013; Harrison, et al. 2001; Inaba, et al. 2021). Nowadays the improvement of multidrug chemotherapy protocols and the novel therapies considering prognostic factors led to a more favorable prognosis and to a complete remission in 85% of cases, while the 20% of patients still relapse with only the 20-45% of cure rate (Nguyen, et al. 2008; Bourquin and Izraeli, 2010; Conter, et al 2010).

Recently, a new high risk subgroup denominated Philadelphia-like (Ph-like) has been defined, (Den Boer, et al. 2009; Mullighan, et al. 2009), as having a genetic expression pattern similar to the one of the Philadelphia positive ALL, despite not having the characteristic chromosomal fusion BCR-ABL1. However, the Ph-like or BCR-ABL1-like subgroup is connoted by alterations of *ABL1/ABL2*, *PDGFRB/A*, *MCSF1R*, *CRLF2*, *PAX5*, *EPOR* and *JAK2* genes (Roberts, et al. 2017; Boer, et al. 2017; Shiraz, et al. 2020; Fazio, et al. 2022), that are altered in 90% of the affected subgroup (Herold and Gokbuget, 2017). Ph-like genomic profile is heterogeneous and characterized by lesions activating tyrosine kinases and/or signaling pathways downstream kinase receptors, making this ALL class a good candidate for alternative treatment therapies with specific kinase inhibitors. Depending on the type of kinase involved in rearrangements, a distinction in ABL-class or JAK2-class can be done, and this is particularly relevant to better

understand to whom class of appropriate tyrosine kinase inhibitor there could be associated with the sensibility of treatment (Boer, et al 2017). JAK2 is a non-receptor tyrosine kinase, fundamental for the hematopoiesis and involved in different signaling pathways and cellular processes, such as cellular proliferation and survival. JAK2 is known to be deregulated in leukemias and lymphomas as characterized by copy number variations, mutations and chromosomal translocations (Meyer, et al 2015; Ehrentraut, et al 2013). While JAK2 mutations have been widely studied in the last years, neoplasms deriving from JAK2 translocations are still poorly characterized (Ehrentraut, et al 2013). In particular, fusion genes involving *JAK2* are found in about 5% of the pediatric Ph-like ALL (Tasian, et al 2017; Shiraz, et al 2020; Tran and Tasian, 2021), in which JAK2 maintains its catalytic domain at 3' of the fusion gene. JAK2 is an appealing target of a large group of tyrosine kinase inhibitors (TKIs) available to date (Tran and Tasian, 2021) There are mainly JAK2 class I-TKIs, but in the last years the production of class II TKIs is increasing, because they could overcome the limits of class I TKIs acting directly on the inactive conformation of JAK2 (Harrison, et al 2017). Ruxolitinib is probably the most diffused class I TKI directed to JAK2 which binds its target in its active form; even though its efficacy, it showed some limitations in leukemia and myeloproliferative diseases' treatment, as efficacy at high dosages, persistence and hyperphosphorylation of JAK2 and STATs, determining a "paradoxical effect" (Koppikar, et al. 2012; Tvorogov, et al. 2018). Class II TKIs bind their targets in the inactive conformation and considering JAK2 as target, the novel compound CHZ868 showed promising results *in-vitro* and *in-vivo* acting significantly on both

leukemias and myeloproliferative diseases in presence of JAK2 point mutations (Bose, et al 2017; Meyer, et al 2015; Tvorogov, et al 2018; Wu, et al 2015; Zhang, et al 2018). Considering CHZ868 efficacy in these settings, we developed the present study with the aim of targeting JAK2 in the context of pediatric BCP-ALL samples derived from patients carrying *JAK2* fusion genes, in an *ex-vivo* and *in-vivo* preclinical setting. The aim was to investigate and assess the CHZ868 specificity and efficacy for this specific subgroup, lacking specific chemotherapy drugs for this type of fusions.

MATERIALS AND METHODS

Patients' cohort.

In this study, we have analyzed samples of primary bone marrow (BM) tumor cells (blasts) of pediatric patients affected by ALL, enlisted in the AIEOP-BFM ALL 2009 protocol. We selected a large cohort of BCP-ALL pediatric patients, as being defined as high risk by PCR MRD analysis at TP1/day 33.

Next Generation Sequencing RNA target capture and whole transcriptome analyses.

We applied the Next Generation Sequencing (NGS) RNA target capture strategy on a large cohort of PCR MRD high risk (HR) BCP-ALL pediatric patients, implementing RNA target capture NGS on Illumina platform (either the *Illumina TruSight RNA Pan-Cancer Library Prep* (Illumina, Inc., San Diego, CA, USA) or the Tecan Genomics Custom Panel), as previously described by Grioni, et al. 2019, starting from total RNA extracted during diagnosis from bone marrow mononuclear cells. For single cases, whole transcriptome analysis has been performed by

using the Universal RNAseq kit (Nugen, Tecan) following the manufacturer's protocol. Briefly, 100 ng nanogram amounts of total RNA obtained from BM cells have been processed to obtain double-stranded cDNA generation using a mixture of random priming, adaptor ligation, strand selection, targeted transcript depletion with AnyDeplete for ribosomal and globin genes, and PCR amplification to produce the final library. The libraries have been analyzed by paired-end sequencing on NextSeq550 Illumina platform, 2x75, sequencing 12 samples on a High Output v2.5 150 cycles cartridge. In the present study, we include exclusively patients carrying chromosomal rearrangements causing *JAK2* fusion genes, identified by bioinformatics analysis performed using TOPHAT and Dragen software (Basespace Illumina cloud, www.basespace.illumina.com) or an internal pipeline (Grioni, et al. 2019).

***JAK2* fusion genes validation.**

NGS identified JAK2 fusions were validated by RT-PCR and Sanger sequencing, and/or FISH. Briefly, 1µg of total RNA was used to obtain cDNA by reverse transcription using the SuperScript® II Reverse Transcriptase enzyme (Invitrogen, Thermo Fisher Scientific, Waltham, MA, USA), according to manufacturer's instructions. Subsequently, samples were analyzed by RT-PCR, with specific designed primers for each fusion (**Supplementary table 1**), using Platinum™ *Taq* DNA polymerase (Invitrogen, Thermo Fisher Scientific), according to manufacturer's instructions. RT-PCR products were purified and analyzed by Sanger sequencing.

Cell lines

MUTZ5 (CRLF2r and JAK2m R683G) and MHH-CALL-4 (CRLF2r) human B-precursor ALL cell lines, and SET2 (JAK2m) of acute megakaryoblast leukemia, were used as positive controls for JAK2/STAT pathway in short time points phosphoflow.

Human-murine xenografts for in-vivo expansion of patients' blasts. An *in-vivo* Patient-Derived-Xenograft (PDX) model has been setup in Immunodeficient NOD.Cg-Prkdc^{scid} Il2^{rgtm1Wjl}/SzJ (NSG) mice to expand primary patients' blasts isolated from diagnostic Bone Marrow. NSG mice were sub-lethally pre-irradiated (125 rad, 12mA, 190V) using X-RAY RADGIL instrument (Gilardoni s.p.a, Mandello del Lario, Italy) and after 4-6 hours, each mouse received a caudal intravenous injection of 1-1.5 x 10^6 patients' blasts. Periodically, we evaluated the leukemic engraftment in transplanted mice by intrafemoral BM aspirate, in general anesthesia using inhalatory isoflurane and oxygen. Mice were sacrificed at the treatment end point or when the human disease engraftment was evident (about 80% or higher), or when evident signs and symptoms of leukemia or suffering (curved posture, weight loss, anorexia, catatonia, matted hair) were observed. Tibia, femur, spleen, and meninges were collected and processed, in order to obtain leukemic cells of BM, spleen (SP) and central nervous system (CNS). Cells were analyzed for phenotype (FACS) and then cryopreserved in FBS-10%DMSO for long term storage.

Engraftment evaluation and immune-phenotype by flow cytometry.

To evaluate the leukemic engraftment in mice, BM and organ cell suspensions (previously processed to lyse red cells by NH_4Cl) were

stained with antibodies to make a cytometric analysis of surface antibodies. The antibodies used were: Fc portion of human and mouse immunoglobulins, mCD45.1-PE (30-F11, 12-0451, eBioscience™, Thermo Fisher), hCD45-PERCP (2D1, 345809, BD Biosciences, San Jose, CA, USA), hCD10-APC (CB-CALLA, 17-0106, eBioscience™, Thermo Fisher), hCD19-FITC (HIB19, 11-0199, eBioscience™, Thermo Fisher). After 15 minutes of dark incubation at room temperature, cells pellets were washed with PBS, resuspended in 200µl of PBS and analyzed at BD LSR X20 FORTESSA cytometer (BD) and FACS Diva software (BD).

Co-culture of leukemic blasts on a layer of human bone marrow stromal cells (HBMS).

Blasts derived from xenografts were seeded on a layer of cellular line of human bone marrow stromal cells, named HBMS. Stromal cell layer was prepared at the concentration of 2 x 10^4 in each of the wells of a 96 multiwell (Corning Incorporated, New York, USA), three days prior to reach confluence. Leukemic blasts were plated at 2 x 10^5 concentration, in presence of 200 µl in each well of AIM V (Thermo Fisher). Blasts in co-culture were treated with each drug in monotherapy at different concentrations to determine IC50, for 48h. Furthermore, three different concentrations (including IC50) were tested for each drug, in monotherapy or in combination of drug pairs. After 48h treatment, leukemic cells were isolated from stromal cells, by processing cells as follows: 8 times of scraping and 8 times of resuspension in PBS for each well. Levels of apoptosis-viability of blasts were evaluated by a staining with anti-hCD10-APC (CD10 PE-Cy™7 #565282 RRID: AB_2739153, BD Biosciences) and contemporarily with Annexin V-PE

and 7-AAD (kit GFP CERTIFIED Apoptosis/Necrosis detection, Enzo Life Science, Inc., Lausen, Switzerland)), following manufacturer's instructions. The experiments were performed in biological triplicate and technical duplicate. Analysis by FACS used BD LSR X20 FORTESSA cytometer (BD Biosciences) and FACSDiva software.

For the described experiments we used two TKIs, CHZ868 and ruxolitinib, which have been dissolved in DMSO for a 10mM STOCK and a 28mg/mL STOCK respectively, then aliquoted and preserved at -20°C. Dexamethasone was used as well, available in a liquid solution of 4mg/mL (preserved at 4°C), and Nintedanib/BIBF1120, which was received at stock solution of 10nM, in DMSO, and kept at -20°C. For each individual *ex-vivo* experiment we prepared fresh dilutions of each drug at specific experimental working concentrations.

The following parameters have been used to determine the efficacy of drug treatment, both in monotherapy and combination, as well as to determine if the combinations of drugs were additive, synergic or antagonistic:

- IC50: to determine the efficacy of drugs to inhibit 50% of their targets. (Beck, et al. 2004; Cheng and Prusoff, 1973; Sebaugh, et al. 2011)
- BLISS score: formula used to determine synergic (OE>EE), additive (OE=EE) or antagonist (OE<EE) activity between the drugs used in experiments Exy=Ex+Ey- (Ex X Ey), considering the expected effect (EE) of single drugs together Ex and Ey, and the Observed Effect (OE) really observed in experiments. (Greco, et al 1995, Zhao, et al 2014)
- Compusyn software: based on the Chou-Talalay's combination index theorem (CI) to evaluate the effect of interaction between n drugs: CI<1

stands for synergy, CI=1 for additivity, CI>1 for antagonism (Chou, et al. 2006).

Functional phosphoflow on JAK2 related pathways.

We evaluated the levels of phosphorylation of JAK/STAT, PI3K-AKT and MAPK pathway by Phosphoflow, in patients' blasts expanded by murine xenografts, and in cell lines, at basal level or after CHZ868, ruxolitinib or BIBF1120/nintedanib treatment. As previously setup in our lab (Cazzaniga, et al. 2015), after starvation, cells were fixed with 1.6% paraformaldehyde (PFA), permeabilized with 90% cold methanol, washed with Staining Buffer, dark stained 30 minutes at room temperature with antibodies. Only for the evaluation of CHZ868, ruxolitinib and BIBF1120 treatment effects, before the fixation with paraformaldehyde cells were treated with the drugs (IC50 concentration) at different time points. Stained cells were analyzed by FACS, using BD LSR X20 FORTESSA cytometer (BD Biosciences) and FACSDiva software. Antibodies used for the evaluation of phosphorylation were: pJAK2 (Tyr1007+Tyr1008, #bs-2485R Bioss Antibodies, Woburn Massachusetts), anti-STAT5(pY694)(#612598 BD Biosciences), anti-STAT3(pS727) (#558085 BD Biosciences), PI3K-AKT (PDPK1 (Anti-PDPK1 pS241 #560092 RRID: AB_1645523 BD Biosciences), pAkt (Ser473) (Phospho-Akt Ser473 #4075 Cell Signaling), pAkt (Thr308) (Anti-Akt pT308 #558275 RRID: AB_2225329 BD Biosciences), pS6 (Anti-S6 pS235/pS236 #560435 RRID: AB_2869348 BD Biosciences) and 4pEBP1 (Phospho-4E-BP1 Thr37/46 #2846 Cell Signaling)), and MAPK (pERK (T202/Y204), #560314 BD Biosciences) pathways, after 48H of CHZ868 or ruxolitinib treatment on blasts on a layer of HBMS.

Autophagy evaluation after TKIs treatment.

Blast cells, on a layer of HBMS, were treated for 44 hours with CHZ868 or ruxolitinib in monotherapy. Chloroquine, an autophagy inhibitor, was then added for 4 hours. Evaluation of autophagy induction was determined by observing LC3-II (LC3B #65299, Cell Signaling), total LC3 (LC3A/B #13611, Cell Signaling) expression and active caspase 3 (Anti-active caspase-3 #559341, Bd Biosciences) positive cells by FACS (LSR X20 FORTESSA, BD Biosciences).

CHZ868 in-vivo targeting.

NSG mice were xenotransplanted with leukemic blasts carrying PAX5::JAK2, ATF7IP::JAK2 or ZEB2::JAK2 fusions. After at least a 10% engraftment of leukemia, evaluated by periodic bone marrow aspiration and cytofluorimetric immunophenotyping evaluation for CD10+CD19+ blasts, we randomized animals in two groups and started the drug administration with either 30mg/Kg of CHZ868 (treatment group) or by vehicle (H2O, EtOH, Kolliphor) (vehicle group) for 2 weeks with washout on the weekend. Based on literature data, we previously performed a dose finding study treating mice carrying PAX5::JAK2 fusion with either 30mg/Kg or 40mg/Kg dosages of CHZ868, which resulted 30mg/kg as being efficacious but no toxic. Leukemia reduction after CHZ868 treatment was evaluated by the % and absolute number of human CD10+CD19+ blasts in Bone marrow, spleen, peripheral blood and meninges of central nervous system (FACS analysis).

Blasts cells isolated from BM of CHZ868 and vehicle treated mice were starved for 1.30h, fixed with 4% of PFA, permeabilized with 90% cold methanol, washed with Staining Buffer, dark stained 30 minutes at

room temperature with antibodies directed to JAK2/STATs, PI3K-AKT, and MAPk pathways as described above.

***Ex-vivo* drug screening experiments of leukemic blasts**

Ex-vivo extended drug screening was performed as previously described (Bhatia, et al. 2018; Fazio, et al. 2022). Briefly the DMSO dissolved compound library (MedChemExpress, NJ, USA) was dispensed with increasing concentrations of the inhibitors in 6 dilution steps (0.008 - 25 μM) using digital dispenser (D300e, Tecan, Mannedorf, Switzerland), which ensures precise and robotic compound application in randomized fashion. Differential responses were monitored with ATP-dependent CellTiter-Glo Luminescent cell viability kit (Promega, Madison, USA) after 72 h of inhibitor exposure using Microplate reader (Spark 10M, Tecan). Drug sensitivity scores (DSS) for the inhibitors were determined, followed by heat map and volcano plots visualization, and unsupervised hierarchical clustering of the DSS scores were performed using R package gplots (Yadav, et al. 2014)

Statistical analysis. Statistical analyses from *in-vivo*, *ex-vivo* and phosphoflow experiments were performed by GraphPad Prism software (ver·9); Anova and T test is shown as *p<0.05, **p<0.01, ***p<0.001, ****p<0.0001.

RESULTS

JAK2 rearrangements were identified in a cohort of pediatric patients affected by acute lymphoblastic leukemia.

Through a large NGS screening we identified, among the others, a total of 13 cases carrying a *JAK2* fusion gene (**Supplementary table 2)**.

Beyond the already described fusions ATF7IP::JAK2 and PAX5::JAK2, which was recurrent in n=6 cases, novel fusions were found and validated by RT-PCR and Sanger Sequencing: ZEB2::JAK2, GIT2::JAK2, TLE4::JAK2, RAB7A::JAK2, MPRIP::JAK2 (n=2). In all the JAK2t cases identified, *JAK2* maintains its kinase domain at the 3', fused at the 5' with the partner gene. We also selected two patients as positive controls, identified by NGS as carrying P2RY8::CRLF2 rearrangements and $JAK2_{R683G}$ mutation, and additional two as negative controls, whose cells were wild type for *JAK2* and negative for any fusion gene by RNA NGS analysis.

JAK/STAT pathway is hyperphosphorylated in JAK2r blasts.

We developed a model of *in-vivo* human-mouse xenograft in sublethally-irradiated NSG mice to expand available primary cells from 3 patients, carrying a PAX5::JAK2 (patient 1), an ATF7IP::JAK2 (patient 2) and a ZEB2::JAK2 (patient 3) fusion, respectively, previously validated by RT-PCR and Sanger sequencing (**Figure 1A-D**). After an assessment of engraftment higher than 80% of human blasts ($CD10^+/CD19^+$) by BM aspirate samples of transplanted mice (FACS analysis), we recovered leukemic blasts from BM, SPL and CNS from mice, which were used to set up the cell biology experiments of this study.

First, we wanted to characterize the signaling pathways involved in the three cases carrying JAK2 fusions, investigating if JAK2 was effectively active at basal level in absence of specific stimuli. To this purpose, by phosphoflow technique we evaluated the level of phosphorylation of the two residues Y1007-1008 in the loop of activation of JAK2, corresponding to constitutive activation of JAK2

itself. We compared the basal phosphorylation levels of our patients to primary cells of two patients characterized by *CRLF2* rearrangements, known to have JAK/STAT pathway active (Savino, et al 2017), and thus considered as positive controls. We detected significantly higher levels of basal activation of pJAK2 in all the three patients (+17+70%) (**Figure 1E),** expressed as median of phosphorylation in basal conditions, compared to positive controls. Further, we evaluated the levels of phosphorylation of STAT5 (pY694) and STAT3 (pS727), two JAK2 downstream effectors on the JAK/STAT pathway, demonstrating that the JAK2 constitutive activation induced the activation of its effector at basal levels in all three patients without any stimuli (**Figure 1F-G**).

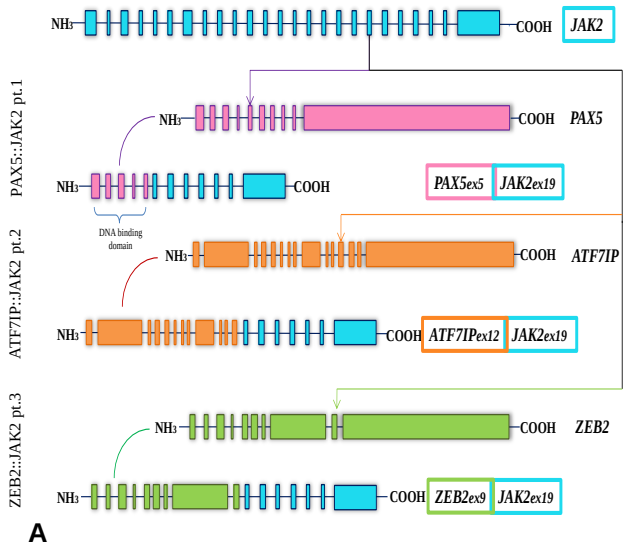

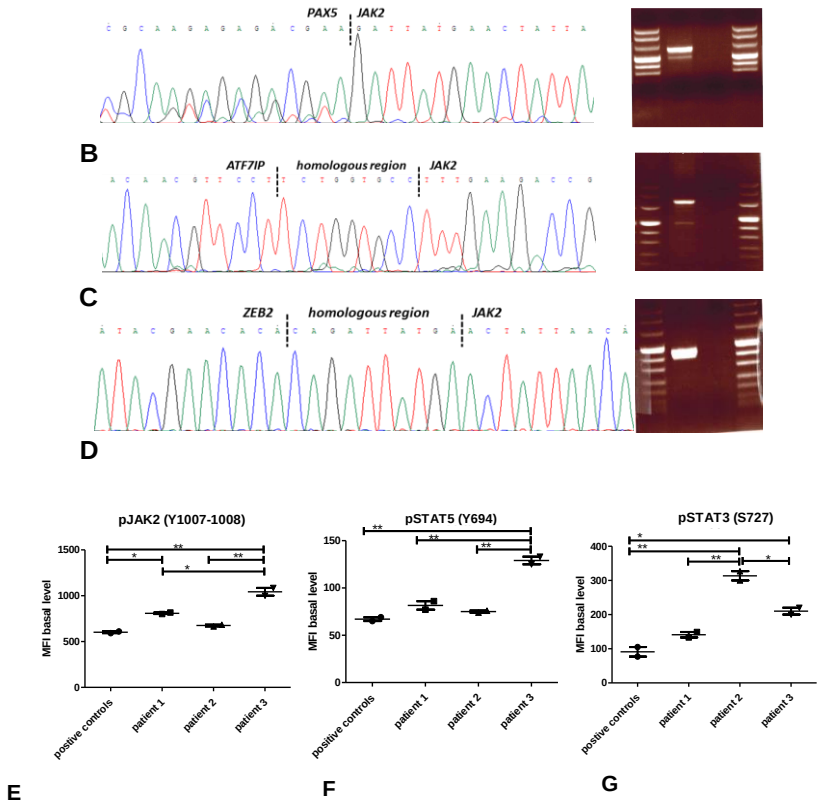

Figure 1. Features of three pediatric patients carrying JAK2 rearrangements. A. Representation of fusion breakpoints of patient 1 PAX5::JAK2, patient 2 ZEB2::JAK2, patient 3 ATF7IP::JAK2, each maintaining JAK2 kinase domain. **B-D.** Sanger indicating the breakpoint of fusions and RT-PCR of patient 1 PAX5::JAK2 (B), patient 2 ATF7IP::JAK2 (C), patient 3 ZEB2::JAK2 (D). **E-F**. Basal level of phosphorylation of pJAK2 (Y1007-1008) (E), pSTAT5 (Y694) (F), pSTAT3 (S727) (D) of the three patients carrying JAK2r compared to positive controls, carrying both a CRLF2 rearrangement, and one of them a JAK2 R683G mutation. P values: *p<0.05; **p<0.01; ***p<0.001.

The JAK2t patients also showed a significant hyperphosphorylation of pJAK2, pSTAT5 and pSTAT3 compared to negative controls, represented by primary cells of two patients carrying a wild type *JAK2* gene, considering both fusion and SNV/CNV mutations, who didn't

have a constitutive activation of pJAK2, therefore a low activation of STAT3 and STAT5 compared to JAK2t blasts (**Supplementary Figure S1A-C**).

Cell lines (SET2, CALL4, MUTZ5), considered positive controls for JAK/STAT pathway, showed little expression of JAK/STAT effectors without stimuli (**Supplementary figure S1D-F**).

Conventional chemotherapy drugs and JAK2 tyrosine kinase inhibitors as single agents show efficacy on JAK fusions.

We executed Annexin V- 7-AAD apoptosis-vitality assay of co-culture of patients' blasts on HBMS, treated with CHZ868, a JAK2 TKI of class II and ruxolitinib, a JAK2 TKI of class I, in monotherapy to determine patient-specific IC50s at 48h. We determined that PAX5::JAK2 and ATF7IP::JAK2 cells were more sensitive to CHZ868, having 0.270μM IC50 (Compusyn analysis), compared to ZEB2::JAK2 sample, which was more resistant (IC50 of 0.338 μM, as shown in **Supplementary figure S2A**). By ruxolitinib dose finding study, we detected IC50 values 100-fold higher than the CHZ868 ones (**Supplementary figure S2B**). Furthermore, we treated PAX5::JAK2 blasts with dexamethasone, a conventional chemotherapy drug used in AIEOP BFM 2017 protocol, determining an IC50 of 7ng/mL IC50, which was considered also for pt.2 and pt.3 (**Supplementary figure S2C**). IC50s are reported in **supplementary figure S2D**.

CHZ868 reduces JAK2/STATs pathway basal hyperphosphorylation in JAK2t leukemic blasts.

We evaluated whether the CHZ868 treatment reduces the phosphorylation of its target JAK2. We treated blasts with CHZ868 and ruxolitinib in monotherapy at IC50 patient-specific doses at different shorter time points than 48h, observing after 30 minutes of treatment a significant patient-specific reduction of phosphorylation of Y1007-1008 residues of the catalytic loop of activation of JAK2 (-33-71%). CHZ868 30 minutes of treatment also caused a significant reduction of phosphorylation on pSTAT5 (Tyr694) (-12-52%) and pSTAT3 (Tyr705) (-37-48%), the two main downstream effectors of JAK2, as an effect of the reduced phosphorylation in JAK2 (**Figure 2A-C**). Overall ruxolitinib showed higher efficacy on pSTAT5 (up to -62%) rather than on pJAK2 (up to -22%) after 30 minutes (**Figure 2D-F**), with patient specific responses.

SET2, CALL4 and MUTZ5 cell lines overall showed similar sensitivity to both TKIs on JAK2/STATs pathway after 30 minutes of treatment (**Supplementary figure S3).**

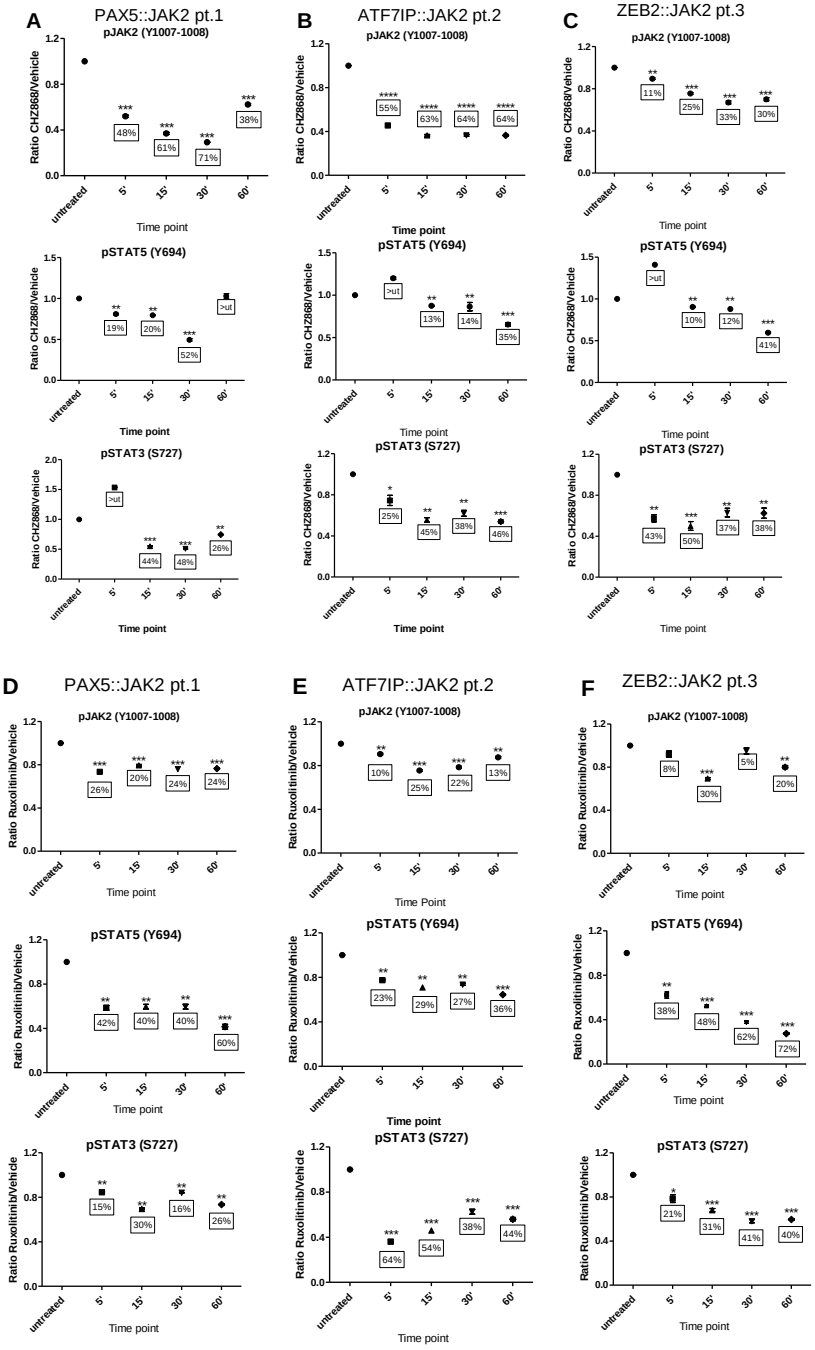

Figure 2. Targeting of three JAK2 rearranged patients with tyrosine kinase inhibitors at short time points, evaluating the phosphorylation levels on JAK2/STATs pathway by phosphoflow. A-C. CHZ868, type-II TKI, targeting of

pJAK2 (Y1007-1008), pSTAT5 (Y694) and pSTAT3 (S727) at short time points on patient 1 carrying a PAX5::JAK2 fusion (A), on patient 2 carrying a ATF7IP::JAK2 fusion (B) and on patient 3 carrying a ZEB2::JAK2 fusion (C). **D-F**. Ruxolitinib, type-I TKI, targeting of pJAK2 (Y1007-1008), pSTAT5 (Y694) and pSTAT3 (S727) at short time points on patient 1 carrying a PAX5::JAK2 fusion (D), on patient 2 carrying a ATF7IP::JAK2 fusion (E) and on patient 3 carrying a ZEB2::JAK2 fusion (F). N=3, 1 representative experiment shown. P values: *p<0.05; **p<0.01; ***p<0.001.

After treatment of blast cells in co-culture on a layer of HBMS cells with CHZ868 for 48 hours, in PAX5::JAK2 blasts, even though pJAK2 was significantly reduced (-40%, p<0.001), pSTAT5 was hyperphosphorylated (+75%, p<0.001) (**Figure 3A)**, probably due to the presence of *PAX5* in the fusion gene, which leads to pSTAT5 hyperphosphorylation (Cazzaniga, et al. 2015). Instead, ATF7IP::JAK2 and ZEB2::JAK2 samples showed a significant reduction of phosphorylation in both pJAK2 (-25-50%) and pSTAT5 (-20-65%)(**Figure 3B-C**), while CHZ868 had effect on pSTAT3 (-50%, p<0.0001) only in ATF7IP::JAK2. At 48h, ruxolitinib had no effect on pJAK2 and pSTAT3 on PAX5::JAK2 positive blasts, while it simultaneously induced pSTAT5 hyperphosphorylation (+50%, p<0.001) (**Figure 3D**). Moreover, while it didn't show an effect on pJAK2 also on ATF7IP::JAK2 positive blasts, ruxolitinib inhibited pSTAT5 (-45%, p<0.0001) and pSTAT3 (-50%, p<0.0001) (**Figure 3E-F**). Conversely, ruxolitinib exerted a significant effect on pJAK2 (-33%) and pSTAT5 (-50%) of ZEB2::JAK2 blasts (**Figure 3G-I**)

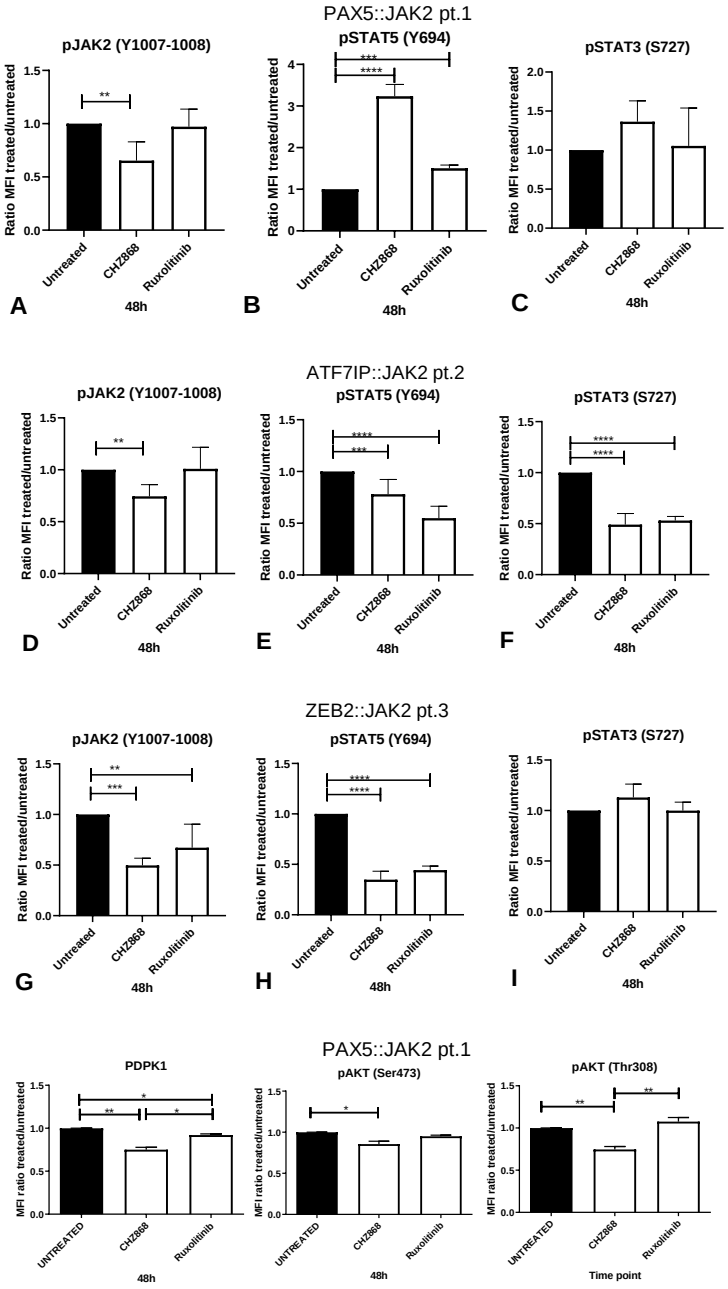
PAX5::JAK2 pt.1
pJAK2 (Y1007-1008)
pSTAT5 (Y694)
pSTAT3 (S727)
Ratio MFI treated/untreated
Untreated
CHZ868
Ruxolitinib
48h
A
B
C
ATF7IP::JAK2 pt.2
D
E
F
ZEB2::JAK2 pt.3
G
H
I
PAX5::JAK2 pt.1
PDPK1
pAKT (Ser473)
pAKT (Thr308)
MFI ratio treated/untreated
UNTREATED
Time point

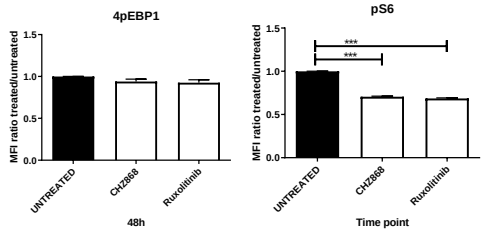
4pEBP1
pS6
MFI ratio treated/untreated
UNTREATED
CHZ868
Ruxolitinib
48h
Time point

J

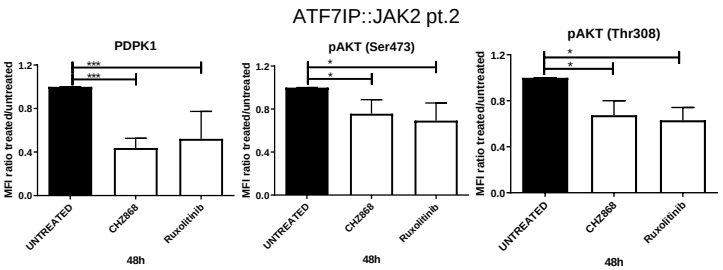
ATF7IP::JAK2 pt.2
PDPK1
pAKT (Ser473)
pAKT (Thr308)
MFI ratio treated/untreated
UNTREATED
CHZ868
Ruxolitinib
48h

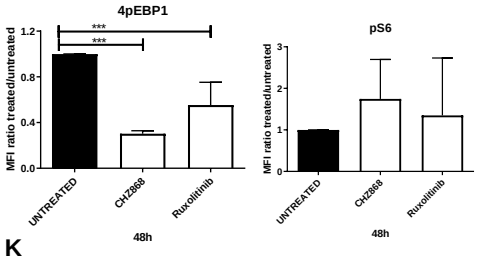
4pEBP1
pS6
MFI ratio treated/untreated
UNTREATED
CHZ868
Ruxolitinib
48h

K

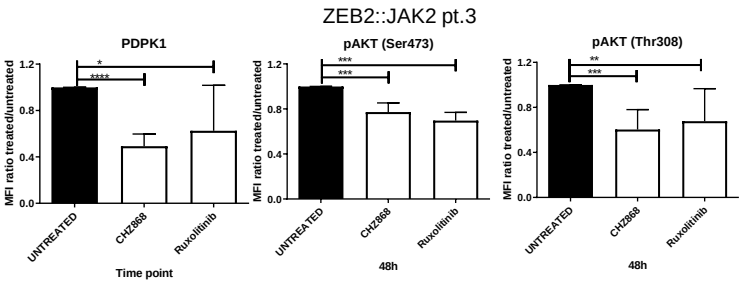
ZEB2::JAK2 pt.3
PDPK1
pAKT (Ser473)
pAKT (Thr308)
MFI ratio treated/untreated
UNTREATED
CHZ868
Ruxolitinib
Time point
48h

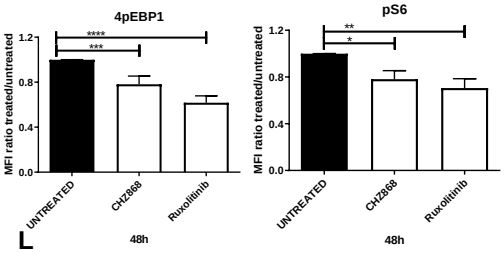
4pEBP1
pS6
MFI ratio treated/untreated
UNTREATED
CHZ868
Ruxolitinib
48h

L

Figure 4. Mean fluorescence intensity (MFI) inhibition of JAK2 related downstream pathways after 48h of treatment with TKIs on blasts carrying JAK2 fusions in co-culture on HBMS, evaluated by phosphoflow. A-C. pJAK2 (Y1007-1008) (A), pSTAT5 (Y694) (B) and pSTAT3 (S727) (C) inhibition after CHZ868 or ruxolitinib treatment on patient 1 blasts carrying a PAX5:.JAK2 fusion. **D-F.** pJAK2 (Y1007-1008) (D), pSTAT5 (Y694) (E) and pSTAT3 (S727) (F) inhibition after CHZ868 or ruxolitinib treatment on patient 2 blasts carrying a ATF7IP:.JAK2 fusion. **G-I.** pJAK2 (Y1007-1008) (G), pSTAT5 (Y694) (H) and pSTAT3 (S727) (I) inhibition after CHZ868 or ruxolitinib treatment on patient 3 blasts carrying a ZEB2:.JAK2 fusion. **J.** PI3K-AKT pathway effectors inhibition [PDPK1, pAKT (S473), pAKT (T308), 4pEBP1, pS6] after CHZ868 or ruxolitinib treatment on patient 1 blasts carrying a PAX5:.JAK2 fusion. **K.** PI3K-AKT pathway effectors inhibition [PDPK1, pAKT (S473), pAKT (T308), 4pEBP1, pS6] after CHZ868 or ruxolitinib treatment on patient 2 blasts carrying a ATF7IP:.JAK2 fusion. **L.** PI3K-AKT pathway effectors inhibition [PDPK1, pAKT (S473), pAKT (T308), 4pEBP1, pS6] after CHZ868 or ruxolitinib treatment on patient 3 blasts carrying a ZEB2:.JAK2 fusion. P values: *p<0.05; **p<0.01; ***p<0.001. N=3 experiments, in technical duplicate (A-L).

Furthermore, we also checked PI3K-AKT and MAPK pathways after 48h of treatment, as they are more downstream JAK2 related pathways, expecting an effect of the TKIs later in time. CHZ868 and ruxolitinib significantly downregulated PI3K-AKT pathway's effectors in all the three JAK2t samples, with similar effects (**Figure 3J-L**), while we evaluated patient-specific responses on pERK (**Supplementary figure S4).**

CHZ868 shows a JAK2t specific pharmacological effect in combination with ruxolitinib and dexamethasone in *ex-vivo* treatments.

CHZ868 was given for 48h in combination with dexamethasone and ruxolitinib to blast cells on HBMS. We found its statistically significant and synergistic effect with ruxolitinib in all the three fusions settings (-62-90%, $0.01<p<0.001$ vs untreated). While patient 2 and 3 showed a resistance to conventional chemotherapy drug dexamethasone, patient 1 (PAX5::JAK2) was quite sensitive and we evaluated a statistically significant synergy between dexamethasone and CHZ868 (-95%, $p<0.001$ vs. untreated). The combination between CHZ868 and dexamethasone on patients 3 (ZEB2::JAK2) showed a tendency to overcome the resistance as we evaluated an additive effect by bliss score, driven mainly by CHZ868 ($p<0.001$ vs. dexamethasone only), while the combination on patient 2 (ATF7IP::JAK2) didn't give and advantage compared to monotherapy due to the high resistance to dexamethasone **(Figure 4A-C).** We assessed synergistic/additive effects in the combinations as indicated by bliss score in figures 4D and combination index in **Supplementary table 3A**, with patient specific responses.

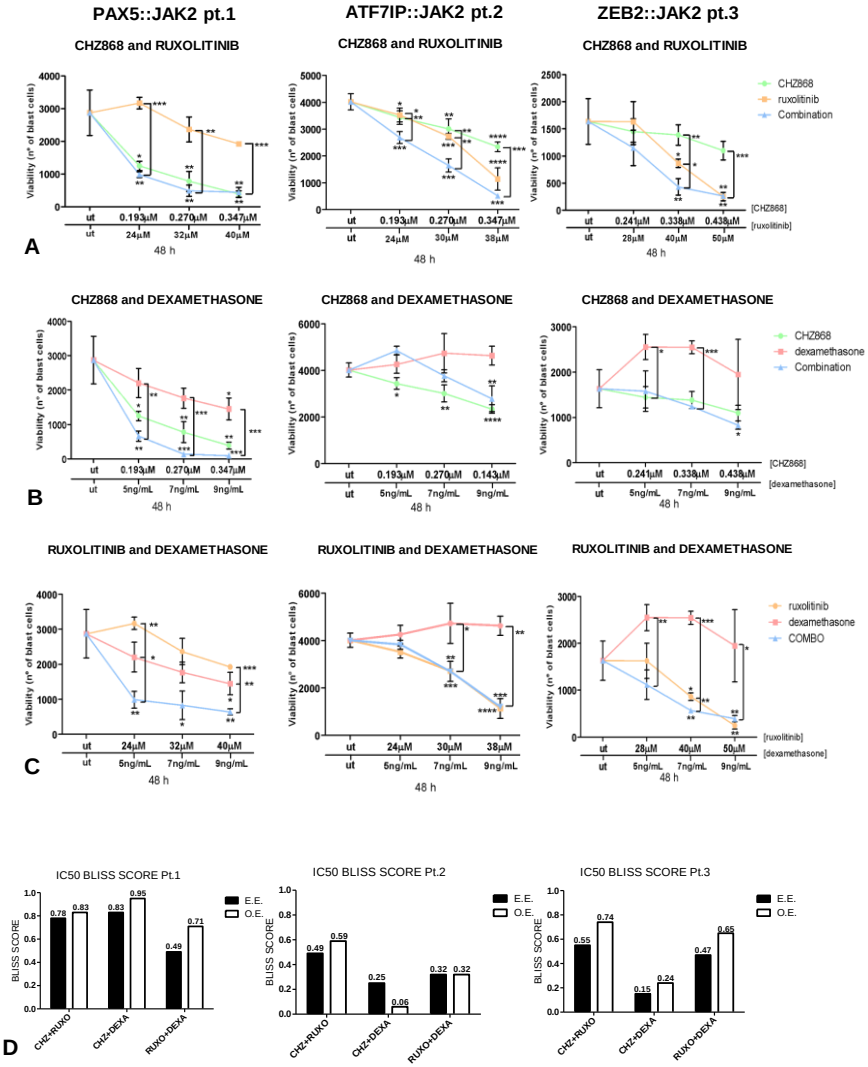

Figure 4 Ex-vivo apoptosis/viability assays of combination of pairs of drugs, given at three different dosages, on BM blasts derived from patients carrying JAK2 rearrangements, treated for 48h in co-culture with HBMS. Viability was assessed by Annexin V-PE/7AAD staining, as difference from apoptosis and necrosis. A. Combinations on PAX5::JAK2 positive blasts. **B**. Combinations on ATF7IP::JAK2 positive blasts. **C**. Combinations of ZEB2::JAK2 positive blasts. **D**. Bliss score of the combinations in pair of the drugs, comparing expected event(EE) and observed event(OE), to evaluate synergy. P values: *p<0.05; **p<0.01;

***p<0.001. N=3 experiments, in technical duplicate. Each column represents results on 1 patient. The internal control is represented by untreated (ut) cells.

The same apoptosis-vitality assays were performed on blasts derived from two pediatric patients defined as negative controls, as they didn't have JAK2t rearrangements, and on two CRLF2r blasts of pediatric patients defined positive controls, using the same range of dosages for the three chemotherapy drugs defined for the PAX5::JAK2 patient. CHZ868 was not significantly effective on positive controls compared to ruxolitinib treatment, highlighting CHZ868 JAK2t specificity. Overall, CRLF2r control n.2 was more sensitive to all treatments, both in monotherapy and in combination, as also suggested by bliss score (**Supplementary figure S5A-B**). Moreover, negative controls were particularly sensitive to dexamethasone treatment, and negative control n.1 was also sensitive to ruxolitinib treatment (IC50 -60%, p<0.01 vs untreated), despite the absence of JAK2 fusions or mutations, remarking ruxolitinib nonspecific activity. CHZ868 had no significant effect in both negative controls (**Supplementary figure S5C-D**). Eventual synergistic or additive effects shown by combination index on CRLF2r and negative controls are exclusively driven by dexamethasone or ruxolitinib (**Supplementary table 3B**).

CHZ868 exerts a synergistic combination with nintedanib on PAX5::JAK2 treated blasts.

Considering the patient 1 carrying PAX5::JAK2 fusion gene, we performed a dose finding study for the kinase inhibitor nintedanib (BIBF1120), which showed efficacy in the treatment of leukemic cells

characterized by *PAX5* fusion genes (Cazzaniga V. et al., 2015, Fazio G. et al., 2022), determining a 10nM IC50 value for BIBF1120 (**Figure 5A**). We also demonstrated the activation at basal level of LCK downstream pathway, known to be regulated by PAX5 and targeted by BIBF1120 (Fazio, et al. 2022), evaluating the phosphorylation levels of PDPK1, pAKT (Thr308 and Ser473), pS6 and 4pEBP1 (**Figure 5B**). After 48 hours of BIBF1120 monotherapy treatment of blast cells on HBMS, we observed a significant downregulation of PI3K-AKT pathway effectors (PDPK1 $p<0.001$, AKT Ser473 $p<0.05$, pAKT Thr308 $p<0.01$, pS6 $p<0.001$, 4pEBP1 $p<0.01$) (**Figure 5C-G**). Moreover, we performed a combination treatment between CHZ868 and BIBF1120, in addition to a combination treatment experiment between ruxolitinib and BIBF1120, using three different drug concentrations (the IC50, one lower and one higher dosage, defined by a constant ratio between the two drugs). After 48h treatment, a more significant effect on cell viability by the combination between CHZ868 and BIBF1120 (-64%, $p<0.001$) than the ruxolitinib-BIBF1120 one (-50%, $p<0.05$) was observed (**Figure 5H-I**). Bliss score also showed that both CHZ868 and dexamethasone combination, both the ruxolitinib and dexamethasone combination are synergistic. (**Figure 5J**).

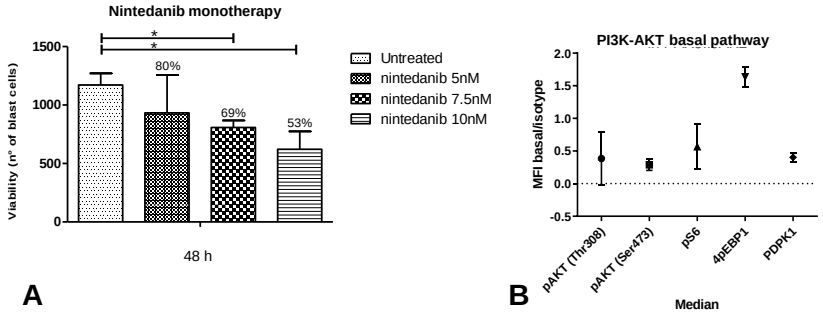

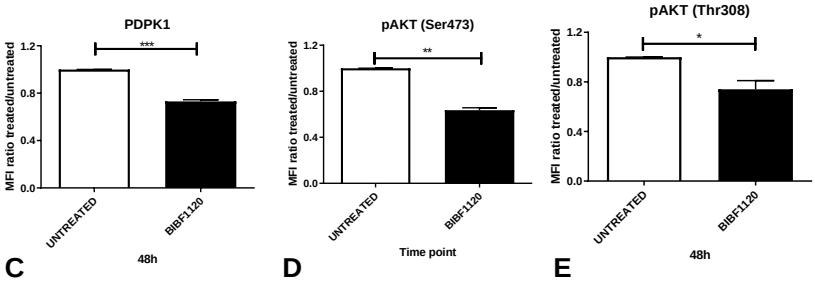
PDPK1
MFI ratio treated/untreated
UNTREATED
BIBF1120
48h
C
pAKT (Ser473)
Time point
D
pAKT (Thr308)
E

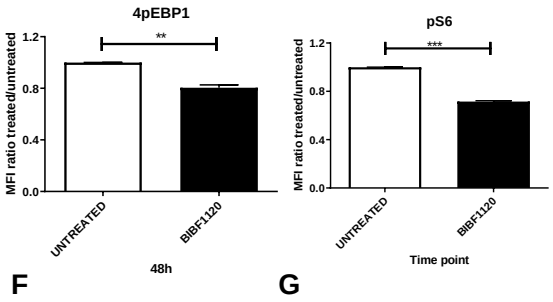
4pEBP1
pS6
F
G

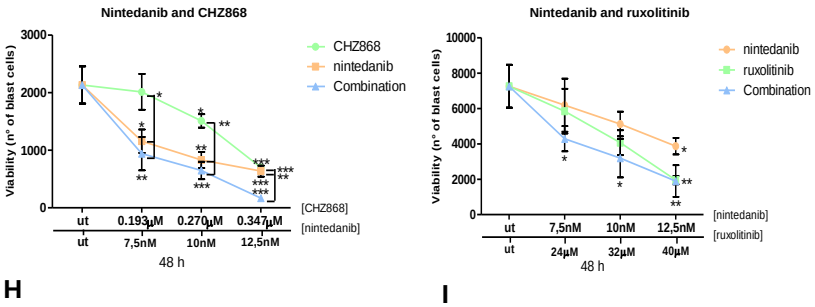
Nintedanib and CHZ868
Viability (n° of blast cells)
CHZ868
nintedanib
Combination
[CHZ868]
[nintedanib]
48 h
H
Nintedanib and ruxolitinib
ruxolitinib
[ruxolitinib]
I

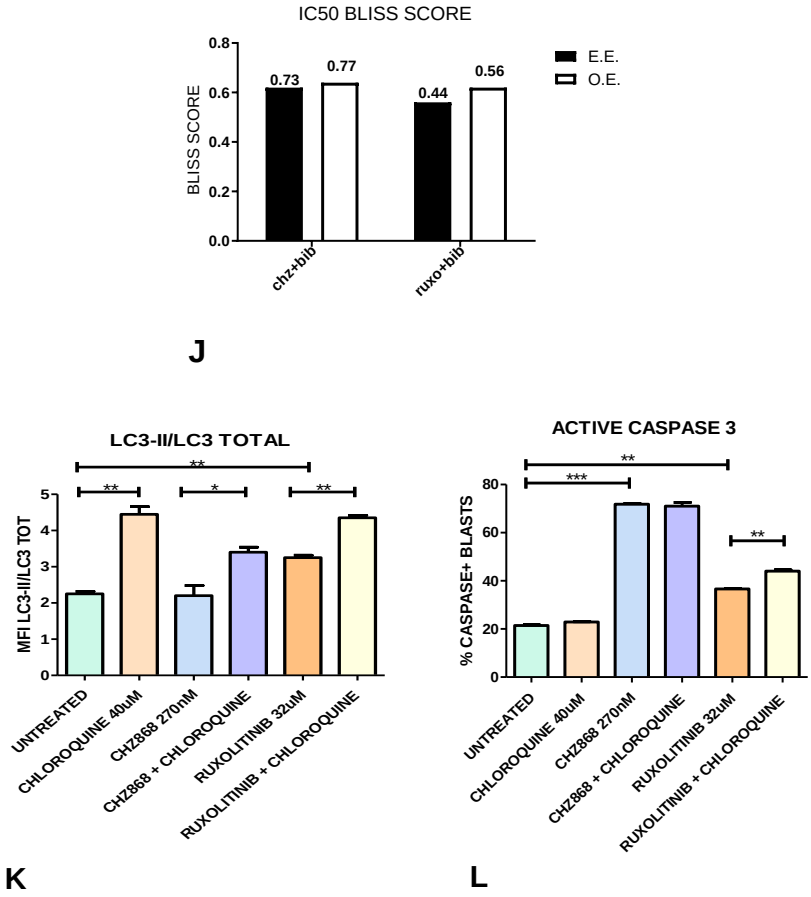

Figure 5. Overview of function characterization of PAX5::JAK2 patient 1 blast cells. A. Viability of blasts in co-culture on HBMS after 48h monotherapy treatment with BIBF1120/Nintedanib to determine IC50. N=3 experiments in technical duplicate. **B**. Basal level evaluation of expression of PI3K-AKT pathway effectors. **C-G**. Mean fluorescence intensity of PI3K-AKT pathway effectors PDPK1 (**C**), pAKT (S473) (**D**), pAKT (T308) (**E**), 4pEBP1 (**F**), pS6 (**G**), after 48h BIBF1120 treatment of blasts on HBMS, evaluated by phosphoflow. N=3 experiments in technical duplicate. **H-I** Ex-vivo iability of blasts after BIBF1120-CHZ868 (**H**) and BIBF1120-ruxolitinib (**I**) combinations after 48h treatment on HBMS, evaluated as difference from necrosis and apoptosis by Annexin V-PE/7AAD staining. N=3 experiments in technical duplicate. **J**. Bliss score of the combinations of the TKIs with BIBF1120, indicating a synergistic effect with combination index CI<1. **K**.

LC3II expression, indicated as MFI ratio on LC3 total, on untreated and treated blasts in co-culture on HBMS for 44h + 4h with chloroquine. N=3, 1 representative experiment shown. **L**. % of blast cells positive to active caspase 3 after treatment with TKIs, BIBF1120 and chloroquine, indicating cells in apoptosis due to drug efficacy. N=3, 1 representative experiment shown.
P values: *p<0.05; **p<0.01; ***p<0.001.

Ruxolitinib, but not CHZ868, exerts a reduction of its apoptotic effect on PAX5::JAK2 blasts as blasts undergo autophagy.

In cases carrying *JAK2* single nucleotide mutations (JAK2m), ruxolitinib is known to reduce its apoptotic effect but inducing autophagy (Machado-Neto, et al. 2020), therefore we investigated autophagy involvement in presence of *JAK2* fusions. We treated blasts, on a layer of HBMS, for 44 hours with CHZ868 or Ruxolitinib alone, then we added chloroquine for 4 hours and we evaluated the MFI. After autophagy inhibition by chloroquine treatment, levels of LC3-II, a marker of autophagy, were assessed by flow cytometry, demonstrating significantly higher levels of LC3-II in chloroquine treated blasts (+115%, p<0.01) and also ruxolitinib treated cells (+45%, p<0.01) compared to untreated blasts, whereas no difference has been observed in CHZ868 treated cells (**Figure 5K**). Moreover, we observed an increase of active caspase 3, in blasts treated with ruxolitinib and chloroquine combination (+20%, p<0.01), compared to ruxolitinib only treated blasts, while CHZ868 and chloroquine combination treatment did not increased apoptosis compared to CHZ868 only (**Figure 5L**). Furthermore, ruxolitinib induced autophagy exclusively in PAX5::JAK2 blasts, and not in ATF7IP::JAK2 and ZEB2::JAK2 treated cells (**Supplementary figure S6A-D**).

CHZ868 treatment targets leukemic blasts carrying *JAK2* fusions in *in-vivo* PDX preclinical model.

As CHZ868 proved to be more effective than ruxolitinib in *ex-vivo* treatments, we evaluated its effect in patient-derived xenograft NSG mice, treated by either CHZ868 (30 mg/kg) or vehicle. After two weeks of treatment, we analyzed the levels of human CD10+CD19+ blasts in the two experimental groups. In all the three subtypes of fusions, we detected a statistically significant reduction of the percentage of the hCD10+CD19+ blasts (**Figure 6A-C**) in the hematopoietic organs, as bone marrow (-43-85%), spleen (-72-89%), peripheral blood (-46-80%) and meninges of central nervous system (-13-62%), and of the number of hCD10+CD19+ (**Supplementary figure S7A-C**). Overall, CHZ868 showed a higher efficacy on spleens, in particular leading to a highly significant reduction of spleens weights (37-60%). We also detected a significant reduction of the levels of phosphorylation in BM derived cell of CHZ868 treated mice, for all the three patients, in pJAK2(-18-30%, $p<0.05$) and pSTAT5(-23-45%, $p<0.05$), therefore CHZ868 maintains its capacity to downregulate JAK/STAT pathway (**Supplementary figure S8A-C**). We detected patient specific responses among the effectors of PI3K and MAPk pathways, suggesting a CHZ868 overall efficacy mainly on JAK2/STAT5 pathway (**Supplementary figure S8D-I**).

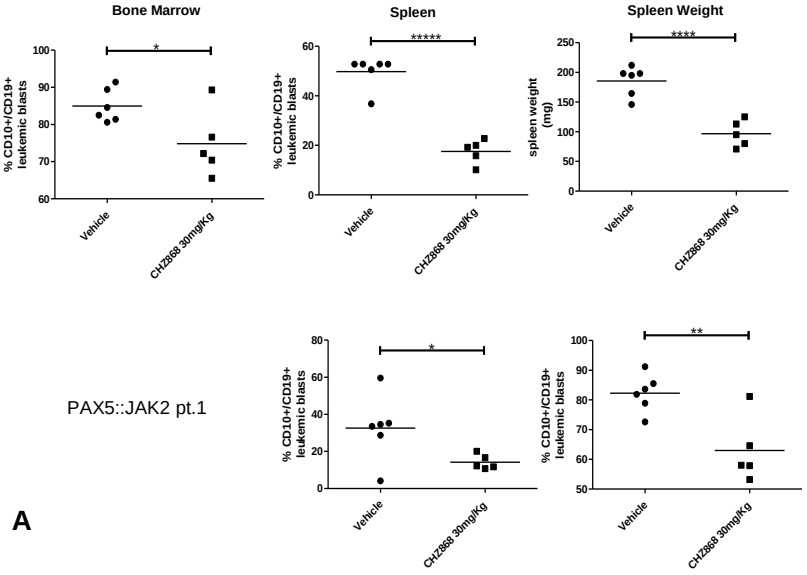
Bone Marrow
Spleen
Spleen Weight
% CD10+/CD19+ leukemic blasts
spleen weight (mg)
Vehicle
CHZ868 30mg/Kg
PAX5::JAK2 pt.1
A

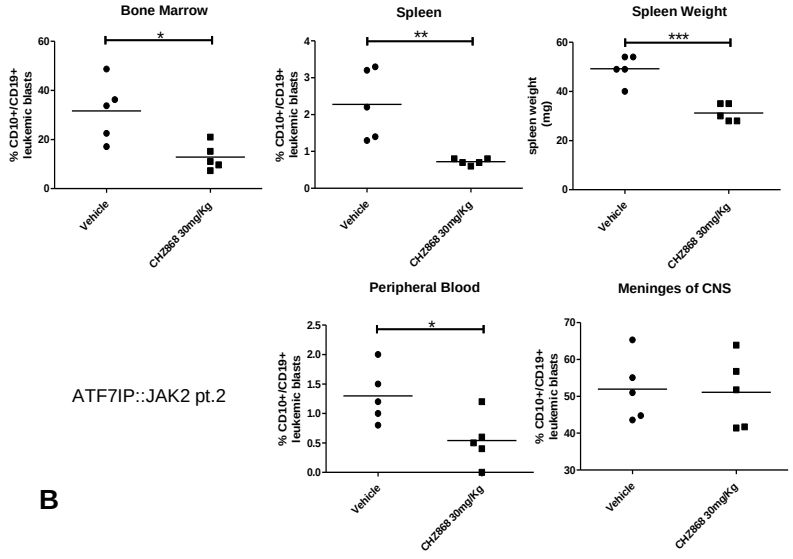
Bone Marrow
Spleen
Spleen Weight
Peripheral Blood
Meninges of CNS
% CD10+/CD19+ leukemic blasts
spleen weight (mg)
Vehicle
CHZ868 30mg/Kg
ATF7IP::JAK2 pt.2
B

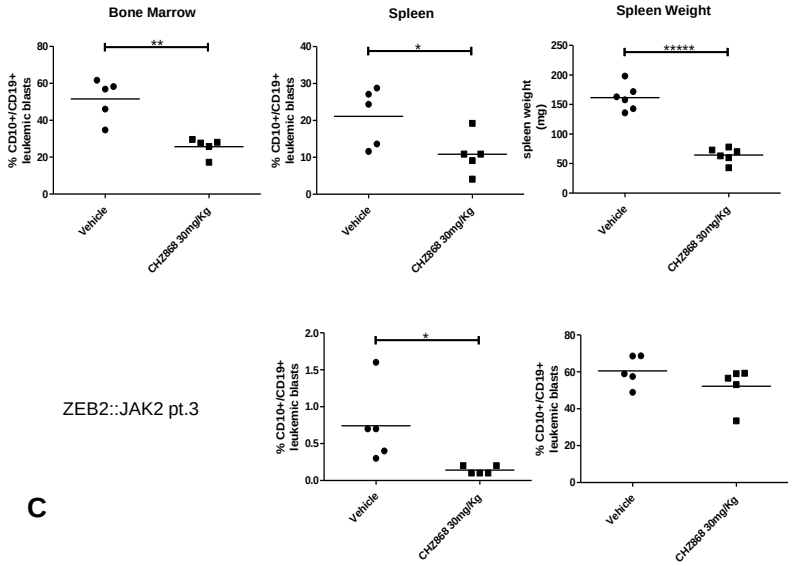

Figure 6. In-vivo CHZ868 treatment of mice xenotransplanted with blasts carrying JAK2r. **A**. Reduction of the % of CD10+CD19+ leukemic blasts in CHZ868 treated mice compared to vehicle, in bone marrow, spleen, peripheral blood and meninges, and reduction of spleen weight, in the setting of PAX5::JAK2 fusion. **B**. Reduction of the % of CD10+CD19+ leukemic blasts in CHZ868 treated mice compared to vehicle, in bone marrow, spleen, peripheral blood and meninges, and reduction of spleen weight, in the setting of ATF7IP::JAK2 fusion. **C**. Reduction of the % of CD10+CD19+ leukemic blasts in CHZ868 treated mice compared to vehicle, in bone marrow, spleen, peripheral blood and meninges, and reduction of spleen weight, in the setting of ZEB2::JAK2 fusion. P values: *p<0.05; **p<0.01; ***p<0.001. At least N=5 mice for each group.

A wide drug screening of FDA-approved drugs identified additional potential JAK2 inhibitors in *ex-vivo* treated PDX cells.

Furthermore, as CHZ868 showed promising effects on JAK2r, we investigated if also other available compounds would act as inhibitors targeting JAK2/STATs pathway, to be considered for the treatment of this specific subgroup of patients. We applied a wide *ex-vivo* drug

screening with 174 FDA-approved drugs and inhibitors in clinical trials (**Supplementary table 5**), to find effective drugs on JAK2 rearranged PDXs. We demonstrated efficacy and specificity to n=4 JAK2t cases (carrying PAX5::JAK2, ZEB2::JAK2, ATF7IP::JAK2, GIT2::JAK2 respectively). After 72h of treatment, we evaluated the differential drug sensitivity score (dDSS) of JAK2t samples, comparing their DSS to CRLF2r and JAK2m cell lines (MUTZ5) and control B-cell lymphoblastoid cell lines (LCLs), derived from healthy donors. Considering patient-specific responses, as reported in **figure 7A**, PAX5::JAK2 was the most sensitive sample to several drugs, belonging both to conventional chemotherapy drugs currently used in the AIEOP BFM 2017 protocol for ALL in children, and to TKIs. Interestingly, we demonstrated that ruxolitinib is not effective on all the JAK2t at the tested dosages, ranging from 8nM up to 25uM.

Among the TKIs targeting JAK2, AT9283 was found to be the highest specific and effective compound to JAK2t (Dawson, et al. 2010), compared to MUTZ5, used as positive controls, and healthy controls ($p<0.05$), on which it had no effect. Additionally, this extended screening led us to identify drugs, not belonging to JAK inhibitors, specific and non-toxic for JAK2t cohort, such as Birinapant (Smac mimetic) (Richmond, et al. 2016), which showed a significant specificity for JAK2t ($p<0.05$) (**Figure 7B**).

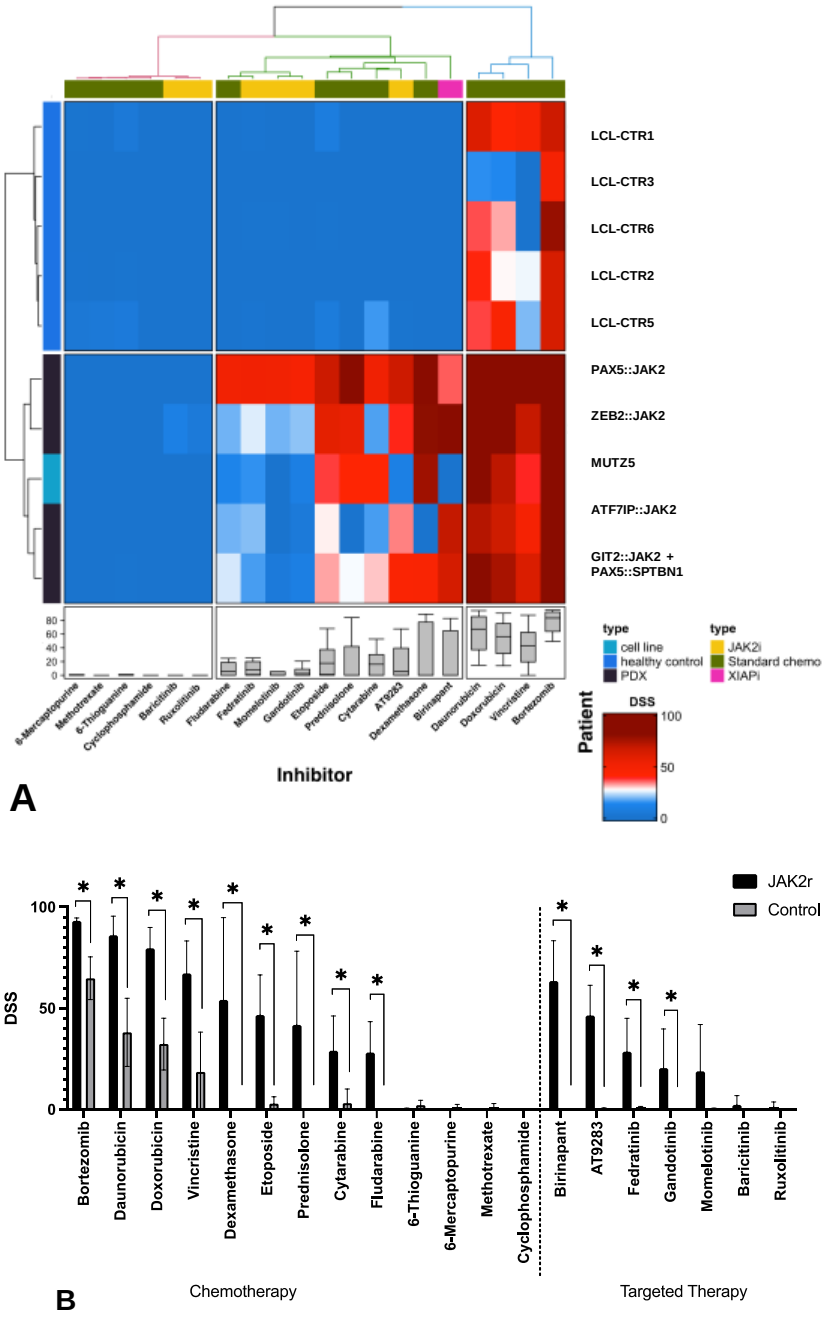

Figure 7. Drug screening results on PDXs carrying JAK2 rearrangements. A. Unsupervised clustering of 4 JAK2r, one positive control (MUTZ5 cell line) and 5

healthy controls (LCLs) expressing the DSS values proportional to the efficacy of a group of standard chemotherapy drugs currently used in the AIEOP BFM 2017 protocol, and a group of inhibitors known to target JAK. **B**. Mean of DSS values of 4 PDXs per drug, with comparison of responses between treated 4 JAK2r and treated 5 LCLs controls. P values: *p<0.05; **p<0.01; ***p<0.001.

DISCUSSION

JAK2 rearrangements (JAK2r) represent about 5% of pediatric Philadelphia-like patients (Tran and Tasian, 2021) and still lacks their specific inhibitors. To target JAK2 alterations, type-I and type-II tyrosine kinase inhibitors are available. As Ruxolitinib, type I-TKI, showed limitations in JAK2 alterations treatments (Roberts, et al. 2012; Maude, et al. 2012; Tvorogov, et al. 2018), we focused on CHZ868, type-II TKI, as it showed to be effective on JAK2 mutations (Meyer, et al. 2015; Wu, et al. 2015), for the treatment of JAK2 rearrangements, aiming to demonstrate CHZ868 specificity for the JAK2r subgroup of Ph-like.

By NGS sequencing we defined a cohort of 13 pediatric patients carrying *JAK2* fusions, in which we evaluated that JAK2 maintains its catalytic domain at 3', having known (ZEB2::JAK2, GIT2::JAK2, TLE4::JAK2, RAB7A::JAK2, MPRIP::JAK) and already described (PAX5, ATF7IP,) partner genes . A subset of primary samples, according to material availability, has been *in-vivo* expanded in a xenograft NSG murine model, to obtain enough cells to proceed with our *ex-vivo* experiments.

We demonstrated, by phosphoflow, that JAK2 rearrangements are defined by a basal hyperphosphorylation of JAK2/STATs pathway, compared both to positive controls, defined by CRLF2 rearrangements

and JAK2 mutations, know to activate JAK/STAT pathway (Savino, et al. 2017), and to negative controls, wild type for JAK/STAT pathway, confirming the role of JAK2 fusions. We determined monotherapy efficacy of CHZ868 at 100-fold lower dosages than ruxolitinib, with patient specific IC50s, in 48h treatments of co-culture of blasts cells on HBMS layers. We included ruxolitinib as it currently involved in clinical trials in the subset of Philadelphia-like positive adolescents and young adults, with rCRLF and mJAK2 (clinicaltrials.gov NCT02723994), and pediatric patients with the same genetic subtypes (clinicaltrials.gov NCT03571321). We also included dexamethasone as a standard chemotherapy drug currently used in the AIEOP BFM 2017 protocol for pediatric ALL, to evaluate its combination effect with the two chosen TKIs. To check CHZ868 specificity on JAK2 related pathway, we did a phosphoflow on blast cells, observing that CHZ868 significantly downregulates JAK/STAT pathway with more specificity and efficacy on pJAK2 compared to ruxolitinib, which instead showed higher affinity for pSTAT5 at short time point. After 48h of treatment, CHZ868 maintains its activity on p JAK2 on all the patients, while ruxolitinib has not effect on PAX5::JAK2 setting. To note, due to the presence of PAX5 in the fusion, both the TKIs loose effect on p STAT5 and p STAT3 in patient 1 carrying the PAX5::JAK2 fusion compared to untreated cells, has PAX5 rearrangements are known to hyperactivate STAT5 (Cazzaniga, et al. 2015). Moreover, also PI3K-AKT pathway was downregulated, at higher levels in CHZ868 treatment than ruxolitinib treatment, showing that JAK2 TKIs regulates not only overexpressed JAK/STAT pathway but also AKT pathway in JAK2r.

Demonstrated CHZ868 high specificity for JAK2, we combined CHZ868 with ruxoltinib and dexamethasone, observing the apoptosis induction after 48h of treatment. The combination of CHZ868 and ruxolitinib was synergistic in all the three patients, indicating a combinatorial approach of targeting on both active (ruxolitinib) and inactive (CHZ868) JAK2 conformation, leading to cell death. The combination with dexamethasone were less effective as patient 2 (ATF7IP::JAK2) and 3 (ZEB2::JAK2) were resistant to dexamethasone. To note, even though patient 3 was resistant, in the combination with CHZ868 we observed an additive effect, which is a promising result to consider for CHZ868 introduction in trials with resistant patient to standard chemotherapy drugs.

As we previously demonstrated that PAX5 fusions can be targeted by BIBF1120 leading to PI3K-AKT pathway inhibition (Fazio, et al. 2022), we demonstrated its efficacy in patient 1 (PAX5::JAK2), having also an additive effect in combination with either CHZ868 or ruxolitinib.

It was previously demonstrated that cell lines carrying JAK2 mutations undergo autophagy when treated with ruxolitinib, with consequent reduction of apoptosis, that could be increase combining the TKI with autophagy inhibitors (Machado-Neto, et al. 2020). Interestingly, we observed an autophagic mechanism of escape to ruxolitinib treatment in PAX5::JAK2 blasts, as LC3-II levels are significantly higher than untreated cells. Moreover, the combination of ruxolitinib and chloroquine, which is an autophagy inhibitor, led to an apoptotic increase compared to ruxolitinib single treatment, while in CHZ868 treated blasts we couldn’t observe any autophagy evidence. It is

important to consider as PAX5::JAK2 fusion is among the most frequent in B-ALL pediatric patients, therefore CHZ868 should be favored for their treatment rather than ruxolitinib.

We also set up an *in-vivo* targeting of JAK2 fusions demonstrating the efficacy of CHZ868 in a xenograft mouse model derived from blasts carrying JAK2 fusions. We decided not to test ruxolitinib *in-vivo* because we already proved that it not effective on leukemic cells even at very high concentration, whereas CHZ868 had higher *ex-vivo* efficacy at 100-fold lower dosages. Overall, CHZ868 proved to significantly reduce CD10+CD19+ positive blasts in bone marrow, meninges and peripheral blood of mice treated. Remarkably, CHZ868 showed high efficacy on spleens, reducing not only leukemic blasts, but also spleen weight, important aspect to consider in patients with JAK2 alterations characterized by splenomegaly (Song, et al. 2018). Moreover, it downregulated the phosphorylation of JAK2 and STAT5 in all patients, confirming that JAK/STAT pathway is the main involved pathway in JAK2 rearrangements. Moreover, it overcame the hyperphosphorylation of STATs that was observed in long *ex-vivo* exposure in blasts carrying the PAX5::JAK2 fusion. PI3K pathway, except from pAKTS473, and MAPK pathways were not involved.

Furthermore, we investigated also other available compounds that can act as inhibitors targeting JAK2/JAK2 pathway, and thus that could be considered for the treatment of this specific subgroup pf patients. Therefore, we applied a wide high-throughput ex-vivo drug screening using a library of 174 FDA approved drugs and inhibitors in early to late clinical trials. Four PDXs carrying JAK2 fusions have been targeted for 72h (PAX5::JAK2, ZEB2::JAK2, ATF7IP::JAK2, GIT2::JAK2

respectively). Differential drug sensitivity score (dDSS), assessed comparing JAK2r responses to control B-cell lymphoblastoid cell lines (LCLs), derived from healthy donors, led us to identify, among the TKIs inhibitors related to JAK targeting, AT9283 as the most effective specifically on JAK2r (Dawson, et al. 2010), as it didn't show an effect on JAK2m. Moreover, also Birinapant, which already demonstrated its efficacy on CRLF2 translocations (Richmond, et al. 2016), is among the top candidates not belonging to JAK2 inhibitors, for JAK2r. Conversely, even though ruxolitinib is currently tested in clinical trials for JAK2r, it didn't show any effect on our JAK2r patients. AT9283 and Birinapant may be considered for future preclinical validations on JAK2r. To note, the fusion PAX5::JAK2 revealed to be the most sensitive to most of the screened drugs, an important consideration for its more feasible treatment with several already available drugs in pediatric patients of BCP-ALL.

To note, our drug screening may be the starting point of novel preclinical models for JAK2 fusions.

In conclusion our findings showed the good potential of CHZ868 both in monotherapy and in combination with other kinase inhibitors as ruxolitinib and BIBF1120, in *ex-vivo* and *in-vivo* settings on JAK2r leukemia. It may be considered as an appealing candidate for a targeted therapy of JAK2 rearrangements in pediatric BCP-ALL.

SUPPLEMENTARY MATERIALS

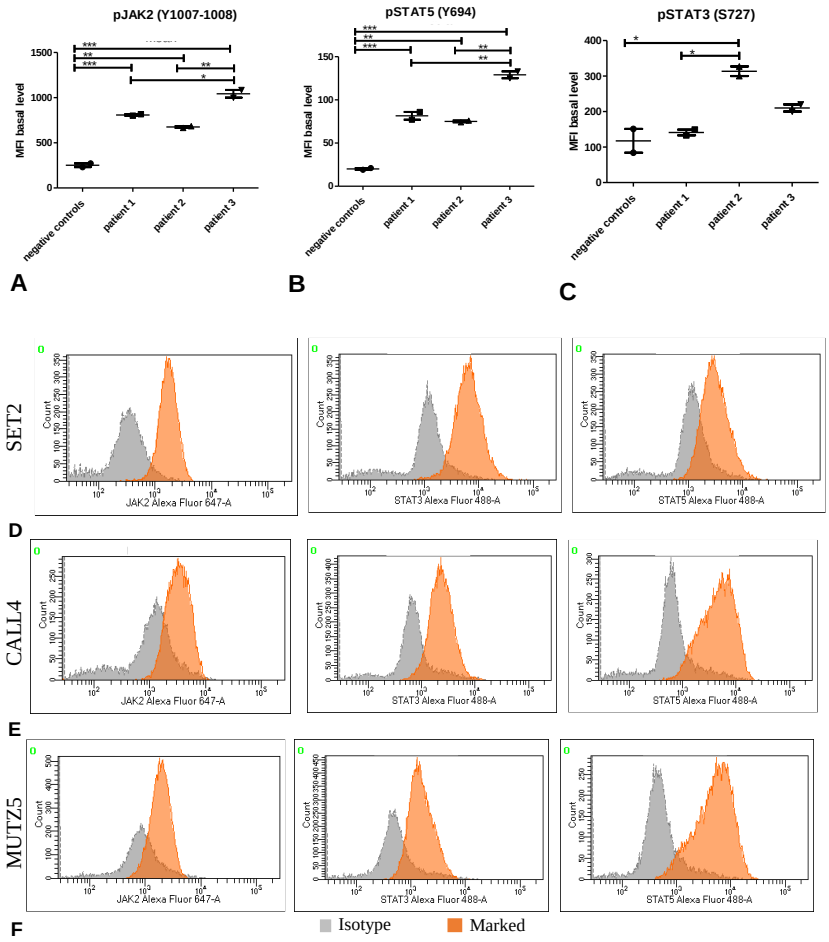

Supplementary figure S1. A-C. Basal level of phosphorylation of pJAK2 (Y1007-1008) (A), pSTAT5 (Y694) (B), pSTAT3 (S727) (C) of three patients carrying a JAK2 fusion compared to negative controls, wild type for JAK2 and negative for any fusion gene. P values: *p<0.05; **p<0.01; ***p<0.001. **D-F.** Representation of SET2 (D), CALL4 (E) and MUTZ5 (F) cell lines basal level expression of pJAK2 (Y1007-1008), pSTAT5 (Y694) and pSTAT3 (S727) compared to isotypes controls.

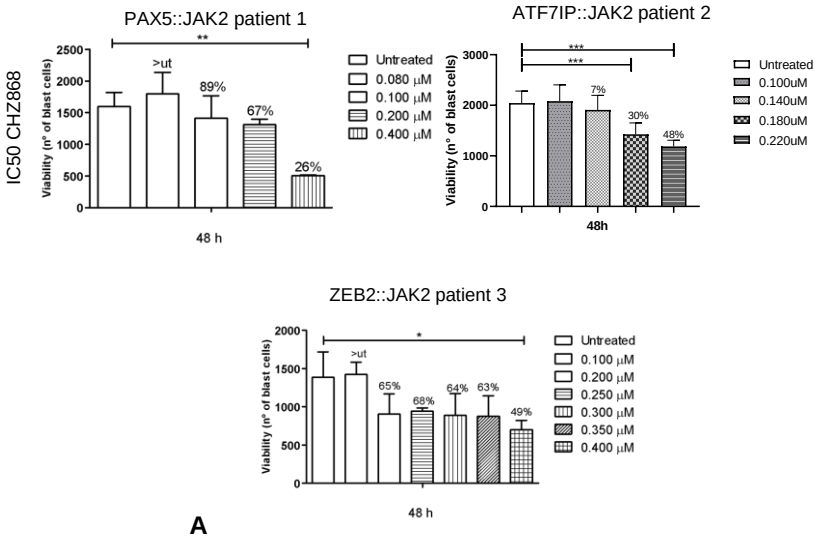

A

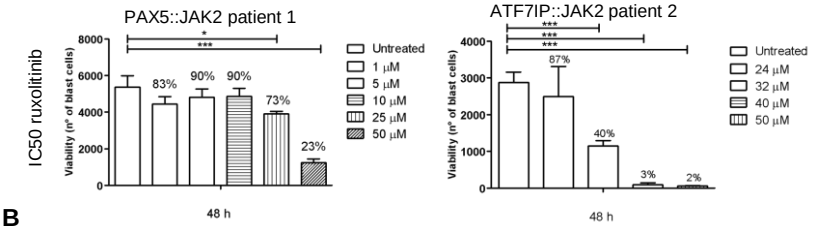

B

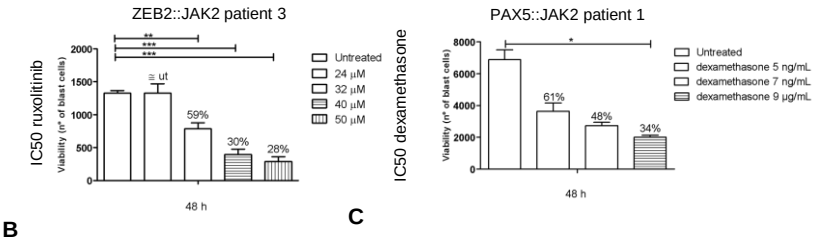

B **C**

Patients fusions	Drug	CHZ868			ruxolitinib			dexamethasone		
	Doses	Lower	IC50	Higher	Lower	IC50	Higher	Lower	IC50	Higher
Patient 1 PAX5::JAK2		0,193μM	0,270μM	0,347μM	24μM	32μM	40μM	5ng/ mL	7ng/ mL	9ng/ mL
Patient 1 ATF7IP::JAK2		0,193μM	0,270μM	0,347μM	24μM	30μM	38μM	5ng/ mL	7ng/ mL	9ng/ mL
Patient 1 ZEB2::JAK2		0,241μM	0,338μM	0,438μM	28μM	40μM	50μM	5ng/ mL	7ng/ mL	9ng/ mL

D

Supplementary figure S2. Evaluation of monotherapy treatments with CHZ868, ruxolitinib and dexamethasone on JAK2 rearranged patients expressed as viability of blasts, derived as difference from apoptosis and necrosis in Annexin V-PE/7AAD staining, treated for 48h in co-culture on HBMS. A. Three experiments of monotherapy treatment with CHZ868 on patient 1 (PAX5::JAK2), patient 2 (ATF7IP::JAK2) and patient 3 (ZEB2::JAK2). **B.** Three experiments of monotherapy treatment with ruxolitinib on patient 1 (PAX5::JAK2), patient 2 (ATF7IP::JAK2) and patient 3 (ZEB2::JAK2). **C.** Monotherapy treatment with CHZ868 on patient 1 (PAX5::JAK2). **D**. Table indicating patient specific IC50s for each drug, and additional lower and higher doses used for the ex-vivo experiments. N=3 experiments, in technical duplicate. P values: *p<0.05; **p<0.01; ***p<0.001.

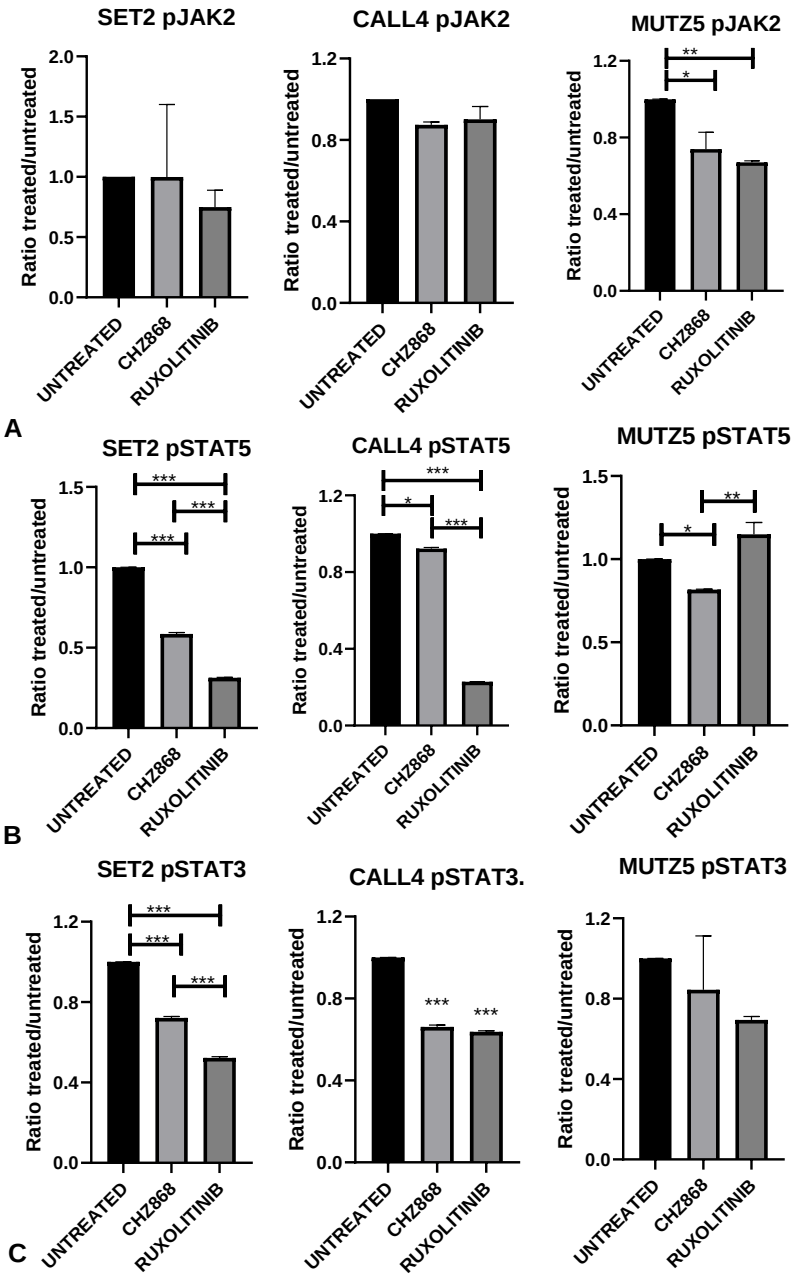

Supplementary figure S3. Targeting of cell lines with tyrosine kinase inhibitors for 30 minutes, evaluating the phopshorylation levels on JAK2/STATs pathway by phosphoflow. A. CHZ868 (300nM) and ruxolitinib (30uM) targeting of pJAK2 (Y1007-1008) in SET2, CALL4 and MUTZ5 for 30 minutes. **B.** CHZ868 (300nM)

and ruxolitinib (30uM) targeting of pSTAT5 (Y694) in SET2, CALL4 and MUTZ5 for 30 minutes **C.** CHZ868 (300nM) and ruxolitinib (30uM) targeting of pSTAT3 (S727) in SET2, CALL4 and MUTZ5 for 30 minutes **D-F**. N=3 experiments. P values: *p<0.05; **p<0.01; ***p<0.001.

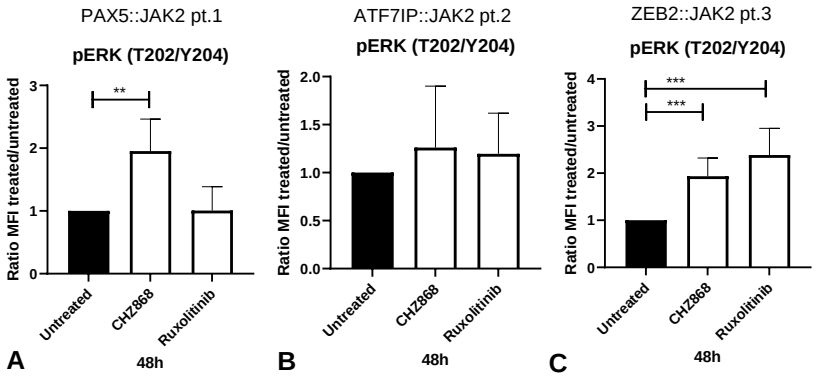

Supplementary figure S4. Mean fluorescence intensity (MFI) inhibition of pERK(T202/Y204) after 48h of TKIs treatments on patient 1 (PAX5::JAK2) (**A**), patient 2 (ATF7IP::JAK2) (**B**) and patient 3 (ZEB2::JAK2) (**C**) blasts in co-culture on HBMS, evaluated by phosphoflow. P values: *p<0.05; **p<0.01; ***p<0.001. N=3 experiments, in technical duplicate.

CI<1	SYNERGY
CI=1	ADDITIVISM
CI>1	ANTAGONISM

	IC50 COMBINATION INDEX		
PATIENT	CHZ868+RUXOLITINIB	CHZ868+DEXAMETHASONE	RUXOLITINIB+DEXAMETHASONE
PAX5::JAK2	0,93	0,87	0,69
ATF7IP::JAK2	0,83	4,17	1
ZEB2::JAK2	0,74	0,62	0,72

A

	IC50 COMBINATION INDEX		
PATIENT	CHZ868+RUXOLITINIB	CHZ868+DEXAMETHASONE	RUXOLITINIB+DEXAMETHASONE
Positive Control 1	0,67	0	0,47
Positive Control 2	0,8	0,78	0,98
Negative Control 1	0,71	0,95	1,16
Negative Control 2	2,14	0,93	0,85

B

Supplementary Table 3. Combination Index tables for JAK2 rearranged patients (**A**), and positive and negative controls (**B**).

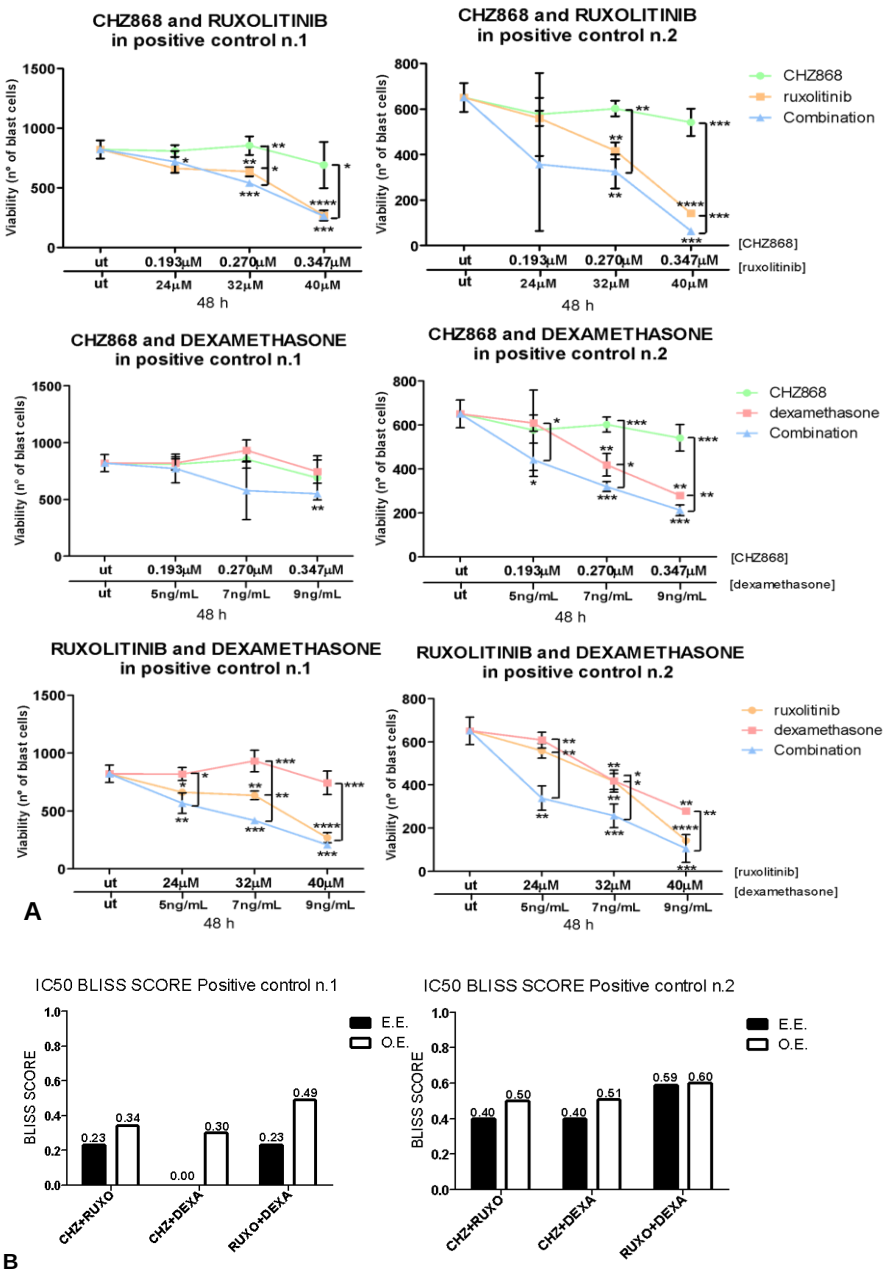
CHZ868 and RUXOLITINIB
in positive control n.1
CHZ868 and RUXOLITINIB
in positive control n.2
CHZ868
ruxolitinib
Combination
Viability (n° of blast cells)
ut
0.193µM
0.270µM
0.347µM
24µM
32µM
40µM
[CHZ868]
[ruxolitinib]
48 h
CHZ868 and DEXAMETHASONE
in positive control n.1
CHZ868 and DEXAMETHASONE
in positive control n.2
CHZ868
dexamethasone
Combination
5ng/mL
7ng/mL
9ng/mL
[CHZ868]
[dexamethasone]
RUXOLITINIB and DEXAMETHASONE
in positive control n.1
RUXOLITINIB and DEXAMETHASONE
in positive control n.2
ruxolitinib
dexamethasone
Combination
[ruxolitinib]
[dexamethasone]
A
IC50 BLISS SCORE Positive control n.1
IC50 BLISS SCORE Positive control n.2
BLISS SCORE
E.E.
O.E.
0.23
0.34
0.00
0.30
0.23
0.49
0.40
0.50
0.40
0.51
0.59
0.60
CHZ+RUXO
CHZ+DEXA
RUXO+DEXA
B

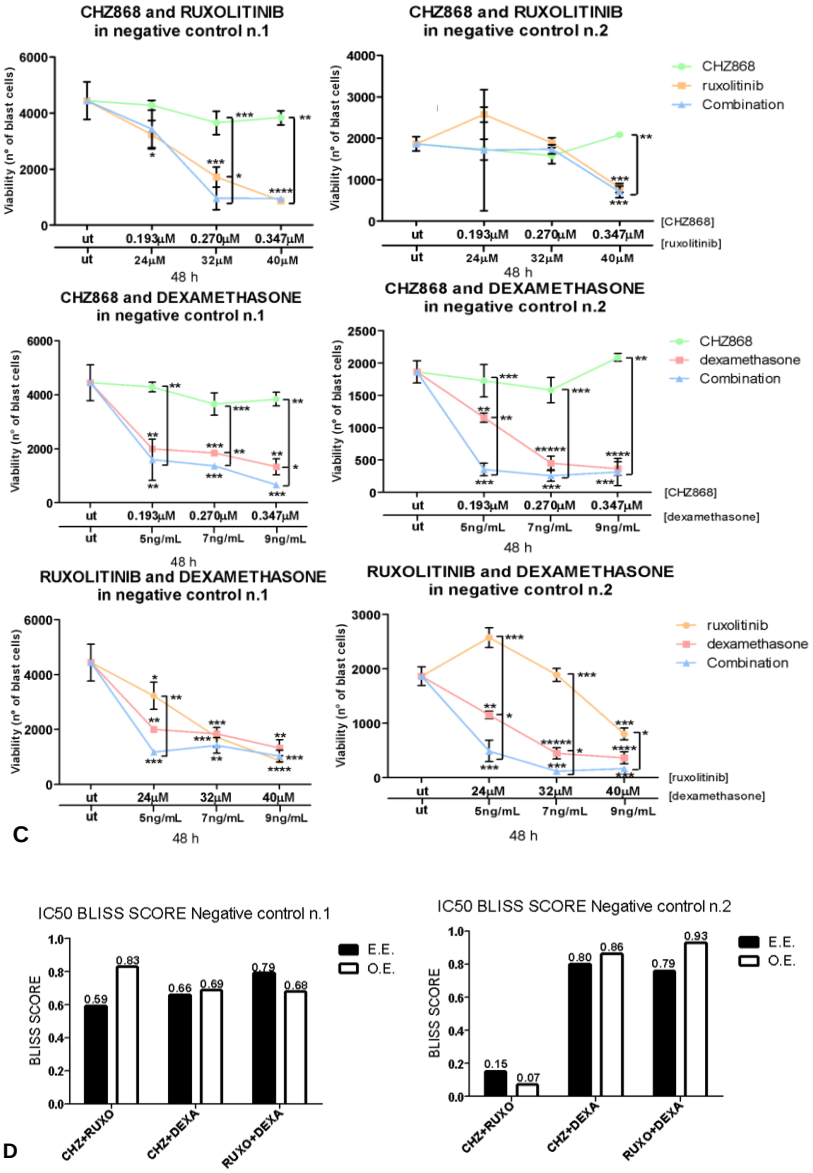

Supplementary figure S5. Apoptosis/viability assays of combination of pairs of drugs, given at three different dosages, on primary blasts of positive and negative controls, treated for 48h in co-culture on HBMS. Viability was asses from apoptosis and necrosis after staining with Annexin V-PE/7AAD. A. Combinations on two positive controls, carrying CRLF2 rearrangements and a JAK2 mutation. **B**. Combinations on two negative controls. **C**. Bliss score of the combinations in pair of

the drugs, comparing expected event (EE) and observed event (OE), to evaluate synergy, additive or antagonism. P values: *p<0.05; **p<0.01; ***p<0.001. N=3 experiments, in technical duplicate.

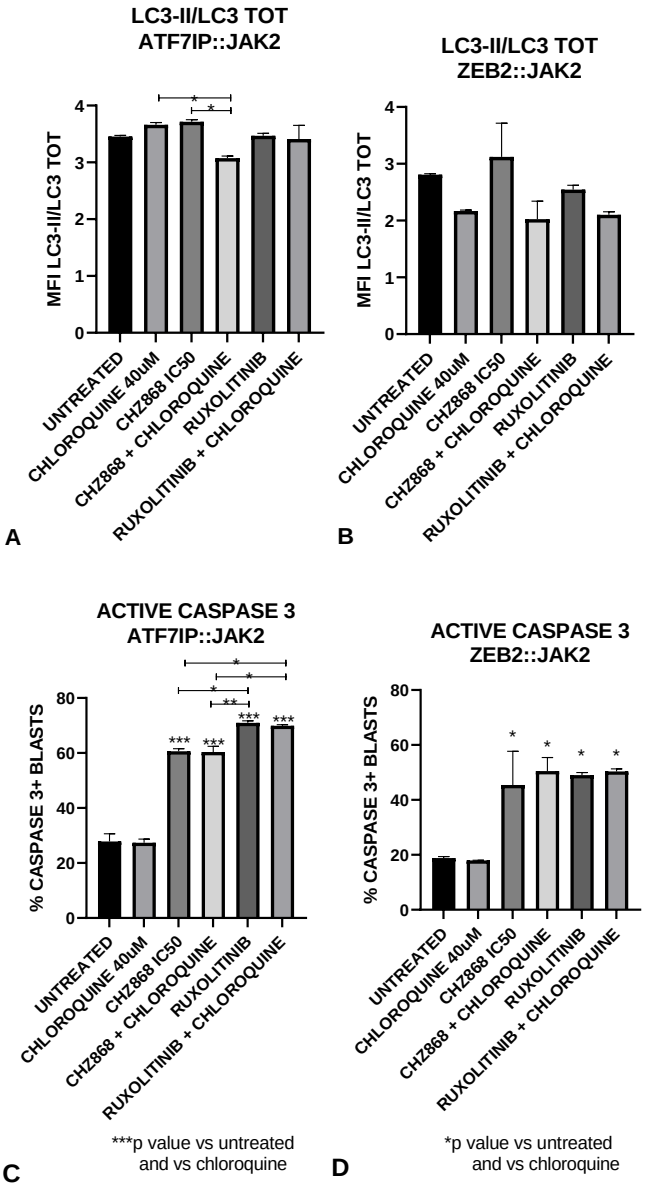

Supplementary figure S6. Autophagy evaluation on two patient's blasts carrying JAK2 fusions. A-B. LC3II expression, indicated as MFI ratio on LC3 total, on untreated and treated blasts in co-culture on HBMS for 44h + 4h with chloroquine, in patient 2 (ATF7IP::JAK2) (A) and patient 3 (ZEB2::JAK2) (B). N=3, 1 representative experiment shown. **C-D**. % of blast cells positive to the active caspase 3 after treatment with TKIs, BIBF1120 and chloroquine, indicating cells in apoptosis due to drug efficacy. N=3, 1 rappresentative experiment shown.

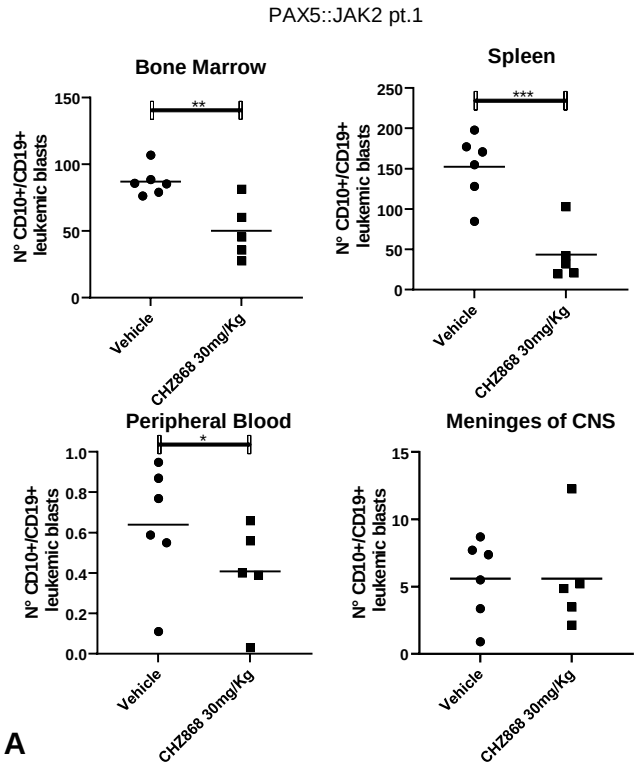

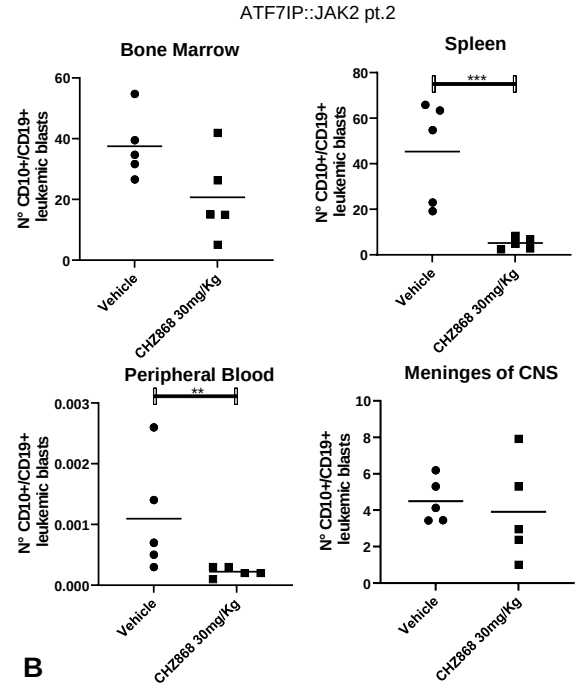
ATF7IP::JAK2 pt.2
Bone Marrow
Spleen
Peripheral Blood
Meninges of CNS
N° CD10+/CD19+ leukemic blasts
Vehicle
CHZ868 30mg/Kg
***
**
B

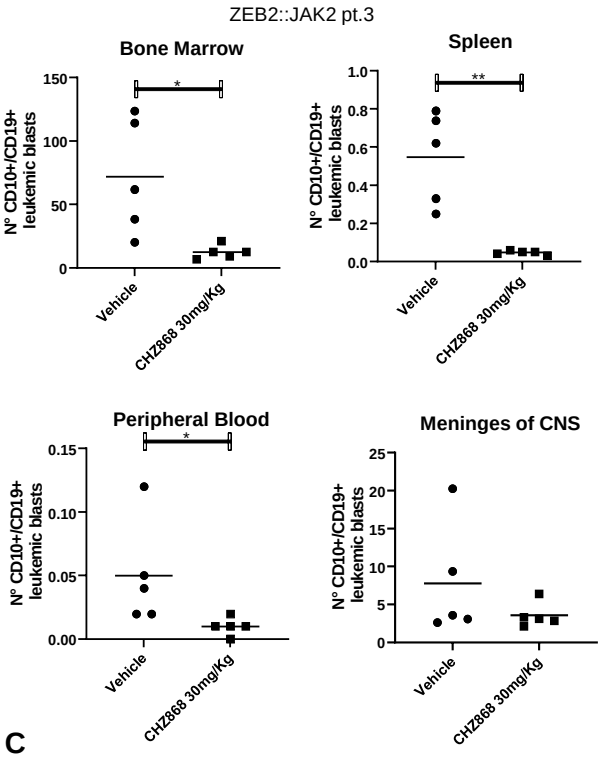
ZEB2::JAK2 pt.3
Bone Marrow
Spleen
Peripheral Blood
Meninges of CNS
N° CD10+/CD19+ leukemic blasts
Vehicle
CHZ868 30mg/Kg
*
**
C

Supplementary figure S7. In vivo CHZ868 treatment of mice xenotransplanted with blasts carrying JAK2r. A. Reduction of the n° of CD10+CD19+ leukemic blasts in CHZ868 treated mice compared to vehicle, in bone marrow, spleen, peripheral blood and meninges, in PAX5::JAK2 setting (A), ATF7IP::JAK2 setting (B) and ZEB2::JAK2 setting (C). P values: *p<0.05; **p<0.01; ***p<0.001. At least N=5 mice for each group.

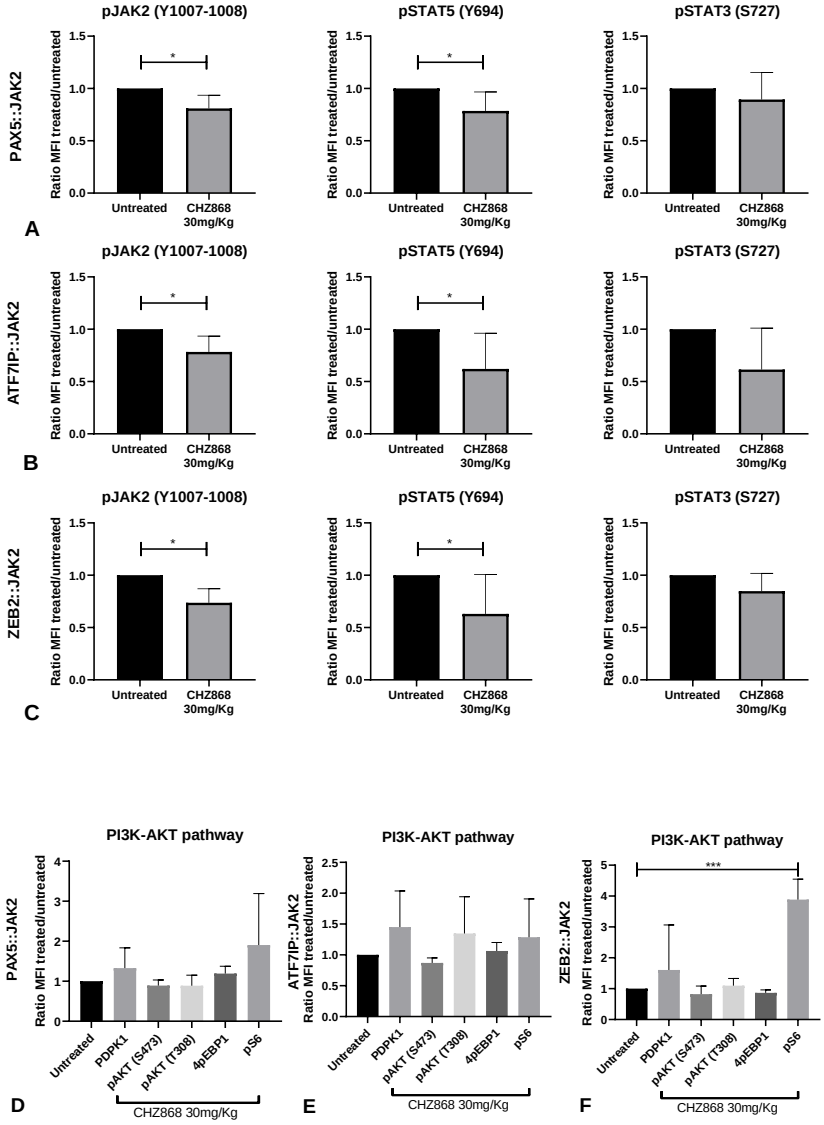

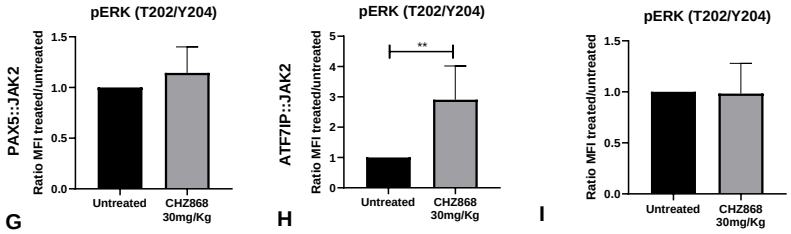

Supplementary figure S8. Mean fluorescence intensity (MFI) inhibition of JAK2 related downstream pathways after in-vivo treatment with CHZ868, evaluated by phosphoflow. A. pJAK2 (Y1007-1008), pSTAT5 (Y694) and pSTAT3 (S727) inhibition after CHZ868 in-vivo treatment of patient 1 PAX5:.JAK2 fusion setting. **B**. pJAK2 (Y1007-1008), pSTAT5 (Y694) and pSTAT3 (S727) inhibition after CHZ868 in-vivo treatment of patient 2 ATF7IP:.JAK2 fusion setting. **C**. pJAK2 (Y1007-1008), pSTAT5 (Y694) and pSTAT3 (S727) inhibition after CHZ868 in-vivo treatment of patient 3 ZEB2:.JAK2 fusion setting. **D**. PI3K-AKT pathway effectors inhibition [PDPK1, pAKT (S473), pAKT (T308), 4pEBP1, pS6] after CHZ868 in-vivo treatment on patient 1 PAX5:.JAK2 setting. **E**. PI3K-AKT pathway effectors inhibition [PDPK1, pAKT (S473), pAKT (T308), 4pEBP1, pS6] after CHZ868 in-vivo treatment on patient 2 ZEB2:.JAK2 setting. **F**. PI3K-AKT pathway effectors inhibition [PDPK1, pAKT (S473), pAKT (T308), 4pEBP1, pS6] after CHZ868 in-vivo treatment on patient 3 ATF7IP:.JAK2 setting. **G**. pERK (T202/Y204) inhbiition after CHZ868 in-vivo treatment on patient 1 PAX5::JAK2 setting. **H**. pERK (T202/Y204) upregulation after CHZ868 in-vivo treatment on patient 2 ATF7IP::JAK2 setting. **I**. pERK (T202/Y204) inhbiition after CHZ868 in-vivo treatment on patient 3 ZEB2::JAK2 setting. P values: *p<0.05; **p<0.01; ***p<0.001. At least N=5 per group.

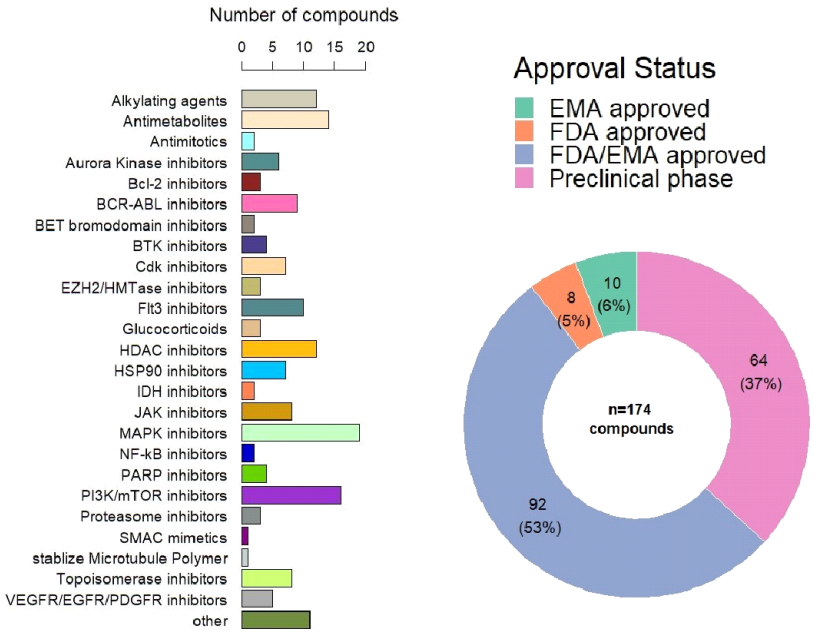

Supplementary figure S9. Subdivision in groups of FDA/EMA approved, or in preclinical phase, drugs and compounds used for the high throughput drug screening.

primer	lenght (bp)	sequence 5' - 3'	Fusion Breakpoint	Patients
PAX5ex3_F	20	ACGCCAAAATCCCACCATGT	PAX5ex5-JAK2ex19	Pt. 1, Pt.5, Pt.6, Pt.10, Pt.11, Pt.12
JAK2ex20_R	20	AGCACTGTAGCACACTCCCT		
ATF7IPex10_F	25	AACCCATACAACCAGCACCGCCTCT	ATF7IPex12-JAK2ex19	Pt.2
JAK2ex20_R	25	CGGCACATCTCCACACTCCCAAAAT		
ZEB2ex_9F	20	AGACTCCGACTCCTGTCTGT	ZEB2ex9-JAK2ex19	Pt.3
JAK2ex_20R	20	AGCACTGTAGCACACTCCCT		
GIT2ex11_F	20	AACGGTCGTCCCCTTTCTTC	GIT2ex13-JAK2ex19	Pt.4
JAK2ex20_R	20	AGCACTGTAGCACACTCCCT		
MPRIPex 9_F	21	ACATCAGCAGGTTGAAGGAGC	MPRIPex10-JAK2ex11	Pt.7; Pt.8
JAK2ex11_R	20	GCTTTGGGGGACAGCATTTA		
TLE4ex7_F	20	GCTCTAGGAGGTCAGTCCCA	TLE4ex10-JAK2ex19	Pt.9
JAK2ex20_R	20	AGCACTGTAGCACACTCCCT		
RAB7Aex1_F	20	GTTTAGTCTCCTCCTCGGCG	RAB7Aex1--JAK2ex11	Pt.11
JAK2ex12_R	20	TGCAGTTGACCGTAGTCTCC		

Supplementary Table 1. Primers used for validation of fusion involving JAK2.

Patient	Age	Phenotype	Blast %	MRD stratification	Protocol	JAK2 fusion gene
pt.1	2	B-III	80	medium risk	2009	chr9-chr9 PAX5-JAK2
pt.2	6	B-II	nk	medium risk	2009	chr12-chr9 ATF7IP-JAK2
pt.3	16	B-II	nk	medium risk	2000-R2006	chr2-chr9 ZEB2/JAK2
pt.4	11	B-II	89	high risk	2017	chr12-chr9 GIT2/JAK2 + chr2-chr9 PAX5/SPTBN1
pt.5	2	B-II	60	standard risk	2017	chr9-chr9 PAX5-JAK2
pt.6	14	B-II	70	early high risk	2017	chr9-chr9 PAX5-JAK2
pt.7	12	B-II	60	standard risk	2017	chr9-chr17 MPRIP--JAK2
pt.8	14	B-II	nk	medium risk	2000-R2006	chr9-chr17 MPRIP/JAK2
pt.9	15	B-II	53	high risk	2009	chr9-chr9 TLE4/JAK2
pt.10	17	B-II	80	high risk	2017	chr9-chr9 PAX5-JAK2
pt.11	5	B-III	60	high risk	2017	chr3-chr9 RAB7A/JAK2
pt.12	12	B-II	95	high risk	2017	chr9-chr9 PAX5-JAK2
pt.13	4	B-II	82	early high risk	2017	chr9-chr9 PAX5-JAK2

Supplementary Table 2. Cohort of JAK2r patients identified by NGS, with summary of the main clinical characteristics.

REFERENCES

Beck B, Chen YF, Dere W, et al. Assay Operations for SAR Support. 2012 May 1 [updated 2017 Nov 20]. Assay Guidance Manual [Internet]. Bethesda (MD): Eli Lilly & Company and the National Center for Advancing Translational Sciences; 2004–.

Bhatia S, Diedrich D, Frieg B, et al. Targeting HSP90 dimerization via the C terminus is effective in imatinib-resistant CML and lacks the heat shock response. Blood. 2018 Jul 19;132(3):307-320. doi: 10.1182/blood-2017-10-810986.

Boer, J.M., Steeghs, E.M., Marchante, et al. (2017) Tyrosine kinase fusion genes in pediatric BCR-ABL1-like acute lymphoblastic leukemia. *Oncotarget,* **8,** 4618-4628

Bose P, Verstovsek S. JAK Inhibition for the Treatment of Myelofibrosis: Limitations and Future Perspectives. Hemasphere. 2020 Jul 21;4(4):e424. doi: 10.1097/HS9.0000000000000424.

Bourquin JP, Izraeli S. Where can biology of childhood ALL be attacked by new compounds? Cancer Treat Rev. 2010 Jun;36(4):298-306. doi: 10.1016/j.ctrv.2010.02.005.

Cazzaniga V, Bugarin C, Bardini M, Giordan M, te Kronnie G, Basso G, Biondi A, Fazio G, Cazzaniga G. LCK over-expression drives STAT5 oncogenic signaling in PAX5 translocated BCP-ALL patients. Oncotarget. 2015 Jan 30;6(3):1569-81. doi: 10.18632/oncotarget.2807.

Cheng Y, Prusoff WH. Relationship between the inhibition constant (K1) and the concentration of inhibitor which causes 50 per cent inhibition (I50) of an enzymatic reaction. Biochem Pharmacol. 1973 Dec 1;22(23):3099-108. doi: 10.1016/0006-2952(73)90196-2.

Chou TC. Theoretical basis, experimental design, and computerized simulation of synergism and antagonism in drug combination studies. Pharmacol Rev. 2006 Sep;58(3):621-81. doi: 10.1124/pr.58.3.10.

Conter V, Aricò M, Basso G, et al. Long-term results of the Italian Association of Pediatric Hematology and Oncology (AIEOP) Studies 82, 87, 88, 91 and 95 for childhood acute lymphoblastic leukemia. Leukemia. 2010 Feb;24(2):255-64. doi: 10.1038/leu.2009.250.

Dawson MA, Curry JE, Barber K, et al. AT9283, a potent inhibitor of the Aurora kinases and Jak2, has therapeutic potential in myeloproliferative disorders. Br J Haematol. 2010 Jul;150(1):46-57. doi: 10.1111/j.1365-2141.2010.08175.x. Epub 2010 May 7.

Den Boer ML, van Slegtenhorst M, De Menezes RX, et al. A subtype of childhood acute lymphoblastic leukaemia with poor treatment outcome: a genome-wide classification study. Lancet Oncol. 2009 Feb;10(2):125-34. doi: 10.1016/S1470-2045(08)70339-5. Epub 2009 Jan 8.

Ehrentraut S, Nagel S, Scherr ME, et al. t(8;9)(p22;p24)/PCM1-JAK2 activates SOCS2 and SOCS3 via STAT5. PLoS One. 2013;8(1):e53767. doi: 10.1371/journal.pone.0053767. Epub 2013 Jan 23.

Fazio G, Bresolin S, Silvestri D, et al. PAX5 fusion genes are frequent in poor risk childhood acute lymphoblastic leukaemia and can be targeted with BIBF1120. EBioMedicine. 2022 Sep;83:104224. doi: 10.1016/j.ebiom.2022.104224. Epub 2022 Aug 16.

Greco WR, Bravo G, Parsons JC. The search for synergy: a critical review from a response surface perspectivee. Pharmacol Rev. 1995 Jun;47(2):331-85.

Grioni A, Fazio G, Rigamonti S, et al. A Simple RNA Target Capture NGS Strategy for Fusion Genes Assessment in the Diagnostics of Pediatric B-cell Acute Lymphoblastic Leukemia. Hemasphere. 2019 Jun 4;3(3):e250. doi: 10.1097/HS9.0000000000000250.

Harrison CJ. Acute lymphoblastic leukaemia. Best Pract Res Clin Haematol. 2001 Sep;14(3):593-607. doi: 10.1053/beha.2001.0156.

Harrison CN, Mead AJ, Panchal A, et al. Ruxolitinib vs best available therapy for ET intolerant or resistant to hydroxycarbamide. Blood. 2017 Oct 26;130(17):1889-1897. doi: 10.1182/blood-2017-05-785790.

Herold T, Gökbuget N. Philadelphia-Like Acute Lymphoblastic Leukemia in Adults. Curr Oncol Rep. 2017 May;19(5):31. doi: 10.1007/s11912-017-0589-2.

Inaba H, Greaves M, Mullighan CG. Acute lymphoblastic leukaemia. Lancet. 2013 Jun 1;381(9881):1943-55. doi: 10.1016/S0140-6736(12)62187-4. Epub 2013 Mar 22.

Inaba H, Pui CH. Advances in the Diagnosis and Treatment of Pediatric Acute Lymphoblastic Leukemia. J Clin Med. 2021 Apr 29;10(9):1926. doi: 10.3390/jcm10091926.

Koppikar P, Bhagwat N, Kilpivaara O, et al. Heterodimeric JAK-STAT activation as a mechanism of persistence to JAK2 inhibitor therapy. Nature. 2012 Sep 6;489(7414):155-9. doi: 10.1038/nature11303.

Machado-Neto JA, Coelho-Silva JL, Santos FPS, Scheucher PS, Campregher PV, Hamerschlak N, Rego EM, Traina F. Autophagy inhibition potentiates ruxolitinib-induced apoptosis in JAK2^{V617F} cells. Invest New Drugs. 2020 Jun;38(3):733-745. doi: 10.1007/s10637-019-00812-5. Epub 2019 Jul 8.

Maude SL, Tasian SK, Vincent T, et al. Targeting JAK1/2 and mTOR in murine xenograft models of Ph-like acute lymphoblastic leukemia. Blood. 2012 Oct 25;120(17):3510-8. doi: 10.1182/blood-2012-03-415448. Epub 2012 Sep 6

Meyer SC, Keller MD, Chiu S, et al. CHZ868, a Type II JAK2 Inhibitor, Reverses Type I JAK Inhibitor Persistence and Demonstrates Efficacy in Myeloproliferative Neoplasms. Cancer Cell. 2015 Jul 13;28(1):15-28. doi: 10.1016/j.ccell.2015.06.006.

Meyer SC, Keller MD, Chiu S, et al. CHZ868, a Type II JAK2 Inhibitor, Reverses Type I JAK Inhibitor Persistence and Demonstrates Efficacy in Myeloproliferative Neoplasms. Cancer Cell. 2015 Jul 13;28(1):15-28. doi: 10.1016/j.ccell.2015.06.006.

Mullighan CG. Genomic analysis of acute leukemia. Int J Lab Hematol. 2009 Aug;31(4):384-97. doi: 10.1111/j.1751-553X.2009.01167.x. Epub 2009 May 18.

Nguyen K, Devidas M, Cheng SC, La M, Raetz EA, et al. Children's Oncology Group. Factors influencing survival after relapse from acute lymphoblastic leukemia: a Children's Oncology Group study. Leukemia. 2008 Dec;22(12):2142-50. doi: 10.1038/leu.2008.251. Epub 2008 Sep 25

Richmond J, Robbins A, Evans K, et al. Acute Sensitivity of Ph-like Acute Lymphoblastic Leukemia to the SMAC-Mimetic Birinapant. Cancer Res. 2016 Aug 1;76(15):4579-91. doi: 10.1158/0008-5472.CAN-16-0523.

Roberts KG. The biology of Philadelphia chromosome-like ALL. Best Pract Res Clin Haematol. 2017 Sep;30(3):212-221. doi: 10.1016/j.beha.2017.07.003. Epub 2017 Jul 6.

Savino AM, Sarno J, Trentin L, et al. The histone deacetylase inhibitor givinostat (ITF2357) exhibits potent anti-tumor activity against CRLF2-rearranged BCP-ALL. Leukemia. 2017 Nov;31(11):2365-2375. doi: 10.1038/leu.2017.93.

Sebaugh JL. Guidelines for accurate EC50/IC50 estimation. Pharm Stat. 2011 Mar-Apr;10(2):128-34. doi: 10.1002/pst.426.

Shiraz P, Payne KJ, Muffly L. The Current Genomic and Molecular Landscape of Philadelphia-like Acute Lymphoblastic Leukemia. Int J Mol Sci. 2020 Mar 22;21(6):2193. doi: 10.3390/ijms21062193.

Song MK, Park BB, Uhm JE. Understanding Splenomegaly in Myelofibrosis: Association with Molecular Pathogenesis. Int J Mol Sci. 2018 Mar 18;19(3):898. doi: 10.3390/ijms19030898.

Tasian SK, Hurtz C, Wertheim GB, et al. High incidence of Philadelphia chromosome-like acute lymphoblastic leukemia in older adults with B-ALL. Leukemia. 2017 Apr;31(4):981-984. doi: 10.1038/leu.2016.375. Epub 2016 Dec 9.

Tran TH, Tasian SK. Has Ph-like ALL Superseded Ph+ ALL as the Least Favorable Subtype? Best Pract Res Clin Haematol. 2021 Dec;34(4):101331. doi: 10.1016/j.beha.2021.101331. Epub 2021 Oct 23.

Tvorogov D, Thomas D, Liau NPD, Dottore M, Barry EF, Lathi M, Kan WL, Hercus TR, Stomski F, Hughes TP, Tergaonkar V, Parker MW, Ross DM, Majeti R, Babon JJ, Lopez AF. Accumulation of JAK activation loop phosphorylation is linked to type I JAK inhibitor withdrawal syndrome in myelofibrosis. Sci Adv. 2018 Nov 28;4(11):eaat3834. doi: 10.1126/sciadv.aat3834.

Wu SC, Li LS, Kopp N, et al. Activity of the Type II JAK2 Inhibitor CHZ868 in B Cell Acute Lymphoblastic Leukemia. Cancer Cell. 2015 Jul 13;28(1):29-41. doi: 10.1016/j.ccell.2015.06.005.

Yadav B, Pemovska T, Szwajda A, et al. Quantitative scoring of differential drug sensitivity for individually optimized anticancer therapies. Sci Rep. 2014 Jun 5;4:5193. doi: 10.1038/srep05193.

Zhang Q, Shi C, Han L, et al. Inhibition of mTORC1/C2 signaling improves anti-leukemia efficacy of JAK/STAT blockade in *CRLF2* rearranged and/or *JAK* driven Philadelphia chromosome-like acute B-cell lymphoblastic leukemia. Oncotarget. 2018 Jan 17;9(8):8027-8041. doi: 10.18632/oncotarget.24261.

Zhao W, Sachsenmeier K, Zhang L, et al. A New Bliss Independence Model to Analyze Drug Combination Data. J Biomol Screen. 2014 Jun;19(5):817-21. doi: 10.1177/1087057114521867. Epub 2014 Feb 3.

Chapter 3

PAX5 fusion genes are frequent in poor risk childhood acute lymphoblastic leukaemia and can be targeted with BIBF1120

EBioMedicine 2022 Sep;83:104224. doi: 10.1016/j.ebiom.2022.104224. Epub 2022 Aug 16.

PAX5 fusion genes are frequent in poor risk childhood acute lymphoblastic leukaemia and can be targeted with BIBF1120

Grazia Fazio,[1] Silvia Bresolin,[2] Daniela Silvestri,[3] Manuel Quadri,[1] Claudia Saitta,[1] Elena Vendramini,[2] Barbara Buldini,[2] Chiara Palmi,[1] Michela Bardini,[1] Andrea Grioni,[1] Silvia Rigamonti,[1] Marta Galbiati,[1] Stefano Mecca,[1] Angela Maria Savino,[1,4] Alberto Peloso,[2] Jia-Wey Tu,[5] Sanil Bhatia,[5] Arndt Borkhardt,[5] Concetta Micalizzi,[6] Luca Lo Nigro,[7] Franco Locatelli,[8] Valentino Conter,[9] Carmelo Rizzari,[9] Maria Grazia Valsecchi,[3] Geertruij te Kronnie,[2] Andrea Biondi,[1,9], Giovanni Cazzaniga.[1,10]

1. Centro Ricerca M. Tettamanti, Paediatrics, University of Milano Bicocca, Monza, Italy
2. Paediatric Haematology, Oncology and Stem Cell Transplant Division, Women and Child Health Department, Padua University and Hospital, Padua, Italy
3. Centre of Biostatistics for Clinical Epidemiology, School of Medicine and Surgery, University of Milano-Bicocca, Monza, Italy.

4. Molecular Pharmacology Program, Memorial Sloan Kettering Cancer Center, New York, NY 10065, USA
5. Department of Paediatric Oncology, Haematology and Clinical Immunology, Heinrich-Heine University Dusseldorf, Medical Faculty, Düsseldorf, Germany
6. Haematology/Oncology Unit, G. Gaslini Children's Hospital, Genoa, Italy
7. Center of Paediatric Haematology Oncology, Azienda Ospedaliero-Universitaria "Policlinico Vittorio Emanuele", Catania, Italy.
8. Department of Paediatric Haematology/Oncology and Cell and Gene Therapy, IRCCS Ospedale Pediatrico Bambino Gesù, Department of Paediatrics, Sapienza University of Rome, Rome, Italy.
9. Paediatrics, University of Milano Bicocca, Fondazione MBBM/San Gerardo Hospital, Monza, Italy.
10. Medical Genetics, University of Milano Bicocca, School of Medicine and Surgery, Monza, Italy.

Correspondence to:
Fazio Grazia, grazia.fazio@unimib.it
Cazzaniga Giovanni, giovanni.cazzaniga@unimib.it
Centro Ricerca Tettamanti, University of Milano-Bicocca
Via Pergolesi 33 - 20900 Monza (MB), Italy
Tel. +39 (0)39 2333661

Running Title: PAX5 fusions in ALL are targeted with BIBF1120

ABSTRACT

Background

Despite intensive risk-based treatment protocols, 15% of paediatric patients with B-Cell Precursor Acute Lymphoblastic Leukaemia (BCP-ALL) experience relapse. There is urgent need of novel strategies to target poor prognosis subgroups, like PAX5 translocated.

Methods

We considered 289 childhood BCP-ALL cases consecutively enrolled in Italy in the AIEOP-BFM ALL2000/R2006 protocols and we performed extensive molecular profiling, integrating gene expression, copy number analyses and fusion genes discovery by target-capture NGS. We developed novel preclinical strategies to target PAX5 fusion genes.

Findings

We identified 135 cases without recurrent genetic rearrangements. Among them, 59 patients (43·7%) had a Ph-like signature; the remaining cases were identified as ERG-related (26%), High-Hyperdiploid-like (17%), ETV6::RUNX1-like (8·9%), MEF2D-rearranged (2·2%) or KMT2A-like (1·5%). A poor prognosis was associated with the Ph-like signature, independently from other high-risk features.

Interestingly, *PAX5* was altered in 54·4% of Ph-like compared to 16·2% of non-Ph-like cases, with 7 patients carrying *PAX5* fusions (PAX5t), involving either novel (*ALDH18A1*, *IKZF1*, *CDH13*) or known (*FBRSL1*, *AUTS2*, *DACH2*) partner genes. PAX5t cases have a specific

driver activity signature, extending to multiple pathways including LCK hyperactivation. Among FDA-approved drugs and inhibitors, we selected Dasatinib, Bosutinib and Foretinib, in addition to Nintedanib, known to be LCK ligands. We demonstrated the efficacy of the LCK-inhibitor BIBF1120/Nintedanib, as single agent or in combination with conventional chemotherapy, both *ex-vivo* and in patient-derived xenograft model, showing a synergistic effect with dexamethasone.

Interpretation

This study provides new insights in the high-risk Ph-like leukaemia and identifies a potential novel therapy for targeting *PAX5*-fusion poor risk group.

Funding

Ricerca Finalizzata-Giovani Ricercatori (Italian Ministry of Health), AIRC, Transcall, Fondazione Cariparo.

Keywords: childhood ALL, PAX5 fusion genes, Ph-like ALL, BIBF1120, Nintedanib

Research in context

Evidence before this study

The discovery of the Philadelphia-like (or BCR/ABL-like) subgroup of patients affected by acute lymphoblastic leukaemia is the most relevant recent advancement in the definition of the ALL genetic landscape, and even more relevant, a step forward in the identification of new patients' subgroups targetable with precision therapy. In addition to the pioneer studies by Mulligan's and Den Boer's groups (in 2009), we considered

several independent studies which further characterized Ph-like patients and reviewed both by Pui in 2017 and Shiraz in 2020. Moreover, further new genetic subgroups of ALL emerged, with association with outcome and potential for targeting, in a continuous path for the definition of ALL heterogeneity and a chance for improving the cure rate by emerging therapies. More specifically in this context, we focused our attention on the ALL subgroup with PAX5 gene alterations, summarized by the two most recent studies by Gu 2019 and Jung 2020, our own previous studies on both i) PAX5 fusions in infant ALL patients and ii) on the functional characterization of the activated pathways downstream to PAX5 fusions, as a potential target for therapies.

Added value of this study

In this paper, in addition to the description of the Ph-like subgroup in the Italian population of childhood ALL, we extend the genomic landscape with further details of other '-like' subgroups and additional copy number abnormalities. A main advantage of this study is the long follow up of the populations in our study allows, with a more stable outcome profile.

Compared to previously published studies, our focus on PAX5 gene rearrangements allowed us to detail the characterization of the PAX5 gene fusion with several different partners. Herewith, we show that PAX5 fusion genes are more recurrent among Ph-like patients and they have their own specific signature, which is here detailed. Moreover, we show that PAX5 fusions can be targeted by Dasatinib, Bosutinib and Foretinib, in addition to the kinase inhibitor BIBF1120/Nintedanib, which is directed against the Lymphocyte-specific tyrosine kinase (LCK), which is over-activated in PAX5 translocated cases.

Implications of all the available evidence

The ex-vivo and in-vivo testing of the LCK inhibitor BIBF1120/Nintedanib sustains the rationale for developing novel preclinical strategies to target PAX5 fusion genes, a step forward in the precision medicine for childhood ALL. In the next future, patients carrying PAX5 fusions may benefit from a novel therapeutic approach.

INTRODUCTION

Despite intensive risk-based treatment protocols, 15% of paediatric patients with B-Cell Precursor Acute Lymphoblastic Leukaemia (BCP-ALL) experience disease relapse. Technological improvement progressively refined the molecular characterization of childhood ALL, identifying among other features the "Ph-like" subgroup (also known as "BCR/ABL1-like").[1,2] Ph-like patients are characterized by poor outcome regardless of treatment protocol, with a high incidence of relapse in children, adolescents and adult cohorts.[3,4] Ph-like ALL was also recognized as a provisional entity in the 2016 revision to the World Health Organization (WHO) classification of haematologic neoplasms,[5] and there is general agreement on the importance to identify the Ph-like subtype. Those patients are characterized by recurrent molecular alterations, mainly fusion genes, classifiable as either ABL-class (involving *ABL1*, *ABL2*, *PDGFRA*, *PDGFRB*, *CSF1R, LYN*) or JAK/STAT-class (affecting *JAK2*, *CLRF2*, *EPOR*).[4,6] The pathogenetic involvement of kinase pathways sustained the use of kinase inhibitors already in use in trials for Ph-positive ALL.[7,8]

In addition, other molecular lesions have been discovered in the Ph-like subgroup, whom prognostic impact still needs to be elucidated, also in

association with cooperative lesions, e.g., IKZF1-plus profile.[9] Namely, *PAX5* gene alterations have been frequently detected in Ph-like ALL, however, their relation with the Ph-like signature, association with outcome and targeting have been poorly elucidated. The *PAX5* gene, which encodes for a B-cell related transcription factor, is altered in about 30% of BCP-ALL as being involved in deletions, amplifications, mutations and translocations that determine the formation of fusion genes encoding aberrant transcription factors.[10,11] Recently, Gu et al. characterized PAX5 alterations (PAX5alt) as an heterogeneous group in childhood and adult cohorts,[12] including cases carrying either PAX5 fusion genes, P80R variant and others, with P80R representing a subgroup with intermediate prognosis.[12,13] Importantly, the PAX5alt signature cluster is very tight and partially overlaps with the Ph-like one, whereas PAX5 P80R has a completely separated pattern.[12] Overall, PAX5alt and PAX5 P80R account for 9·7% of B-other ALL and have a significant role in leukaemia initiation, prognosis and risk stratification, thus requiring an early identification and target therapy.[12]

Our previous studies, in murine pre-BI cells as well as in primary patient cells, showed that *PAX5* fusions sustain survival of leukemic cells through overexpression of the Lymphocyte kinase (LCK) gene,[14,15] a directly repressed target of PAX5.[16] We demonstrated that LCK hyperactivation upon *PAX5* fusion expression leads to STAT5 activation and survival advantage, and that LCK phosphorylation can be specifically targeted by the kinase inhibitor BIBF1120, also known as Nintedanib (Boehringer Ingelheim, Ingelheim am Rhein, Germany),[15] a small molecule which acts as a triple kinase inhibitor with anti-angiogenic anti-tumour effect.[17] Nintedanib is approved for

the treatment of patients with idiopathic pulmonary fibrosis,[18] in use in phase 3 and 4 trials for solid tumors[19] (e.g. pancreatic, hepatocellular, ovarian cancers and lung carcinomas), as well as in three clinical studies for relapsed/refractory adult AML (www.clinicaltrial.gov). It binds the ATP pocket domain of many molecules and it blocks the activity of many receptor-tyrosine kinases,[20] such as the VEGF/FGF/PDGF receptors and the non-receptor tyrosine kinases Src-family members, including LCK.[17,20]

The present study aimed at the characterization of *PAX5* rearranged cases among the Ph-like subgroup of children with BCP-ALL diagnosed in Italy. We herewith tested *ex-vivo* and *in-vivo* the efficacy of the LCK inhibitor Nintedanib/BIBF1120, setting the rationale for developing novel preclinical strategies to target PAX5 fusion genes.

MATERIAL AND METHODS

Patients' cohort

We considered a cohort of 289 consecutive childhood BCP-ALL cases enrolled in Italy in the AIEOP-BFM ALL2000/R2006 protocols (Eudract number: 2007-004270-43).[21] Among them, we identified 135 cases defined as "B-others" by excluding patients with the recurrent t(9;22), t(12;21), t(4;11) or t(1;19) translocations, or cases either with High Hyperdiploidy state (DNA index≥1·16) or carrying constitutional trisomy 21. To confirm that the study cohort was representative of the whole B-other population, the features of the study cohort of N=135 cases were compared with the whole B-other population of 837 patients enrolled in the same period in Italy in the AIEOP-BFM ALL2000/R2006 protocols. Analyses did not reveal any difference

considering gender, age or MRD stratification. Although the study cohort was, likely by chance, enriched for high-risk features (i.e., prednisone response and WBC and consequently stratification to the final High-Risk group), nonetheless, the estimated 5 years EFS did not differ between analysed and not-analysed patients (74.2±3.8 vs 76.5±1.6, respectively, p=0.48) (data not shown).

Ethics

Investigation has been conducted in accordance with the ethical standards of the Declaration of Helsinki and following national and international guidelines. The study is approved by each institutional review board (Eudract number: 2007-004270-43). A written informed consent was obtained from patients or legal representatives. Regarding animal work, ethical approval was obtained by the Animal Welfare Office of the University of Milano-Bicocca prior to submit the request to the Ministry of Health. Animal testing was conducted in accordance with current European and National legislation (authorization n° 09/2018, protocolFB7CC·38 released by the Italian Minister of Health).

Gene expression profiling and Leukaemia diagnostic classification model

Patients were analysed using HG-U133 Plus 2.0 microarray (Affymetrix, Santa Clara, CA, USA) to assess Gene expression profiles. Leukaemia subtypes were classified accordingly to the previously published diagnostic GEP categories using The Diagnostic Classifier (DC) model. The model is based on all-pairwise linear classifiers for the 18 distinct classes of leukaemia, MDS and healthy control, developed for the Microarray Innovation LEukemia (MILE) study, as described in previous studies.[22] Data were normalized using Robust

Multiarray Average (RMA) method using Bioconductor R package (r-package.org). ComBat function in the sva package was used to correct the batch effect of different protocol for microarray preparation. Unsupervised analyses were generated using the top 1000 variable (based on variance) probe sets and processed by t-SNE algorithm with a perplexity score of 30. Data are available at GEO (accession numbers GSE79547, GSE13164, GSE13159, GSE13204). A data-driven network inference algorithm (NetBID, https://jyyulab.github.io/NetBID/)[23] was applied to identify drivers in PAX5-translocated BCP-ALL patients, and a scalable solution of the Algorithm was used for the Reconstruction of Accurate Cellular Networks (SJARACNe).[24] The top 44 drivers for PAX5t were selected using default parameters reported in the package and P value < 0·05 on the primary comparison PAX5t versus BCP-ALL excluding BCR-ABL-like group. Genes resulted with a positive driver activity in PAX5t by NetBID2 analysis ($p<0.05$) were subjected to DGIdbv4.2.0 software analysis to identified drug approved interactions. Cytoscape v3.9.0 was used to build gene-drug interaction network.

Copy Number Alteration analysis in B-others cohort

DNA material of BM at diagnosis was available from 131/135 patients for Copy Number Alteration (CNA) analysis using Multiplex Ligation-dependent Probe Amplification (MLPA)[25] or the Affymetrix Cytogenetics Whole Genome 2.7M Array or Cytoscan-HD (Affymetrix, Santa Clara, CA) according to the manufacturer's protocol.

DNA and RNA Target Capture NGS analysis and Bioinformatics

RNA or DNA target capture Next Generation Sequencing analysis has been performed for 86/135 patients, following a bioinformatic pipeline previously setup in our laboratory.[26] Total RNA was extracted during diagnosis from bone marrow mononuclear cells by the guanidinium thiocyanate–phenol–chloroform method and the RNA CaptureSeq 'TruSight RNA PanCancer' (Illumina, San Diego, CA, USA) was applied. If RNA was not available, we applied a DNA target panel including 17 genes, by Nextera Rapid Capture Custom panel (Illumina). We used the Illumina MiSeq platform. FASTQ files are available in the ArrayExpress database (www.ebi.ac.uk/arrayexpress) under accession number E-MTAB-11319. Fusion genes were validated by RT-PCR (experimental details are provided in Supplementary Table S7).

***In vivo* expansion of leukemic cells and drug experiments**

Primary patient-derived xenograft (PDX) samples were obtained by intravenous injection of BM cells at diagnosis of PAX5 translocated BCP-ALL patients into female NSG mice (NOD/SCID gamma-/- mice, Charles River Laboratories, Calco, Italy) after at least two weeks of acclimatization and then after sublethal irradiation (125 Rad, X-ray) with Radgil (Gilardoni, Mandello del Lario, Italy). Leukaemia engraftment expansion was periodically evaluated by intra-femoral BM aspiration and assessed by FACS as positive to hCD10 (eBioCB-CALLA, APC, #17-0106, RRID AB_11043552, eBiosciences, Thermofisher) and to CD19 (HIB19, FITC, #11-0199, RRID AB_10669461, eBiosciences, Thermofisher). We monitored weekly the engraftment and for signs of distress or toxicity, such as shaggy fur, walking problems and weight loss (if more than 20% the animal is considered for the humanitarian end-point). At bulk disease detection

of hCD10/CD19 positive cells (>10% by intra-femoral BM aspiration), we randomized mice (at least N=5 for each group) and we started a daily treatment by either BIBF1120 (40mg/kg, by oral gavage (o.g)) or dexamethasone (0·5mg/kg, by intraperitoneal injection (i.p.)), or in combination, for 2 weeks and wash out during the weekend. No animals have been excluded. The vehicle group has been treated both by o.g. BIBF1120 vehicle (Kolliphor/ethanol/water) and by i.p. physiological solution. At the end of treatment, we sacrificed animals and analysed data in hematopoietic tissues and organs, such as Bone Marrow (BM), Peripheral Blood (PB), Spleen (SP), and meninges of Central Nervous Systems (CNS). Spleen weight was recorded prior to cell recovery. We collected the absolute number of cells for organs and we assessed the percentage of human cells (hCD10/CD19/CD45) vs. murine cells (mCD45) by FACS, to assess leukaemia engraftment (hCD45, Clone 2D1, #347464, RRID: AB_400307, BD Biosciences; mCD45, 30-F11, #12-0451, RRID AB_465668, eBioscience). According to experimental needs and international guidelines, we estimated to include N=5 animals to each group (groups of animals, included in a single cage), N=4 groups in each experiment, for a total of N=20 animals in each experiment. The experimental staff was aware during the conduction of the experiment and analysis, not during the allocation and a strategy for potential confounders was not applied. We performed the power analyses according to Freedman, using a log-rank statistic test and the 3Rs rules. In details, the number of animals was calculated by considering either the final number of animals, the total number of events, the proportion of surviving in the control group and the estimated proportion of surviving in the experimental group,

calculating a difference of 30% in survival outcome. We obtained to use 20 mice per single experiment, composed by 4 independent treatment groups of 5 mice each.

***Ex vivo* drug screening experiments of leukemic blasts**

Ex vivo extended drug screenings were performed as previously described.[27-30] Briefly the DMSO dissolved compound library (MedChemExpress, NJ, USA) was dispensed with increasing concentrations of the inhibitors in 6 dilution steps (0.008 - 25 µM) using digital dispenser (D300e, Tecan, Männedorf, Switzerland), which ensures precise and robotic compound application in randomized fashion. Differential responses were monitored with ATP-dependent CellTiter-Glo Luminescent cell viability kit (Promega, Madison, USA) after 72 h of inhibitor exposure using Microplate reader (Spark® 10M, Tecan). Drug sensitivity scores (DSS) for the inhibitors were determined, followed by heat map visualization and unsupervised hierarchical clustering of the DSS scores were performed using R package gplots.[31]

***Ex vivo* apoptosis experiments of leukemic blasts in co-culture with human bone marrow stromal cells**

Blasts derived from xenografts were plated on a layer of human bone marrow stromal cells (HBMS). Stromal cells were seeded at the concentration of $2x10^4$/well in MW96, three days prior to reach confluence and then leukemic blasts were plated at $2x10^5$/well in 200µl of AIM V (ThermoFisher). At 48h we tested three different concentrations (including IC50) for each drug, in monotherapy or combination. Apoptosis/viability was evaluated by Annexin V-PE and 7-AAD staining (kit GFP CERTIFIED Apoptosis/Necrosis detection,

Enzo Life Science Inc., Lausen, Switzerland) on leukemic cells positive by anti-hCD10-APC (BD Biosciences). Vincristine (stock 1mg/mL), dexamethasone (4mg/mL), L-asparaginase (kidrolase, stock 4000 IU/mL) and BIBF1120/Nintedanib (stock 10nM) were tested. In order to determine the efficacy of drug treatments and their combinations, the following parameters have been used: IC50 to determine the efficacy of drugs to inhibit the 50% of their targets and BLISS score: formula used to determine synergic (OE>EE), additive (OE=EE) or antagonist (OE<EE) activity between the drugs used in experiments Exy=Ex+Ey-(Ex*Ey), considering the expected effect (EE) of single drugs together Ex and Ey, and the Observed Effect (OE) really observed in experiments. Furthermore, we analysed data by Compusyn software, based on the Chou-Talalay's combination index theorem (CI) to evaluate the effect of interaction between n drugs: CI<1 stands for synergy, CI=1 for additivity, CI>1 for antagonism.

Phosphoflow analysis

As previously setup and validated in our lab,[15] the phosphoflow test was used to evaluate the levels of phosphorylation of PDPK1, Akt (Ser473), Akt (Thr308), S6 (S235/S236), 4EBP1 (Thr37/46), in leukemic cells (CD10+) derived from mice treated with vehicle or Nintedanib mice. After 1·5h serum starvation in X-VIVO at 37°C leukemic cells were then fixed for 10 minutes at room temperature by 1,5% PFA/mL and then permeabilized with 90% cold methanol, kept on ice for 30 minutes then washed with Staining Buffer. Further, cells were dark stained for 30 minutes at room temperature with antibodies directed to PDPK1 (Anti-PDPK1 pS241 #560092 RRID: AB_1645523 BD Biosciences), pAkt (Ser473) (Phospho-Akt Ser473 #4075 Cell Signaling), pAkt

(Thr308) (Anti-Akt pT308 #558275 RRID: AB_2225329 BD Biosciences), pS6 (Anti-S6 pS235/pS236 #560435 RRID: AB_2869348 BD Biosciences) and 4pEBP1 (Phospho-4E-BP1 Thr37/46 #2846 Cell Signaling). Cells were also stained for CD10 (CD10 PE-Cy™7 #565282 RRID: AB_2739153 BD Biosciences), in order to clearly detect B leukemic cells.

FACS experiments

BD FACS CANTOII or LSRX20 FORTESSA cytometer (BD Biosciences) and FACSDiva software were used.

Statistical analysis

Analysis of clinical characteristics of patients were performed by the chi-square test for association, when appropriate. Event-free survival (EFS) was calculated from the date of diagnosis to the date of the first event. Events considered were resistance, relapse, death or second malignant neoplasms, whichever occurred first. EFS curves were estimated according to the Kaplan-Meier method, with standard errors (SE) according to the Greenwood formula; differences between groups were evaluated using the log-rank test. Cumulative incidence of relapse (CIR) curves accounting for competing events, were estimated according Kalbfleisch and Prentice and compared using the Gray test. SAS software, version 9.4, was used for analysis. Statistical analyses from *in vivo*, *ex vivo* and phosphoflow experiments were performed by GraphPad Prism software (ver·9); Anova and T test is shown as *p<0·05, **p<0·01, ***p<0·001. Normality of phosphoflow data was demonstrated by normal distribution test (Excel). Moreover, for each experimental set of data of *ex vivo* and *in vivo* drug treatments

experiments, data were analysed for D'Agostino-Pearson omnibus K2 normality test (alpha=0.05) by GraphPad Prism software (ver·9).

Role of Funders

This work was supported by Ricerca Finalizzata-Giovani Ricercatori (Italian Ministry of Health) for reagents used in *ex vivo* and *in vivo* experiments. Moreover, AIRC and Transcall grants contributed to expenses for patients' data collection, molecular profiling and characterization. Fondazione Cariparo supported costs due for data analysis. The funders did not have any role nor in study design, data collection, data analyses, interpretation or writing of report.

RESULTS

With the aim to define targetable subgroups, we considered consecutively diagnosed 289 BCP-ALL patients and defined 135 cases referred to as 'B-others' according to the workflow (outlined in figure S1) which excluded recurrent aberrations and specific gene expression signatures. B-others were scrutinized for specific GEP profiles and fusion transcripts by RNA-seq, and unsupervised t-distributed stochastic neighbour embedding (tSNE) analysis (Figure 1a) allowed to recognize several BCP-ALL subtypes based on the expression of the first 1000 most variable genes and fusion transcripts. Patients with a Ph-like profile formed the largest group of 59/135 of B-other patients. The remaining cases clustered together with known groups and were denominated accordingly.

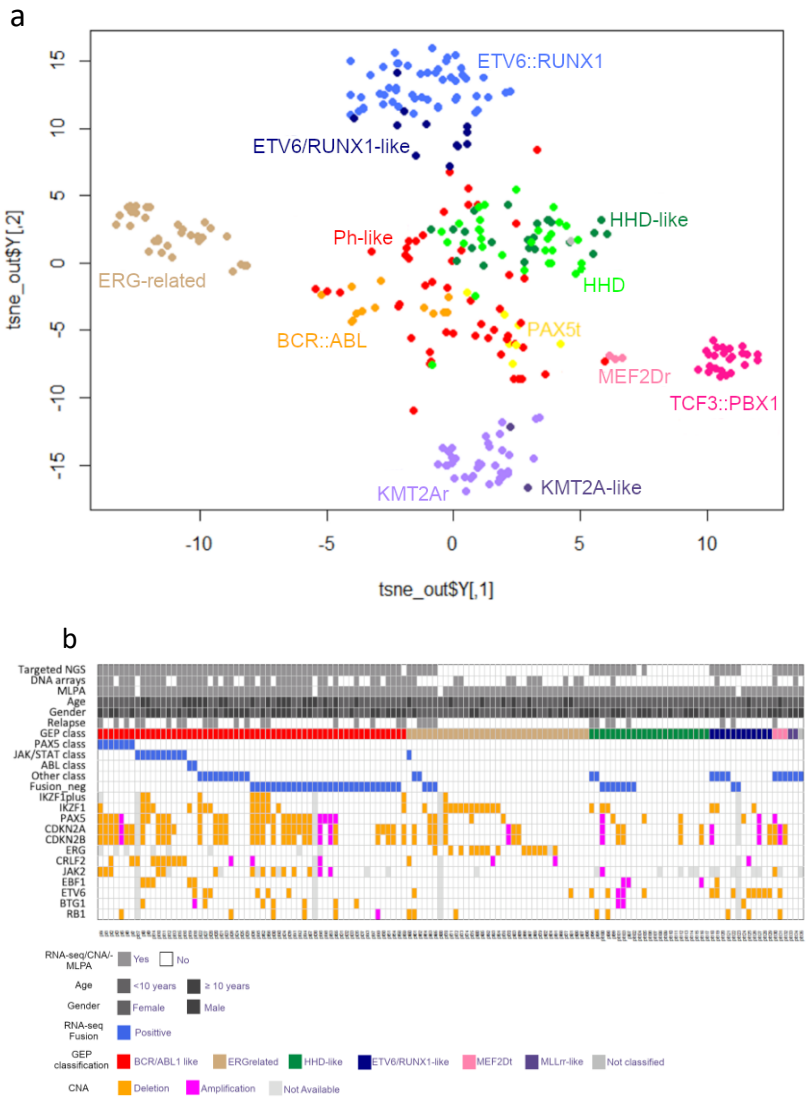

Figure 1. (a) Two dimensional tSNE plot of 289 paediatric BCP-ALL cases based on the top 1000 variable genes of gene expression data. The BCP-ALL subgroups are represented with different colours. Colour label indicated the different subgroups. Yellow highlights a subgroup of Ph-like patient carrying PAX5-translocations (PAX5t). Groups recognized as "like" cluster together with samples carrying the associated translocations, which is attributed to a similar gene expression profile. (b) Plot summarizing the molecular characterization of B-other cohort in childhood ALL:

assessment of specific genetic subtypes, as reported in details in Supplementary Table S2.

A significant poor risk was confirmed for our Ph-like patients' cohort. In fact, Ph-like cases had a significantly inferior EFS (5-year figure (SE) of 59·9% (6·5) for Ph-like versus 85·2% (4·1) for non-Ph-like, p=0·001), mainly due to a higher CIR (Table 1; Figure 2, panel a, left and middle, p=0·01). The Overall Survival is inferior in Ph-like vs. non-Ph-like (5-year, 75·4% vs. 94·6%, p=0·003). The significantly poor EFS and OS were confirmed when excluding cases already classified as high risk (HR) (p=0·02 and p=0·049, Figure 2, panel b left and right), with a trend for higher CIR (Figure 2, panel b middle). In HR patients the 5-year EFS (SE) was 35·7% (12·8) for Ph-like vs. 76·5% (10·3) for non-Ph-like (p=0·03, Figure 2, panel c left), with a trend for a difference in CIR (50·0% (13·4) vs. 17·6% (9·6), p=0·08) (Figure 2, panel c right). Notably, the survival in Ph-like is 42·9% vs. 82·4% in non-Ph-like (p=0·029). When medium risk (MR) and standard risk (SR) patients were considered separately, the Ph-like outcome was associated with worse prognosis only in MR (60·1% vs. 85·4%, p=0·02, Supplementary Figure S2a and S2b). The EFS analysis of the most represented B-other subgroups (Ph-like, ERG-related, ETV6/RUNX1-like and HHD-like, whose clinical characteristics are described in Supplementary Table S1) confirmed that Ph-like patients show the worst outcome (Supplementary Figure S3a), even excluding HR patients (Supplementary Figure S3b). Events according to subgroups are shown in Supplementary Table S2. Of relevance, among 32/135 B-other cases experiencing relapse (23·7%), 20 were Ph-like (34%), as indicated in Table 1, and their clinical characteristics

are shown in Supplementary Table S3. Moreover, a Cox model was fitted on our cohort of 135 patients; given the relatively small sample, we adjusted for the main characteristics known as generally associated to outcome. A highly significant impact on EFS was confirmed for Ph-like (hazard ratio (HR)=2·93, p-value=0·003) as well as for assignment to final High-Risk group (HR=2·25, p-value=0·03), while age and WBC at diagnosis did not have a significant impact on outcome (Table 2).

a. Ph-like vs non Ph-like: overall analysis

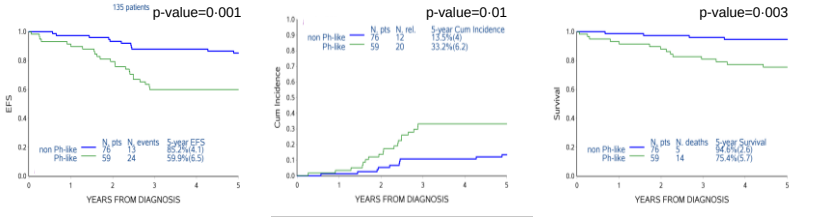

b. Ph-like vs non Ph-like: No high risk patients

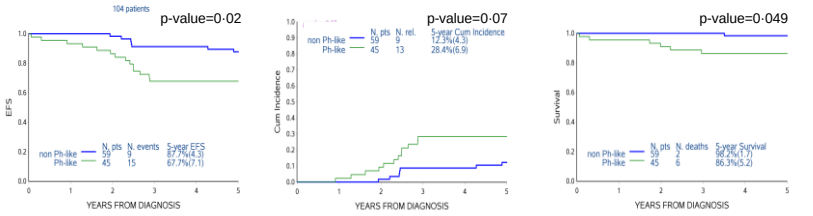

c. Ph-like vs non Ph-like: High risk only patients

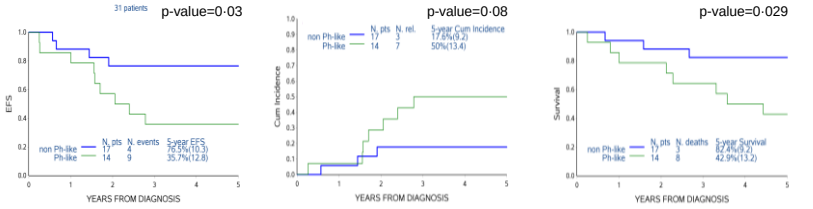

d. Ph-like patients accordingly to different class fusions

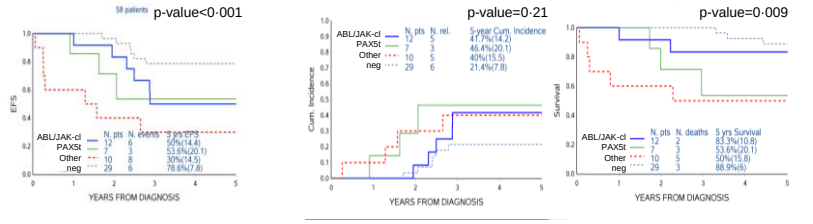

Figure 2. Outcome analysis of AIEOP B-Other cohort, in terms of EFS (on the left column) and CIR (in the middle column) and OS (in the right), comparing Ph-like vs. non-Ph-like patients overall (a), in no High Risk (b), in HR patients (c), respectively; (d) EFS, CIR and OS analyses according to the fusion classes reveal statistical significance in Ph-like cases, classified accordingly to different class fusions, such as ABL/JAK-class, PAX5t, other fusions and negative after NGS analysis.

In addition, we collected data from immunophenotype analysis of the complete cohort (N=135) and we classified data according to phenotype profiles, according to Ph-like signature: Non-Ph-like: pre-pre-B: 9%; call: 60%, pre-B: 18%; preB/B: 1%; Biclonal B: 4%and B-lineage: 8%; whereas Ph-like were distributed as follows: pre-pre-B: 2%; call: 81%, pre-B: 14% and B-lineage: 3%. Thus, overall, the majority of cases were classified as having call phenotype in both groups.

In Ph-like patients, CNAs were recurrent in leukaemia-associated genes, such as *CDKN2A* and/or *CDKN2B* (33·6%), *PAX5* (25·2%), *IKZF1* (24·4%), *ETV6* (15·3%), *RB1* (10%) and *CLRF2* (8·4%) (Figure 1b), with the IKZF-plus profile accounting for 7% of cases (Supplementary Table S4). The mean number of CNA events per Ph-like patient is almost double (2·77 events/pt) compared to ERG-related patients (1·53 events/pt) or non-Ph-like B-other patients overall (1·57 events/pt).

Fusion genes were identified in 30/58 (52%) Ph-like cases analysed (see heatmap of Figure 1b and Supplementary Table S4). Among those 30 fusion genes, 21 included 8 P2RY8::CLRF2, 7 PAX5-translocated cases (PAX5t), 2 IGH::CRLF2 (by FISH), 2 ABL-class fusion (EBF1::PDGFRB) and single cases carrying either TCF3::HLF or BCL9::MEF2D. The remaining 9/30 were novel fusion genes, not previously reported in normal or cancer tissues (FusionHub database, https://fusionhub.demopersistent.com/) and classified as 'other fusions' in Supplementary Table S4. Notably, fusion genes were detected in 19/32 relapsed patients, of which 14/20 (70%) in Ph-like and only 5/12 (42%) in non-Ph-like relapsed patients. Overall, the 59

Ph-like cases could be sub grouped according to fusions as 2 ABL-class, 10 JAK-class, 7 PAX5-class, 9 carrying other fusions in addition to two single cases carrying either TCF3::HLF or BCL9::MEF2D and 28 remaining negative after NGS analyses. One case had no available RNA for fusion analysis but was IKZF1-plus as described below.

CRLF2 rearrangements were almost exclusively found in the Ph-like group (Figure 1b and Supplementary Table S4), and also the IKZF1-plus profile was prevalent in Ph-like cases (8/9) and associated with a poor outcome (5-year EFS (SE) 37·5% (17·1) vs 65·5% (7·0) for non-IKZF1-plus cases) (Supplementary Figure S4). Interestingly, also *PAX5* gene lesions were mostly associated with the Ph-like signature. Considering CNAs and translocations, the *PAX5* gene was involved in 43/131 B-other patients (32·8%), with 31/57 (54·3%) in Ph-like and 12/74 (16%) in non-Ph-like cases. (Supplementary Tables S4 and S5). Notably, all the 7 PAX5t were found in the Ph-like group (Supplementary Table S5). Validation primers are reported in Supplementary Table S6). As showed in Figure 2d, EFS ($p<0·001$) and OS ($p=0·009$) analyses according to the fusion classes reveal statistical significance in Ph-like cases, classified accordingly to different class fusions, such as ABL/JAK-class, PAX5-class, other fusions and negative cases after NGS analysis. In fact, the PAX5t cases have a poor EFS, similar to ABL/JAK-class patients (53% and 50%, respectively) and lower than Ph-like cases negative for any fusion gene (78%). Moreover, PAX5t OS was inferior respect to ABL/JAK-class and negative cases (about 53% vs. 83·3% and 88·9%). However, CIR analysis was not different among the subgroups ($p=0·21$). In details among PAX5t had 3 events out of 7, corresponding to BM relapse and

they died later; among N=12 ABL/JAK, they had one death post HSCT and 5 relapses (4 BM and 1 CNS) with only one death (the 4 non-deceased all have an adequate post-relapse follow-up)

These features of PAX5t cases prompted us to explore the feasibility of targeting patients with this aberration. By applying the NetBID2 data-driven network interference algorithms (Figure 3a), we constructed the BCP-ALL interactome and identified the hub drivers' activity (DA) based on network gene interaction on either PAX5 translocated patients versus all BCP-ALL excluding Ph-like (Figure 3b, left column) or versus Ph-like (Figure 3b, middle column). We also assessed a Differential Expression (DE) of genes belonging to these pathways (Figure 3c). Interestingly, in the top NetBID2 drivers we identified the LCK signalling factor showing a significantly higher activity in PAX5t compared to other BCP-ALL subgroups (Figure 3d). Furthermore, analysis of LCK activity in BCP-ALL patients with known PAX5 status (N=131) revealed that it is an exclusive signature of PAX5t cases, with statistically significance compared to all the categories, such as patients with amplification or deletion or being wild type for PAX5 gene (Figure 3e). Moreover, among the 22 genes resulted with a positive driver activity in PAX5t vs. Ph-like by NetBID2 analysis ($p<0.05$) were subjected to DGIdbv4.2.0 software analysis to identified drug approved interactions and among them we found 7 genes that can be targeted, including LCK by Nintedanib (Supplementary Table S7 and Supplementary Figure S5a). Further, a positive enrichment of upregulated genes has been determined interacting with LCK signalling in these patients (Supplementary Figure S5b). These data pointed LCK-signalling as a potential signalling to target in this subgroup of patients.

Thus, in agreement with our previous data on Pax5t targeting by the kinase inhibitor BIBF1120/Nintedanib in murine preBI cells and in primary patients' cells,[15] and sustained by independent studies in which Nintedanib is reported to be effective in LCK targeting as summarized in the Drug Gene Interaction Database (https://www.dgidb.org/genes/LCK#_interactions), we developed a LCK targeting strategy in a preclinical model of PAX5 fusion PDX. Moreover, we applied a wider ex-vivo drug screening with FDA-approved drugs and inhibitors in early to late clinical trials, and we selected Dasatinib, Bosutinib and Foretinib, known to be among the top 10 most potent LCK ligands, as assed by Kinome DiscoveRx study (http://www.discoverx.com/services/drug-discovery-development-services/kinase-profiling/kinomescan)[32,33] in addition to Nintedanib/BIBF1120. Here we demonstrated their potential therapeutic efficacy and specific to (N=3) PAX5t cases (carrying PAX5::AUTS2, PAX5::DACH2 and PAX5::SOX5, respectively), by evaluating the differential drug sensitivity score of PAX5t samples and including both MLLr (ALL-PO, KOPN8, RS4;11 and SEM) and CRLF2r cell lines (MUTZ5) and control B-cell lymphoblastoid cell lines (derived from healthy donors). As shown in Figure 3f and in Supplementary Figure S6 and Table S8, Nintedanib demonstrated to be the highest specific and effective compound to PAX5t, considering the statistics (One way Anova test), compared to leukaemia cell lines and controls. We also tested other kinase inhibitors, not directly related to LCK but to BCR/ABL targeting, were not effective on PAX5t cases, whereas conventional chemotherapy drugs were effective, e.g., Dexamethasone, Vincristine among other (Supplementary Figure S6).

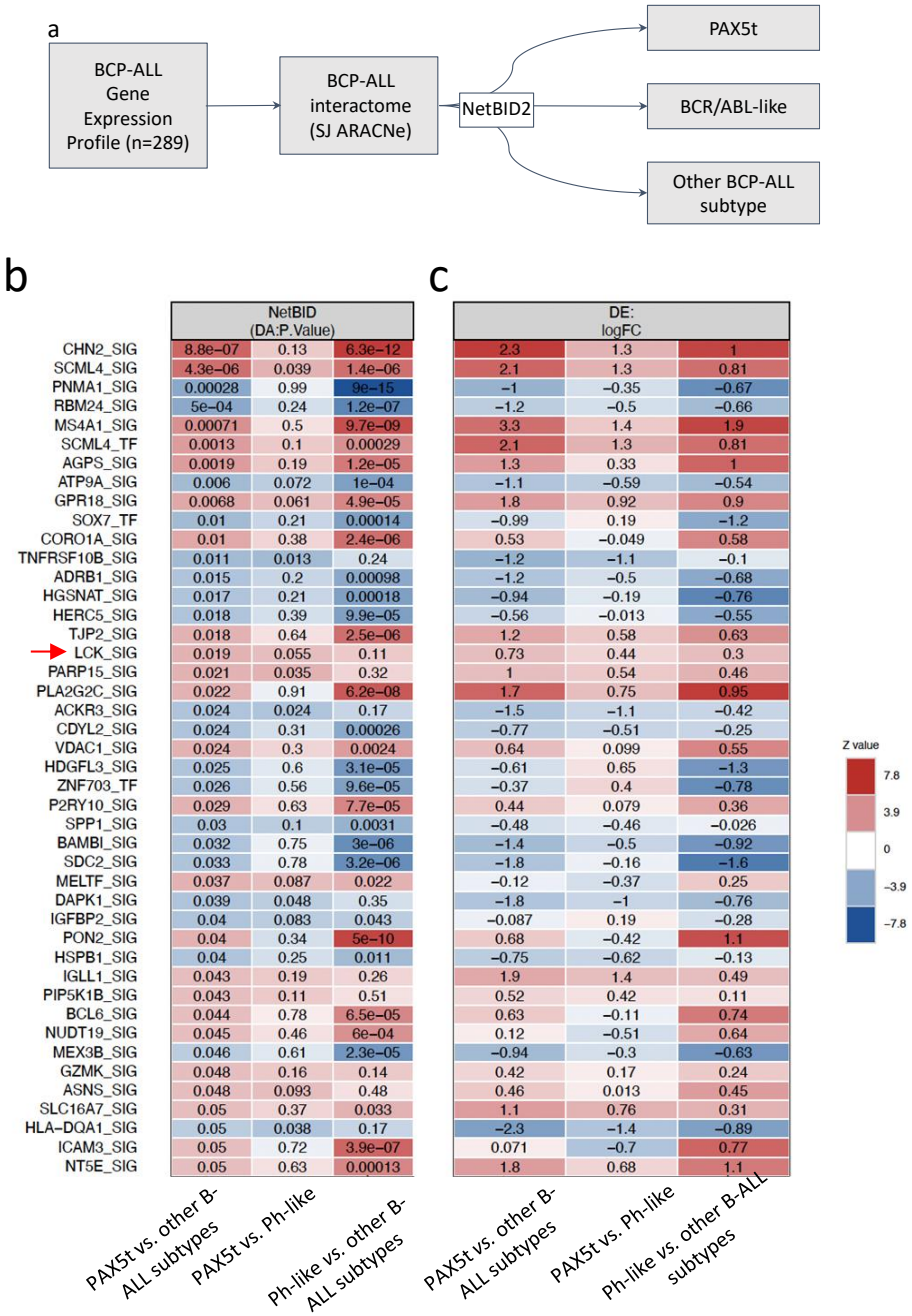
a
BCP-ALL Gene Expression Profile (n=289)
BCP-ALL interactome (SJ ARACNe)
NetBID2
PAX5t
BCR/ABL-like
Other BCP-ALL subtype
b
c
NetBID (DA:P.Value)
DE: logFC
CHN2_SIG 8.8e−07 0.13 6.3e−12 2.3 1.3 1
SCML4_SIG 4.3e−06 0.039 1.4e−06 2.1 1.3 0.81
PNMA1_SIG 0.00028 0.99 9e−15 −1 −0.35 −0.67
RBM24_SIG 5e−04 0.24 1.2e−07 −1.2 −0.5 −0.66
MS4A1_SIG 0.00071 0.5 9.7e−09 3.3 1.4 1.9
SCML4_TF 0.0013 0.1 0.00029 2.1 1.3 0.81
AGPS_SIG 0.0019 0.19 1.2e−05 1.3 0.33 1
ATP9A_SIG 0.006 0.072 1e−04 −1.1 −0.59 −0.54
GPR18_SIG 0.0068 0.061 4.9e−05 1.8 0.92 0.9
SOX7_TF 0.01 0.21 0.00014 −0.99 0.19 −1.2
CORO1A_SIG 0.01 0.38 2.4e−06 0.53 −0.049 0.58
TNFRSF10B_SIG 0.011 0.013 0.24 −1.2 −1.1 −0.1
ADRB1_SIG 0.015 0.2 0.00098 −1.2 −0.5 −0.68
HGSNAT_SIG 0.017 0.21 0.00018 −0.94 −0.19 −0.76
HERC5_SIG 0.018 0.39 9.9e−05 −0.56 −0.013 −0.55
TJP2_SIG 0.018 0.64 2.5e−06 1.2 0.58 0.63
LCK_SIG 0.019 0.055 0.11 0.73 0.44 0.3
PARP15_SIG 0.021 0.035 0.32 1 0.54 0.46
PLA2G2C_SIG 0.022 0.91 6.2e−08 1.7 0.75 0.95
ACKR3_SIG 0.024 0.024 0.17 −1.5 −1.1 −0.42
CDYL2_SIG 0.024 0.31 0.00026 −0.77 −0.51 −0.25
VDAC1_SIG 0.024 0.3 0.0024 0.64 0.099 0.55
HDGFL3_SIG 0.025 0.6 3.1e−05 −0.61 0.65 −1.3
ZNF703_TF 0.026 0.56 9.6e−05 −0.37 0.4 −0.78
P2RY10_SIG 0.029 0.63 7.7e−05 0.44 0.079 0.36
SPP1_SIG 0.03 0.1 0.0031 −0.48 −0.46 −0.026
BAMBI_SIG 0.032 0.75 3e−06 −1.4 −0.5 −0.92
SDC2_SIG 0.033 0.78 3.2e−06 −1.8 −0.16 −1.6
MELTF_SIG 0.037 0.087 0.022 −0.12 −0.37 0.25
DAPK1_SIG 0.039 0.048 0.35 −1.8 −1 −0.76
IGFBP2_SIG 0.04 0.083 0.043 −0.087 0.19 −0.28
PON2_SIG 0.04 0.34 5e−10 0.68 −0.42 1.1
HSPB1_SIG 0.04 0.25 0.011 −0.75 −0.62 −0.13
IGLL1_SIG 0.043 0.19 0.26 1.9 1.4 0.49
PIP5K1B_SIG 0.043 0.11 0.51 0.52 0.42 0.11
BCL6_SIG 0.044 0.78 6.5e−05 0.63 −0.11 0.74
NUDT19_SIG 0.045 0.46 6e−04 0.12 −0.51 0.64
MEX3B_SIG 0.046 0.61 2.3e−05 −0.94 −0.3 −0.63
GZMK_SIG 0.048 0.16 0.14 0.42 0.17 0.24
ASNS_SIG 0.048 0.093 0.48 0.46 0.013 0.45
SLC16A7_SIG 0.05 0.37 0.033 1.1 0.76 0.31
HLA−DQA1_SIG 0.05 0.038 0.17 −2.3 −1.4 −0.89
ICAM3_SIG 0.05 0.72 3.9e−07 0.071 −0.7 0.77
NT5E_SIG 0.05 0.63 0.00013 1.8 0.68 1.1
PAX5t vs. other B-ALL subtypes
PAX5t vs. Ph-like
Ph-like vs. other B-ALL subtypes
PAX5t vs. other B-ALL subtypes
PAX5t vs. Ph-like
Ph-like vs. other B-ALL subtypes
Z value
7.8
3.9
0
−3.9
−7.8

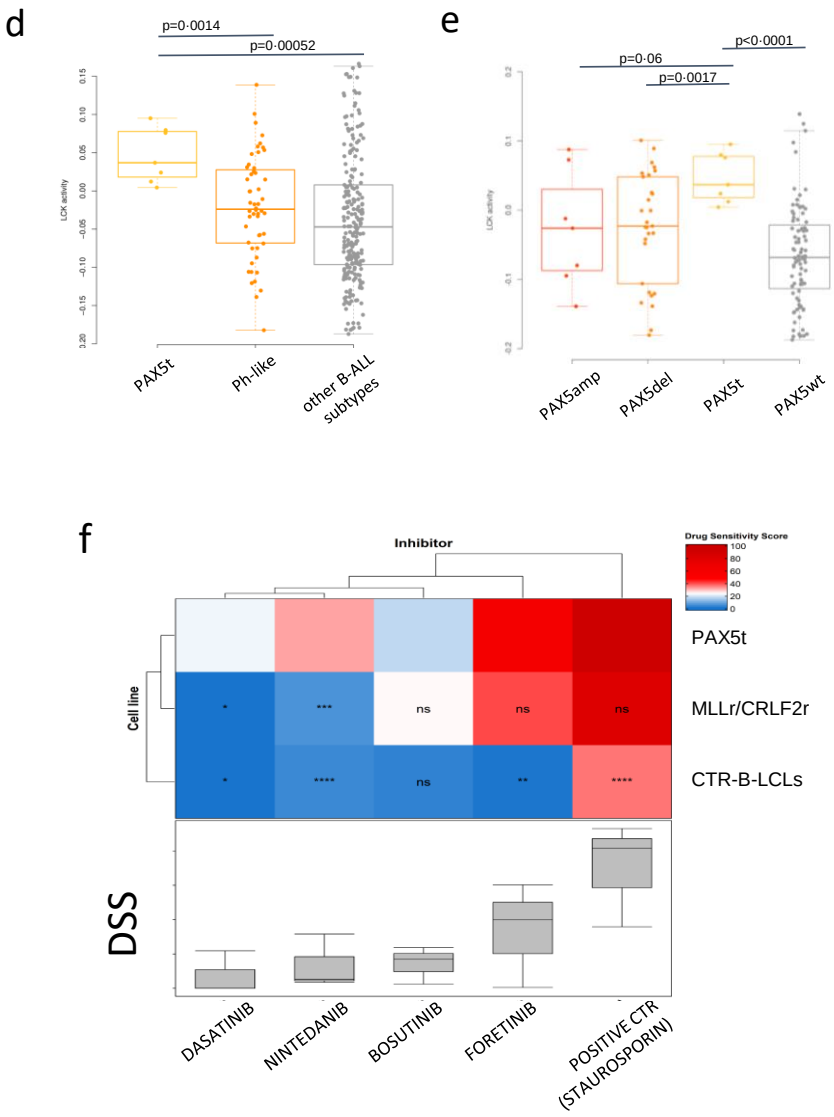

Figure 3. PAX5 translocated cases (or PAX5t) have a specific interactome signature. (a) Schema of NetBID2 analysis in BCP-ALL at diagnosis to identify driver in PAX5t BCP-ALL patients. To construct the BCP-ALL interactome the SJARCNe algorithm was employed on gene expression profiles of BCP-ALL patients (n=289), and driver gene networks in PAX5t patients were identified in comparison with BCR/ABL-like or all other BCP-ALL subtypes. (b) Heatmap of the top 44 predicted driver's activity (DA) and (c) differentially expressed (DE) in the BCP-ALL interactome based on

PAX5t patients. Drivers were ranked according to p-value. Colour code was generated by z-score. (left column= PAX5t vs. other BCP-ALL subtypes; middle column=PAX5t vs. Ph-like, right column=Ph-like vs other BCP-ALL subtypes). (d) Boxplot of LCK activity by NetBID2 analysis of PAX5 translocated patients compared between Ph-like and all other BCP-ALL subtypes using gene expression data. P-value was calculated using Welch T-test. (e) Boxplot of LCK activity in BCP-ALL patients with known PAX5 status (N=131). P-value was calculated by Welch t-test. PAX5amp: patients with amplification of PAX5 gene; PAX5del: patients with deletion of PAX5 gene; PAX5t: patients with translocation of PAX5 gene; PAX5wt: patients with PAX5 gene without aberrations. (f) Comparative cellular viability of different sub-groups of leukemia (PAX5t, MLLr or CRLFr) samples and control-B-lymphoblastoid cell lines (CTR-B-LCSs), measured by ATP-Glo based luminescent based assay after exposure of the depicted drugs, whereas Staurospsorin was taken as a positive control. Drug sensitivity scores (DSS) are plotted as a clustered heat map, followed by unsupervised hierarchical clustering. The horizontal and the vertical axis of the dendrogram illustrates the dissimilarity between clusters, whereas the color of the cell is related to its position along with a DSS gradient. The p-values are calculated with the one-way Anova test related to PAX5t group, **** ($p<0.0001$), *** ($p<0.001$), ** ($p < 0.01$); * ($p < 0.05$); ns = not significant.

To investigate drug sensitivity and efficacy, we assessed apoptosis in leukemic cells. We performed *ex-vivo* cell incubation by BIBF1120 alone or in combination with chemotherapeutic drugs used as standard therapy in ALL treatment protocols, such as Dexamethasone, Vincristine or Asparaginase. Figure 4 shows a representative experiment in four different *PAX5*-fusion BCP-ALL samples at 48h (2 PAX5::AUTS2 pt.1 and pt.2, PAX5::DACH2 pt.3 and PAX5::SOX5 pt.4). After treatment viability has been determined, as difference from apoptosis and necrosis, by Annexin V-PE and 7-AAD staining. BIBF1120 had a synergistic effect with either Dexamethasone or

Vincristine, rather than additive with Asparaginase (Combination index values are reported in Supplementary Figure S7 a-b, as Bliss score), specifically in cases carrying PAX5 fusions, whereas it did not show any activity in PAX5-deleted or -wild type cases, regardless of their Ph-like profile (N=4 cases, Supplementary Figure S7 panel c).

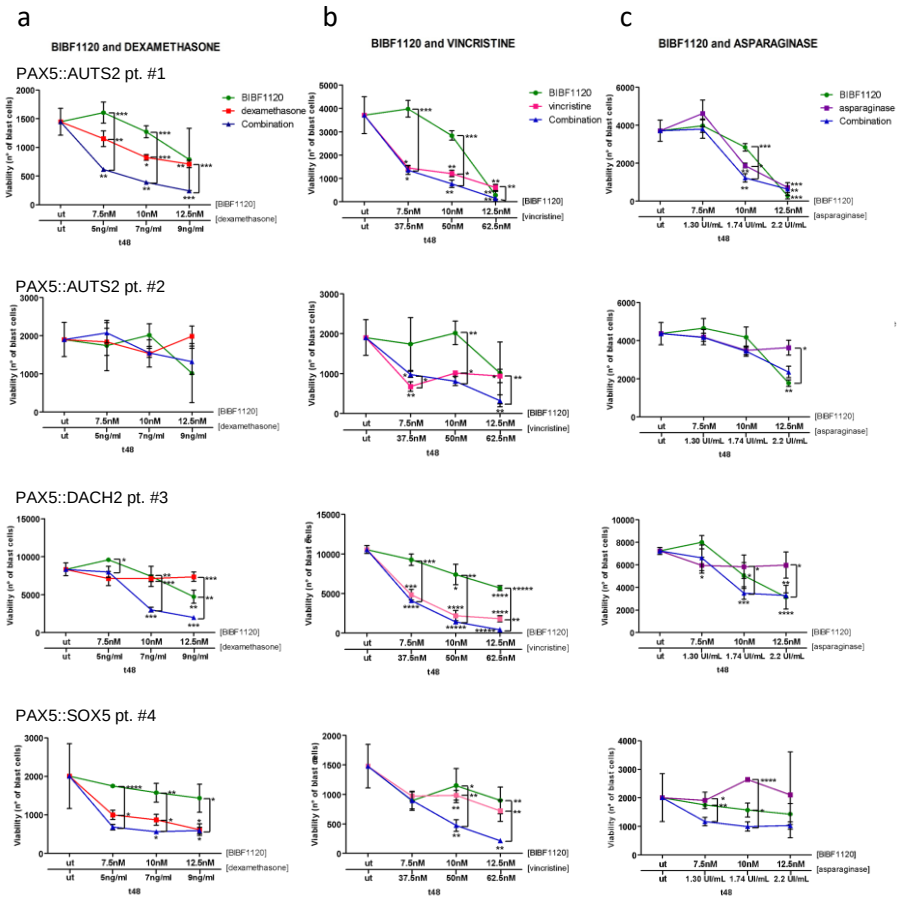

Figure 4. *Ex-vivo* treatment by BIBF1120 either alone or in combination with Dexamethasone (a), Vincristine (b) or Asparaginase (c). Experiments have been performed in presence of different PAX5 fusion genes, such as PAX5::AUTS2 in Pt. n°1 and n°2, or alternatively carrying PAX5::DACH2 as in Pt. n°3 or PAX5::SOX5 in Pt. n°4. After drug treatment, viability has been determined, as difference from

apoptosis and necrosis, by Annexin V-PE and 7-AAD staining. Untreated samples (ut) have been analysed as internal control.

According to the synergistic effect of dexamethasone and BIBF1120 in *ex vivo* experiments, their efficacy was further assessed in the *in vivo* PDX mouse model. The BIBF1120 dose finding experiments were carried out in secondary transplants of PAX5::AUTS2 pt.1, determining 40mg/kg as the most effective dose of BIBF1120 in absence of toxicity, phenotypic symptoms or weight loss (data not shown). Further, as schematically shown in Figure 5a, we performed secondary transplants with cells carrying either PAX5::AUTS2 (pt.1) or PAX5::DACH2 (pt.3). At bulk disease detection (hCD10/CD19 positive cells >10%, by BM aspiration), animals were randomized into four groups (vehicle, BIBF1120 alone, dexamethasone alone, combination) and we started treatment.

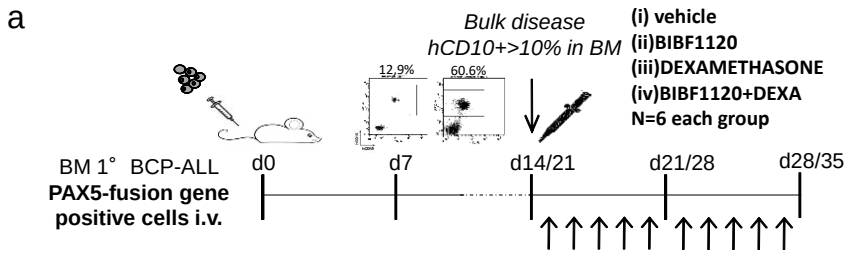

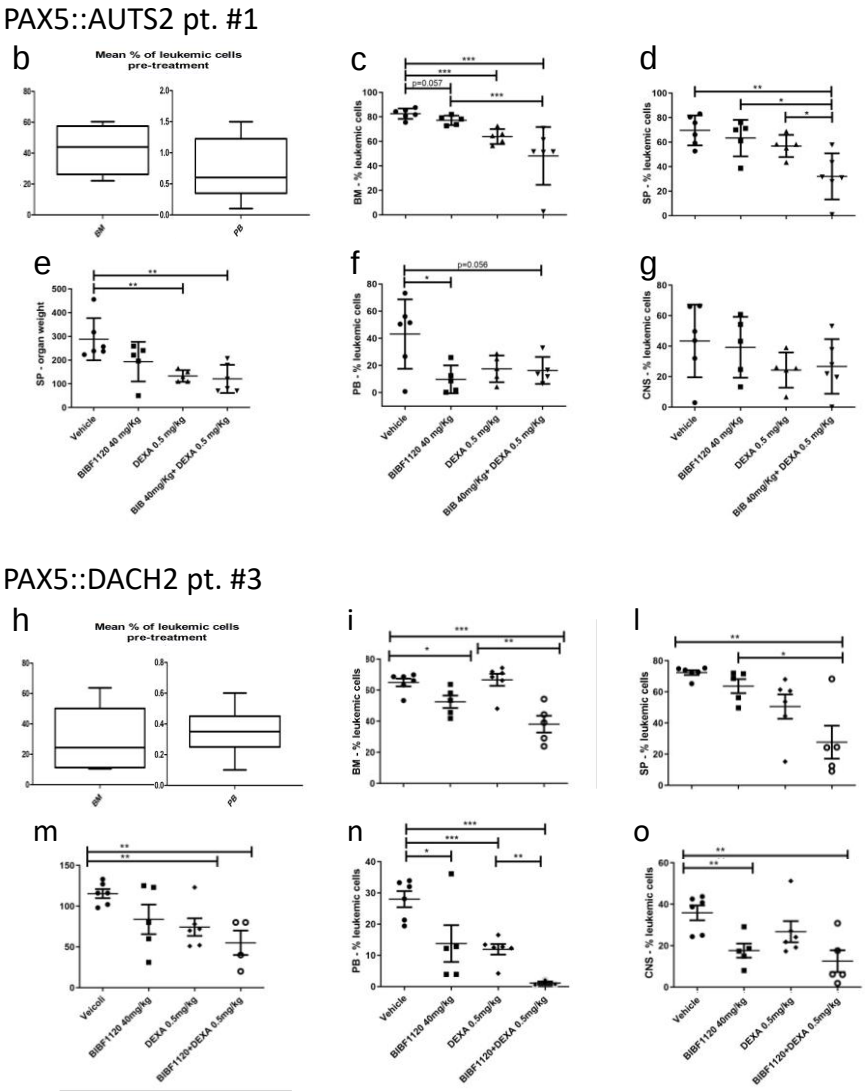

Figure 5. *In vivo* treatment by BIBF1120 either administered alone or in combination with Dexamethasone. The experimental plan is depicted in panel (a): NSG mice were transplanted with human leukemic cell carrying different PAX5 fusion genes, namely PAX5::AUTS2 as in Pt. n°1 (panels b-g) or PAX5::DACH2 as in Pt. n°3 (panels h-o). Human leukaemia engraftment was evaluated in hematopoietic tissues prior to start treatment in Bone Marrow and Peripheral Blood (panels b and h, in both patients, respectively) and after two weeks of treatment, in all hematopoietic organs, such as Bone Marrow for Pt.1 (panel c) and Pt.3 (panel i), in Spleen as percentage (panel d

and l) and weight (panels e and m), in Peripheral Blood, f and n) and in Central Nervous System Meninges (g and o). Data are expressed as percentages of human CD10+ cells. Statistical analyses have been performed by GraphPad Prism software and T test is shown as *p<0·05, **p<0·01, ***p<0·001.

In PAX5::AUTS2 pt.1, the daily treatment was started at day14 with 42% hCD10 positive cells mean engraftment detection in BM (ranging from 23·3 to 60·6%, Figure 5b). After two weeks, we sacrificed animals and assessed the disease levels as percentage of tumour cells in each organ, as reported in Figure 5 panels from c to g and the mean engraftment in vehicle BM was 82·6% (range 75·5-86·7%). As shown in Figure 5c, in the PAX5::AUTS2 PDX mice we detected a mild effect in the BM of BIBF1120 alone (disease reduction of 24%, p=0·057), further enhanced by the combination with dexamethasone (-49%, p=0·005, with a mean engraftment in vehicle mice of 82·6%). In the spleen (Figure 5d and S8c), the efficacy was highly significant both for BIBF1120 (-52%, p=0·025) and the combination (-91%, p=0·015, mean engraftment vehicle 69·5%). We also observed a macroscopic effect on spleen weight decrease by the combination treatment (Figure 5e). A similar statistically significant effect was observed also in peripheral blood (Figure 5f and S8d), whilst, BIBF1120 alone showed a specific significant efficacy in CNS meninges, considering both percentages and absolute number of leukemic cells, as showed in Figure 5g and S8e, respectively. Moreover, data were further confirmed by evaluation of the tumour burden, defined as the absolute number of human CD10 positive (hCD10+) leukemic cells over the total number of cells in each organ (BM, spleen, CNS and PB), as shown in Supplementary Figure S8 panel from b to e.

The efficacy of treatment was further confirmed in the PAX5::DACH2 PDX mice. We started treatment at day21, with 15% BM Engraftment (range 10-34·3%, Figure 5h). After two weeks, the number of human leukemic cells in BM deceased of 47% using BIBF1120 alone (p=0·02 as % and p=0·004 as n° cells, Figure 5i and S8f, respectively), further diminished by the combination (-70% vs. vehicle, p=0·001 as % and p=0·00001 as n° cells, with a mean engraftment in vehicle mice of 65%, ranging from 53·3 to 70%) (Figure 5i and S8f). As shown in Figure 5l and Supplementary Figure S8g, in the spleen, the efficacy was highly significant both with BIBF1120 (-45·6%, p=0·00003 as % and p=0·03 n° cells) and the combination (-97·5% tumour burden, p=0·0008, mean engraftment vehicle 72·4%), with considerable effects on spleen weight (Figure 5m). Strikingly, BIBF1120 treatment alone showed similar efficacy in PB and CNS, with leukaemia decrease as much as -45% (p=0·04) and -76% (p=0·007), respectively. Dexamethasone alone was not effective in the BM and spleen (Figures 5i and 5l), whereas it decreased the leukaemia bulk both in PB (-65%, p=0·0004, Figure 5n) and CNS (-52·8%, p=0·03, Figure S8i). Importantly, the combination with BIBF1120 nearly achieved remission in PB (-94%, p=0·0001, Figure 5n and S8h) and it was significant in CNS (-84·7%, p=0·005, Figure 5o and S8i).

Since the AKT signalling pathway was activated downstream LCK via the PIP3 signalling pathway,[34] we hypothesised a molecular regulation mechanism involving both kinases, as depicted in Figure 6 panel a. To sustain this molecular regulation, we investigated the *in vivo* Nintedanib/BIBF1120 treatment both in four patients' primary cells and in PAX5::AUTS2 mice (Supplementary Figure S9). In PDX cells

phosphoflow analysis showed a marked inhibition of pAKT-Thr308 (-29%, p<0·01) and the downstream effectors pS6 (-64%, p<0·001) and 4pEBP1 (-26%, p<0·05), comparing BIBF1120 vs. vehicle group (Figure 6b). Inhibitor treatment mildly affected pAKT-Ser473 (-9%) and PDPK1 (-13%, p<0·05) phosphorylation levels. As shown in Figure 6c, we confirmed results in PAX5::DACH2 mice, demonstrating a reliable AKT inhibition, with consistent decreased phosphorylation levels of both pAKT-Thr308 (-34%, p<0·01) and pAKT-Ser473 (-61%, p<0·001), respectively. Moreover, also PDPK1 (-37%, p<0·05), 4pEBP1 (-38%, p<0·001) and pS6 (-78%, p<0·0001) were decreased.

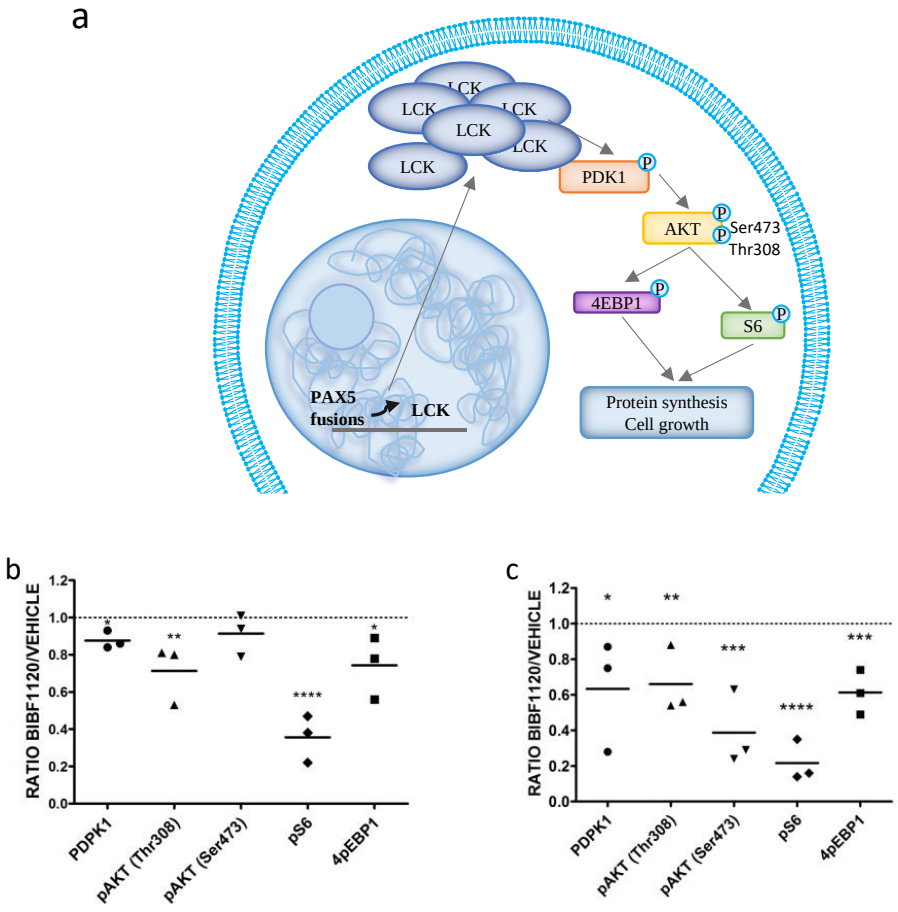

Figure 6. LCK and Akt pathway involvement in leukemic cells with PAX5 fusion genes. (a) A schematic view of molecular hypothesised mechanism of LCK and Akt interaction. After in vivo BIBF1120 treatment vs. vehicle mice, in (b) pt.#1 PAX5::AUTS2 and (c) pt.#3 PAX5::DACH2, respectively. PDPK1, pAKT-Ser473 and -Thr308, pS6 and 4pEBP1 are analysed by FACS. Data are expressed as ratio of Phosphorylation levels, considering vehicle phosphoprotein levels equal to 1 (dotted line) and symbols are correspondent to single BIBF1120-treated mice. Statistical analyses have been performed by GraphPad Prism software and T test is shown as *p<0·05, **p<0·01, ***p<0·001.

DISCUSSION

After a first definition,[1,2] several studies identified the BCR/ABL1-like or Ph-like group both in paediatric and in adult cohorts of BCP-ALL, demonstrating an association with poor MRD response and overall outcome.[3] Thus, the terms 'BCR/ABL1-like' or Ph-like have been included as provisional entity in the 2016 WHO classification of ALL.[5]In the present study, we identified and characterized the Ph-like subgroup in an AIEOP cohort of BCP-ALL patients, enrolled into the AIEOP-BFM ALL2000/R2006 protocol.[21] A Ph-like signature was defined at transcriptome level,[22] and targeted RNAseq data identified underlining molecular lesions. In addition, signatures for ERG-related, HHD-like, ETV6/RUNX1-like, KMT2A-like and MEF2Dr subgroups were recognized.

Among B-others ALL patients, which accounted for 47% of a series of 289 new BCP-ALL diagnoses, the Ph-like profile was identified in 43·7%, corresponding to about 20% of the entire BCP-ALL cohort, in agreement with frequency previously reported.[3] The study cohort was, likely by chance, enriched for high-risk features (i.e., prednisone response and WBC and consequently stratification to the final High-

Risk group but not for MRD stratification, gender or age), possibly due to the relatively limited number of samples available for analysis from the total cohort of 837 B-other patients recruited in the study period. Nonetheless, the estimated 5 years EFS did not differ between analysed and not-analysed patients (74.2±3.8 vs 76.5±1.6, p=0.48). Ph-like ALL patients are characterized by a poor outcome, independently of any other commonly used risk features, even in homogeneous risk groups, including HR patients. Importantly, the Cox model demonstrated the highly significant impact on EFS for Ph-like (hazard ratio (HR)=2.93, p-value=0.003) as well as for assignment to final High-Risk group (HR=2.25, p-value=0.03).

The Ph-like group showed molecular characteristics known to be associated to high-risk features,[3,4] including the IKZF1-plus profile.[9] In addition, a driver fusion gene was identified in more than 50% of Ph-like cases; including the well-known ABL- or JAK/STAT-class in 20% of cases. Many studies are ongoing to target those genetic lesions mainly by deploying Tyrosine Kinase Inhibitors (TKIs) or JAK Inhibitors (JAKi)[7,35] as well as with CAR-based immunotherapy approaches.[36] These new therapeutic observations support the rationale to enrol Ph-like ALL patients in a specific clinical treatment protocol to improve treatment response with the use of TKIs.[6,8]

Here, we show that *PAX5* fusion genes are particularly recurrent among Ph-like patients: while PAX5 lesions overall account for more than 50% of Ph-like cases, PAX5t were identified exclusively in Ph-like,[12] they have their specific signature and are associated with a poor EFS similar to ABL/JAK-class patients (around 50%), and an inferior OS (about 53% vs. 83%) unacceptable for childhood ALL. Likewise, we recently

reported that PAX5 fusions are recurrent and associated with poor outcome in infant ALL patients (<1 year at diagnosis), not carrying a KMT2A/MLL rearrangement.[37]

Importantly, and in agreement with our previous studies,[14,15] we demonstrated that PAX5 fusions are characterized by LCK activity upregulation and are targetable by the Nintedanib/BIBF1120 inhibitor.[14,15,17,20] *Ex-vivo* treatment with Nintedanib/BIBF1120 demonstrated to promote apoptosis of leukemic cells, both in monotherapy and in combination with chemotherapy agents (Vincristine, Dexamethasone or Asparaginase). Strikingly, Dexamethasone and BIBF1120 had a synergistic effect, as further assessed *in vivo* assays in PDX NSG mice with two different PAX5 fusions (PAX5::AUTS2 and PAX5::DACH2), in which we observed a significant efficacy in different organs by BIBF1120 alone and in drug combination. Overall BIBF1120 alone was more effective than Dexamethasone in reducing tumour burden. Furthermore, ex-vivo drug screening revealed differential sensitivity of Nintedanib and Dasatinib against PAX5t leukemia samples when compared to MLLr/CRLFr samples. Our findings are also in agreement with the role and targeting of LCK in T-ALL setting, in which they demonstrate both the role of LCK in pathogenesis and how it is possible to target with specific inhibitors such as Dasatinib and Nintedanib, through gene silencing LCK in Patient-Derived Xenograft model.[38,39]

Moreover, we demonstrated that BIBF1120 was also effective on the AKT signalling in PAX5t, by inhibiting both the pAkt-Thr308 and pAkt-Ser473 residues, essential to activate the pathway.[40] This novel finding reveals a role for alternative mechanisms of PAX5t leukaemia,

considering that AKT is involved in apoptosis, metabolism and multidrug resistance in CLL and other malignancies.[34]

In conclusions, PAX5 lesions are amongst the most recurrent aberrations in Ph-like BCP-ALL, they have a specific signature and an unacceptable prognosis; PAX5t involve multiple pathways that can be targeted by Nintedanib/BIBF1120. The drug could be inserted in a second line of treatment, both to allow the identification of the patient's profile and to integrate this information with the MRD analysis data. In this way it could be possible to assign these patients to an experimental group, where they receive this inhibitor in addition to the chemotherapy drugs already in use. This drug has an acceptable tolerability profile and is already approved in clinical trials for idiopathic pulmonary fibrosis by the US Food and Drug Administration (FDA) since October 2014 and by the European Medicines Agency (EMA) since January 2015, and it is tested in several cancers, with anti-angiogenic and anti-tumour effects.[17,18,20]

These results strongly encourage further studies for a tailored treatment of patients with PAX5 fusions, implementing the deployment of inhibitors in combination with chemotherapy.

Tables

	Ph-like		Non-Ph-like	
	N	%	*N*	%
Total n. of patients	59	*43·7*	76	*56·3*
GENDER				
Male	36	*61·0*	37	*48·7*
Female	23	*39·0*	39	*51·3*
p-value=0·15				
AGE				
1-5 yrs	28	*47·5*	42	*55·3*
6-9 yrs	11	*18·6*	23	*30·2*
10-17 yrs	20	*33·9*	11	*14·5*
p-value=0·02				
WBC				
<20000	25	*42·4*	47	*61·8*
20-100000	28	*47·4*	20	*26·3*
>=100000	6	*10·2*	9	*11·9*
p-value=0·04				
Prednisone RESPONSE				
Good	52	*88·1*	61	*80·3*
Poor	7	*11·9*	15	*19·7*
p-value=0·22				
MRD stratification				
Standard	15	*28·8*	17	*27·4*
Medium	28	*53·9*	38	*61·3*
High	9	*17·3*	7	*11·3*
Not known	7		14	
p-value (NK excluded)=0·60				
FINAL RISK				
Standard	14	*23·7*	16	*21·0*
Medium	31	*52·6*	43	*56·6*
High	14	*23·7*	17	*22·4*
p-value=0·89				
Non Ph-like subgroups				
ETV6::RUNX1-like			12	*15·8*
HHD-like			23	*30·3*
KMT2A-like			2	*2·6*
ERG-related			35	*46·0*
MEF2Dr			3	*4·0*
Class-tie (not evaluable)			1	*1·3*
Events				
Resistant	0		0	
Death in Induction	1	*1·7*	0	
Relapses	20	*33·9*	12	*15·8*
- BM	*17*		*5*	
- CNS	*1*		*0*	
- BM+other	*2*		*7*	
Death in CCR	3	*5·1*	0	
- After CHEMO	2			
- After HSCT	1			
SMN	0		1	*1·3*
Alive in CCR	35	*59·3*	63	*82·9*

***Table 1*: Clinical Characteristics and outcome of Ph-like vs. non-Ph-like subgroups, in AIEOP ALL 2000/R2006.**

	Cox model on EFS		
	Hazard Ratio	*p*-value	95% Confidence Interval
Ph-like			
Non Ph-like	1		
Ph-like	2·93	0·003	1·46-5·87
Final risk			
Non High Risk	1		
High Risk	2·25	0·03	1·09-4·67
Age at diagnosis			
1-9 years	1		
10-17 years	1·10	0·80	0·51-2·37
WBC at diagnosis			
<100000	1		
≥100000	1·16	0·78	0·42-3·21

***Table 2*: Cox model analysis on study cohort of 135 B-other patients.**

Supplementary materials

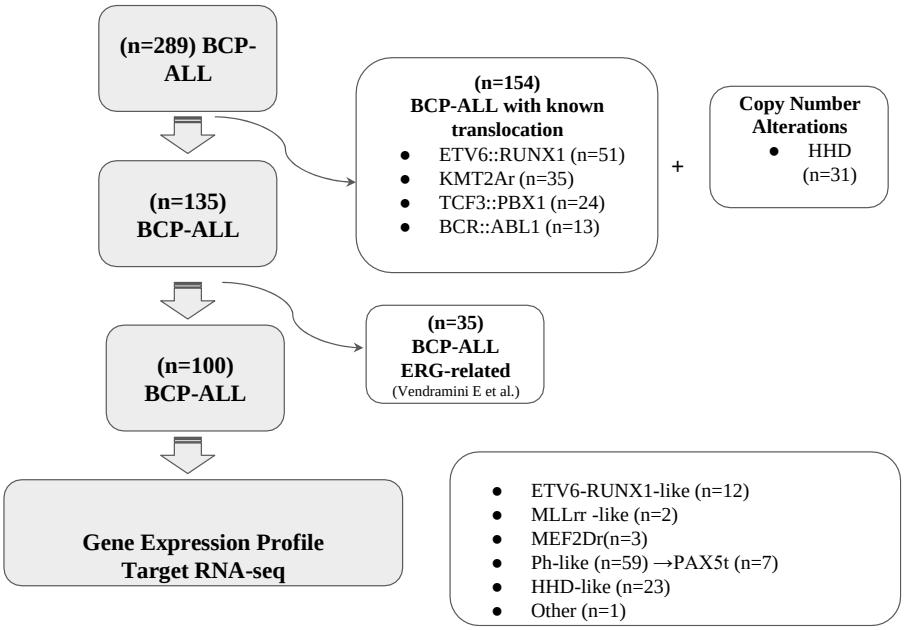

Supplementary figure S1. Flow-chart of strategy aiming to identify subgroups of BCP-ALL patients with targetable aberrations by characterizing cases according to gene expression and molecular profiles.

a

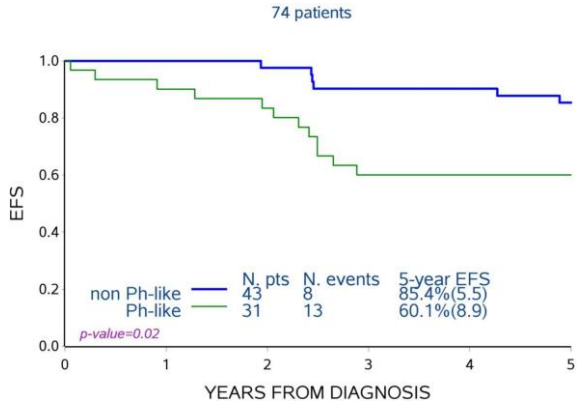

b

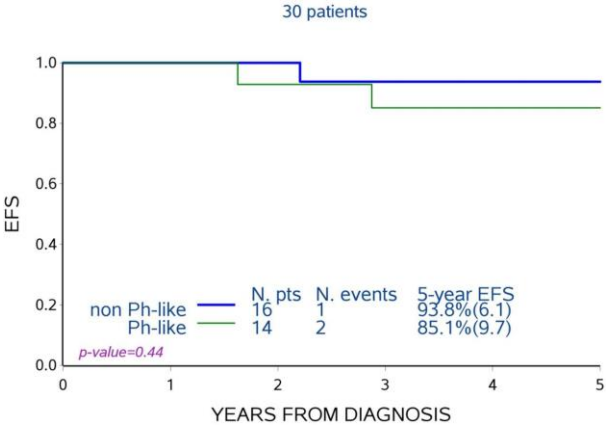

(All events are relapses)

Supplementary figure S2. Outcome analysis of the B-Other cohort, in terms of Events Free Survival or EFS In Medium Risk (a) and in Standard Risk groups (b).

a

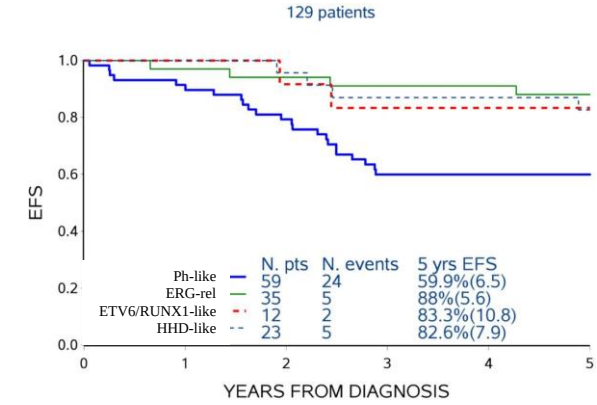

b

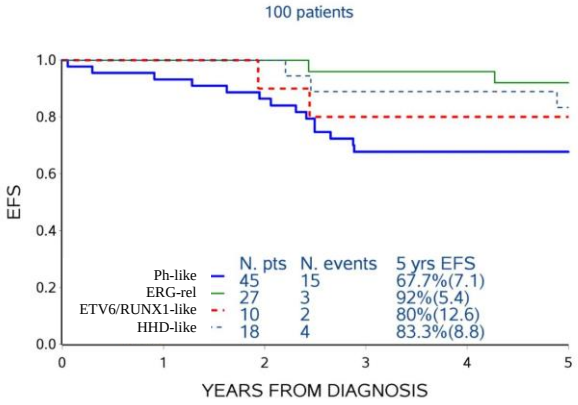

Supplementary figure S3. AIEOP ALL 2000/R2006 by GEP class in all risk (a) and in non-High-Risk patients (b).

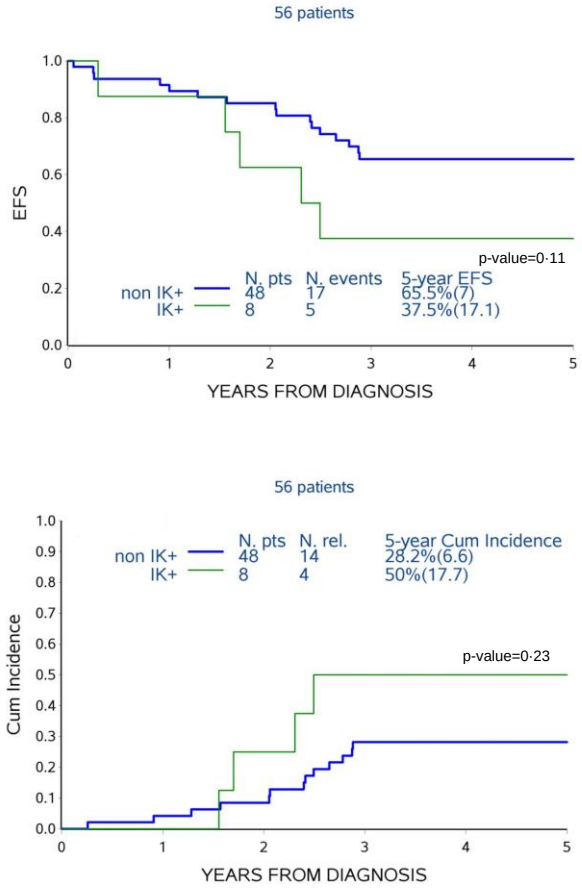

Supplementary figure S4. EFS and CIR analyses of IKAROS-plus vs. non IKAROS-plus patients in Ph-like subgroup.

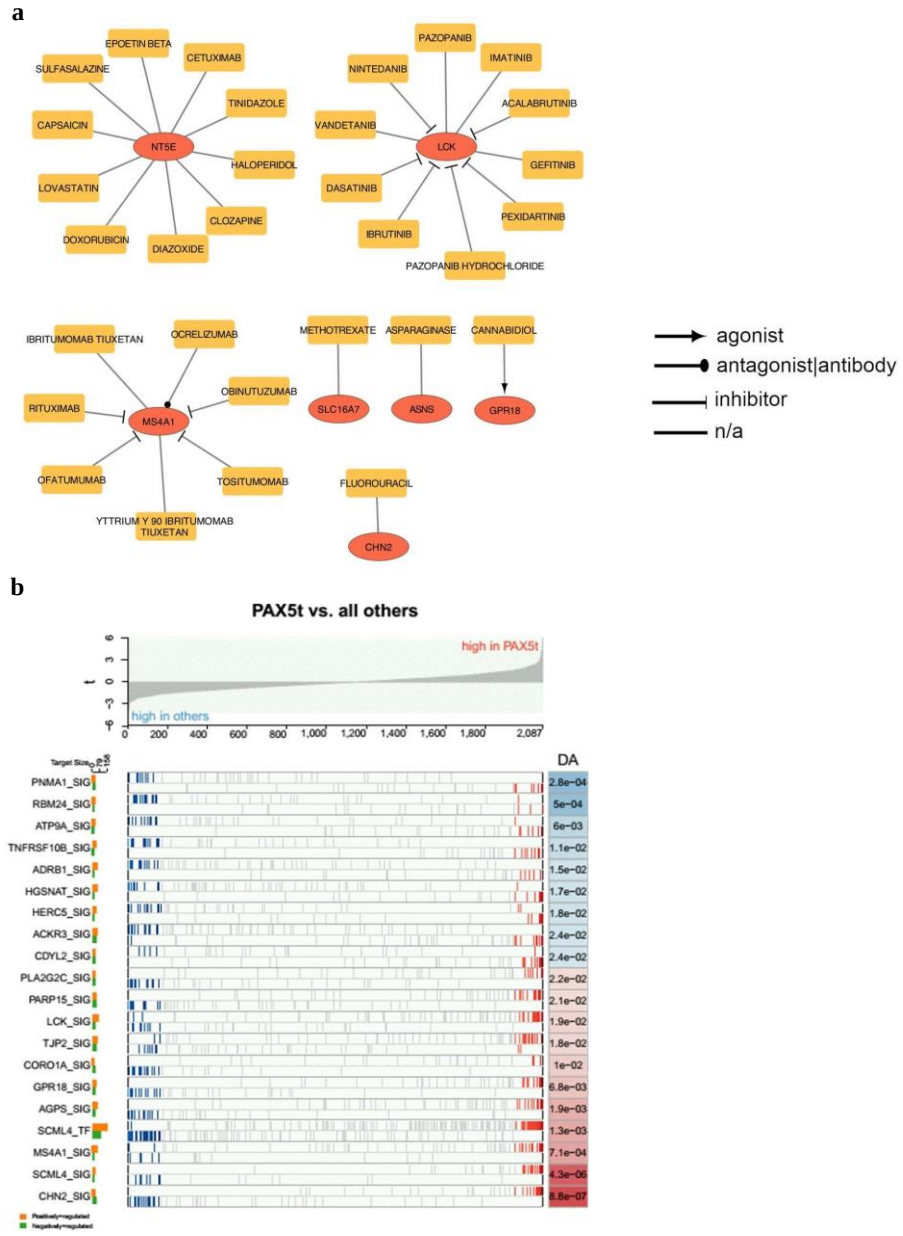

Supplementary figure S5. Activity of each driver inferred with NETBID2 in PAX5 translocated versus all BCP-ALL subtypes excluding Ph-like. Top panel (a) represents the expression ranking genes: at left the highest expressed in all BCP-ALL subtypes excluded Ph-like, at right in PAX5 translocated cases (PAX5t). Bottom panel (b) shows the impact of the expression patterns of each driver activity. In red, positively-

regulated target genes with significantly upregulation in PAX5 translocated compared to others BCP-ALL; in blue negatively-regulated target genes have significantly downregulation in PAX5 translocated compared to others BCP-ALL.

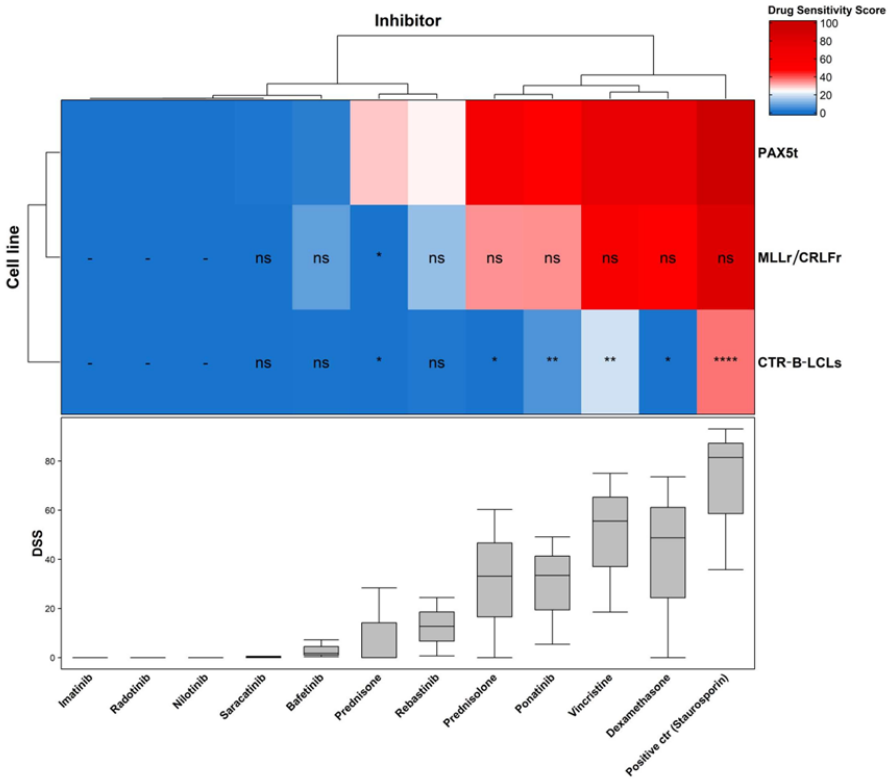

Supplementary figure S6. Comparative cellular viability of different sub-groups of leukemia (PAX5t, MLLr or CRLFr) samples and control-B-lymphoblastoid cell lines (CTR-B-LCSs), measured by ATP-Glo based luminescent based assay after exposure of the depicted drugs, whereas Staurospsorin was taken as a positive control. Drug sensitivity scores (DSS) are plotted as a clustered heat map, followed by unsupervised hierarchical clustering. The horizontal and the vertical axis of the dendrogram illustrates the dissimilarity between clusters, whereas the color of the cell is related to its position along with a DSS gradient. The P-values are calculated with the one-way Anova test related to PAX5t group, **** (P<0.0001), *** (P<0.001), ** (P<0.01);

*(P<0.05); ns=not significant. - represent significance cannot be calculated as DSS are 0, i.e., respective candidate is inactive.

a

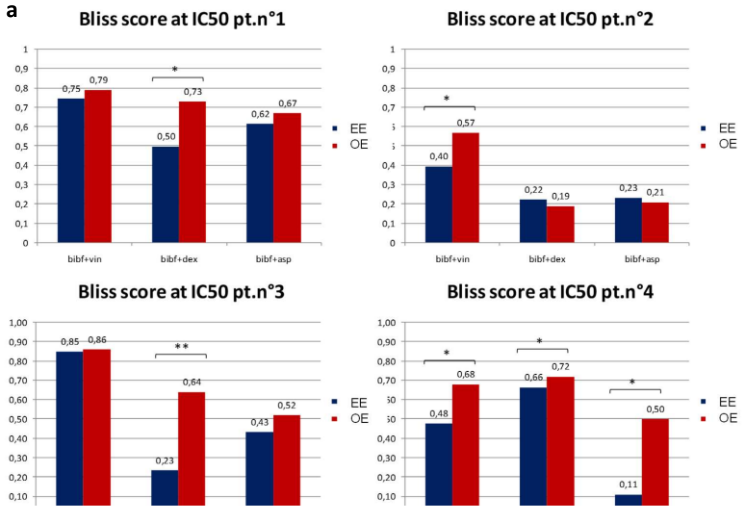

b

	Vincristine			Dexamethasone			Asparaginase		
	SYNERGISTIC EFFECT	ADDITIVE EFFECT	ANTAGONIST EFFECT	SYNERGISTIC EFFECT	ADDITIVE EFFECT	ANTAGONIST EFFECT	SYNERGISTIC EFFECT	ADDITIVE EFFECT	ANTAGONIST EFFECT
Pt. #1 PAX5/AUTS2		x		x				x	
Pt. #2 PAX5/AUTS2	x				x			x	
Pt. #3 PAX5/DACH2		x		x				x	
Pt. #4 PAX5/SOX5	x			x			x		

c

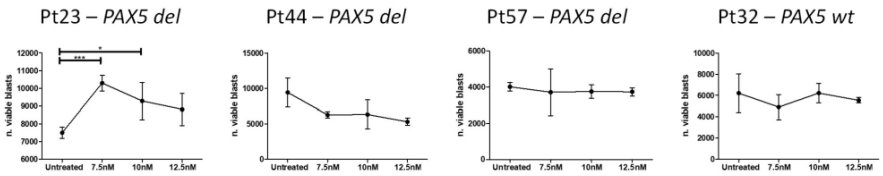

Supplementary figure S7. BIBF1120 combination index with Vincristine, Dexamethasone and Asparaginase, evaluated as Bliss score are shown in panel (a), while a summary of results is reported in panel (b), in patients' samples carrying a PAX5-fusion gene. Moreover, in panel (c), BIBF1120 treatment in N=5 Ph-like patients either PAX5-deleted or -wildtype status did not show any efficacy at 48h, evaluated as Annexin V/7-AAD by FACS.

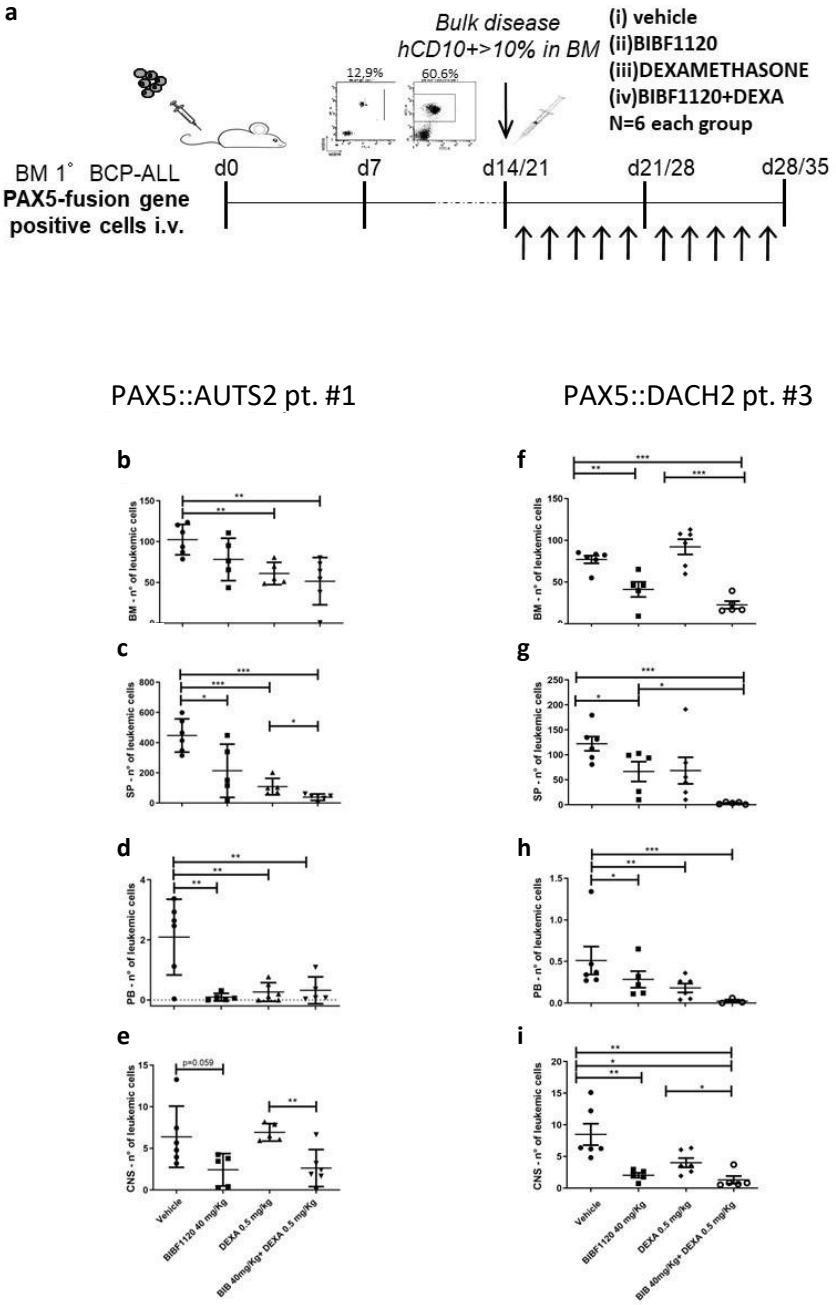

Supplementary figure S8. *In vivo* treatment by BIBF1120 alone or in combination with Dexamethasone. The experimental plan is depicted in panel (a): NSG mice were transplanted with human leukemic cell carrying different PAX5 fusion genes, namely

PAX5::AUTS2 as in Pt. n°1 (left panels) or PAX5::DACH2 as in Pt. n°3 (right panels). Data are expressed as absolute number of leukemic cells per organ, calculated mean of number of cells normalized for % human CD10 positive cells in hematopoietic tissues, such as Bone Marrow for Pt.1 (panel b) and Pt.3 (panel f), Spleen (panel c and g), Peripheral Blood (d and h) and Central Nervous System Meninges (e and i). Statistical analyses have been performed by Graphpad prism software and T test is shown as *P<0·05, **P<0·01, ***P<0·001.

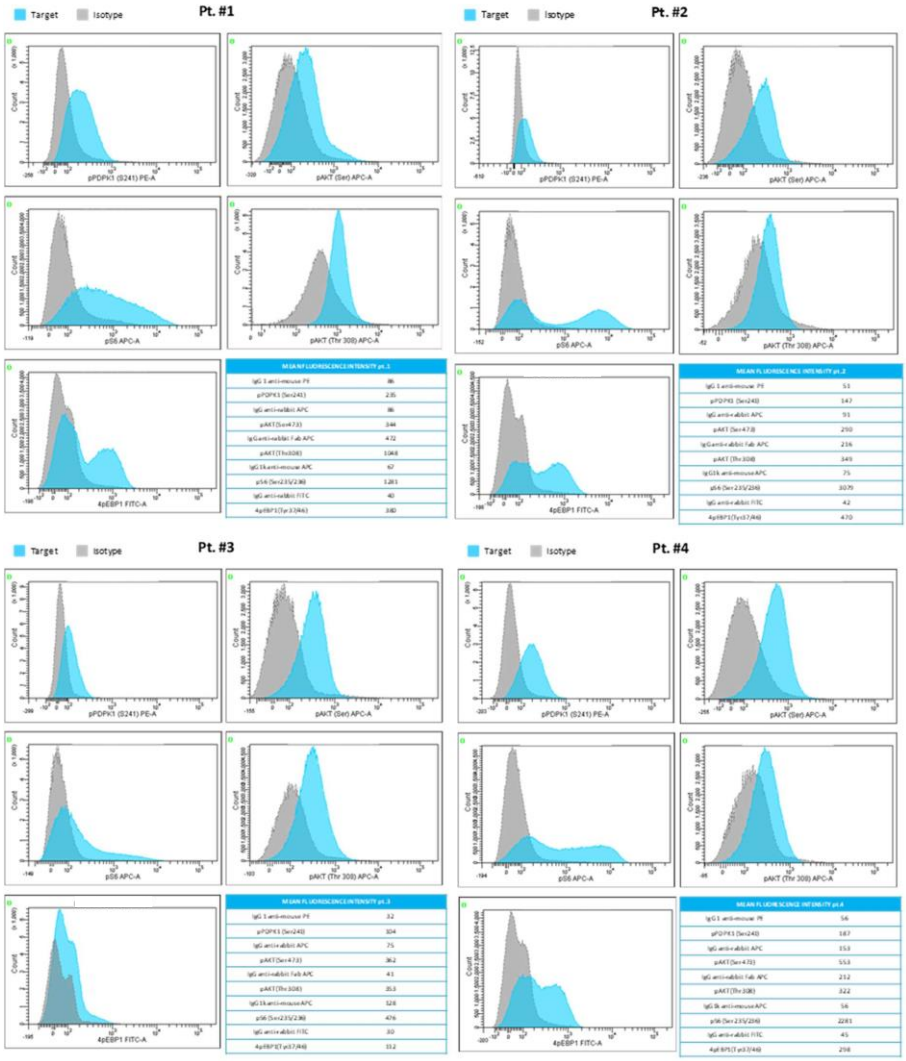

Supplementary figure S9. Phosphoflow Flow Cytometry images of AKT pathway, at basal level in primary patients' blast cells.

	Ph-like		ERG-related		ETV6/RUNX1 like		HHD-like	
	N	**%**	**N**	**%**	**N**	**%**	**N**	**%**
Total n. of patients	59		35		12		23	
GENDER								
Male	36	*61·0*	13	*37·1*	5	*41·7*	14	*60·9*
Female	23	*39·0*	22	*62·9*	7	*58·3*	9	*39·1*
AGE								
1-5 yrs	28	*47·5*	14	*40·0*	6	*50·0*	20	*87·0*
6-9 yrs	11	*18·6*	12	*34·3*	5	*41·7*	3	*13·0*
10-17 yrs	20	*33·9*	9	*25·7*	1	*8·3*	0	
WBC								
<20000	25	*42·4*	26	*74·3*	6	*50·0*	12	*52·2*
20-100000	28	*47·4*	8	*22·9*	2	*16·7*	9	*39·1*
≥100000	6	*10·2*	1	*2·8*	4	*33·3*	2	*8·7*
Prednisone RESPONSE								
Good	52	*88·1*	29	*82·9*	10	*83·3*	18	*78·3*
Poor	7	*11·9*	6	*17·1*	2	*16·7*	5	*21·7*
MRD stratification								
Standard	15	*28·8*	5	*16·1*	1	*11·1*	9	*56·3*
Medium	28	*53·9*	21	*67·7*	8	*88·9*	7	*43·7*
High	9	*17·3*	5	*16·1*	0	*10·0*	0	
Not known	7		4		3		7	
FINAL RISK								
Standard	14	*23·7*	5	*14·3*	1	*8·3*	8	*34·8*
Medium	31	*52·6*	22	*62·9*	9	*75·0*	10	*43·5*
High	14	*23·7*	8	*22·8*	2	*16·7*	5	*21·7*

3 MEF2Dr patients: 1 male, 2 females; 2 with WBC <20000, 1 with WBC ≥100000; 2 PGR and 1 PPR
2 KMT2A-like patients: 2 females; 1 with WBC 20-100, 1 with WBC ≥100000; 1 PGR and 1 PPR.

Table S1. AIEOP ALL 2000/R2006 GEP class characteristics.

	Ph-like		ERG-related		ETV6/RUNX1-like		HHD-like	
	N	**%**	**N**	**%**	**N**	**%**	**N**	**%**
Total n. of patients	**59**		35		12		23	
Resistant	0		0		0		0	
Death IND	1	*1·7*	0		0		0	
Relapses	**20**	*33·9*	**4**	*11·4*	**2**	*16·7*	**5**	*21·7*
- *BM*	*17*		2		1		1	
- *CNS*	*1*		0		0		0	
- *BM+other*	*2*		2		1		4	
Death in CCR	**3**	*5·1*	0		0		0	
- *After CHEMO*	2							
- *After HSCT*	1							
SMN	0		1	*2·9*	0		0	
Alive in CCR	**35**	*59·3*	30	*85·7*	10	*83·3*	18	*78·3*

Table S2. Characteristics of events among different GEP class subgroups.

	Ph-like			Non-Ph-like		
	N	***%***	***%****	**N**	***%***	***%****
Total n. of patients	20			12		
GENDER						
Male	13	*65·0*	*36·1*	5	*41·7*	*13·5*
Female	7	*35·0*	*30·4*	7	*58·3*	*17·9*
AGE						
1-5 yrs	13	*65·0*	*46·4*	7	*58·3*	*16·7*
6-9 yrs	1	*5·0*	*9·1*	5	*41·7*	*21·7*
10-17 yrs	6	*30·0*	*30·0*	0		
WBC						
<20000	8	*40·0*	*32·0*	2	*16·7*	*4·3*
20-100000	10	*50·0*	*35·7*	8	*66·6*	*40·0*
≥100000	2	*10·0*	*33·3*	2	*16·7*	*22·2*
Prednisone RESPONSE						
Good	18	*90·0*	*34·6*	9	*75·0*	*14·8*
Poor	2	*10·0*	*28·6*	3	*25·0*	*20·0*
MRD stratification						
Standard	2	*10·5*	*13·3*	1	*10·0*	*5·9*
Medium	11	*57·9*	*39·3*	8	*80·0*	*21·1*
High	6	*31·6*	*66·7*	1	*10·0*	*14·3*
Not known	1		*14·3*	2		*14·3*
FINAL RISK						
Standard	2	*10·0*	*14·3*	1	*8·3*	*6·3*
Medium	11	*55·0*	*35·5*	8	*66·7*	*18·6*
High	7	*35·0*	*50·0*	3	*25·0*	*17·7*

(*) calculated on total number of patients with a specific characteristic.

Table S3. Ph-like vs non-Ph-like characteristics of relapsed pts (protocol AIEOP ALL 2000/R2006).

MO	Final GEP	age (years)	MRD stratification	final stratification	RELAPSE (EFS)	FUSION GENE	FUSION-class	PAX5 STATUS	IKZF1plus	IKZF1	PAX5	CDKN2A	CDKN2B	ERG	CRLF2	JAK2	EBF1	ETV6	BTG1	RB1	n° CNV	Targeted-dNGS	MLPA	DNA array	GEP array
pt1	Ph-like	1	MR	MR	no	chr7-chr9 PAX5::ALT52	PAX5-class	PAX5 TRdel	neg	0	1	1	1	0	0	1	0	0	0	0	4	yes	yes	yes	yes
pt2	Ph-like	1	SR	SR	no	chr9-chr10 PAX5::ALDH18A1 + chrX-chrX P2RY8::CRLF2	PAX5-class	PAX5 TRdel	0	0	1	1	1	0	1	1	0	0	0	0	5	yes	yes	yes	yes
pt3	Ph-like	1	n.a.	MR	yes	chr9-ch12 PAX5::FBRSL1	PAX5-class	PAX5 TRdel	0	0	1	1	1	nk	0	0	0	0	0	0	3	yes	yes	yes	yes
pt4	Ph-like	2	SR	SR	yes	chr7-chr9 PAX5::ALT52	PAX5-class	PAX5 TRdel	nk	1	1	1	1	nk	0	1	0	0	0	0	5	yes	yes	yes	yes
pt5	Ph-like	2	MR	MR	no	chr7-chr9 PAX5::IZKF1 + chr14-chrX IgH::CRLF2	PAX5-class	PAX5 TRdel	0	0	2	2	2	0	0	0	0	0	0	1	4	yes	yes	yes	yes
pt6	Ph-like	1	MR	MR	yes	chr9-chrX PAX5::DACH2	PAX5-class	PAX5 TRdel	0	0	0	1	1	nk	0	0	0	0	0	0	2	yes	yes	yes	yes
pt7	Ph-like	8	SR	SR	no	chr9-chr16 PAX5::CDH13 + chrX-chrX P2 RY8::CRLF2	PAX5-class	PAX5 TRdel	0	0	0	1	1	0	1	0	0	0	0	0	3	yes	yes	yes	yes
pt8	Ph-like	10	MR	MR	yes	chr14-chrX IgH::CRLF2	JAK/STAT-class	PAX5 DEL	1	1	1	1	1	0	0	0	1	0	1	0	6	yes	yes	yes	yes
pt9	Ph-like	12	HR	HR	no	chr14-chrX IgH::CRLF2	JAK/STAT-class	PAX5 DEL	1	1	1	0	0	0	0	0	1	0	0	0	3	yes	yes	yes	yes
pt10	Ph-like	3	MR	MR	no	chrX-chrX P2RY8::CRLF2	JAK/STAT-class	PAX5 DEL	0	0	1	1	1	0	1	1	0	0	0	0	5	yes	yes	yes	yes
pt11	Ph-like	2	MR	MR	no	chrX-chrX P2RY8::CRLF2	JAK/STAT-class	PAX5 DEL	0	0	1	1	1	0	1	1	0	0	0	0	5	yes	yes	yes	yes
pt12	Ph-like	5	MR	MR	yes	chrX-chrX P2RY8::CRLF2	JAK/STAT-class	PAX5 DEL	0	0	1	1	1	nk	1	nk	0	0	0	0	4	yes	yes	no	yes
pt13	Ph-like	5	SR	SR	no	chrX-chrX P2RY8::CRLF2	JAK/STAT-class	PAX5 WT	0	0	0	1	0	0	1	0	0	0	0	0	2	yes	yes	no	yes
pt14	Ph-like	5	MR	MR	no	chrX-chrX P2RY8::CRLF2	JAK/STAT-class	PAX5 WT	0	1	0	0	0	nk	1	0	1	0	0	0	3	yes	yes	yes	yes
pt15	Ph-like	1	SR	SR	yes	chrX-chrX P2RY8::CRLF2	JAK/STAT-class	PAX5 WT	0	0	0	0	0	0	1	0	0	0	0	0	1	yes	yes	yes	yes
pt16	Ph-like	10	MR	MR	yes	chrX-chrX P2RY8::CRLF2	JAK/STAT-class	PAX5 WT	0	0	0	0	0	0	1	0	0	0	0	0	1	yes	yes	yes	yes
pt17	Ph-like	4	MR	MR	yes	chrX-chrX P2RY8::CRLF2	JAK/STAT-class	nk	nk	nk	nk	nk	nk	nk	1	nk	nk	nk	nk	nk	nk	yes	yes	no	yes
pt18	Ph-like	13	HR	HR	death in CCR after HSCT	chr5-chr5 EBF1::PDGFRB	ABL-class	PAX5 WT	0	0	0	0	0	0	0	0	1	1	2	0	3	yes	yes	yes	yes
pt19	Ph-like	11	HR	HR	no	chr5-chr5 EBF1::PDGFRB	ABL-class	PAX5 WT	0	1	0	0	0	0	0	0	1	0	0	0	2	yes	yes	yes	yes
pt20	Ph-like	4	MR	MR	yes	chr5-chr10 EBF1::JMJD1C + chr10-chr10 JMJD1C::VTI1A	other	PAX5 DEL	0	0	1	1	1	0	0	1	0	0	0	0	4	yes	yes	no	yes
pt21	Ph-like	13	n.a.	MR	death in induction	chr22-chr22 MAP4K1::PPM1F	other	PAX5 DEL	0	0	1	1	1	0	0	nk	0	0	0	0	3	yes	yes	yes	yes
pt22	Ph-like	12	n.a.	MR	death in CCR after chemotherapy	chr5-chr5 CAMK2A::CD74 + chr16-chr16 SLC7A6::CYBA	other	PAX5 DEL	1	1	1	1	1	0	0	0	0	0	0	0	4	yes	yes	yes	yes
pt23	Ph-like	13	MR	HR	death in CCR after chemotherapy	chr1-chr1 MEF2D::BCL9	MEF2Dr	PAX5 DEL	0	0	1	1	1	0	0	0	0	0	0	0	3	yes	yes	no	yes
pt24	Ph-like	4	MR	MR	yes	chr5-chr5 CAMK2A::CD74	other	PAX5 WT	0	0	0	0	0	0	0	0	0	0	0	0	0	yes	yes	no	yes
pt25	Ph-like	8	SR	SR	no	chr2-chr11 SPTBN1::MLL4T1	other	PAX5 WT	0	0	0	0	0	0	0	0	0	0	0	0	0	yes	yes	no	yes
pt26	Ph-like	9	MR	HR	no	chr9-chr12 SET::RASA3	other	PAX5 WT	0	0	0	0	0	0	2	0	0	0	0	1	2	yes	yes	yes	yes
pt27	Ph-like	10	MR	HR	yes	chr7-chr7 IKZF1::DOCK	other	PAX5 WT	0	1	0	0	0	0	0	0	0	1	1	0	3	yes	yes	yes	yes
pt28	Ph-like	3	MR	MR	yes	chr12-chr12 BCL7A::MXI1	other	PAX5 WT	0	1	0	0	0	nk	0	0	0	1	0	0	2	yes	yes	no	yes
pt29	Ph-like	3	HR	HR	yes	chr17-chr19 TCF3::HLF	other	PAX5 WT	0	0	0	0	0	0	0	0	0	0	0	0	0	yes	yes	yes	yes
pt30	Ph-like	5	HR	HR	yes	chr5-chr5 CAMK2A::CD74 + chr5-chr5 ARSI::CD74	other	PAX5 WT	0	0	0	0	0	0	0	0	0	0	0	0	0	yes	yes	yes	yes
pt31	Ph-like	4	SR	SR	no	neg	neg	PAX5 WT	0	0	0	0	0	0	0	0	0	0	0	0	0	yes	yes	no	yes
pt32	Ph-like	7	n.a.	MR	no	neg	neg	PAX5 WT	0	0	0	0	0	0	0	0	0	0	0	0	0	yes	yes	no	yes
pt33	Ph-like	9	SR	SR	no	neg	neg	PAX5 WT	0	0	0	0	0	0	0	0	0	0	0	0	0	yes	yes	yes	yes
pt34	Ph-like	15	SR	SR	no	neg	neg	PAX5 DEL	0	0	1	1	1	0	0	1	0	0	0	0	4	yes	yes	yes	yes
pt35	Ph-like	10	HR	HR	yes	neg	neg	PAX5 WT	0	0	0	0	0	0	0	0	0	0	1	0	1	yes	yes	yes	yes
pt36	Ph-like	15	SR	SR	no	neg	neg	PAX5 DEL	1	1	1	1	1	0	2	1	0	0	0	0	8	yes	yes	yes	yes
pt37	Ph-like	5	MR	HR	no	neg	neg	PAX5 WT	0	0	0	0	0	0	0	0	0	0	0	0	0	yes	yes	no	yes
pt38	Ph-like	11	MR	MR	no	neg	neg	nk	nk	nk	nk	nk	nk	nk	0	nk	nk	nk	nk	nk	nk	yes	yes	no	yes
pt39	Ph-like	14	SR	SR	no	neg	neg	PAX5 DEL	0	0	1	1	1	0	0	0	0	1	0	0	4	yes	yes	yes	yes
pt40	Ph-like	13	MR	MR	no	neg	neg	PAX5 WT	0	1	0	0	0	0	0	nk	0	0	0	0	1	yes	yes	yes	yes
pt41	Ph-like	3	MR	MR	no	neg	neg	PAX5 DEL	0	0	1	1	1	0	0	1	0	0	0	0	4	yes	yes	yes	yes
pt42	Ph-like	5	MR	MR	no	neg	neg	PAX5 DEL	0	0	1	1	0	nk	0	0	0	0	0	0	2	yes	yes	yes	yes
pt43	Ph-like	3	SR	HR	no	neg	neg	PAX5 WT	0	0	0	0	0	0	0	nk	0	0	0	0	0	yes	yes	no	yes
pt44	Ph-like	16	n.a.	MR	no	neg	neg	PAX5 DEL	0	0	1	1	1	0	0	0	0	0	1	1	3	yes	yes	yes	yes
pt45	Ph-like	2	SR	SR	no	neg	neg	PAX5 DEL	1	1	1	1	1	0	0	nk	0	1	0	0	5	yes	yes	no	yes
pt46	Ph-like	6	SR	SR	no	neg	neg	PAX5 AMP	0	0	2	2	2	nk	2	2	0	0	0	0	3	yes	yes	yes	yes
pt47	Ph-like	4	SR	SR	no	neg	neg	PAX5 DEL	0	0	1	1	1	0	0	1	0	0	1	1	6	yes	yes	yes	yes
pt48	Ph-like	12	MR	MR	no	neg	neg	PAX5 AMP	0	0	2	0	0	0	0	0	0	0	0	0	1	yes	yes	yes	yes
pt49	Ph-like	9	n.a.	MR	no	neg	neg	PAX5 WT	0	0	0	1	1	0	0	0	0	0	0	2	2	yes	yes	yes	yes
pt50	Ph-like	5	MR	MR	no	neg	neg	PAX5 WT	0	0	0	1	0	0	0	0	0	0	0	0	1	yes	yes	no	yes
pt51	Ph-like	6	n.a.	MR	no	neg	neg	PAX5 WT	0	0	0	1	1	0	0	nk	0	0	0	0	2	yes	yes	yes	yes
pt52	Ph-like	1	MR	MR	yes	neg	neg	PAX5 DEL	1	1	1	1	1	0	0	1	0	0	1	0	6	yes	yes	yes	yes
pt53	Ph-like	9	MR	MR	no	neg	neg	PAX5 AMP	0	0	2	2	2	0	0	2	0	0	0	0	4	yes	yes	no	yes
pt54	Ph-like	9	MR	MR	no	neg	neg	PAX5 WT	0	0	0	1	1	0	0	0	0	0	0	0	2	yes	yes	yes	yes
pt55	Ph-like	11	HR	HR	yes	neg	neg	PAX5 AMP	0	0	2	1	1	0	0	0	0	0	1	1	5	yes	yes	yes	yes
pt56	Ph-like	12	HR	HR	yes	neg	neg	PAX5 DEL	1	1	1	0	0	0	0	0	0	1	0	0	3	yes	yes	yes	yes
pt57	Ph-like	15	MR	MR	no	neg	neg	PAX5 DEL	0	0	1	1	1	0	0	1	0	0	0	0	4	yes	yes	yes	yes
pt58	Ph-like	8	MR	MR	yes	neg	neg	PAX5 WT	0	0	0	0	0	0	0	0	0	0	0	0	0	yes	yes	yes	yes
pt59	Ph-like	3	HR	HR	yes	nk	nk	PAX5 WT	1	1	0	1	1	0	0	0	0	0	0	0	3	no	yes	yes	yes

Table S4. Clinical and Molecular Characteristics of AIEOP ALL 2000/R2006 B- other cohort, such as GEP-class, CNV data, Fusion genes. Legend: 0=wt; 1=del; 2=amp; n.a.=not applicable; n.k.=not known.

	Ph-like		Not Ph-like	
	N	***%***	**N**	***%***
Total n. of patients with available PAX5 status	57(59)	*96·6*	74(76)	*97·4*
PAX5wt	26	*45·6*	62	*83·8*
PAX5del	20	*35·1*	9	*12·2*
PAX5amp	4	*7*	3	*4*
PAX5t	7	*12·3*	0	*0*

Table S5. *PAX5* gene status in B-other cohort, according to Ph-like (or not) profiles.

FUSION GENE	Forward primer	Sequence 5' - 3'	Reverse primer	Sequence 5' - 3'	PCR product size
chr1-chr1 MEF2D::BCL9	MEF2Dex5	CCCTGGTGACATCATCCCTC	BCL9ex10	GTGAGAAAGTGGCTGGGTCA	209
chr5-chr5 EBF1::PDGFRB	EBF1ex14	CACGAGCATGAACGGATACGGCTCT	PDGFRBex12	ATGGCCGTCAGAGCTCACAGACTCA	442
chr5-chr5 CAMK2A::CD74	CD74ex4	TGCAGAATGCCACCAAGTATG	CAMK2Aex4	TCAGGTAGTGGTGTCCCTCC	443
chr5-chr10 EBF1::JMJD1C	EBF1ex9	GAGTGAAGGATGGACGACGG	JMJD1Cex8	TGGTGTGGGTGGTCTGGATA	733
chr7-chr9 PAX5::AUTS2	PAX5ex3	ACGCCAAAATCCCACCATGT	AUTS2ex6	GATGCCTTCGTCTCTCTTGC	609
chr7-chr9 PAX5::IKZF1	PAX5ex3	ACGCCAAAATCCCACCATGT	IKZF1ex4	CGTTCTCCAGTGTGGCTTCT	664
chr9-chr10 PAX5::ALDH18A1	PAX5ex2	CTCATCAAGGTGTCAGGCCC	ALDH18A1ex5	GCACAGATGCTGTACTGGGT	934
chr9-chr12 PAX5::FBRSL1	PAX5ex5	GACACCAACAAGCGCAAGAG	FBRSL1ex12	CCCAACACGTGCTCACCTT	403
chr9-chr16 PAX5::CDH13	PAX5ex3	ACGCCAAAATCCCACCATGT	CDH13ex3	GGACGAACAGAGTTTTGCCC	658
chr9-chrX PAX5::DACH2	PAX5ex3	ACGCCAAAATCCCACCATGT	DACH2ex5	GCAGCCATGTTGGCAATAGT	341
chr10-chr10 JMJD1C/VTI1A	JMJD1Cex3	GTGCCTTTCAGCCCTACCAG	VTI1Aex4-5	AGATGTGCCCTCTGGTTCTC	847
chr11-chr11 MLL::USP2	MLLex19	AAGGTCCTGGAGAACCAGACT	USP2ex5	AGATGGGCTCACCACATCATT	701
chr12-chr13 ETV6::EEF1DP3	ETV6ex3		EEF1DP3intr1-2	CTGCAAAACTCACTCAGGCA	539
chr12-chr16 ZNF384::CREBBP	CREBBPex6	ATGCCAGTGACAAGCGAAAC	ZNF384ex3	ATTCTGGGTAACGGACGCTT	536
chr12-chr19 ZNF384::TCF3	TCF3ex7	CATGAAGGGGACCTCCCAGTA	ZNF384ex10	GTGGCAGCACGGATCTCTAA	341
chr12-chr21 ETV6::RUNX1 atypical	ETV6ex4	GGTGATGTG CTCTATGA ACTC CTTCAGCA TATTC	RUNX1ex4	AACGCCTCGCTCATCTTGC	245
chr17-chr19 TCF3::HLF	TCF3ex16	CACCAGCCTCATGCACAAC	HLFex4	GGGCCGAGTTCTCCTTCTCCAGGA	213+intron
chr19-chr19 TCF3::OAZ1	OAZ1ex1	CGGATGGTGAAATCCTCCCTG	TCF3ex6	TCTCCCGAAGGAGGCATAGG	343
chrX-chrX P2RY8::CRLF2	P2RY8ex1	GGACAGATGGAAACTGGAAGG	CRLF2ex3	GTCCCATTCCTGATGGAGAA	511

Supplemental Table S6. Fusion gene validation RT-PCR primers.

Gene	Drug	Interaction_types	Database Sources	PMIDs
CHN2	FLUOROURACIL	NA	PharmGKB	24444404
MS4A1	OCRELIZUMAB	antagonist antibody	TdgClinicalTrial | ChemblInteractions | GuideToPharmacology | TTD	27343722 | 27756172
	OFATUMUMAB	antibody | inhibitor	MyCancerGenome | TdgClinicalTrial | ChemblInteractions | GuideToPharmacology | PharmGKB | TTD	19427037 | 18386516 | 17968100
	TOSITUMOMAB	inhibitor | antibody	TdgClinicalTrial | ChemblInteractions | TEND | GuideToPharmacology | PharmGKB | TTD	11418316 | 14748653 | 11879282 | 12899647 | 11752352 | 15023434 | 13129395
	YTTRIUM Y 90 IBRITUMOMAB TIUXETAN	NA	ChemblInteractions	
	IBRITUMOMAB TIUXETAN	NA	TdgClinicalTrial | TEND | PharmGKB | TTD	
	RITUXIMAB	antibody | inhibitor	MyCancerGenome | TdgClinicalTrial | ChemblInteractions | TEND | GuideToPharmacology | PharmGKB | TTD	19704735 | 20350667 | 11752352 | 20350663
	OBINUTUZUMAB	antibody | inhibitor	TdgClinicalTrial | ChemblInteractions | GuideToPharmacology | PharmGKB | TTD | FDA	19513948 | 24795454
GPR18	CANNABIDIOL	NA	GuideToPharmacology	26264914
LCK	WANDETANIB	NA	DTC	
	IBRUTINIB	inhibitor	GuideToPharmacology	
	IMATINIB	NA	DTC	
	GEFITINIB	NA	DTC	
	DASATINIB	multitarget | inhibitor	TdgClinicalTrial | ChemblInteractions | TEND | TTD	17154512 | 20072833 | 11752352
	PAZOPANIB	NA	DTC	
	PEXIDARTINIB	inhibitor	GuideToPharmacology	
	NINTEDANIB	inhibitor	TALC	18559334 | 31016670
	ACALABRUTINIB	inhibitor	GuideToPharmacology	
	PAZOPANIB HYDROCHLORIDE	inhibitor	ChemblInteractions	
ASNS	ASPARAGINASE	NA	NCI | CNIC | PharmGKB	28069604 | 24268318 | 11568548
SLC16A7	METHOTREXATE	NA	PharmGKB	
NTSE	CAPSAICIN	NA	NCI	2492344
	DOXORUBICIN	NA	NCI	7927909
	CETUXIMAB	NA	CNIC	25320391
	HALOPERIDOL	NA	NCI	11490180
	LOVASTATIN	NA	NCI	11884371
	EPOETIN BETA	NA	NCI	16469051
	CLOZAPINE	NA	NCI	11490180
	SULFASALAZINE	NA	NCI	9435300
	TINIDAZOLE	NA	NCI	14553936
	DIAZOXIDE	NA	NCI	16271703
SCML4	No interactions			
AGPS	No interactions			
CORO1A	No interactions			
TJP2	No interactions			
PARP15	No interactions			
PLA2G2C	No interactions			
VDAC1	No interactions			
PZRY10	No interactions			
IGFBP2	No interactions			
PON2	No interactions			
IGLL1	No interactions			
PIP5K1B	No interactions			
BCL6	No interactions			
GDMK	No interactions			
PTPRJ	No interactions			

Supplemental Table S7. List of genes resulted with a positive high driver activity in

PAX5t versus BCR/ABL like patients by NetBID2 analysis (P<0.05); when present, names of drug with interaction among the genes is reported.

		PAX5t			MLLr/CRLFr					CTR B-LCLs				
Inhibitor	Target	pt. #1 PAX5::AUTS2	pt. #3 PAX5::DACH2	pt. #4 PAX5::SOX5	ALL-PO	KOPN8	RS4;11	SEM	MUTZ5	CTR #1	CTR #2	CTR #3	CTR #4	CTR #5
Foretinib	VEGFR2; c-MET	89,56	11,34	79,90	60,10	39,61	21,33	58,05	20,17	0,02	0,01	0,01	2,23	0,04
Bosutinib	Bcr-Abl; Src;	5,16	16,33	29,20	25,72	37,39	13,39	35,57	6,40	2,11	1,19	1,98	5,63	1,27
Dasatinib (Hydrochlorid)	Bcr-Abl; Src;	22,74	42,65	0,00	0,00	0,00	0,00	0,00	0,00	0,00	0,00	0,00	0,00	0,00
Nintedanib (BIBF1120)	LCK inhibitor	27,33	34,69	32,62	0,00	17,73	0,61	5,94	1,91	3,40	1,39	2,27	9,03	1,50
Staurosporin, pos ctr	Multiple non-selective inhibitor of protein kinases	92,31	92,29	94,51	84,05	91,34	76,46	90,51	64,77	30,28	30,15	28,39	53,04	37,03

mean dss	PAX5t	MLLr/CRLFr	CTR B-LCLs
Foretinib	60,27	44,77	0,46
Bosutinib	16,90	28,02	2,43
Dasatinib	21,80	0,00	0,00
Nintedanib	31,55	6,07	3,52
Staurosporin	93,04	85,59	35,78

Table S8. Differential drug sensitivity score data by drug screening in PAX5t

Author contributions.

GF, SB and GC initiated the project; GF and SB performed experiments; DS and MGV collected patients data and performed survival analyses; EV and SB developed the signature classification; AG and AP performed bioinformatic analyses; SR, CS and MQ performed NGS analyses and RT-PCR validation tests; CP and MG completed the CNA analyses; GF, CS, MQ, CP, MB, SM, AMS developed the in vivo work; CS and MQ setup the ex-vivo and phosphoflow experiments; BB performed immunophenotypic analyses; SBh, JWT and AB developed and analysed drug screening; CM, LLN, FL, VC, CR and ABi provided patients, treated in their centres; GF, SB, GtK and GC analysed data and wrote the paper, with contributions from all co-authors. GF, SB, DS, MGV, Gtk and GC have verified the underlying data. Moreover, all authors read and approved the final version of the manuscript.

Data Sharing Statement

GEP data are available at GEO (accession numbers GSE79547, GSE13164, GSE13159, GSE13204).

Target capture Next Generation Sequencing FASTQ files are available in the ArrayExpress database (www.ebi.ac.uk/arrayexpress) under accession number E-MTAB-11319.

Declaration of Interests. The authors declare no competing financial interests.

Acknowledgements

This work was supported by the Italian Ministry of Health, grant Ricerca Finalizzata-Giovani Ricercatori (GR-2016-02364753 to GF, CP and MB), Associazione Italiana Ricerca per la Ricerca sul Cancro (AIRC) IG2015 no. 17593 (GC) and IG2017 no. 20564 (to AB), TRANSCALL-2 (ID 189) to AB, Fondazione Cariplo project number 2018-0339 to CP and supporting MQ fellow. Fondazione Cariparo no. 17/07_1FCR (to SB) and no. 20/12 (to BB). CS and MQ were supported from the Doctoral Program in Molecular and Translational Medicine (DIMET, University of Milano-Bicocca). We are grateful to Prof. Beppe Basso, who since the beginning was enthusiast for the contribution of gene expression profiling to the dissection of ALL, and fully supported this project. We thank the Paediatric Oncology BioBank of Padua for providing the biological material. The authors thank the BioBank of the Laboratory of Human Genetics (former Galliera Genetic Bank) member of "Network Telethon of Genetic Biobanks" (project no. GTB18001), funded by Telethon Italy, and of the EuroBioBank Network and the Assi Gulliver Associazione Sindrome di Sotos Italia provided as with specimens". The authors deeply thank the

“Comitato Maria Letizia Verga” for its support with “Passaporto Genetico” project.

REFERENCES

1. Den Boer ML, van Slegtenhorst M, De Menezes RX, Cheok MH, Buijs-Gladdines JG, Peters ST, et al. A subtype of childhood acute lymphoblastic leukaemia with poor treatment outcome: a genome-wide classification study. *The Lancet Oncology* 2009; **10**(2): 125-34.
2. Mullighan CG, Su X, Zhang J, Radtke I, Phillips LA, Miller CB, et al. Deletion of IKZF1 and prognosis in acute lymphoblastic leukemia. *N Engl J Med* 2009; **360**(5): 470-80.
3. Pui CH, Roberts KG, Yang JJ, Mullighan CG. Philadelphia Chromosome-like Acute Lymphoblastic Leukemia. *Clin Lymphoma Myeloma Leuk* 2017; **17**(8): 464-70.
4. Shiraz P, Payne KJ, Muffly L. The Current Genomic and Molecular Landscape of Philadelphia-like Acute Lymphoblastic Leukemia. *Int J Mol Sci* 2020; **21**(6).
5. Arber DA, Orazi A, Hasserjian R, Thiele J, Borowitz MJ, Le Beau MM, et al. The 2016 revision to the World Health Organization classification of myeloid neoplasms and acute leukemia. *Blood* 2016; **127**(20): 2391-405.
6. Izraeli S. Beyond Philadelphia: 'Ph-like' B cell precursor acute lymphoblastic leukemias - diagnostic challenges and therapeutic promises. *Curr Opin Hematol* 2014; **21**(4): 289-96.
7. Roberts KG, Li Y, Payne-Turner D, Harvey RC, Yang YL, Pei D, et al. Targetable kinase-activating lesions in Ph-like acute lymphoblastic leukemia. *N Engl J Med* 2014; **371**(11): 1005-15.
8. Cario G, Leoni V, Conter V, Attarbaschi A, Zaliova M, Sramkova L, et al. Relapses and treatment-related events contributed equally to poor prognosis in children with ABL-class fusion positive B-cell acute lymphoblastic leukemia treated according to AIEOP-BFM protocols. *Haematologica* 2020; **105**(7): 1887-94.
9. Stanulla M, Dagdan E, Zaliova M, Moricke A, Palmi C, Cazzaniga G, et al. IKZF1(plus) Defines a New Minimal Residual Disease-Dependent Very-Poor Prognostic Profile in Pediatric B-Cell Precursor Acute Lymphoblastic Leukemia. *J Clin Oncol* 2018; **36**(12): 1240-9.
10. Cobaleda C, Schebesta A, Delogu A, Busslinger M. Pax5: the guardian of B cell identity and function. *Nature Immunology* 2007; **8**(5): 463-70.

11. Mullighan CG, Goorha S, Radtke I, Miller CB, Coustan-Smith E, Dalton JD, et al. Genome-wide analysis of genetic alterations in acute lymphoblastic leukaemia. *Nature* 2007; **446**(7137): 758-64.

12. Gu Z, Churchman ML, Roberts KG, Moore I, Zhou X, Nakitandwe J, et al. PAX5-driven subtypes of B-progenitor acute lymphoblastic leukemia. *Nat Genet* 2019; **51**(2): 296-307.

13. ung M, Schieck M, Hofmann W, Tauscher M, Lentes J, Bergmann A, et al. Frequency and prognostic impact of PAX5 p.P80R in pediatric acute lymphoblastic leukemia patients treated on an AIEOP-BFM acute lymphoblastic leukemia protocol. *Genes, chromosomes & cancer* 2020; **59**(11): 667-71.

14. Fazio G, Cazzaniga V, Palmi C, Galbiati M, Giordan M, te Kronnie G, et al. PAX5/ETV6 alters the gene expression profile of precursor B cells with opposite dominant effect on endogenous PAX5. *Leukemia* 2013; **27**(4): 992-5.

15. Cazzaniga V, Bugarin C, Bardini M, Giordan M, Te Kronnie G, Basso G, et al. LCK over-expression drives STAT5 oncogenic signaling in PAX5 translocated BCP-ALL patients. *Oncotarget* 2015; **6**(3): 1569-81.

16. Delogu A, Schebesta A, Sun Q, Aschenbrenner K, Perlot T, Busslinger M. Gene repression by Pax5 in B cells is essential for blood cell homeostasis and is reversed in plasma cells. *Immunity* 2006; **24**(3): 269-81.

17. Hilberg F, Roth GJ, Krssak M, Kautschitsch S, Sommergruber W, Tontsch-Grunt U, et al. BIBF 1120: triple angiokinase inhibitor with sustained receptor blockade and good antitumor efficacy. *Cancer Res* 2008; **68**(12): 4774-82.

18. Keating GM. Nintedanib: A Review of Its Use in Patients with Idiopathic Pulmonary Fibrosis. *Drugs* 2015; **75**(10): 1131-40.

19. Awasthi N, Schwarz RE. Profile of nintedanib in the treatment of solid tumors: the evidence to date. *Onco Targets Ther* 2015; **8**: 3691-701.

20. Wind S, Schmid U, Freiwald M, Marzin K, Lotz R, Ebner T, et al. Clinical Pharmacokinetics and Pharmacodynamics of Nintedanib. *Clin Pharmacokinet* 2019; **58**(9): 1131-47.

21. Conter V, Bartram CR, Valsecchi MG, Schrauder A, Panzer-Grumayer R, Moricke A, et al. Molecular response to treatment redefines all prognostic factors in children and adolescents with B-cell precursor acute lymphoblastic leukemia: results in 3184 patients of the AIEOP-BFM ALL 2000 study. *Blood* 2010; **115**(16): 3206-14.

22. Haferlach T, Kohlmann A, Wieczorek L, Basso G, Kronnie GT, Bene MC, et al. Clinical utility of microarray-based gene expression profiling in the diagnosis and subclassification of leukemia: report from the International Microarray Innovations in Leukemia Study Group. *J Clin Oncol* 2010; **28**(15): 2529-37.

23. Du X, Wen J, Wang Y, Karmaus PWF, Khatamian A, Tan H, et al. Hippo/Mst signalling couples metabolic state and immune function of CD8alpha(+) dendritic cells. *Nature* 2018; **558**(7708): 141-5.

24. Khatamian A, Paull EO, Califano A, Yu J. SJARACNe: a scalable software tool for gene network reverse engineering from big data. *Bioinformatics* 2019; **35**(12): 2165-6.

25. Palmi C, Lana T, Silvestri D, Savino A, Kronnie GT, Conter V, et al. Impact of IKZF1 deletions on IKZF1 expression and outcome in Philadelphia chromosome negative childhood BCP-ALL. Reply to "incidence and biological significance of IKZF1/Ikaros gene deletions in pediatric Philadelphia chromosome negative and Philadelphia chromosome positive B-cell precursor acute lymphoblastic leukemia". *Haematologica* 2013; **98**(12): e164-5.

26. Grioni A, Fazio G, Rigamonti S, Bystry V, Daniele G, Dostalova Z, et al. A Simple RNA Target Capture NGS Strategy for Fusion Genes Assessment in the Diagnostics of Pediatric B-cell Acute Lymphoblastic Leukemia. *Hemasphere* 2019; **3**(3): e250.

27. Pemovska T, Kontro M, Yadav B, Edgren H, Eldfors S, Szwajda A, et al. Individualized systems medicine strategy to tailor treatments for patients with chemorefractory acute myeloid leukemia. *Cancer discovery* 2013; **3**(12): 1416-29.

28. Bhatia S, Diedrich D, Frieg B, Ahlert H, Stein S, Bopp B, et al. Targeting HSP90 dimerization via the C terminus is effective in imatinib-resistant CML and lacks the heat shock response. *Blood* 2018; **132**(3): 307-20.

29. Dietrich S, Oles M, Lu J, Sellner L, Anders S, Velten B, et al. Drug-perturbation-based stratification of blood cancer. *The Journal of clinical investigation* 2018; **128**(1): 427-45.

30. Flumann R, Rehkamper T, Nieper P, Pfeiffer P, Holzem A, Klein S, et al. An Autochthonous Mouse Model of Myd88- and BCL2-Driven Diffuse Large B-cell Lymphoma Reveals Actionable Molecular Vulnerabilities. *Blood Cancer Discov* 2021; **2**(1): 70-91.

31. Yadav B, Pemovska T, Szwajda A, Kulesskiy E, Kontro M, Karjalainen R, et al. Quantitative scoring of differential drug sensitivity for individually optimized anticancer therapies. *Scientific reports* 2014; **4**: 5193.

32. Davis MI, Hunt JP, Herrgard S, Ciceri P, Wodicka LM, Pallares G, et al. Comprehensive analysis of kinase inhibitor selectivity. *Nat Biotechnol* 2011; **29**(11): 1046-51.

33. Wodicka LM, Ciceri P, Davis MI, Hunt JP, Floyd M, Salerno S, et al. Activation state-dependent binding of small molecule kinase inhibitors: structural insights from biochemistry. *Chem Biol* 2010; **17**(11): 1241-9.

34. Talab F, Allen JC, Thompson V, Lin K, Slupsky JR. LCK is an important mediator of B-cell receptor signaling in chronic lymphocytic leukemia cells. *Mol Cancer Res* 2013; **11**(5): 541-54.

35. Boer JM, den Boer ML. BCR-ABL1-like acute lymphoblastic leukaemia: From bench to bedside. *European journal of cancer* 2017; **82**: 203-18.

36. Maus MV. CD19 CAR T cells for adults with relapsed or refractory acute lymphoblastic leukaemia. *Lancet* 2021; **398**(10299): 466-7.

37. Fazio G, Bardini M, De Lorenzo P, Grioni A, Quadri M, Pedace L, et al. Recurrent genetic fusions redefine MLL germ line acute lymphoblastic leukemia in infants. *Blood* 2021; **137**(14): 1980-4.

38. Serafin V, Capuzzo G, Milani G, Minuzzo SA, Pinazza M, Bortolozzi R, et al. Glucocorticoid resistance is reverted by LCK inhibition in pediatric T-cell acute lymphoblastic leukemia. *Blood* 2017; **130**(25): 2750-61.

39. Shi Y, Beckett MC, Blair HJ, Tirtakusuma R, Nakjang S, Enshaei A, et al. Phase II-like murine trial identifies synergy between dexamethasone and dasatinib in T-cell acute lymphoblastic leukemia. *Haematologica* 2021; **106**(4): 1056-66.

40. Wei Y, Zhou J, Yu H, Jin X. AKT phosphorylation sites of Ser473 and Thr308 regulate AKT degradation. Biosci Biotechnol Biochem 2019; 83(3): 429-35.

Chapter 4

Recurrent genetic fusions redefine MLL germline acute lymphoblastic leukemia in infants

Blood. 2021 Apr 8;137(14):1980-1984.
doi:10.1182/blood.2020009032.

Recurrent genetic fusions redefine MLL germline acute lymphoblastic leukemia in infants

Grazia Fazio,[1,*] Michela Bardini,[1,*] Paola De Lorenzo,[2] Andrea Grioni,[1,3] Manuel Quadri,[1] Lucia Pedace,[4] Lilia Corral Abascal,[1] Sonia Palamini,[1] Chiara Palmi,[1] Barbara Buldini,[4] Luciana Vinti,[5] Rosanna Parasole,[6] Elena Barisone,[7] Marco Zecca,[8] Claudio Favre,[9] Franco Locatelli,[5] Valentino Conter,[10] Carmelo Rizzari,[10] Maria Grazia Valsecchi,[2,11] Andrea Biondi,[10,†] and Giovanni Cazzaniga[1,12,†]

[1]Centro Ricerca Tettamanti, Pediatrics, University of Milan-Bicocca, Fondazione Monza e Brianza per il Bambino e la sua Mamma (MBBM)/San Gerardo Hospital, Monza, Italy; [2]Centro Operativo di Ricerca Statistica, Fondazione Tettamanti, School of Medicine and Surgery, University of Milan-Bicocca, Monza, Italy; [3]Central European Institute of Technology, Brno, Czech Republic; [4]Woman and Child Health Department, OncoHematology Laboratory, University of Padua, Padua, Italy; [5]Department of Pediatric Hematology-Oncology, Istituto di Ricovero e Cura a Carattere Scientifico (IRCCS), Bambino Gesu`

Children's Hospital, University of Rome, Rome, Italy; [6]Department of Pediatric Hemato-Oncology, Azienda Ospedaliera di Rilievo Nazionale Santobono Pausilipon, Napoli, Italy; [7]Department of Pediatric Onco-Hematology, Regina Margherita Children's Hospital, Turin, Italy; [8]Pediatric Hematology/Oncology, Fondazione IRCCS Policlinico San Matteo, Pavia, Italy; [9]Department of Onco-Hematology, Tumori Pediatrici e Trapianto di Cellule Staminali, Azienda Ospedaliero-Universitaria Meyer, Florence, Italy; [10]Pediatrics, University of Milan-Bicocca, Fondazione MBBM/San Gerardo Hospital, Monza, Italy; and [11]Bicocca Bioinformatics, Biostatistics and Bioimaging Centre, School of Medicine and Surgery, and [12]Genetics, School of Medicine and Surgery, University of Milan-Bicocca, Monza, Italy

*GF and MB equally contributed; °GC and AB share the senior author position

Running Title: Genetic redefinition of MLL-germline Infant ALL

Corresponding author:

Giovanni Cazzaniga

Centro Ricerca Tettamanti /University of Milano-Bicocca

Centro Maria Letizia Verga - via Cadore snc - 20900 Monza (MB) Italy

Tel. +39 (0)39 233. 3661; email: giovanni.cazzaniga@unimib.it

Letter to Blood

B-cell precursor (BCP) acute lymphoblastic leukemia (BCP-ALL) in infants (ie, children age <1 year) is a rare disease traditionally subdivided into MLL-rearranged (alias KMT2A; MLL-R) and MLL germ line (MLL-G) subtypes. MLL gene rearrangements occur in ~75% of infants with BCP-ALL[1-3] and are typically associated with a mixed-lineage phenotype.[4] MLL rearrangements originate prenatally in utero[5] and play a role in transcription factor dysregulation.6 MLL-R BCP-ALL in infants is associated with dismal outcomes.[1-3]

Infants with MLL-G ALL treated with intensive therapies in the Interfant-06 protocol may have a relatively favorable prognosis, with a 6-year event-free survival (EFS) rate of 73.9%,[2] slightly inferior to that observed in older children with BCP-ALL.[1,2] Of interest, a recent study from the Japanese Pediatric Leukemia/ Lymphoma Study Group MLL-10 trial reported more favorable outcomes in infants with MLL-G ALL, with a 3-year EFS rate of 93.3%.[7] However, it must be noted that in the Japanese study, the cohort of patients was relatively small (15 patients with MLL-G ALL were enrolled, compared with 167 patients in the Interfant-06 Consortium, which includes many national groups from different countries with different outcomes), and the chemotherapy treatment was overall more intensive, with additional high-dose cytarabine and L-asparaginase in early consolidation. Despite the great interest and efforts in clarifying the biology of MLL-G BCP-ALL in infants, the information available on genetic alterations is still rather limited.[8] Conversely, BCP-ALL in noninfants is MLL-G in 98% of the

cases, and it is characterized by a great diversity of chromosomal aberrations and gene rearrangements, which correlate with favorable or unfavorable early treatment response and prognosis and are currently used, in association with minimal residual disease (MRD) assessment, for treatment stratification.[9-12] The identification of specific genetic abnormalities in MLL-G BCP-ALL in infants might be crucial for selecting appropriate personalized treatments and improving outcomes.[13] Recently, the *NUTM1* gene was found to be rearranged in MLL-G BCP-ALL in pediatric, as well as infant cases, and the presence of *NUTM1* fusions was associated with favorable outcomes in both settings.[14,15] Herein, we report results on the incidence and associated outcomes of fusion genes in a cohort of 30 infants with MLL-G BCP-ALL. We retrospectively analyzed 30 of 37 consecutive infant patients with MLL-G BCP-ALL treated in centers of the Italian Association of Pediatric Hemato-Oncology from 2006 to 2019 within the Interfant-06 (n=29)[2] or Italian Association of Pediatric Hemato-Oncology/Berlin-Frankfurt-Munster ALL2017 (n=1) protocols for whom biological material was available. The study was approved by the ethics committees of the participating institutions, and written consent was obtained from parents. Split-signal fluorescence in situ hybridization analysis was mandatory to assess MLL rearrangements; multiplex reverse transcription polymerase chain reaction and genomic breakpoint cloning were performed to identify MLL fusion partners.[16] RNA samples were analyzed using a custom next-generation sequencing (NGS) panel, with probes capturing 95 leukemia-related genes, including *ABL1, JAK2, PAX5, EBF1, PDGFRB, CRLF2,* and *TCF3* (Nugen, Tecan, CA). Sequencing analysis was performed in

2x150 paired ends on NextSeq550 (Illumina, San Diego, CA). Fusion genes were identified by STAR-Fusion, Dragen RNA, and an in-house bioinformatic pipeline.[17] In a subset of cases, whole-transcriptome RNA sequencing analysis was also performed (Nugen). All identified fusions were validated by reverse transcription polymerase chain reaction and Sanger sequencing (supplemental Figure 1; supplemental Tables 1-2, available on the Blood Web site). EFS was defined as time from diagnosis to first event (ie, resistance, relapse, death resulting from any cause, or second malignancy, whichever occurred first). Observation periods were censored at time of last contact when no events were reported. EFS was estimated according to the Kaplan-Meier method (with Greenwood standard error). Median follow-up was 4.0 years (range, 0.4-10.2 years). Analyses were performed using SAS software (version 9.4).

Overall, 30 infant patients with MLL-G BCP-ALL were screened. Table 1 describes their main features: 24 patients were aged >6 months, 29 had white blood cell count < 300 x 10^9/L at presentation, and two thirds were female. In contrast to MLL-R cases, which are typically CD102, a CD101 immunophenotype was observed in 28 (93%) of 30 MLL-G cases. Supplemental Table 3 reports the details of cytogenetic data. In addition, 26 of 30 cases were prednisone good responders, and all achieved complete remission at the end of induction therapy. Of 21 patients with available data, MRD at the end of induction therapy was negative in 7 (33%), low (<5 x 10^{-4}) in 11 (52%), and high (≥5 x 10^{-4}) only in 3 cases (14%). Only 1 (5%) of 19 patients had high MRD (≥5 x 10^{-4}) at the end of consolidation phase 1B. These data confirm that MLL-G BCP-ALL in infants is associated with favorable clinical

features at diagnosis (ie, age >6 months and low white blood cell count) and favorable initial response to therapy (ie, prednisone good response and low MRD level).[2]

Strikingly, the NGS analysis revealed that MLL-G BCP-ALL in infants is characterized by a high rate of fusion genes. Indeed, among these 30 patients, as many as 22 (73%) carried a fusion gene. *NUTM1* fusions were the most frequent, identified in 9 cases (30%), with *ACIN1* (n=5), *CUX1* (n=2), *BRD9* (n=1), and *ZNF618* (n=1) as fusion partners (Figure 1A). *NUTM1* class patients (mean age at diagnosis, 8.8 months) had a 3-year EFS rate of 100% (Figure 1C). This finding suggests that *NUTM1* fusions are associated with very good outcomes, in agreement with recent data from an ongoing International collaborative 'Ponte di Legno' Childhood ALL Working Group project.[15] Remarkably, we found that rearrangement of the PAX5 gene was also recurrent, detected in 6 (20%) of 30 cases, with *DNAJA1* (n=3), *FBRSL1* (n=1), *MBNL1* (n=1), and *GRHPR* (n=1) as fusion partner genes (Figure 1B). To our knowledge, these *PAX5* fusion partners have not been reported in the literature or databases as common *PAX5* partners in older patients.[18] As in older children, the PAX5 fusion genes found in most of the infant patients retained the DNA binding domain and the homeodomain, with *PAX5/GRHPR* as the only exception, where the first exon of *PAX5* is fused with almost the entire structure of *GRHPR*. Whether the disruption of *PAX5* or the expression of *GRPHR* under the *PAX5* promoter might represent the driver event for leukemogenesis must be further explored. In contrast with *NUTM1* class patients, patients carrying *PAX5* fusions had a mean age at diagnosis of 11.4 months and had poorer outcomes, with 4 events (bone marrow relapse, n=3; death

in first remission, n=1) occurring in 6 patients, leading to a 3-year EFS rate of 25.0% (±20.4%; Figure 1C). Notably, the outcomes of *PAX5* patients did not differ from those of 65 concurrent MLL-R BCP-ALL patients, whose 3-year EFS rate was 43.6% (66.5%; supplemental Figure 2). Moreover, in 7 cases (23%), other fusion transcripts were detected, including *TCF3* (with different partner genes) and *ABL* class fusions. We identified the following: *TCF3/PBX1* (n=2), *TCF3/ZNF384* (n=1), *ETV6/ABL1* (n=1), *P2RY8/CRLF2* (n=1), and a new *KDM2B/GATAD2B* fusion in a pair of monozygotic twins. None of the cases was positive for the fusions more commonly found in patients age >1 year (ie, *ETV6/RUNX1* or *BCR/ABL1*). The 3-year EFS rate in this heterogeneous group was 57.1% (±18.7%; Figure 1C). Finally, no fusion genes were detectable in the remaining 8 cases (27%), neither by the RNA-targeted NGS approach nor by whole-transcriptome RNA sequencing screening. Interestingly, 3 of 4 patients for whom we had cytogenetic data were hyperdiploid. These negative cases had a 3-year EFS rate of 83.3% (±15.2%; Figure 1C), with 1 testis relapse occurring 3.1 years after diagnosis in this subgroup.

Overall, this study shows that MLL-G BCP-ALL in infants is characterized by remarkable genetic heterogeneity. An unexpectedly high rate of fusion genes was found, associated with distinct treatment responses and outcomes. This study shows for the first time that *PAX5* fusions are recurrent in MLL-G BCP-ALL in infants and associated with worse outcomes compared with *NUTM1* class fusions. The major limitation in this study is the small size of the patient cohort and subgroups. Because of the rarity of the disease, confirmation of these findings can only be pursued through large international collaborations.

If confirmed, the detection of *PAX5* and *NUTM1* class (and potentially other) fusions by either fluorescence in situ hybridization and/or NGS targeted strategies[17] might be applied prospectively to stratify more properly infant patients with ALL in the context of a dedicated clinical protocol. The dismal prognosis observed in infant ALL with *PAX5* fusions is of particular interest, because these patients may benefit from novel therapeutic approaches, such as the kinase inhibitor nintedanib. This compound, also known as BIBF1120, Vargatef, or Ofev (Boehringer Ingelheim, Ingelheim am Rhein, Germany), has antiangiogenic and antitumoral effects in several cancers[19,20] and is already used in patients with pulmonary fibrosis.[21] Of note, we previously demonstrated the in vitro and ex vivo antileukemic activity of nintedanib in $PAX5^+$ ALL cells from pediatric patients (age .1 year at diagnosis), both alone and in combination with standard chemotherapy.[22,23] Other innovative therapies (eg, immunotherapy) may be considered in infants with MLL-G BCP-ALL not associated with *NUTM1* fusions, because prognosis in these patients seems unfavorable. In summary, if confirmed in a larger cohort, these data would support the redefinition of the infant MLL-G BCP-ALL subgroup, where specific genetic features might have prominent biological and prognostic roles, with a rationale for risk stratification and potential benefit from genetically driven or other innovative treatments.

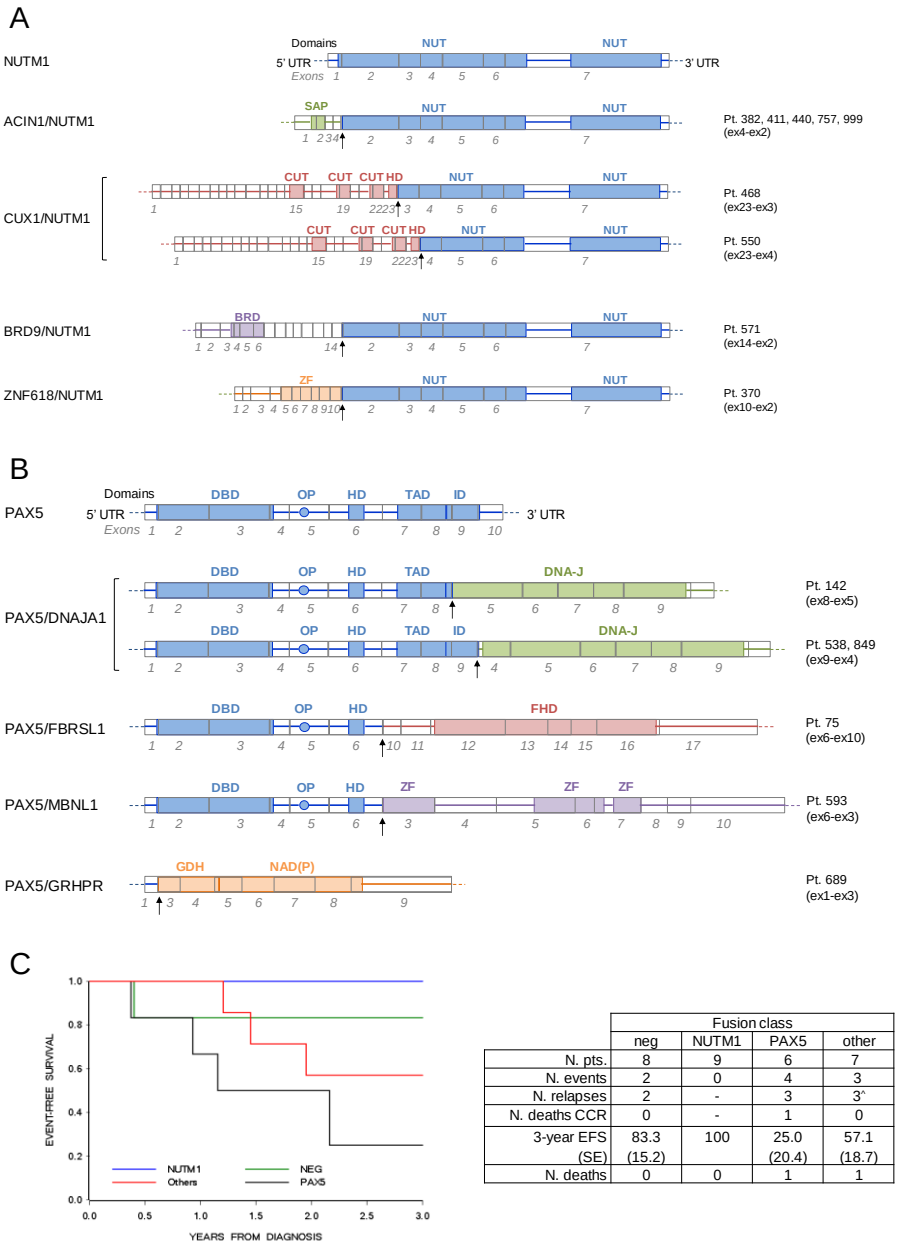

	Fusion class			
	neg	NUTM1	PAX5	other
N. pts.	8	9	6	7
N. events	2	0	4	3
N. relapses	2	-	3	3*
N. deaths CCR	0	-	1	0
3-year EFS (SE)	83.3 (15.2)	100	25.0 (20.4)	57.1 (18.7)
N. deaths	0	0	1	1

Figure 1. Genomics and outcome of infant patients with MLL-G BCP-ALL. Schematic representation of NUTM1 (A) and PAX5 (B) fusion genes identified in infant patients with MLL-G B-ALL compared with the respective wild-type genes.

For each gene, exons and relevant protein domains are indicated at the bottom and top, respectively. Arrows indicate the fusion breakpoints. (C) EFS according to the class of fusion transcript detected in 30 infant patients with MLL-G BCP-ALL. The negative (NEG; no fusion gene detected) curve does not depict 1 relapse (testis) that occurred at 3.1 years. Table reports the details of patients and events. ^Relapses occurred in: TCF3 class (n 5 1; died after relapse), ABL class (n 5 1), and CRLF2 class (n 5 1). BRD, bromodomain; CUT, CUT DNA binding motif; DBD, DNA binding domain; DNA-J, DNA-J peptide binding; FHD, fibrosin homology domain; GDH, glycerate dehydrogenase catalytic domain; HD, homeodomain; ID, inhibitory domain; NAD(P), NAD(P) binding domain; NUT, NUT domain; NUTM1, NUTM1 class fusions; other, other fusions; PAX5, PAX5 fusions; OP, octapepdtie domain; SAP, SAP motif; TAD, transactivation domain; ZF, zinc finger.

Table 1. Clinical and biological features of patients

	Fusion class, no. of patients				
	Negative	NUTM1 class	PAX5 class	Other	Total
Sex					
Male	4	2	2	1	9
Female	4	7	4	6	21
Age at diagnosis, mo					
0 to ,3	1	3	0	0	4
3 to ,6	0	1	0	1	2
6 to ,9	0	2	1	2	5
9 to ,12	7	3	5	4	19
WBC count, 310^9/L					
#100	8	6	5	4	23
100-300	0	2	1	3	6
$300	0	1	0	0	1
Immunophenotype					
CD10[2]	0	1	0	1	2
CD10[1]	8	8	6	6	28
Prednisone response					
PGR	6	8	5	7	26
PPR	1	1	1	0	3
NK	1	0	0	0	1
MRD at EOI, 310^{2*}					
Negative	4 (0)	2 (0)	0	1 (0)	7 (0)
,5	0	5 (0)	2 (1)	4 (2)	11 (3)
$5	0	0	2 (2)	1 (1)	3 (3)
Total	8	9	6	7	30

EOI, end of induction therapy; NK, not known; PGR, prednisone good responder; PPR, prednisone poor responder; WBC, white blood cell.

*Values in parentheses indicate no. of relapses. MRD data were available for 21 patients.

Supplementary Material

Supplementary Figure 1. Validation of NUTM1 (Panel A) and PAX5 (Panel B) fusion genes, identified in the present study. All the fusion transcripts detected by NGS have been validated by RT-PCR and Sanger analysis.

A. *NUTM1* fusions:

Pt. 382 ACIN1ex3-NUTM1ex2 + ACIN1ex4-NUTM1ex2

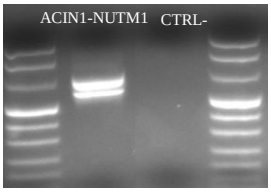

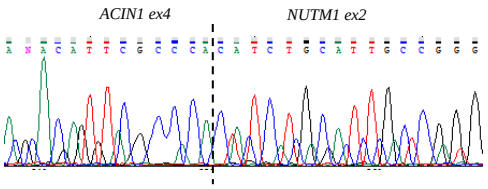

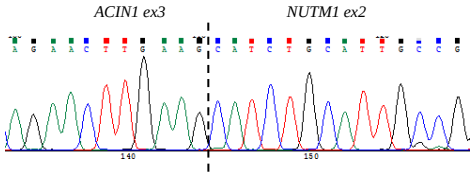

Pt. 411 ACIN1ex3-NUTM1ex3 + ACIN1ex4-NUTM1ex2

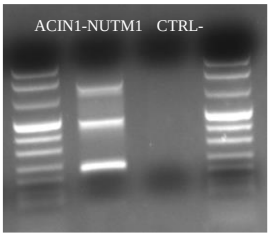

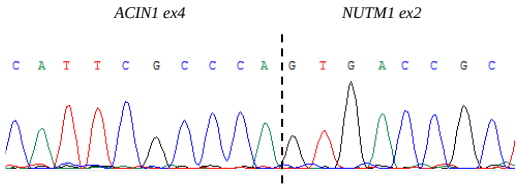

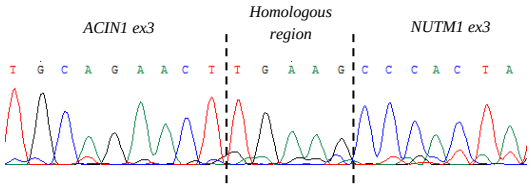

Pt. 999 ACIN1ex4-NUTM1ex2 + ACIN1ex3-NUTM1ex2

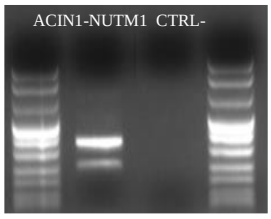

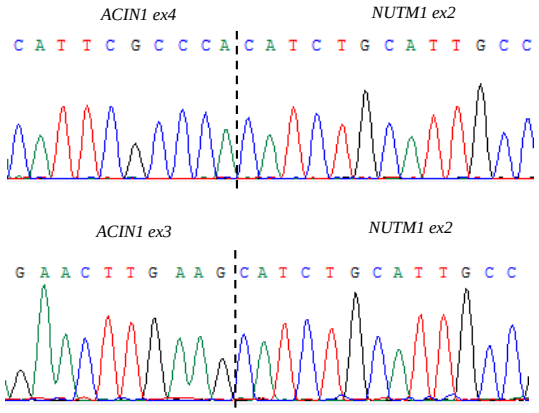

Pt. 468 CUX1ex23-NUTM1ex3 + CUX1ex23-NUTM1ex4

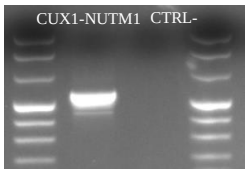

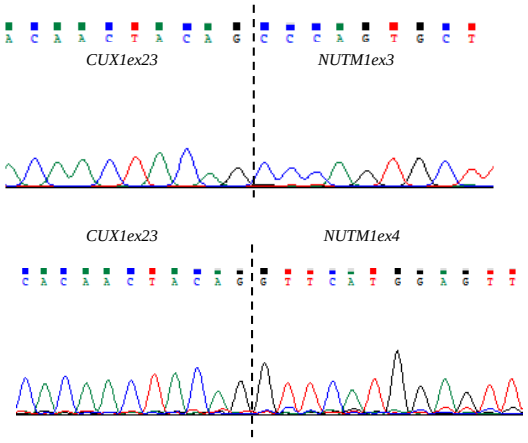

Pt. 550 CUX1ex23-NUTM1ex4

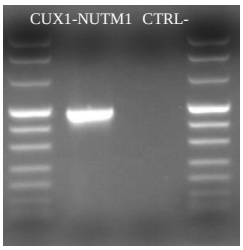

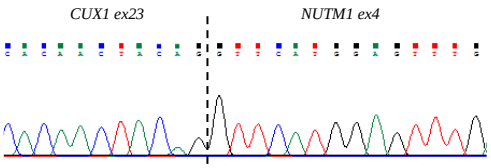

Pt. 571 BRD9ex14-NUTM1ex2

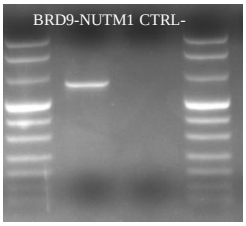

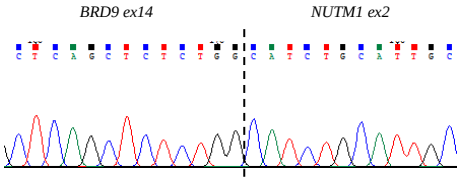

Pt. 370 ZNF618ex10-NUTM1ex2

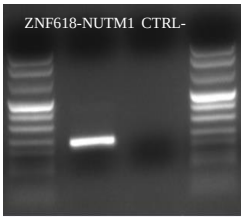

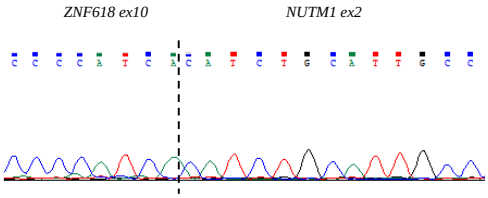

A. *PAX5* fusions:

Pt. 538 PAX5ex9-DNAJA1ex4

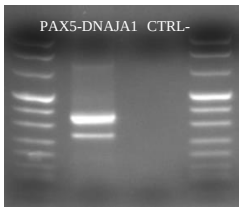

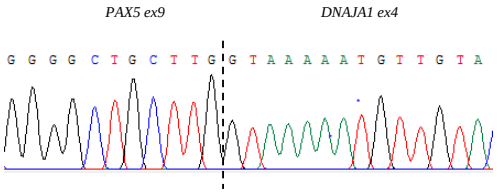

Pt. 849 PAX5ex9-DNAJA1ex4

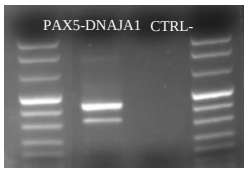

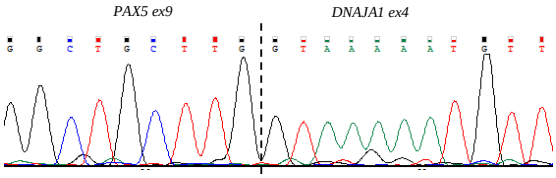

Pt. 142 PAX5ex8-DNAJA1ex5

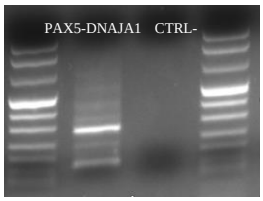

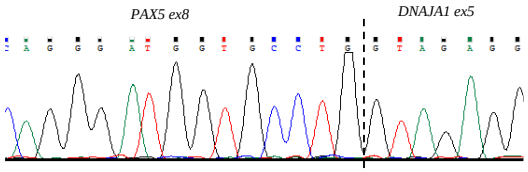

Pt. 689 PAX5ex1-GRHPRex3

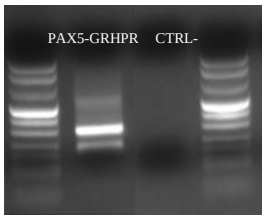

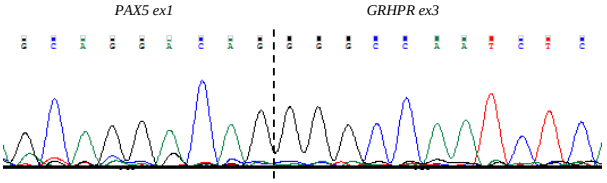

Pt. 593 PAX5ex6-MBNL1ex3

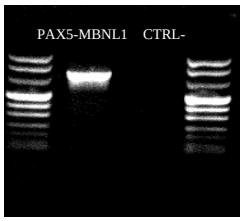

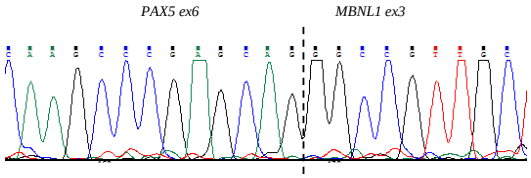

Pt. 75 PAX5ex6-FBRSL1ex10

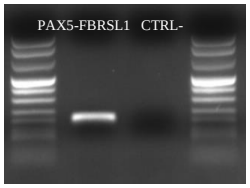

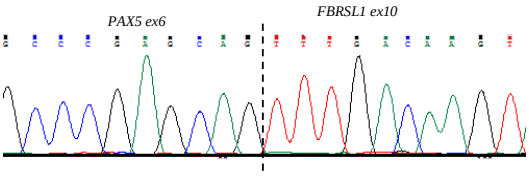

Supplementary Table 1. Sequence of primers used for RT-PCR validations.

Primers	***5'-3' sequence***
NUTM1ex2_R	GGCTGACACCAACAGCCTTA
NUTM1ex4_R	GGGCCCTAGAGGATCAAGTTTC
ACIN1ex2_F	CAACACCCCATGCTGCATTC
ACIN1ex3_F	TACTTAGGCAGCGTCTGGAAC
BRD9ex12_F	GGAGACCACTCTAGGACGC
ZNF618ex9_F	TTAAGAAGAAAGAAGTTAGGCAGTG
CUX1ex22_F	CCAGCGCTTATTTGGGGAGA
PAX5ex1_F	GGGAGCGGAAGGCTTGAATTA
PAX5ex3_F	ACGCCAAAATCCCACCATGT
PAX5ex6_F	GATGCGGGGAGACTTGTTCA

PAX5ex7_F	GCAGTCCTACCCCATTGTGAC
PAX5ex8_F	GTGACTTGGCGAGCACGA
GRHPRex7_R	AATCAGATTGGGCAGCCAGC
MBNL1ex4_R	CACCCGGATTCCCTGTAACC
FBRSL1ex11_R	GGATGGCAGGAGGGAAGG
DNAJAex5_R	GCACTCCATGCACACAGACT
DNAJAex5_R2	TGCATTCCAGTACCTCGGC

Supplementary Table 2. Combination of primer pairs used for RT-PCR validations and size of PCR products. Annealing Temperature was 60°C for all combinations.

Primers pairs		***PCR amplicon (bp)***
ACIN1ex2_F	NUTM1ex2_R	705
ACIN1ex3_F		609
BRD9ex12_F		616
ZNF618ex9_F		230
CUX1ex22_F	NUTM1ex4_R	691
PAX5ex1_F	GRHPRex7_R	328
PAX5ex3_F	MBNL1ex4_R	609
PAX5ex6_F	FBRSL1ex11_R	197
PAX5ex7_F	DNAJAex5_R	442
PAX5ex8_F	DNAJAex5_R2	352

Supplementary Figure 2. Outcome of MLL-rearranged cases and comparison with

	PAX5	**MLL rearranged**
N. pts.	6	65
N. events	4	36
N. induction failures	0	2
N. relapses	3	29
N. deaths CCR	1	5
3-year EFS (SE)	25.0 (20.4)	43.6 (6.5)

PAX5-fusion patients. Overall, N=102 infants were enrolled, of whom N=65 were MLL rearranged. Their outcome did not differ from that of PAX5 rearranged patients (3-year EFS ± SE was 43.6 ± 6.5 vs.25.0 ± 20.4, respectively). Details on type and number of events are given in the table.

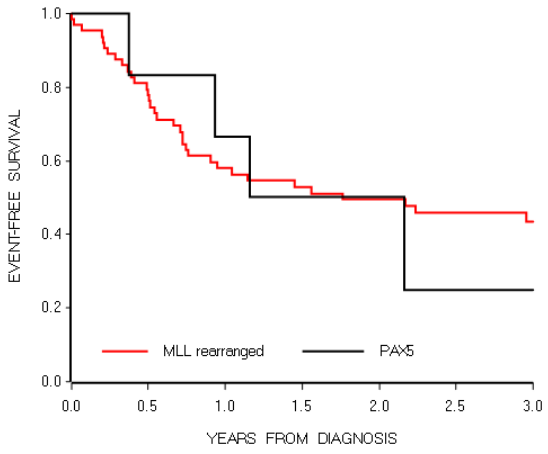

Supplementary Table 3. Cytogenetic features of MLL-G Infant ALL cases analyzed.

Patient Code	Fusion class	Fusion genes	Karyotype
85	neg	neg	n.a.
165	neg	neg	52-54,XY,+Y,+6,+d,+17,+18,+21,+21,inc[cp3]/46,XY
530	neg	neg	49-54,XY,+X,+4,+d,+16 or +17,+18,+21,+21,inc[cp4]/46,XY[4]
604	neg	neg	n.a.
790	neg	neg	54-57,XX,+4,+6,+9,+10,+?14,+21,+21,inc[cp3]/46,XX[6]
809	neg	neg	n.a.
810	neg	neg	n.a.
811	neg	neg	46,XX[15]
370	NUTM1	ZNF618/NUTM1	46,XX,t(9;15)(q34;q15)[6]/46,XX[13]
382	NUTM1	ACIN1/NUTM1	n.a.
411	NUTM1	ACIN1/NUTM1	n.a.
440	NUTM1	ACIN1/NUTM1	46,XX[20]
468	NUTM1	CUX1/NUTM1	46,XX[20]
550	NUTM1	CUX1/NUTM1	46,XY[20]
571	NUTM1	BRD9/NUTM1	46,XX,t(5;6)(q22;q25 or q27),t(5;15)(p15;q11.2)[19]/46,XX[6]
757	NUTM1	ACIN1/NUTM1	n.a.
999	NUTM1	ACIN1/NUTM1	46,XY,ins(15;14)(q1?3;q?12q31)[6]/46,XY[14]
75	PAX5	PAX5/FBRSL1	n.a.
142	PAX5	PAX5/DNAJA1	46,XX,t(2;11)(q10;p10),inv(7)(p15q11),del(9)(p22)[4]/46,XX[13]
538	PAX5	PAX5/DNAJA1	45,XX,-8,der(9)t(8;9)(q13;p13),inv(9)(p21q21)[20]
593	PAX5	PAX5/MBNL1	46,XY,t(3;9)(q21;p13),del(3)(q21q25)[31]
689	PAX5	PAX5/GRHPR	46,XX[13]
849	PAX5	PAX5/DNAJA1	n.a.
58	Others	TCF3/PBX1	n.a.
387	Others	TCF3/PBX1	46,XX,t(1;19)(q23;p13)[3]/47,sl,+8[8]/47,sdl1,der(20)t(?;20)(?;p13)[3]/46,XX[2]
484	Others	TCF3/ZNF384	46,XY[14]
369	Others	ETV6/ABL1	46,XX[20]
625	Others	P2RY8/CRLF2	45,XX,dic(9;20)(p13;q11.2)[16]/46,sl,+9[6]/46,XX[8].ish dic(9;20)(D20Z1+,D9Z1+)[10]
676	Others	KDM2B/GATAD2B	46,XX,t(1;12)(q12;q24.2)[13]/46,XX[1]
677	Others	KDM2B/GATAD2B	n.a.

Ackowledgments

This work was partially supported by the Comitato Maria Letizia Verga, grant IG 2017-20564 from the Italian Association for Cancer Research (AIRC; A.B.), grant PRIN 2017-N. 20178S4EK9 from the Ministero dell'Universita e della Ricerca (M.G.V.), an AIRC fellowship (A.G.), the ` Italian Ministry of Health, and grant GR-2016-02364753 from the Ricerca Finalizzata-GR (C.P., G.F., M.B.).

Authorship

Contribution: G.F., M.B., S.P., C.P., and M.Q. performed NGS and molecular analyses; G.C. initiated the project and supervised the team's work; A.G. performed bioinformatic analyses; P.D.L. and M.G.V. collected clinical data and performed survival analyses; M.Q. performed reverse transcription polymerase chain reaction validation tests; L.P. analyzed the twin patients; L.C.A. performed MRD monitoring; B.B. performed immunophenotypic analyses; R.P., E.B., M.Z., C.F., F.L., L.V., C.R., and A.B. provided information on patients treated in their centers; and G.F., M.B., V.C., P.D.L., and G.C. analyzed data and wrote the paper, with contributions from all authors.

Conflict-of-interest disclosure: The authors declare no competing financial interests.

ORCID profiles: G.F., 0000-0001-7077-8422; A.G., 0000-0003-3268-2918; M.Z., 0000-0002-8818-1744; G.C., 0000-0003-2955-4528.

Correspondence: Giovanni Cazzaniga, Centro Ricerca Tettamanti/ University of Milano-Bicocca, Centro Maria Letizia Verga, via Cadore snc, 20900 Monza (MB) Italy; e-mail: giovanni.cazzaniga@unimib.it.

Footnotes

Submitted 4 September 2020; accepted 22 November 2020; prepublished online on Blood First Edition 22 December 2020.

*G.F. and M.B. contributed equally to this work.

†G.C. and A.B. contributed equally as senior authors.

Genomic data have been uploaded to ArrayExpress: targeted allele sequencing of BCP-ALL pediatric patients (E-MTAB-9971) and wholetranscriptome analysis to detect fusion genes in pediatric BCP-ALL (E-MTAB-9925).

Original data are available upon request; please contact gianni.cazzaniga@ hsgerardo.org.

REFERENCES

1. Pieters R, Schrappe M, De Lorenzo P, et al. A treatment protocol for infants younger than 1 year with acute lymphoblastic leukaemia (Interfant-99): an observational study and a multicentre randomised trial. Lancet. 2007; 370(9583):240-250.

2. Pieters R, De Lorenzo P, Ancliffe P, et al. Outcome of infants younger than 1 year with acute lymphoblastic leukemia treated with the Interfant-06 protocol: results from an international phase III randomized study. J Clin Oncol. 2019;37(25):2246-2256.

3. Silverman LB. Acute lymphoblastic leukemia in infancy. Pediatr Blood Cancer. 2007;49(suppl 7):1070-1073.

4. Slany RK. The molecular biology of mixed lineage leukemia. Haematologica. 2009;94(7):984-993.

5. Greaves MF, Wiemels J. Origins of chromosome translocations in childhood leukaemia. Nat Rev Cancer. 2003;3(9):639-649.

6. Armstrong SA, Look AT. Molecular genetics of acute lymphoblastic leukemia. J Clin Oncol. 2005;23(26):6306-6315.

7. Tomizawa D, Miyamura T, Imamura T, et al. A risk-stratified therapy for infants with acute lymphoblastic leukemia: a report from the JPLSG MLL-10 trial. Blood. 2020;136(16):1813-1823.

8. Cario G, Leoni V, Conter V, et al. Relapses and treatment-related events contributed equally to poor prognosis in children with ABL-class fusion positive B-cell acute lymphoblastic leukemia treated according to AIEOP-BFM protocols. Haematologica. 2020;105(7):1887-1894.

9. Conter V, Bartram CR, Valsecchi MG, et al. Molecular response to treatment redefines all prognostic factors in children and adolescents with B-cell precursor acute lymphoblastic leukemia: results in 3184 patients of the AIEOP-BFM ALL 2000 study. Blood. 2010;115(16):3206-3214.

10. Pui CH, Robison LL, Look AT. Acute lymphoblastic leukaemia. Lancet. 2008;371(9617):1030-1043.

11. Moricke A, Zimmermann M, Valsecchi MG, et al. Dexamethasone vs ¨ prednisone in induction treatment of pediatric ALL: results of the randomized trial AIEOP-BFM ALL 2000. Blood. 2016;127(17): 2101-2112.

12. Stam RW, Schneider P, Hagelstein JAP, et al. Gene expression profilingbased dissection of MLL translocated and MLL germline acute lymphoblastic leukemia in infants. Blood. 2010;115(14):2835-2844.

13. Kumar AR, Sarver AL, Wu B, Kersey JH. Meis1 maintains stemness signature in MLL-AF9 leukemia. Blood. 2010;115(17):3642-3643.

14. Hormann FM, Hoogkamer AQ, Beverloo HB, et al. NUTM1 is a recurrent fusion gene partner in B-cell precursor acute lymphoblastic leukemia associated with increased expression of genes on chromosome band 10p12.31-12.2. Haematologica. 2019;104(10):e455-e459.

15. Boer JM, Valsecchi MG, Hormann FM, et al NUTM1-rearranged infant and pediatric B cell precursor acute lymphoblastic leukemia: a good prognostic subtype identified in a collaborative international study [abstract]. Blood. 2020;136(suppl 1). Abstract 582.

16. Meyer C, Burmeister T, Groger D, et al. The MLL recombinome of acute ¨ leukemias in 2017. Leukemia. 2018;32(2):273-284.

17. Grioni A, Fazio G, Rigamonti S, et al. A simple RNA target capture NGS strategy for fusion genes assessment in the diagnostics of pediatric B-cell acute lymphoblastic leukemia. HemaSphere. 2019;3(3):e250**.**

18. Persistent Labs. Fusion Hub. Available at: https://fusionhub.persistent.co. in. Accessed 31 October 2020.

19. Hilberg F, Roth GJ, Krssak M, et al. BIBF 1120: triple angiokinase inhibitor with sustained receptor blockade and good antitumor efficacy. Cancer Res. 2008;68(12):4774-4782.

20. Awasthi N, Schwarz RE. Profile of nintedanib in the treatment of solid tumors: the evidence to date. OncoTargets Ther. 2015;8:3691-3701.

21. Wind S, Schmid U, Freiwald M, et al. Clinical pharmacokinetics and pharmacodynamics of nintedanib. Clin Pharmacokinet. 2019;58(9):1131-1147.

22. Cazzaniga V, Bugarin C, Bardini M, et al. LCK over-expression drives STAT5 oncogenic signaling in PAX5 translocated BCP-ALL patients. Oncotarget. 2015;6(3):1569-1581.

23. Fazio G, Bresolin S, Saitta C, et al. Pre-clinical efficacy of the novel kinase inhibitor nintedanib on PAX5 fusion genes in pediatric Ph-like B-cell precursor acute lymphoblastic leukemia [abstract]. Blood. 2019; 134(suppl 1). Abstract 745.

Chapter 5

Functional and metabolic characterization of PAX5 and JAK2 rearranged PDXs at single cell level by CyTOF

Functional and metabolic characterization of PAX5 and JAK2 rearranged PDXs at single cell level by CyTOF

Manuel Quadri[1], Jolanda Sarno[2], Andrea Biondi[1], Kara L. Davis[2], Giovanni Cazzaniga[3], Grazia Fazio[1].

Manuscript in preparation

[1]Tettamanti Research Center, Dept. Pediatrics, University of Milano-Bicocca, Fondazione MBBM/San Gerardo Hospital, Monza, Italy.

[2]Department of Pediatrics, Bass Center for Childhood Cancer, Stanford University, Stanford, California, USA

[3]Medical Genetics, School of Medicine and Surgery, University of Milano-Bicocca, Monza, Italy.

ABSTRACT

PAX5 is rearranged in 30% of BCP-ALL cases, having several partner genes as the kinase JAK2. PAX5 is fundamental as a regulator of development of B cells, and its alterations may have opposite effects to wild type PAX5. In addition to the known key role of PAX5 as a

transcription factor in B cells, PAX5 is also considered a metabolic gatekeep, lowering glycolysis and ATP production in B cells. It is still to define whether JAK2 alterations may contribute in metabolic regulation of B cells. To functionally and metabolically characterize PAX5 and JAK2 fusions in leukemic B cells, we set up xenotransplantation in mice of blasts carrying JAK2 and PAX5 rearrangement, obtaining bone marrow cells to simultaneously analyze at single cell level the expression of PAX5 and JAK2 related multiple proteins by CyTOF. We firstly demonstrated a peculiar blockade of maturation at pre-proB, pro-BII and pre-BII stages of cells due to the presence of the fusion genes. As LCK, overexpressed by PAX5 fusions, and kinases are target of dasatinib, we ex-vivo targeted blasts cells with dasatinib observing an inhibition of mainly phosphoproteins related to PAX5 and JAK2 fusions, as pJAK2 and pERK. Moreover, we confirmed that PAX5 and JAK2 fusions lead to an increased glycolysis toward lactate production, with alterations at mitochondria level. We may say that those fusions alter B cells development, and that they can be specifically targeted by dasatinib.

In this chapter, we reported preliminary results on this ongoing study.

INTRODUCTION

PAX5 is considered a metabolic gatekeeper reducing glucose uptake and consumption in PAX5wt cells, while in presence of heterozygous deletion of PAX5, glycolysis increases as marked glucose uptake and ATP production are observed (Chan, et al. 2019).

By sequential developmental stages defined by changes in the surface proteins and intracellular mediator of DNA rearrangements, and

regulation of signaling pathways, intracellular mediators of DNA rearrangements, there is the normal development of B cells (Bendall, et al 2014). By CyTOF application, B cell subpopulations can be finely studied and classified quantified multiple proteins at the same time (Bendall, et al. 2014; Good, et al 2018), an important application to eventually study the many consequences of genetic aberrations of B cells.

Recently, dasatinib has been found to be effective in the T-ALL setting with LCK overexpression (Laukkanen, et al. 2022), being among the most potent inhibitors of LCK (Fazio, et al. 2022). PAX5 fusions are known to have an overexpression of LCK (Cazzaniga, et al. 2015). Moreover, as a general tyrosine kinase inhibitor, dasatinib application may be appealing also on the Philadelphia-like subgroup of BCP-ALL with JAK2 rearrangements. Indeed, it showed efficacy on Philadelphia positive pediatric BCP-ALL (Cerchione, et al. 2021).

The aim is to better functionally and metabolically characterized PAX5 and JAK2 rearrangements at single cell level, to verify the preclinically activity of dasatinib on pediatric leukemic blasts carrying those fusions.

PATIENTS' COHORT DEFINITION

A cohort of 20 patients has been identified by a wide screening of RNA samples of Italian pediatric patients through a next generation sequencing approach. The 20 patients were found to be characterized by the presence of PAX5 and/or JAK2 rearrangements. PAX5r patients had been also divided in different subclasses according to the partner gene function (**Table 1**).

Primary cells from patients were used to set up *in-vivo* xenotransplantations in NSG mice of blasts carrying PAX5r and JAK2r. Bone marrow cells expanded in PDX mice were used for the CyTOF application. Only samples characterized by at least 80% of leukemia cells in BM were used.

We moreover included studies on NALL1 cell line, a cell line carrying a PAX5::ETV6 fusion gene (Hiraki, et al. 1977).

CyTOF SAMPLES PREPARATION

Frozen viably preserved samples of bone marrow of PDXs carrying PAX5 and/or JAK2 fusions were thawed at 37°C and resuspended in RPMI 10% FBS supplemented with 20 U/mL sodium heparin (Sigma-Aldrich, St. Louis, MO, USA), 0.025 U/mL benzonase (Sigma-Aldrich), 1X L-glutamine and 1X penicillin/streptomycin (Invitrogen, Carlsbad, CA, USA). After counting the cells to take from 1 to 2M of cells for each condition, cells were stained for monoisotopic cisplatin viability, by adding 0.2mM of Pt-194 to each condition for 5 minutes and quenching the reaction with RPMI 10%FBS. Cells were washed and a pellet was obtained, resuspended then left in incubator for 30 minutes. Following cisplatin viability staining and starvation, cells were treated 30' with dasatinib (100nM). Cells were then fixed with 1.6% final concentration of PFA for 10 minutes RT. Cells were then barcoded using 20-plex palladium barcoding plates prepared in-house (Zunder, et al. 2015), including one healthy bone marrow as a reference in each of the barcoding plates and NALL-1 cell lines prepared in at least one of the three conditions of treatment (pre-BCR stimulation, IL7 stimulation, dasatinib treatment), to control for batch effects. After

barcoding, cells were washed once with cell staining media (PBS with 0.5% BSA, 0.02% sodium azide), to remove residues of PFA. Cells were blocked 10' RT using purified human Fc receptor binding inhibitor (eBioscience, San Diego, CA, USA). Surface markers antibodies staining was performed for 30' RT on shaker (see CyTOF panels). Cells were then washed in cell staining media (CSM) and permeabilized with 1ml 4°C 100% methanol for 10' at 4°C, washed three times with CSM and stained for intracellular markers antibodies for 30' RT on shaker (see CyTOF panels). Cells were washed with CSM and resuspended in 100uL of CSM, then intercalated with the 1:500 ^{103}Rd DNA intercalator (Fluidigm, South San Francisco, CA, USA) in PBS 1.6%PFA, keeping cells resuspended in 1mL over night at 4°C. Cells were washed one time with CSM and two times with ddH_2O, and resuspended in ^{139}La/^{142}Pr/^{159}Tb/^{169}Tm/^{175}Lu normalization beads (Finck, et al. 2013) before the analysis at Helios CyTOF mass cytometer (Fluidigm). During the readout cells were kept at 4°C introducing no more than 300 cells/sec at CyTOF, keeping the ratio constant.

CyTOF PANELS

We developed two independent panels were developed considering literature data and our functional results on PAX5 and JAK2 rearrangements and consist of both surface and intracellular markers. They were applied to both JAK2 and PAX5 rearranged PDXs bone marrow samples The first panel is related to B cells classification and functions, consisting of mostly signaling related molecules (**Table 3**), while the second panel is related to the metabolism (**Table 4**). Antibodies were conjugated with heavy metals ions following an in-

house protocol based on sequential steps of incubations, filtrations and washes.

CyTOF ANALYSIS

Data were analyzed after beads normalization and files debarcoding (Zunder, et al. 2015, Finck, et al. 2013). Single-cell protein expression data were extracted using in-house software and transformed using the inverse hyperbolic sine (arsinh). Analyses were done using Cytobank and Graphpad.

RESULTS

Classification of PAX5 and JAK2 rearranged PDXs, highlighting leukemic blockade of development in the most delicate phases of B cell maturation

By CyTOF approach, we obtained a high amount of data, that we are still deeply analyzing, therefore herein we reported preliminary data. Firstly, we classified our patients to evaluate at which stage they are collocated on the B cell development from HSC to mature B cells, by aligning each individual PAX5r and JAK2r carrying-cell to its nearest healthy B cell population through a developmental classifier along the healthy B cell trajectory, as done by Good, et al. 2018.

We obtained patient specific classifications, with some similarities among the groups, also considering PAX5 rearranged samples according to the PAX5 partner gene function. However, JAK2 rearranged patients showed more similarity with increased percentage in the pre-BI and pre-BII populations, except from patient MZ2 ATF7IP::JAK2 having a more early blockade of differentiation,

highlighted by the marked pre-pro-B subpopulation (**Figure 1A**). Considering PAX5r, the 'transcription factor' subgroup showed the higher differences in development, due to the different partner genes (**Figure 1B**), while PAX5:.AUTS2, the 2 cases of 'activator of transcription factors' class, showed a good similarity with high from pro-BI to pre-BII cells (**Figure 1C**). The different partner genes in the 'structural protein' group differentially influenced the development of B cells, as well as in the 'enzyme' class (**Figure 1D-E**). In the 'kinase' group, we observed a marked difference between the two patients, therefore MZ3 patient carrying PAX5::JAK2, having instead higher similarity to JAK2r patients development, was finally included in JAK2r class and not in the 'kinase' group for the following results (**Figure 1F**). Finally, the same fusion PAX5::FBRSL1 in the 2 cases of 'RNA binding activity' leads to the same expression of mainly of pro-BII and pre-BII. (**Figure 1G**). NALL1 cell line and MZ10 patient, which share the same fusion PAX5::ETV6, showed a different distribution of populations as NALL1 are markedly pre-BI cells. To note only patients in JAK2r and 'structural protein' group of PAX5r showed very low % of immature BI, immature BII and mature B cells. We moreover combined the % of subpopulations of the 20 PDXs to check which were the main expressed subpopulations in the cohort, observing a significant early blockade of maturation in pre-pro-B, pro-BII and pre-BII stages compared to immature and mature B cells (**Figure 1I**). The expression of the markers used for their classification at basal level is highlighted in **figure 2A**.

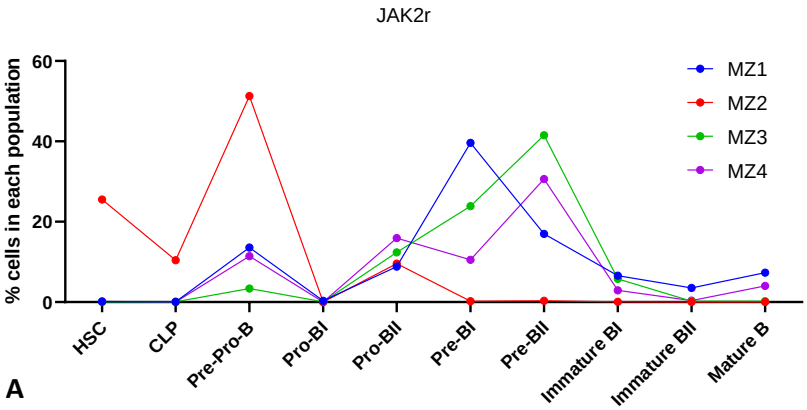
JAK2r
% cells in each population
60
40
20
0
MZ1
MZ2
MZ3
MZ4
HSC
CLP
Pre-Pro-B
Pro-BI
Pro-BII
Pre-BI
Pre-BII
Immature BI
Immature BII
Mature B

A

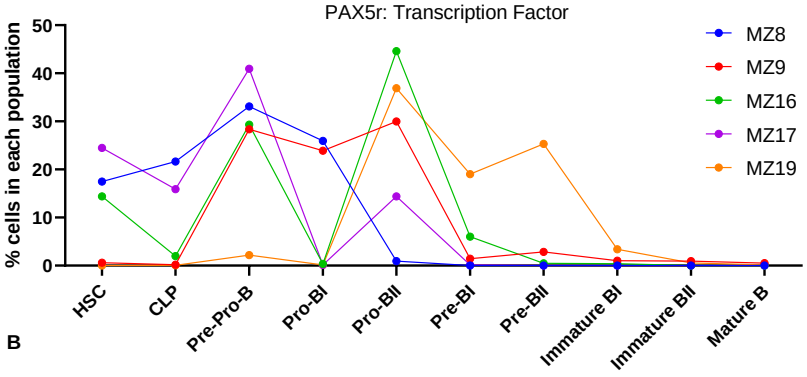
PAX5r: Transcription Factor
% cells in each population
50
40
30
20
10
0
MZ8
MZ9
MZ16
MZ17
MZ19
HSC
CLP
Pre-Pro-B
Pro-BI
Pro-BII
Pre-BI
Pre-BII
Immature BI
Immature BII
Mature B

B

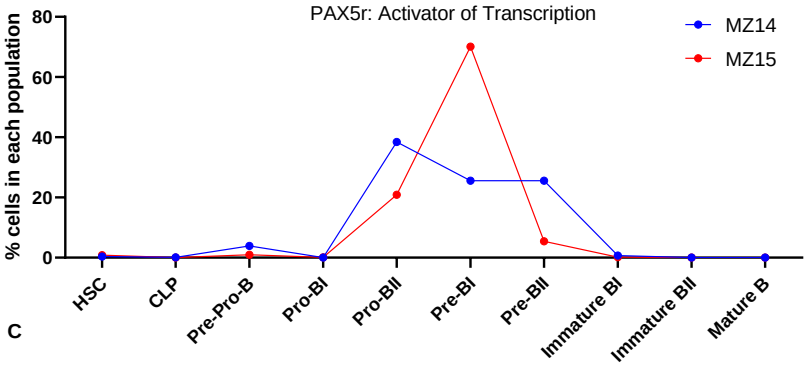
PAX5r: Activator of Transcription
% cells in each population
80
60
40
20
0
MZ14
MZ15
HSC
CLP
Pre-Pro-B
Pro-BI
Pro-BII
Pre-BI
Pre-BII
Immature BI
Immature BII
Mature B

C

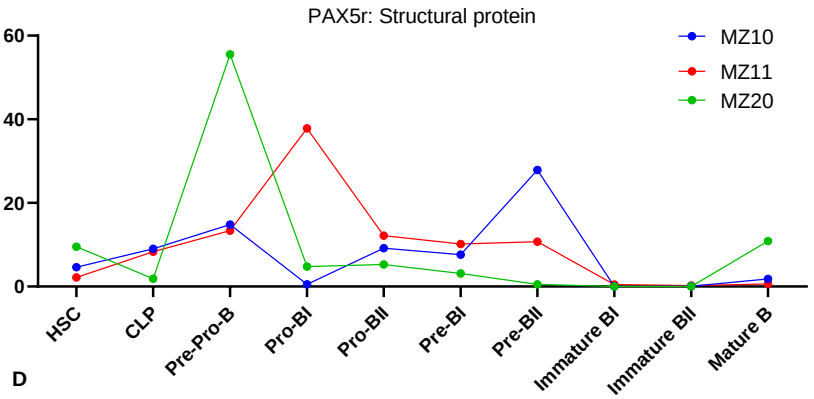
PAX5r: Structural protein
MZ10
MZ11
MZ20
60
40
20
0
HSC
CLP
Pre-Pro-B
Pro-BI
Pro-BII
Pre-BI
Pre-BII
Immature BI
Immature BII
Mature B

D

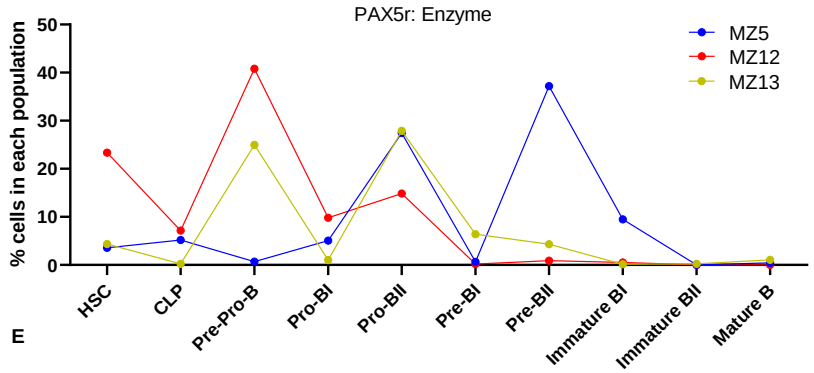
PAX5r: Enzyme
MZ5
MZ12
MZ13
% cells in each population
50
40
30
20
10
0
HSC
CLP
Pre-Pro-B
Pro-BI
Pro-BII
Pre-BI
Pre-BII
Immature BI
Immature BII
Mature B

E

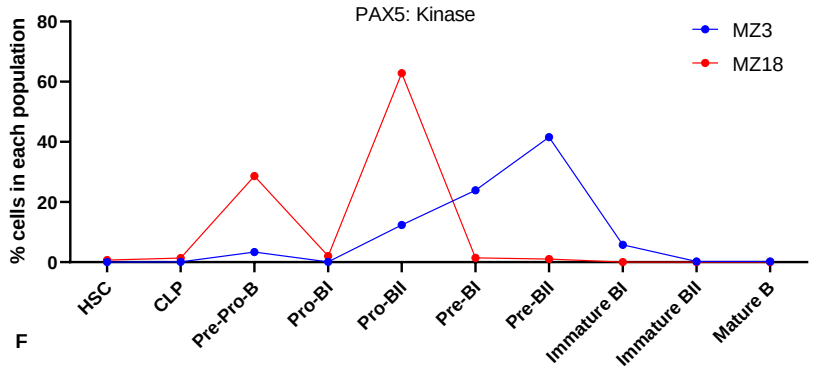
PAX5: Kinase
MZ3
MZ18
% cells in each population
80
60
40
20
0
HSC
CLP
Pre-Pro-B
Pro-BI
Pro-BII
Pre-BI
Pre-BII
Immature BI
Immature BII
Mature B

F

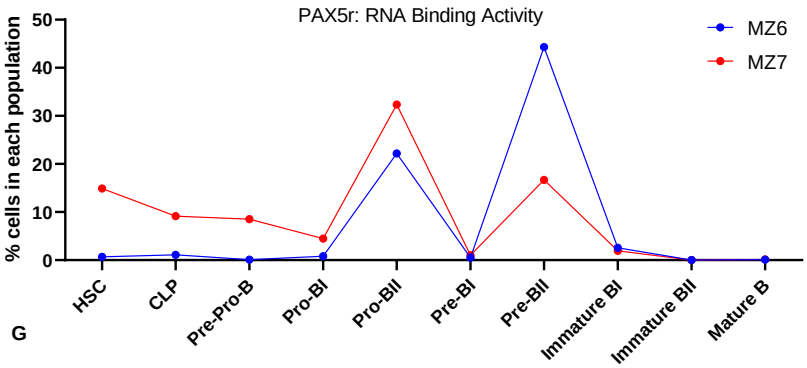
PAX5r: RNA Binding Activity
MZ6
MZ7
% cells in each population
50
40
30
20
10
0
HSC
CLP
Pre-Pro-B
Pro-BI
Pro-BII
Pre-BI
Pre-BII
Immature BI
Immature BII
Mature B

G

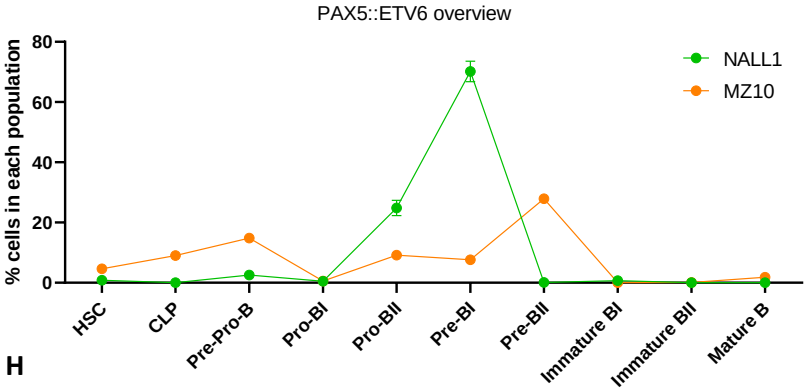
PAX5::ETV6 overview
NALL1
MZ10
% cells in each population
80
60
40
20
0
HSC
CLP
Pre-Pro-B
Pro-BI
Pro-BII
Pre-BI
Pre-BII
Immature BI
Immature BII
Mature B

H

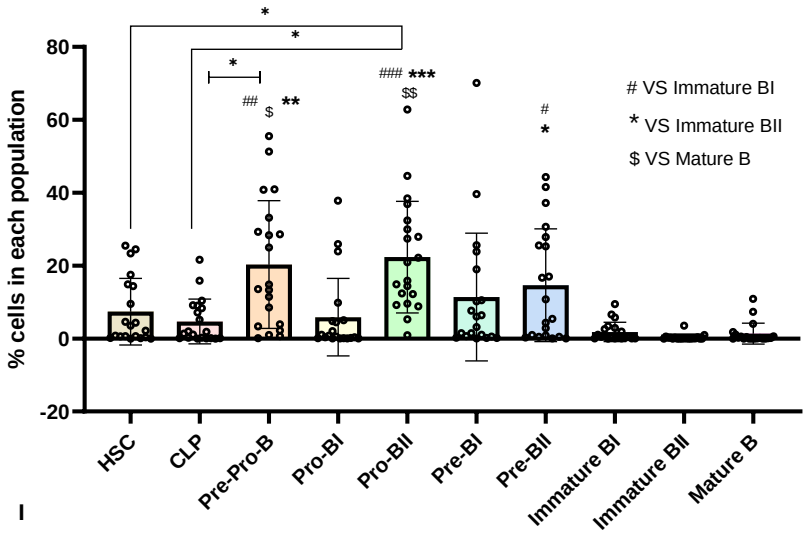
% cells in each population
80
60
40
20
0
-20
VS Immature BI
* VS Immature BII
$ VS Mature B
HSC
CLP
Pre-Pro-B
Pro-BI
Pro-BII
Pre-BI
Pre-BII
Immature BI
Immature BII
Mature B

I

Figure 1. Classification of B cells subpopulations of JAK2 and PAX5 rearranged patients**. A**. JAK2r patients. **B**. PAX5r patients of 'transcription factor' group. **C**. PAX5r patients of 'activator of transcription' group. **D**. PAX5r patients of 'structural protein' group. **E**. PAX5r patients of 'enzyme' group. **F**. PAX5r patients of 'kinase' group. **G**. PAX5r patients of 'RNA binding activity' group. **H**. Nall-1 and MZ10, carrying both a PAX5::ETV6 fusion gene, subpopulations. **I**. Istogram representation of different B cells subpopulations of the entire cohort of PDXs. P values: * $p< 0.05$; ** $p<0.01$; *** $p<0.001$ (same values for # and $ statistics).

Dasatinib treatment acts on PAX5 and JAK2 related targets in PAX5 and JAK2 rearranged samples at B cell level

The treatment of BM PDXs cells for 30 minutes with dasatinib didn't change the expression of proteins of marker used for their classification in subpopulations compared to basal level, at the level of B cell gating, not considering the single subpopulations. Only patient MZ14 showed more evident differences in some markers as increased CD38 and CD19 (**Figure 2B**). We compared dasatinib treatment in PDXs and in treated NALL1 cell lines carrying a PAX5::ETV6 fusion.

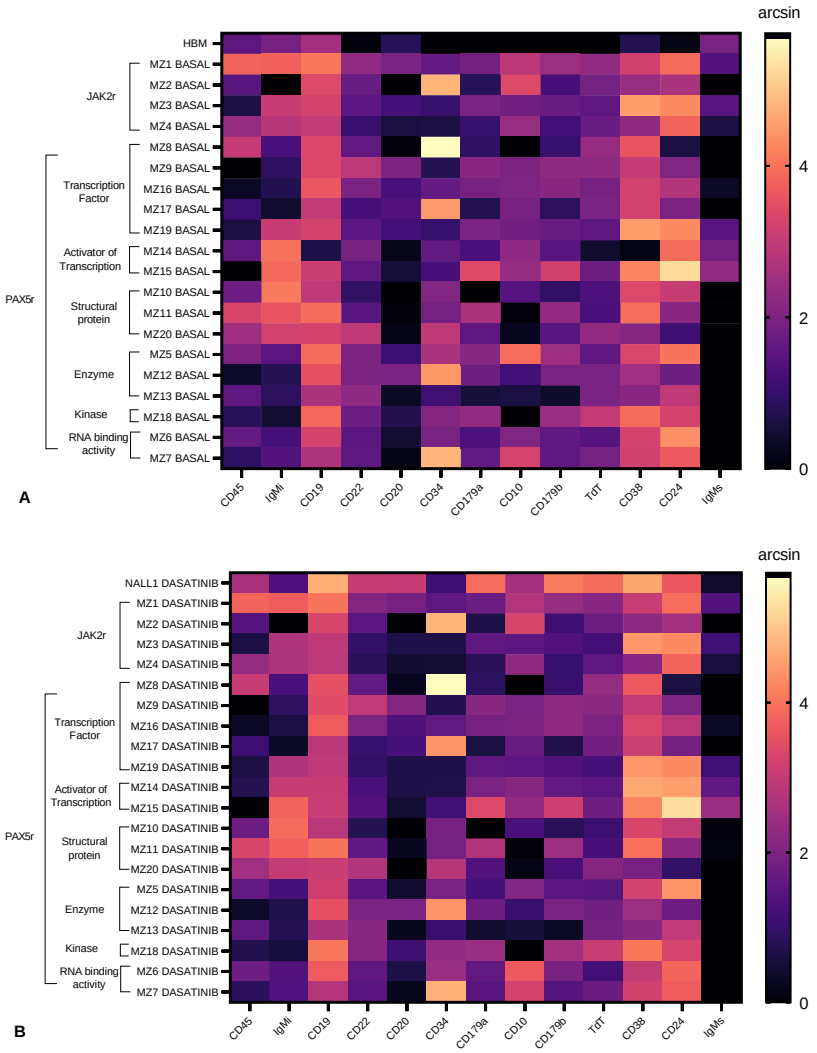

Figure 2. Protein expression of surface and intracellular markers defined to classify B cells' subpopulations in rearranged sample, expressed as arcsinh of expression**. A**. Expression at basal level of B cells classification's markers in HBM and rearranged PDXs. **B**. Expression of B cells classification's markers after dasatinib treatment in NALL-1 and rearranged PDXs.

Dasatinib mediated a fine regulation on PAX5 and JAK2 related factors, as surface proteins, transcription factors and signaling related effectors,

such as phosphoproteins. First, we observed that at basal level PAX5 and JAK2 related proteins have an overall higher expression of proteins compared to HBM, with evidence of some patient specific regulation of expression (e.g., pCREB) (**Figure 3A**). Considering an overview of all the patients, as in **Figure 3B**, we found that dasatinib treatment is significatively effective after 30 minutes of treatment.

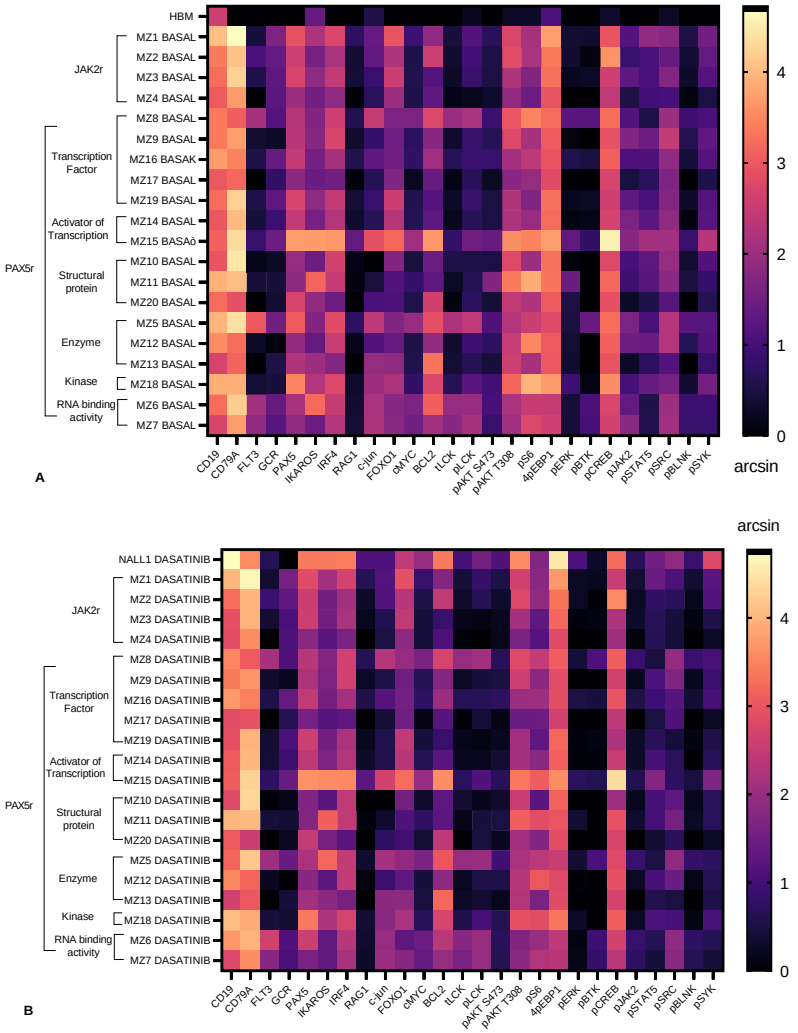

Figure 3. Protein expression of PAX5 and JAK2 related surface and intracellular markers, expressed as arcsinh of expression**. A**. Expression at basal level of PAX5 and

JAK2 related proteins in HBM and rearranged PDXs. **B**. Expression of PAX5 and JAK2 related proteins after dasatinib treatment in NALL-1 and rearranged PDXs.

We also combined the patients dividing them into 6 separated groups depending on the class to which PAX5 partner genes belonged, and 1 group for the JAK2 rearranged PDXs, to check protein expressions into the different subgroups. In general, among the groups, we observed a similar increase of proteins' expression at basal levels compared to HBM (**Figure 4A**). Moreover, there was a similar trend to inhibit some of those proteins after dasatinib treatment, mainly regarding the phosphoproteins such as pJAK2 and pSRC, compared to basal level. The inhibition was also observed comparing different PAX5 subgroups, but also comparing PAX5 subgroups vs JAK2 subgroup (**Figure 4B**).

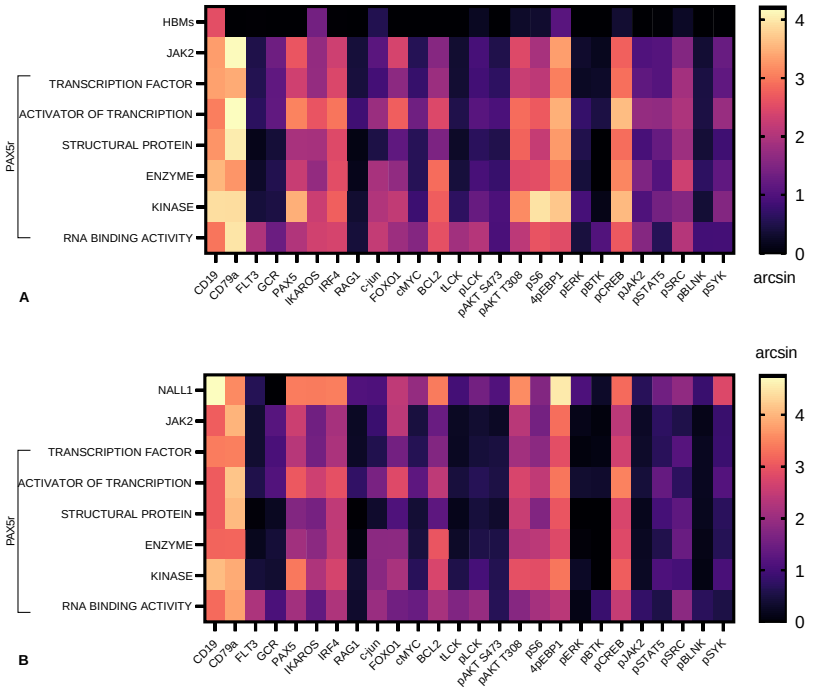

Figure 4. Protein expression of PAX5 and JAK2 related surface and intracellular markers, expressed as arcsinh of expression, evaluated in different subgroups**. A**. Expression at basal level of PAX5 and JAK2 related proteins in HBM and rearranged PDXs divided into 7 groups based on the fusions. **B**. Expression of PAX5 and JAK2 related proteins after dasatinib treatment in NALL-1 and rearranged PDXs divided into 7 groups based on the fusions.

Beside the general overview, we did considerations for each of the subgroups, comparing their basal levels of expression to the expression after dasatinib treatment, observing a wide significant effect of inhibition on most of the proteins.

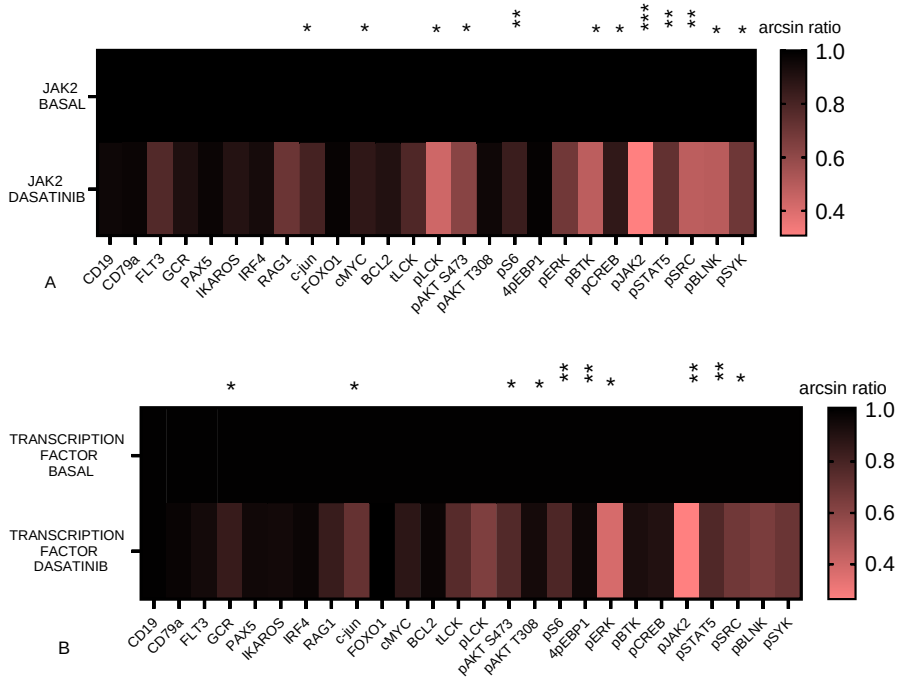

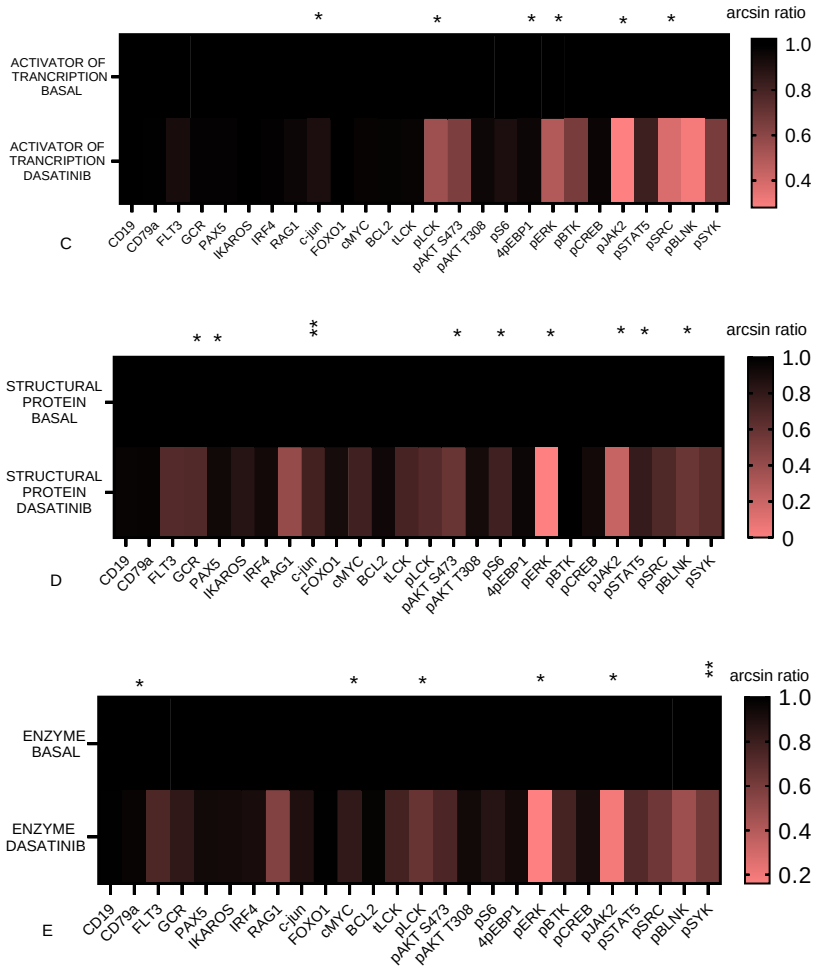
arcsin ratio
1.0
0.8
0.6
0.4
0.2
0
ACTIVATOR OF TRANCRIPTION BASAL
ACTIVATOR OF TRANCRIPTION DASATINIB
STRUCTURAL PROTEIN BASAL
STRUCTURAL PROTEIN DASATINIB
ENZYME BASAL
ENZYME DASATINIB
CD19
CD79a
FLT3
GCR
PAX5
IKAROS
IRF4
RAG1
c-jun
FOXO1
cMYC
BCL2
tLCK
pLCK
pAKT S473
pAKT T308
pS6
4pEBP1
pERK
pBTK
pCREB
pJAK2
pSTAT5
pSRC
pBLNK
pSYK
C
D
E

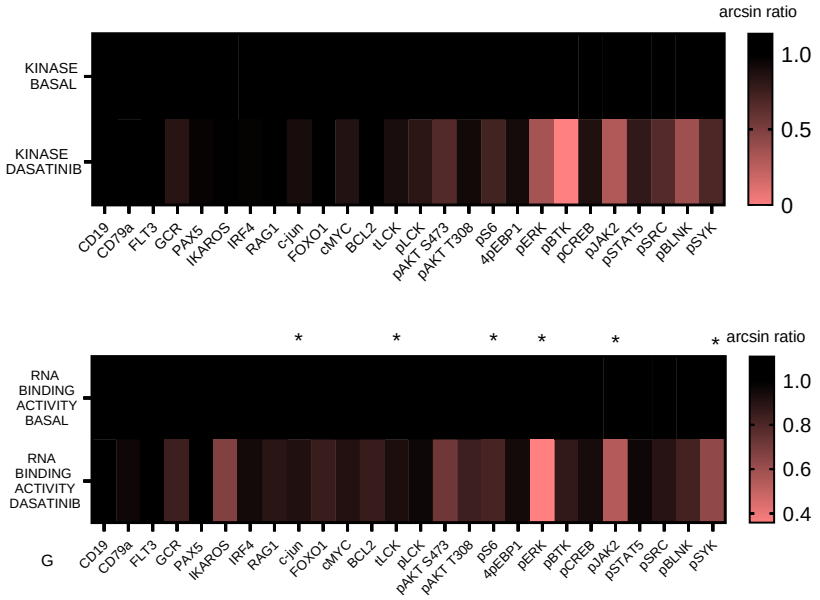

Figure 4. Protein expression of PAX5 and JAK2 related surface and intracellular markers, expressed as ratio of arcsinh(expression) of basal vs dasatinib, evaluated in different subgroups**. A**. Expression of proteins in JAK2r patients, basal vs dasatinib. **B**. Expression of proteins in 'transcription factor' of PAX5r patients, basal vs dasatinib. **C.** Expression of proteins in 'activator of transcriptio' of PAX5r patients, basal vs dasatinib. **D.** Expression of proteins in 'structural protein' of PAX5r patients, basal vs dasatinib. **E.** Expression of proteins in 'enzyme' of PAX5r patients, basal vs dasatinib. **F.** Expression of proteins in 'kinase' of PAX5r patients, basal vs dasatinib. **G.** Expression of proteins in 'RNA binding activity' of PAX5r patients, basal vs dasatinib. P values calculated on treated blasts vs untreated, by One Sample T-test: *p<0.05, **p<0.01, ***p<0.001.

The significant inhibition of proteins due to dasatinib treatment is subgroup dependent, due to the variability among the single patients. We evaluated that dasatinib is slightly more effective on phosphoproteins rather than on other JAK2r and PAX5r related proteins represented. Indeed, overall, surface marker (e.g., CD10, CD79a) and

transcription factors (e.g., IKAROS, FOXO1) are not inhibited. To note, only c-Jun (up to $p<0.01$) is commonly inhibited among most of the subgroups. Considering the phosphoproteins, pJAK2 (up to $p<0.001$), pERK ($p<0.05$) and LCK ($p<0.05$) are the most inhibited overall (**Figure 5A-G**).

PAX5 and JAK2 rearrangements show a peculiar metabolic state

Blast cells carrying PAX5 and JAK2 fusions have been analyzed at basal level, without previous treatment to stimulate the metabolism. Metabolic markers have been analyzed in the Lin- cells population gated to keep only B cells, not in the different subpopulations, as future analysis will implement our findings in subpopulations. MZ13 patients is not included due to lack of cells to apply also the metabolic panel.
Interestingly we demonstrated that JAK2 and PAX5 rearrangements showed an overall expression of the same metabolic markers, with both overexpression and reduction of expression of proteins, compared to healthy BM. To note, differences in protein expression were found at single patient level (**Figure 6A**) but also comparing subtypes of PAX5 rearranged patients which were organized into 6 different classes based on the type of the partner gene of PAX5 (**Figure 6B**).

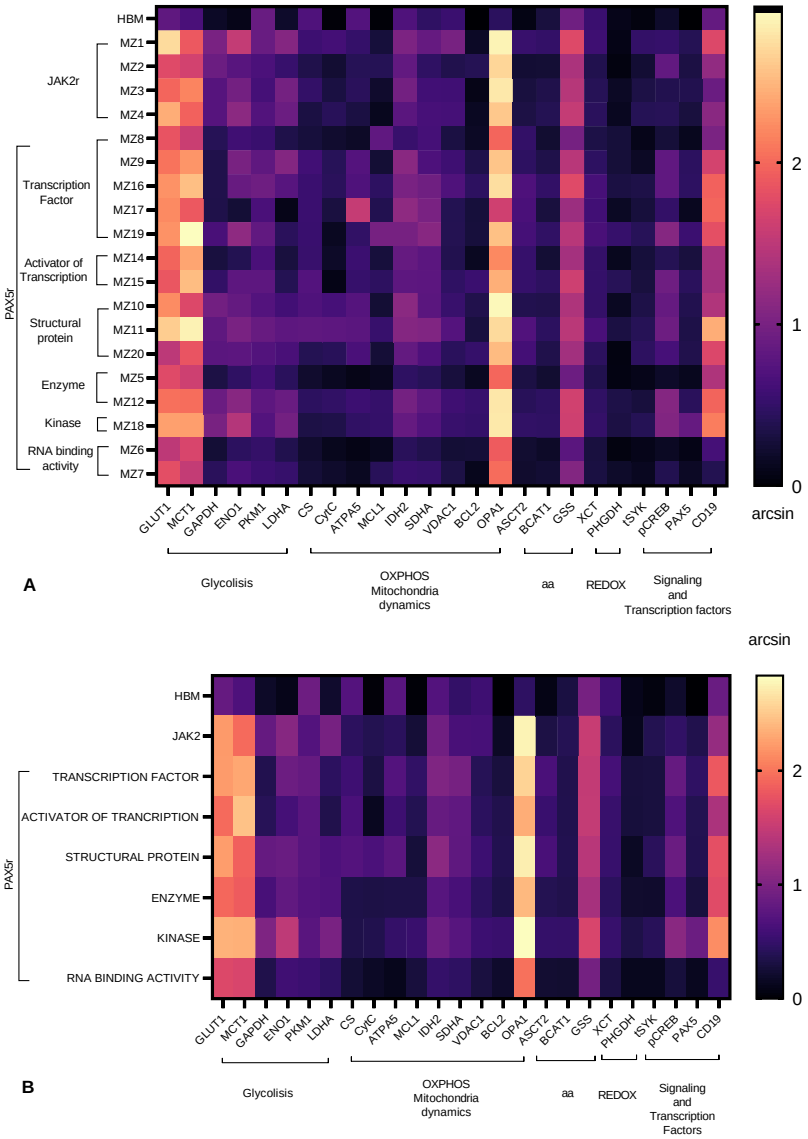

Figure 6. Protein expression of metabolic markers, expressed as arcsinh(expression), evaluated in PAX5r and JAK2r PDXs**. A**. Expression of proteins in basal condition in each patient of the cohort. **B**. Expression of proteins in basal condition in different subgroups of PAX5r and in JAK2r group.

Firstly, the two patients carrying a PAX5::FBRSL1 fusion, representing the 2 cases of the class of 'RNA binding activity', showed a lower activation of metabolism at basal level compared to the other classes of fusions. In all the groups, both JAK2 and PAX5r, we evaluated an increase in glycolysis towards lactate production, with marked expression of GLUT1 and MCT1, followed by a subsequent higher expression of GAPDH, ENO1 and LDHA compared to the healthy BM. Among the 'transcription factors', MZ17 (PAX5::DACH2) patient, showed a marked increased expression of ATPA5 in OXPHOS markers and a reduction of expression of LDHA. MCL1, BCL2, ASCT2, GSS, pSYK, pCREB and PAX5 were little higher expressed compared to healthy BM, while CytC showed a marked lower expression in the 'activator of transcription' group compared to the other PAX5r classes. To note, all the patients showed a strong increased expression of OPA1, indicating a strong alteration of mitochondria dynamics. In JAK2r cases the reduced expression of some proteins was slightly more evident than in PAX5 rearranged cases, as in CS and ATPA5. Patients showed specific responses due to their fusion genes, but overall, they had similar tendency to increase the glycolysis towards lactate production.

TABLES

Patient	First Fusion	Second Fusion	Subgroup
MZ1	ZEB2-JAK2	chr7-chr7 IKZF1-DDC	JAK2r
MZ2	ATF7IP-JAK2	No	JAK2r
MZ3	PAX5-JAK2	No	JAK2r
MZ4	GIT2-JAK2	PAX5-SPTBN1	JAK2r

MZ8	PAX5-ZNF521	No	Transcription Factor
MZ9	PAX5-ETV6	chr19-chr19 TCF3-LMNB	Transcription Factor
MZ16	PAX5-SOX5	No	Transcription Factor
MZ17	PAX5-DACH2	No	Transcription Factor
MZ19	PAX5-ZNF521	No	Transcription Factor
MZ14	PAX5-AUTS2	No	activator of transcription
MZ15	PAX5-AUTS2	No	activator of transcription
MZ10	PAX5-FAM219A	No	Structural protein
MZ11	PAX5-C20orf112	No	Structural protein
MZ20	PAX5-COL13A1	TCF3-ZNF384	Structural protein
MZ5	PAX5-DNAJA1	No	Enzyme
MZ12	PAX5-ALDH18A1	P2RY8-CRLF2	Enzyme
MZ13	PAX5-CHFR	No	Enzyme
MZ6	PAX5-FBRSL1	No	rna binding activity
MZ7	PAX5-FBRSL1	No	rna binding activity

Table 2. Table of the 20 patients, with indication of their first fusion and additional fusions, and the subgroup in which they have been divided depending on the function of the partner gene of PAX5 involved in the fusion.

B cell panel			
Antigen	**Panel (Surface or Iintra)**	**Symb**	**Mass**
CD45	S	Y	89
DNA intercalator			103
mCD45.1	S	In	113
IgMi	I	Cd	116
Cparp	I	La	139
pSRC	I	Pr	141
CD19	S	Nd	142
CD22	S	Nd	143
p4EBP1	I	Nd	144
tIKAROS	I	Nd	145
CD79a	S	Nd	146
CD20	S	Sm	147
CD34	S	Nd	148
CD179a	I	Sm	149
pLCK	I	Nd	150

Metabolic Panel			
Antigen	**Panel (Surface or Intra)**	**Metal**	**Mass**
CD45	S	Y	89
DNA intercalator			103
mCD45.1	S	In	113
IgMi	I	Cd	116
cPARP	I	La	139
PKM1	I	Ce	140
pSRC	I	Pr	141
CD19	S	Nd	142
GAPDH	I	Nd	143
GSS	I	Nd	144
tIKAROS	I	Nd	145
PHGDH	I	Nd	146
CD20	S	Sm	147
CD34	S	Nd	148
CD179a	I	Sm	149

GCR (NR3C1)	I	Eu	151
pAKT (Ser473)	I	Sm	152
total LCK	I	Eu	153
pJAK2	I	Sm	154
pSTAT5	I	Gd	155
CD10	S	Gd	156
AP1 (c-Jun)	I	Gd	157
CD179b	I	Gd	158
BCL-2	I	Tb	159
pBLNK	I	Gd	160
c-myc	I	Dy	161
IRF4	I	Dy	162
RAG1	I	Dy	163
TdT	I	Dy	164
PAX5	I	Ho	165
pSYK	I	Er	166
FOXO-1	I	Er	167
CD38	S	Er	168
pAKT (308)	I	Tm	169
FLT3 (CD135)	S	Er	170
CD24	S	Yb	171
pS6	I	Yb	172
pERK	I	Yb	173
pBTK	I	Yb	174
IgMs	S	Lu	175
pCREB	I	Yb	176
cisplatin monoisotopyc		Pt	194
CD43	S	Pt	198
CD33	S	Bi	209
CD16	S	Bi	209
CD3	S	Bi	209

SDHA	I	Nd	150
GCR (NR3C1)	I	Eu	151
ENO1	I	Sm	152
CS	I	Eu	153
BCAT1	I	Sm	154
CytC	I	Gd	155
VDAC1	I	Gd	156
tSYK	I	Gd	157
ATPA5	I	Gd	158
BCL2	I	Tb	159
NDUFB8	I	Gd	160
HK2	I	Dy	161
G6PD	I	Dy	162
TdT	I	Dy	163
MCL1	I	Dy	164
PAX5	I	Ho	165
ASCT2	S	Er	166
LDHA	I	Er	167
CD38	S	Er	168
XCT	S	Tm	169
IDH2	I	Er	170
CD24	S	Yb	171
MCT1	S	Yb	172
GLS	I	Yb	173
OPA1	I	Yb	174
IgMs		Lu	175
pCREB	I	Yb	176
MPO	I	Pt	196
GLUT1	S	Pt	198
CD33	S	Bi	209
CD16	S	Bi	209
CD3	S	Bi	209

Table 3 and 4. CyTOF Panels. **3.** B cell panel. **4.** Metabolic panel.

DISCUSSION

CyTOF application has become hugely important for the single cell analysis of multiple proteins, both surface and intracellular ones. To note, CyTOF has been fundamental to classify B cells subpopulations in the setting of B cell development, from very early HSC to mature B cells, having the possibility to contemporaneously evaluate multiple B cell protein to consider for their classification (Bendall, et al. 2014). The classifier of B cell subpopulation is a useful tool to define and discover altered protein expressions in leukemic cells, as indicated in Good, et al. 2018. Following the developmental classifier approach, we aligned our single cells carrying PAX and/or JAK2 rearrangement to their nearest healthy B cell populations. We defined the different % of B cells subpopulations in our 20 PDXs, noting a peculiar increase firstly in the pro-BII subpopulations, followed by pre-pro-B and pre-BII settings. This aspect shows that the presence of PAX5 and JAK2 rearrangements blocks B cells maturation at early stage of maturation. Remarkably, PAX5 alteration due to the fusion seems to alter its normal B cell regulation of maturation, blocking cells before pro-BII and pre-BII stage as observed in cases of absence of PAX5 (Matthias, et al. 2005; Cobaleda, et al. 2007), but further analysis on the single subpopulations are ongoing to check the specific protein expression of B cell related markers. To note, all the patients confirmed to be blocked in the B cells development in the early-middle stages, involving only in very few patients among the 20 very low % of immature BI, immature BII and mature B cells (below 10% of the entire population of B cells). Depending on the group considered, the % of populations were similar among the patients, due to the different partner genes of PAX5 or JAK2,

even though sharing the same function within their group. A very reassuring finding is that patients having the same fusion showed enrichments in the same subpopulations, as evaluated in pro-BII to pre-BII in PAX5::AUTS2, and in pro-BII and pre-BII in PAX5::FBRSL1, underlying the evidence of the same mechanism of blockade of differentiation due to PAX5 rearrangement.

Dasatinib is a tyrosine kinase inhibitor which has been preclinically and clinically applied in leukemia setting, know to inhibit multiple kinase pathways. Initially introduced to target BCR::ABL1 in CML (Cerchione, et al. 2021), it also showed high affinity for LCK in T-ALL (Laukkanen, et al. 2022), and discovered to be among the most potent inhibitors of LCK. Considering those premises, we decide to test it on our PAX5 and JAK2 rearranged PDXs. Indeed, PAX5r are known to overexpress LCK and its downstream signaling (Cazzaniga, et al. 2015; Fazio, et al. 2022).

We first evaluated, after 30 minutes of treatment with dasatinib, that overall, on the B cell gating, there were no changes in the expression of proteins used for the classification of the B cell subpopulations among our patients. Interestingly, MZ14 patient showed an increase in the expression of CD19, CD38 and CD24, but further studies are ongoing at the level of the single subpopulations.

Instead, more interesting results were found on the regulation of PAX5 and JAK2 related proteins, such as surface markers, transcription factors and phosphoproteins, defined by patient specific responses but overall, quite similar. If on one side, the effects of inhibition of dasatinib compared to basal level in each group were low on surface markers and transcription factors, with group and patients' specific responses, the

effect of dasatinib was higher on the group of the phosphoproteins. In particular, pJAK2 was among the most inhibited (up to $p<0.001$), a promising preliminary result to consider not only PAX5r targeting by dasatinib, but also JAK2r in future preclinical studies, but also pERK ($p<0.05$). The broad inhibition of proteins' expression due to dasatinib treatment, which was subgroup dependent, confirmed its action as multi kinase inhibitor (e.g, c-Jun $p<0.01$, LCK $p<0.05$). Overall, each subgroup showed specific inhibitions, remarking the importance of the previous determination of the B cell classification and of the protein expression in PAX5 and JAK2 rearranged blasts to predict the efficacy of dasatinib on some of those fusions. Therefore, those findings indicate dasatinib as a promising candidate to target the different PAX5 and JAK2 fusions which harbors their specific signaling alterations depending on the partner genes involved in the fusion.

PAX5 role as metabolic gatekeeper was previously demonstrated in leukemic cell lines double negative for PAX5 due to the introduction of a PAX5 fusion gene, in which PAX5 alteration induced increased glycolysis (Chan, et al. 2017), while JAK2 rearrangements' role in metabolism of BCP-ALL cells is still unknown. Here we demonstrated in a cohort of 16 PDXs carrying PAX5 fusion genes, that we divided into six different subtypes based on PAX5 partner gene in the fusions, the role of PAX5 in the maintenance of a leukemic cells peculiar metabolism that differs from healthy bone marrow. Moreover, we obtained slightly more marked results in a smaller cohort of 4 JAK2 rearranged PDXs, one of them carrying a PAX5::JAK2 fusion gene, therefore with a gene expression supposed to be more similar to Ph-like patients, specifically the JAK2 fusions (Gu, et al. 2019), compared to

PAX5r cases, and a second one carrying one fusion involving JAK2 and an additional second fusion involving PAX5. We confirmed an increased glycolysis in our cells, both JAK2r and PAX5r, with marked overexpression of GLUT1 and MCT1 in particular. Moreover, as CS expression was comparable to health BM, and LDHA and MCT1 expression was higher, we may expect a shift towards aerobic metabolism with lactate production. We may say that leukemic cells carrying PAX5 and JAK2 fusion genes undergo the Warburg effect, known to be activated in cancer cells and being responsible of chemoresistance (Liu, et al. 2021), to produce ATP with anaerobic reactions even in presence of oxygen. Signaling molecules were more expressed (e.g. pCREB, tSYK), with evidence of an activate signaling in cells even at basal level and suggesting the role of signaling molecules in the maintenance of leukemic metabolism (Polak, et al. 2020; Altarejos, et al. 2011).

Further studies are ongoing to better elucidate PAX5 and JAK2 rearrangements in pediatric BCP-ALL at single cell level through their B cell classification and protein expression.

REFERENCES

Altarejos JY, Montminy M. CREB and the CRTC co-activators: sensors for hormonal and metabolic signals. Nat Rev Mol Cell Biol. 2011 Mar;12(3):141-51. doi: 10.1038/nrm3072

Bendall SC, et al. Single-cell trajectory detection uncovers progression and regulatory coordination in human B cell development. Cell. 2014 Apr 24;157(3):714-25. doi: 10.1016/j.cell.2014.04.005.

Cazzaniga V, Bugarin C, Bardini M, Giordan M, te Kronnie G, Basso G, Biondi A, Fazio G, Cazzaniga G. LCK over-expression drives STAT5 oncogenic signaling in PAX5 translocated BCP-ALL patients. Oncotarget. 2015 Jan 30;6(3):1569-81. doi: 10.18632/oncotarget.2807.

Cerchione C, Locatelli F, Martinelli G. Dasatinib in the Management of Pediatric Patients With Philadelphia Chromosome-Positive Acute Lymphoblastic Leukemia. Front Oncol. 2021 Mar 25;11:632231. doi: 10.3389/fonc.2021.632231

Chan LN, Chen Z, Braas D, et al. Metabolic gatekeeper function of B-lymphoid transcription factors. Nature. 2017 Feb 23;542(7642):479-483. doi: 10.1038/nature21076. Epub 2017 Feb 13. Erratum in: Nature. 2018 Jun;558(7711):E5.

Chan LN, Chen Z, Braas D, et al. Metabolic gatekeeper function of B-lymphoid transcription factors. Nature. 2017 Feb 23;542(7642):479-483. doi: 10.1038/nature21076. Epub 2017 Feb 13. Erratum in: Nature. 2018 Jun;558(7711):E5.

Cobaleda C, Schebesta A, Delogu A, Busslinger M. Pax5: the guardian of B cell identity and function. Nat Immunol. 2007 May;8(5):463-70. doi: 10.1038/ni1454.

Fazio G, Bresolin S, Silvestri D, et al. PAX5 fusion genes are frequent in poor risk childhood acute lymphoblastic leukaemia and can be targeted with BIBF1120. EBioMedicine. 2022 Sep;83:104224. doi: 10.1016/j.ebiom.2022.104224. Epub 2022 Aug 16.

Finck R, Simonds EF, Jager A, et al. Normalization of mass cytometry data with bead standards. Cytometry A. 2013 May;83(5):483-94. doi: 10.1002/cyto.a.22271. Epub 2013 Mar 19.

Good Z, Sarno J, Jager A, et al. Single-cell developmental classification of B cell precursor acute lymphoblastic leukemia at diagnosis reveals predictors of relapse. Nat Med. 2018 May;24(4):474-483. doi: 10.1038/nm.4505. Epub 2018 Mar 5.

Gu Z, Churchman ML, Roberts KG, et al. PAX5-driven subtypes of B-progenitor acute lymphoblastic leukemia. Nat Genet. 2019 Feb;51(2):296-307. doi: 10.1038/s41588-018-0315-5.

Hiraki S, Miyoshi I, Kubonishi I, et al. Human leukemic "null" cell line (NALL-1). Cancer. 1977 Nov;40(5):2131-5. doi: 10.1002/1097-0142(197711)40:5<2131::aid-cncr2820400523>3.0.co;2-v.

Laukkanen S, Veloso A, Yan C, et al. Therapeutic targeting of LCK tyrosine kinase and mTOR signaling in T-cell acute lymphoblastic leukemia. Blood. 2022 Oct 27;140(17):1891-1906. doi: 10.1182/blood.2021015106.

Liu C, Jin Y, Fan Z. The Mechanism of Warburg Effect-Induced Chemoresistance in Cancer. Front Oncol. 2021 Sep 3;11:698023. doi: 10.3389/fonc.2021.698023.

Matthias P, Rolink AG. Transcriptional networks in developing and mature B cells. Nat Rev Immunol. 2005 Jun;5(6):497-508. doi: 10.1038/nri1633. PMID: 15928681.

Polak A, Bialopiotrowicz E, Krzymieniewska B, et al. SYK inhibition targets acute myeloid leukemia stem cells by blocking their oxidative metabolism. Cell Death Dis. 2020 Nov 6;11(11):956. doi: 10.1038/s41419-020-03156-8.

Zunder ER, Finck R, Behbehani GK, et al. Palladium-based mass tag cell barcoding with a doublet-filtering scheme and single-cell deconvolution algorithm. Nat Protoc. 2015 Feb;10(2):316-33. doi: 10.1038/nprot.2015.020. Epub 2015 Jan 22.

Chapter 6

Summary, discussion and future perspectives

Summary, discussion and future perspectives

In this project we aimed to develop a preclinical target strategy towards pediatric patients of B-ALL carrying JAK2 and/or PAX5 rearrangements. As they are a delicate and fragile group of patients, lacking their specific and effective drugs, it is fundamental to achieve a personalized medicine regimen.

Firstly, taking advantage of the constant NGS screening performed in our laboratory on RNA samples of all cohort of Italian pediatric leukemic patients enrolled into the AIEOP centers, we have identified a recurrency in JAK2 and PAX5 fusion genes. Indeed, a total of 13 cases has been found to carry JAK2 fusion genes, some of them identified as novel genes (ZEB2::JAK2, GIT2::JAK2, TLE4::JAK2, RAB7::JAK2, MPRIP::JAK2). To note, PAX5::JAK2 fusion was the only recurrent in 6/13 cases, which confirms data referring to PAX5::JAK2 fusion as one of the most frequent in B-ALL (Jia and Gu, et al. 2022). On the other hand, considering PAX5 fusion genes, we recently identified 18 rearrangements, as indicated in chapter 4, in addition to the 7 described in chapter 2. Among PAX5 rearrangements, we found several novel fusion genes such as the ones involving ALDH18A1, IKZF1, CDH13 (Fazio, et al. 2022). We noted that PAX5 fusion genes are particularly recurrent among Ph-like patients. Indeed, while more than 50% of Ph-like patients have PAX5 lesions, we identified PAX5r exclusively in Ph-like, having their specific signature and being associated with a poor EFS similar to ABL/JAK-class patients (around 50%), and an inferior OS (about 53% vs. 83%), unacceptable for childhood ALL (Fazio, et al.

2022). Remarkably, we described for the first time in infants (<1 year at diagnosis) germline for KMT2A an enrichment in fusion genes involving PAX5, identifying novel fusion partner genes involving DNAJA1, FBRSL1, MBNL1, and GRHPR, which lead to a poor outcome (Fazio, et al. 2021).

Therefore, in this project, the large NGS screening applied has been fundamental to define molecular aberrations, specifically fusion genes, which characterize delicate subgroups of patients.

To get to our final goal of a personalized medicine, we expanded *in-vivo* in NSG mice primary blasts derived from ALL patients carrying JAK2 and/or PAX5 rearrangements, in order to use expanded leukemic cells for our *ex-vivo* and *in-vivo* experiments.

We obtained a complete molecular characterization of JAK2 rearrangements from 3 PDXs (PAX5::JAK2, ATF7IP::JAK2, ZEB2::JAK2 respectively). We demonstrated a basal hyperphosphorylation of JAK2r that can be targeted by tyrosine kinase inhibitors directed to JAK2, from short to long exposure. CHZ868, a type-II TKI which is becoming of interest in the setting of JAK2 alterations (Wu, et al 2015; Meyer et al. 2015), proved to be more specific on pJAK2 on all the three patients rather than ruxolitinib, a type-I TKI, which showed more efficacy on STATs family. To note, CHZ868 dosages were 100-fold lower than Ruxolitinib ones, which is important to reduce the toxicity related to the treatment. Moreover CHZ868 had a synergistic effect in combination with Ruxolitinib but also with BIBF1120, applied on the PAX5::JAK2 setting. In addition, we have also demonstrated that BIBF1120 targets PAX5 fusions in pediatric B-ALL (Fazio, et al 2022). Remarkably, CHZ868 proved its

efficacy also in *in-vivo* setting, in mice xenotransplant with primary cells carrying JAK2 fusions. Therefore, CHZ868 proved to be an ideal candidate for JAK2 fusions in presence of an aberrant JAK2/STATs pathway in pediatric B-ALL.

Not only JAK2 rearrangements have been deeply characterized, but also PAX5 fusions. Indeed, we demonstrated that PAX5 fusions cluster and partially overlaps to Philadelphia-like patients; moreover, we deepened our interest on the alterations induced by PAX5 fusions to set up a targeted therapy. In particular, PAX5t cases have a specific driver activity signature, extending to multiple pathways including LCK hyperactivation. We also further demonstrated that in presence of PAX5 fusions there is a peculiar overexpression of LCK in addition to its hyperactivation, that is not seen nor in deleted or wild type PAX5 cases. Moreover, we considered the opportunity to target PAX5 fusion by BIBF1120/Nintedanib, as previously demonstrated in our lab in murine pre-B cells carrying PAX5/ETV6 (Cazzaniga, et al 2015). Indeed, we tested it on our PAX5 rearranged samples, in (N=4) *ex-vivo* and (N=2) *in-vivo* experiments. Interestingly, BIBF1120 proved to be effective at low dosages in monotherapy, and showed synergistic and additive effects in combination with three different standard chemotherapy drugs (*ex-vivo* data). Moreover, *in-vivo* BIBF1120 treatment proved to be significantly effective in PDX mice with PAX5 fusions, not only in monotherapy but also in combination with dexamethasone. We also confirmed LCK regulation of PI3K-AKT pathway, and the capacity of BIBF1120 to downregulate it after in-vivo treatment. Our results on PAX rearranged samples indicate BIBF1120 as a promising candidate drug for the treatment of pediatric B-ALL with PAX5 fusions,

remarking its synergistic effect with dexamethasone to introduce it as a second line treatment. Moreover, among FDA-approved drugs and inhibitors, we also selected Dasatinib, Bosutinib and Foretinib, known to be among the top 10 compound to target LCK, in addition to Nintedanib.

To better understand the mechanisms underlying the development and maintenance of leukemic cells due to the presence of fusion genes involving JAK2 and PAX5, we simultaneously checked the expression of a wide pool of proteins related to B cells and PAX5 and JAK2, through a single cell analysis of mass spectrometry by CyTOF. We observe in a cohort of 20 PDXs that PAX5 and JAK2 fusions lead to a blockade of maturation mainly in the pre-pro-B, pro-BII and pre-BII stag of B cells maturation, meaning that these fusions maintain the leukemic cells in an immature state. We interestingly found that PAX5 and JAK2 fusions have a similar pattern of expression of signaling related molecules, that are mainly upregulated compared to healthy BM, such as phosphoproteins and surface molecules. We confirmed that dasatinib is among the potent inhibitors of LCK (Fazio, et al. 2022) and it is known to target LCK in T-ALL (Serafin, et al. 2017). Moreover, it is a broad range kinase inhibitor used for BCR::ABL1 targeting in Ph+ ALL (Cerchione, et al. 2021). For those reasons, we tested dasatinib on our JAK2 and PAX5 rearranged cases, finding an interesting significant decrease of expression of PAX5 and JAK2 related proteins, such as c-Jun, LCK, pJAK2, pERK, among the others. We have to consider that, due to the classification of our patients in different subgroups, we obtained interesting subgroup specific responses to dasatinib treatment. Those preliminary data proved that dasatinib may be an additional

potential candidate for PAX5 and JAK2 rearrangements targeting in B-ALL. Moreover, we interestingly noted a metabolic switch in our rearranged samples compared to healthy BM, with a peculiar increased glycolysis and lactate production, which may be a potential branch of novel studies for our rearranged cases.

Finally, a high throughput wide drug screening of 174 FDA approved drugs was applied on our JAK2 and PAX5 rearranged PDXs. Having positive and negative controls to compare our results with, we could define a group of ideal candidates that may be used to develop future preclinical models of validation *ex-vivo* and *in-vivo* of their efficacy and specificity on JAK2 or PAX5 fusions in pediatric B-ALL. To note, Birinapant and AT9283 were the most effective drugs on JAK2 rearrangements, while venetoclax may be a potential candidate for PAX5 fusions (see preliminary data).

Therefore, we will deeply analyze our wide data found through the CyTOF evaluation of proteins expression in our cohort of PDXs, not only considering B cells, but going into the details of the subpopulations. This analysis will deepen our knowledge of what led to and sustain the leukemic state in presence of fusion genes and will contribute to predict drug responsiveness.

Remarkably, we obtained some preliminary results on JAK2 rearrangements. By NGS RNAseq, we defined a peculiar gene expression profile, with the top 30 genes expressed indicated in **figure 1**.

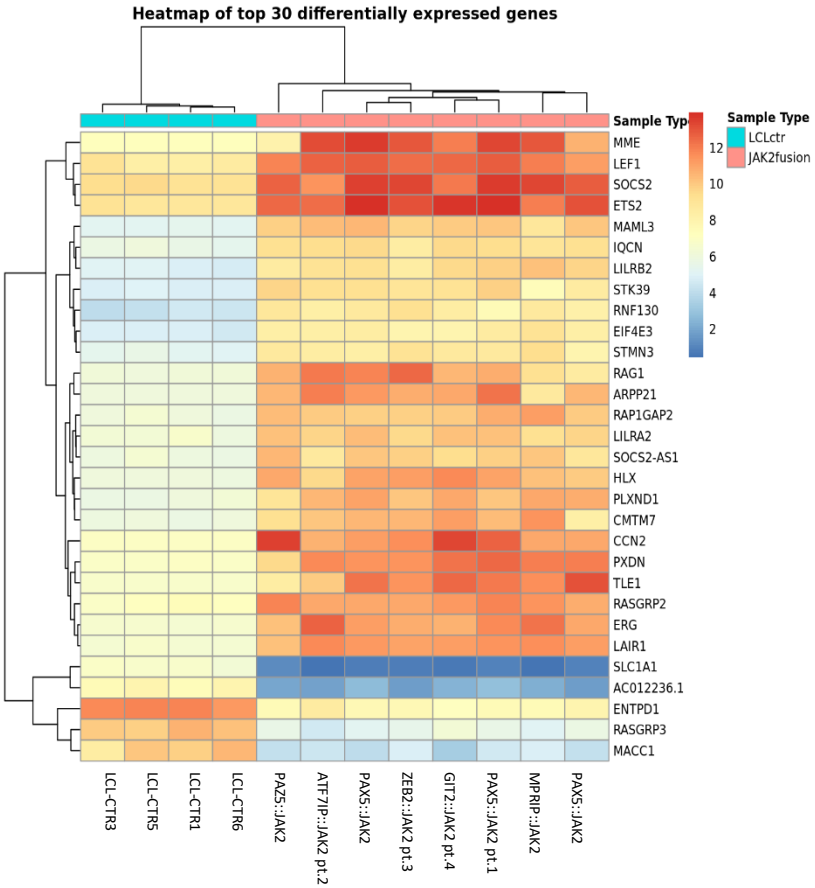

Figure 1. Heatmap of top expressed genes in N=8 JAK2 rearranged pediatric patients compared to N=4 lymphoblastoid cell lines (LCL) used as healthy controls, derived from transcriptome analysis after RNA sequencing.

Considering n=8 JAK2t cases, we applied the RNAseq analysis comparing their gene expression profile to the one of four lymphoblastoid cell lines (LCLs), used as healthy controls. We interestingly found that, among the top 30 differentially expressed genes, MME/CD10, phenotypic marked of pre-B cells in B-ALL

(Mishra, et al. 2016), LEF1 and RAG1, direct targets of PAX5 (Cobaleda, et al. 2007), SOCS2, known to be activated by JAK2 fusions (Ehrentraut, et al. 2013) and ETS2, amplified in JAK2m (Takeda, et al. 2022), were the most upregulated. Conversely, MACC1, a metabolic marker (Lisec, et al. 2021), was among the most downregulated, leading a finding that could be integrated to our CyTOF results on metabolism. Moreover, we are deepening our interest in recent results regarding a high throughput drug screening on PAX5 rearranged PDXs. A library of 174 compounds, from preclinical stage to FDA/EMA approved drugs, has been screened. To dissect compounds with a profound efficacy for PAX5r versus a pool of 14 healthy samples, we considered a threshold from zero to minimal activity on heathy controls. We performed Mann Whitney U-tests on the drug responses of PAX5 rearranged PDXs versus the responses of the healthy controls. We identified 82/174 drugs to be effective in PAX5r-ALL (**Figure 2**).

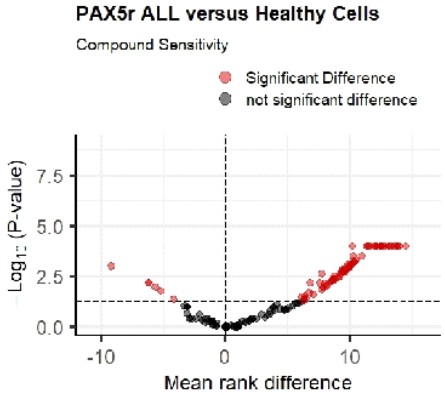

Figure 2. Volcano plot summarizing the statistical significance (y-axis) of the mean rank difference (x-axis) as defined by Mann-Whitney U-test using the DSS sensitivity scores for N=15 PAX5r PDXs against the DSS scores of the cohort of healthy cells (in total n=14; healthy lymphoblastoid B-cell lines: n=5, hematopoietic stem cells-HSCs: n=3 , T cells: n=3, PBMCs: n=3). Highlighted in red the compounds with

statistically significant difference less than 0.05 between PAX5r and the healthy controls. A positive mean rank difference represents higher activity in PAX5r versus the healthy controls while negative mean rank difference corresponds to the opposite effect.

We combined PAX5r drug screening results to the results on other categories of high-risk ALL (KMT2Ar and CRLF2r), applying also stringent selection criteria (median DSS of ALL patients > 50 accompanied by a median DSS of healthy controls <10) determining N=9 compounds to be the most communal effective on the three high-risk subgroups. We decided to start to validate, among them, venetoclax, as it is not only used for the treatment of AML (Samra, et al. 2020), but it is also known to correlate with metabolic changes in leukemic cells (Carter, et al. 2022), important aspect for us considering our promising preliminary data on metabolism obtained by CyTOF technique. So far, we demonstrated its efficacy on N=3 PAX5r cases (**Figure 3**).

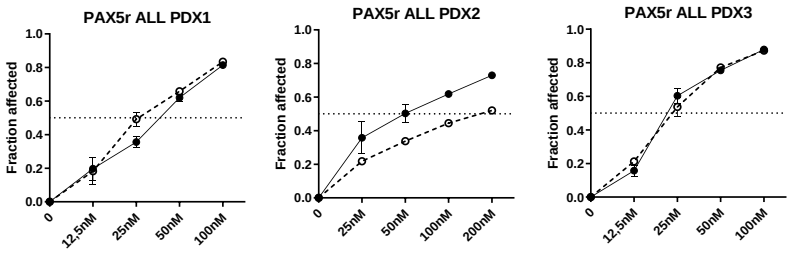

Figure 3. 72h ex-vivo venetoclax treatment of blast cells carrying PAX5 rearrangements after 72h, in biological triplicate and technical duplicate. Apoptosis evaluation by FACS through Annexin V-PE/7AAD staining and affected metabolic activity evaluation by CellTiterGlo through luminescence assay.

In conclusion, on one side we better defined the features sustaining the molecular alterations in novel subgroups of B-ALL, based on the identification of specific fusion genes and analyzing their downstream related altered signaling pathways.

Moreover, on the other side, we identified novel molecular drugs and compounds which could lead novel preclinical targeting approaches specific for JAK2 and PAX5 fusions. In the next future, the final goal would be to introduce those compounds, previously knowing the features of PAX5 and JAK2 rearrangements, into the clinics as novel targeted therapy for a personalized medicine which is still lacking for pediatric patients of B-ALL carrying JAK2 and PAX5 rearrangements. Indeed, Nintedanib/BIBF1120 drug could be considered as a second line of treatment, not only allowing the identification of the patient's profile but also integrating this information with the MRD analysis data. This approach would be fundamental to assign PAX5 rearranged patients to an experimental group, where they could receive BIBF1120 in addition to the chemotherapy drugs already in use.

In future perspective, we will focus on one side on the validation of novel drugs, which have shown to be highly specific and effective on our PAX5 and JAK2 cases. Moreover, more needs to be known about leukemia maintenance and development of leukemia in presence of fusion genes.

REFERENCES

Carter BZ, Mak PY, Tao W, et al. Targeting MCL-1 dysregulates cell metabolism and leukemia-stroma interactions and resensitizes acute myeloid leukemia to BCL-2 inhibition. Haematologica. 2022 Jan 1;107(1):58-76. doi: 10.3324/haematol.2020.260331.

Cazzaniga V, Bugarin C, Bardini M, et al. LCK over-expression drives STAT5 oncogenic signaling in PAX5 translocated BCP-ALL patients. Oncotarget. 2015 Jan 30;6(3):1569-81. doi: 10.18632/oncotarget.2807. PMID: 25595912; PMCID: PMC4359315.

Cerchione C, Locatelli F, Martinelli G. Dasatinib in the Management of Pediatric Patients With Philadelphia Chromosome-Positive Acute Lymphoblastic Leukemia. Front Oncol. 2021 Mar 25;11:632231. doi: 10.3389/fonc.2021.632231

Cobaleda C, Schebesta A, Delogu A, Busslinger M. Pax5: the guardian of B cell identity and function. Nat Immunol. 2007 May;8(5):463-70. doi: 10.1038/ni1454.

Ehrentraut S, Nagel S, Scherr ME, et al. t(8;9)(p22;p24)/PCM1-JAK2 activates SOCS2 and SOCS3 via STAT5. PLoS One. 2013;8(1):e53767. doi: 10.1371/journal.pone.0053767. Epub 2013 Jan 23.

Fazio G, Bardini M, De Lorenzo P, et al. Recurrent genetic fusions redefine MLL germ line acute lymphoblastic leukemia in infants. Blood. 2021 Apr 8;137(14):1980-1984. doi: 10.1182/blood.2020009032. PMID: 33512459.

Fazio G, Bresolin S, Silvestri D, et al. PAX5 fusion genes are frequent in poor risk childhood acute lymphoblastic leukaemia and can be targeted with BIBF1120. EBioMedicine. 2022 Sep;83:104224. doi:

10.1016/j.ebiom.2022.104224. Epub 2022 Aug 16. PMID: 35985167; PMCID: PMC9403348.

Jia Z, Gu Z. *PAX5* alterations in B-cell acute lymphoblastic leukemia. Front Oncol. 2022 Oct 25;12:1023606. doi:10.3389/fonc.2022.1023606. PMID: 36387144; PMCID: PMC9640836.

Lisec J, Kobelt D, Walther W, et al. Systematic Identification of MACC1-Driven Metabolic Networks in Colorectal Cancer. Cancers (Basel). 2021 Feb 26;13(5):978. doi: 10.3390/cancers13050978.

Meyer SC, Keller MD, Chiu S, et al. CHZ868, a Type II JAK2 Inhibitor, Reverses Type I JAK Inhibitor Persistence and Demonstrates Efficacy in Myeloproliferative Neoplasms. Cancer Cell. 2015 Jul 13;28(1):15-28. doi: 10.1016/j.ccell.2015.06.006.

Mishra D, Singh S, Narayan G. Role of B Cell Development Marker CD10 in Cancer Progression and Prognosis. Mol Biol Int. 2016;2016:4328697. doi: 10.1155/2016/4328697. Epub 2016 Nov 14

Samra B, Konopleva M, Isidori A, et al. Venetoclax-Based Combinations in Acute Myeloid Leukemia: Current Evidence and Future Directions. Front Oncol. 2020 Nov 5;10:562558. doi: 10.3389/fonc.2020.562558

Serafin V, Capuzzo G, Milani G, et al. Glucocorticoid resistance is reverted by LCK inhibition in pediatric T-cell acute lymphoblastic leukemia. Blood. 2017 Dec 21;130(25):2750-2761. doi: 10.1182/blood-2017-05-784603. Epub 2017 Nov 3. PMID: 29101238.

Takeda J, Yoshida K, Nakagawa MM, et al. Amplified EPOR/JAK2 Genes Define a Unique Subtype of Acute Erythroid Leukemia. Blood Cancer Discov. 2022 Sep 6;3(5):410-427. doi: 10.1158/2643-3230.BCD-21-0192.

Wu SC, Li LS, Kopp N, et al. Activity of the Type II JAK2 Inhibitor CHZ868 in B Cell Acute Lymphoblastic Leukemia. Cancer Cell. 2015 Jul 13;28(1):29-41. doi: 10.1016/j.ccell.2015.06.005. PMID: 26175414; PMCID: PMC4505625.

Appendix

Publications not included in the thesis

Blood. 2021 Jan 28;137(4):493-499. doi:10.1182/blood.2020006441.

Absent B cells, agammaglobulinemia, and hypertrophic cardiomyopathy in folliculin-interacting protein 1 deficiency

Francesco Saettini [1], Cecilia Poli [2, 3], Jaime Vengoechea [4 ,5], Sonia Bonanomi [1], Julio C Orellana [6], Grazia Fazio [7], Fred H Rodriguez [8,9], Loreani P Noguera [3], Claire Booth [10], Valentina Jarur-Chamy [3], Marissa Shams [5], Maria Iascone [11], Maja Vukic [12], Serena Gasperini [13], Manuel Quadri [7], Amairelys Barroeta Seijas [10], Elizabeth Rivers [10], Mario Mauri [14], Raffaele Badolato [15], Gianni Cazzaniga [7,14], Cristina Bugarin [7], Giuseppe Gaipa [7], Wilma G M Kroes [16], Daniele Moratto [17], Monique M van Oostaijen-Ten Dam [18], Frank Baas [16], Silvère van der Maarel [12], Rocco Piazza [14], Zeynep H Coban-Akdemir [19,20], James R Lupski [19,21], Bo Yuan [19,20], Ivan K Chinn [2,22], Lucia Daxinger [12], Andrea Biondi [1,7]*

**see paper for affiliations*

Abstract

Agammaglobulinemia is the most profound primary antibody deficiency that can occur due to an early termination of B-cell development. We here investigated 3 novel patients, including the first known adult, from unrelated families with agammaglobulinemia, recurrent infections, and hypertrophic cardiomyopathy (HCM). Two of them also presented with intermittent or severe chronic neutropenia. We identified homozygous or compound-heterozygous variants in the gene for folliculin interacting protein 1 (FNIP1), leading to loss of the FNIP1

protein. B-cell metabolism, including mitochondrial numbers and activity and phosphatidylinositol 3-kinase/AKT pathway, was impaired. These defects recapitulated the Fnip1-/- animal model. Moreover, we identified either uniparental disomy or copy-number variants (CNVs) in 2 patients, expanding the variant spectrum of this novel inborn error of immunity. The results indicate that FNIP1 deficiency can be caused by complex genetic mechanisms and support the clinical utility of exome sequencing and CNV analysis in patients with broad phenotypes, including agammaglobulinemia and HCM. FNIP1 deficiency is a novel inborn error of immunity characterized by early and severe B-cell development defect, agammaglobulinemia, variable neutropenia, and HCM. Our findings elucidate a functional and relevant role of FNIP1 in B-cell development and metabolism and potentially neutrophil activity.

Pediatr Hematol Oncol. 2021 Mar;38(2):174-178. doi: 10.1080/08880018.2020.1793849. Epub 2020 Jul 22.

A novel homozygous disruptive PRF1 variant (K285Sfs*4) causes very early-onset of familial hemophagocytic lymphohystiocytosis type 2

F Saettini [1], I Castelli [1], M Provenzi [2], G Fazio [3], M Quadri [3], G Cazzaniga [3,4], S Sala [3], F Dell'Acqua [1], E Sieni [5], M L Coniglio [5], L Pezzoli [6], M Iascone [6], F Vendemini [1], A C Balduzzi [1], A Biondi [1,3], C Rizzari [1], S Bonanomi [1]

doi: 10.1080/08880018.2020.1793849, to see published case report.

Clin Immunol. 2020 Sep;218:108525. doi: 10.1016/j.clim.2020.108525. Epub 2020 Jul 11.

Two siblings presenting with novel ADA2 variants, lymphoproliferation, persistence of large granular lymphocytes, and T-cell perturbations

F Saettini [1], G Fazio [2], P Corti [3], M Quadri [2], C Bugarin [2], G Gaipa [2], F Penco [4], D Moratto [5], M Chiarini [5], M Baronio [6], L Gazzurelli [6], L Imberti [7], S Paghera [7], S Giliani [6], G Cazzaniga [8], A Plebani [6], R Badolato [6], V Lougaris [6], M Gattorno [4], A Biondi [9] *

**see paper for affiliations*

Abstract

The presence of large granular lymphocytes has been reported in patients with ADA2 deficiency and T-LGL leukemia. Here we describe two siblings with novel ADA2 variants, expanding the mutational spectrum of ADA2 deficiency. We show that lymphoproliferation, persistence of large granular lymphocytes, T-cell perturbations, and activation of PI3K pathway, measured by means of phosphorylation levels of S6, are detectable in DADA2 patients without T-LGL leukemia.

Keywords: ADA2 deficiency; DADA2; Hypogammaglobulinemia; Large granular lymphocytes; Lymphopenia; Lymphoproliferation; T-cell repertoire.